THE UNIVERSITY OF QUEENSLAND

AUSTRALIA

Investigating Defensive Colouration in Nudibranch Molluscs using a Novel Analytical Framework for the Study of Animal Colour Patterns

Cedric Pascal van den Berg

MSc

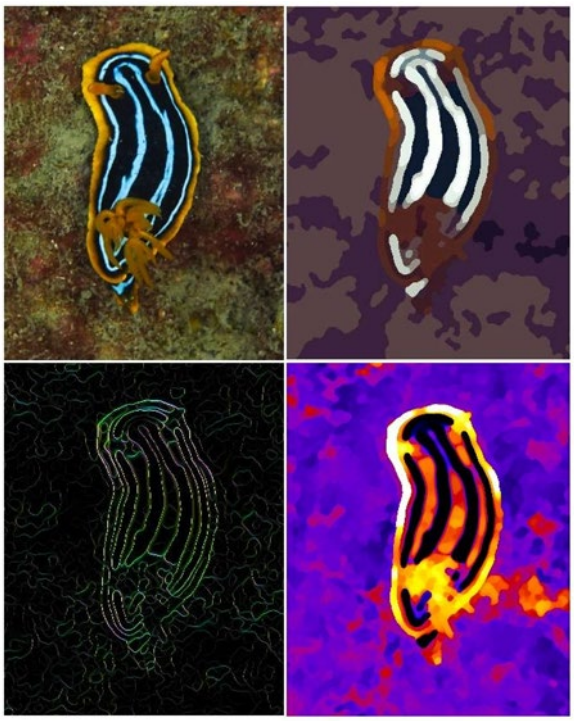

A thesis submitted for the degree of Doctor of Philosophy at

The University of Queensland in 2020

School of Biological Sciences

Abstract

Animal colour patterns are complex and highly diverse traits that are used for intra- and inter-specific communication, thermoregulation and predator avoidance, including aposematism, camouflage and mimicry. To understand the evolution and design of such colouration, it is essential to quantify animal colour patterns and how they appear against their natural background. Visual signals comprise multiple elements, such as luminance, chromaticity and pattern geometry, and the integrated perception of these elements against the background determine how an animal appears to predators, prey and conspecifics. However, despite considerable attention in the literature, the ability of visual ecologists to achieve a comprehensive analysis of complex visual signals has been limited, mainly due to quantitative and qualitative limitations of data acquisition. Importantly, existing pattern analyses failed to integrate the perception of colour-, luminance- and pattern geometry contrast of complex animal colour patterns against their natural background.

In this thesis, I have overcome many limitations of colour pattern analyses by combining calibrated digital photography, visual modelling and comprehensive colour pattern analysis. I first developed a new colour pattern analysis framework (QCPA) (Chapter 2) in a collaborative effort. This resulted in user friendly and open source software running on two separate software platforms (Matlab & ImageJ), accompanied by a website hosting manuals, user guides, worked examples, tutorials and videos, and a user forum.

I used this new methodology to investigate the evolution and design of colour patterns in nudibranch molluscs (Chapter 3). I investigated morphological differences in colour patterns between dorid nudibranchs exclusively active during the night and those active during daytime at dive sites in rocky shore sites in Nelson Bay, NSW, Australia. This chapter investigated a key assumption underlying the use of nudibranch molluscs for the study of defensive colouration, namely that selection pressure by visual predators is the primary cause for colour pattern evolution in nudibranchs. To do this, I obtained a calibrated image database of 23 species of dorid nudibranchs against their natural backgrounds. I found distinct differences in colour pattern morphology between species active at either time of the day, supporting the hypothesis that colour pattern morphology is indeed correlated with daytime activity.

To test assumptions on parameter and model choices using QCPA and deepen our understanding of animal vision, I conducted behavioural experiments using Picasso triggerfish (*Rhinecanthus aculeatus*) to determine thresholds of luminance contrast detection and discrimination of reef fish (Chapter 4). This study found profound context dependant differences in luminance discrimination thresholds, questioning the current use of visual models to describe luminance contrast perception in animals.

The work in this thesis greatly contributes to the ability of researchers to investigate visual perception in non-humans at a quantitative scale, while contributing to our understanding of how animal might perceive spatiochromatic information. My thesis greatly reduces current boundaries to visual modelling and colour pattern analysis by creating a comprehensive and user friendly open-source software and online user platform. My work innovates and expands upon currently used tools for the study of animal vision, while investigating the use of the receptor noise limited model. It also provides specific solutions while outlining potential for future research and development. I also provide a specific example of how to calibrate parameter choice for the QCPA. Finally, the thesis provides a first application of the QCPA framework while highlighting the great suitability of nudibranchs as a model organism of growing importance for the study of defensive animal colouration.

Declaration by Author

This thesis is composed of my original work, and contains no material previously published or written by another person except where due reference has been made in the text. I have clearly stated the contribution by others to jointly-authored works that I have included in my thesis.

I have clearly stated the contribution of others to my thesis, including statistical assistance, survey design, data analysis, significant technical procedures, professional editorial advice, financial support and any other original research work used or reported in my thesis. The content of my thesis is the result of work I have carried out since the commencement of my higher degree by research candidature and does not include a substantial part of work that has been submitted *to qualify for the award of any* other degree or diploma in any university or other tertiary institution. I have clearly stated which parts of my thesis, if any, have been submitted to qualify for another award.

I acknowledge that an electronic copy of my thesis must be lodged with the University Library and, subject to the policy and procedures of The University of Queensland, the thesis be made available for research and study in accordance with the Copyright Act 1968 unless a period of embargo has been approved by the Dean of the Graduate School.

I acknowledge that copyright of all material contained in my thesis resides with the copyright holder(s) of that material. Where appropriate I have obtained copyright permission from the copyright holder to reproduce material in this thesis and have sought permission from co-authors for any jointly authored works included in the thesis.

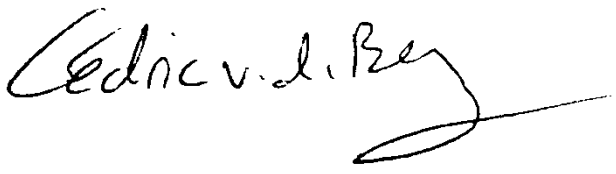

Publications Included in this Thesis

Cedric P. van den Berg, Jolyon Troscianko, John A. Endler, N. Justin Marshall, Karen L. Cheney, Quantitative Colour Pattern Analysis (QCPA): A Comprehensive Framework for the Analysis of Colour Patterns in Nature. *Methods in Ecology and Evolution,* 2019 (October), 1–17. DOI:10.1111/2041-210X.13328

Submitted Manuscripts Included in this Thesis

Cedric P. van den Berg, Michelle Hollenkamp, Laurie J. Mitchell, Erin J. Watson, Naomi F. Green, N. Justin Marshall, Karen L. Cheney, More than noise: Context-dependant luminance contrast discrimination in a coral reef fish (*Rhinecanthus aculeatus*). *bioRxiv* (2020.06.25). DOI: https://doi.org/10.1101/2020.06.25.168443

Other Publications During Candidature

Peer-reviewed Papers

Winters, A. E., Wilson, N. G., **van den Berg, C. P.**, How, M. J., Garson, M. J., Endler. J. A., Marshall, N. J., & Cheney, K. L. (2018), Toxicity and taste: unequal chemical defences in a mimicry ring. *Proceedings of Royal Society of London, B-Biological Sciences*, 285 (1880): 20180457. DOI: 10.1098/rspb.2018.0457

Green, N. F., Urquhart, H. H., **van den Berg, C. P.**, Marshall, N. J., Cheney, K. L. (2018), Pattern edges improve predator learning of aposematic signals. *Behavioral Ecology,* 29 (6): 1481-1486. DOI: doi.org/10.1093/beheco/

Carmen R. B. da Silva, **Cedric P. van den Berg**, Nicholas D. Condon, Cynthia Riginos, Robbie S. Wilson, Karen L. Cheney (2020), Intertidal gobies acclimate rate of luminance change for background matching with shifts in seasonal temperature. *Journal of Animal Ecology*, 89 (7): 1735-1746. DOI: 10.1111/1365-2656.13226

Monique G. G. Grol, Julie Vercelloni, Tania M. Kenyon, Elisa Bayraktarov, **Cedric P. van den Berg**, Daniel Harris, Jennifer A. Loder, Morana Mihaljevic, Phebe I. Rowland, Chris M. Roelfsema (2020), Conservation value of a subtropical reef in south-eastern Queensland, Australia, highlighted by citizen-science efforts. *Marine and Freshwater Research*, DOI: 10.1071/MF19170

Papers in Press

None

Conference Abstracts

Cedric P. van den Berg, Jolyon Troscianko, John A. Endler, N. Justin Marshall, Karen L. Cheney. "Quantitative Colour Pattern Analysis (QCPA): A Novel Analytical Framework for the Study of Animal Colour Patterns". Australasian Society for the Study of Animal Behaviour (ASSAB) Conference 2019, Waiheke Island, New Zealand.

Cedric P. van den Berg, Jolyon Troscianko, John A. Endler, N. Justin Marshall, Karen L. Cheney. "Quantitative Colour Pattern Analysis (QCPA): A Novel Analytical Framework for the Study of Animal Colour Patterns". 6th International Heterobranch Workshop 2018, Freemantle (Perth), Australia.

Cedric P. van den Berg, Michelle Hollenkamp, Erin J. Watson, Naomi F. Green, Laurie J. L. Mitchell, N. Justin Marshall, Karen L. Cheney. "39 Shades of Grey: Luminance detection and Discrimination Thresholds in a Coral Reef Fish (*Rhinecanthus aculeatus*)". Australasian Society for the Study of Animal Behaviour (ASSAB) Conference 2018, Brisbane, Australia.

Cedric P. van den Berg, Jolyon Troscianko, John A. Endler, N. Justin Marshall, Karen L. Cheney. "Quantitative Colour Pattern Analysis (QCPA): A Novel Analytical Framework for the Study of Animal Colour Patterns". International Society for Behavioural Ecology (ISBE) meeting 2018, Minneapolis, United States of America.

Cedric P. van den Berg, Jolyon Troscianko, John A. Endler, N. Justin Marshall, Karen L. Cheney. “A Novel Analytical Framework for the Study of Animal Colour Patterns”. Behaviour 2017 (joint meeting of the 35th International Ethological Conference (IEC) and the 2017 Summer Meeting of the Association for the Study of Animal Behaviour (ASAB), Lisbon, Portugal.

Cedric P. van den Berg, Jolyon Troscianko, John A. Endler, N. Justin Marshall, Karen L. Cheney. “A Novel Approach to Quantitative Pattern Analysis”. Australasian Society for the Study of Animal Behaviour (ASSAB) Conference 2016, Katoomba, Australia.

Contributions by Others to the Thesis

Chapter 1: Karen Cheney provided feedback.

Chapter 2: Jolyon Troscianko and Karen Cheney contributed to original concept. Final software written for ImageJ by Jolyon Troscianko with substantial contributions by Cedric van den Berg. Manuscript & Supplementary Material written by Cedric van den Berg with contributions from Jolyon Troscianko, Karen Cheney and John Endler. Website & user forum conceptualised by Cedric van den Berg. Web-design by Jolyon Troscianko with substantial contributions from Cedric van den Berg. Online user guides were jointly written with Jolyon Troscianko.

Chapter 3: Karen Cheney contributed to original concept. Data collection & analysis was performed with support by various field work assistants. The phylogenetic tree was assembled by Nerida Wilson. Data analysis was performed with advice from Karen Cheney, Simone Blomberg, John Endler and Thomas Guilleman. Chapter reviewed by Karen Cheney.

Chapter 4: Data collection was performed with support by Michelle Hollenkamp, Laurie Mitchell, Erin Watson and Naomi Green. Data analysis was performed with advice from Karen Cheney. Chapter reviewed by Karen Cheney and Naomi Green.

Chapter 5: Reviewed by Karen Cheney.

Statement of Parts of the Thesis Submitted to Qualify for the Award of Another Degree

No works submitted towards another degree have been included in this thesis.

Research Involving Human or Animal Subjects

Chapter 1: No animal or human subjects were involved in this research.

Chapter 2: No animal or human subjects were involved in this research.

Chapter 3: No animal or human subjects were involved in this research.

Chapter 4: Research was carried out with permission of the University of Queensland Animal Ethics Committee (AEC approval number: SBS/077/17).

Chapter 5: No animal or human subjects were involved in this research.

Acknowledgements

I would like to thank the University of Queensland, the School of Biological Sciences, the Queensland Brain Institute and the combined labs of Dr. Karen Cheney and Prof. Justin Marshall for enabling me to conduct my PhD here in Australia. I would especially like to thank Karen Cheney for guiding and supporting me in my successes and failures while skilfully chaperoning my quest to try to do things a little bit different. I could not have asked for a better mentor and supervisor, thank you!

I would like to thank Prof. Justin Marshall for being supportive of my attempts to realise something I often struggled to put into words, while providing a healthy dose of criticism to keep my efforts realistic. Your work is truly inspirational, and it has been a privilege to be part of your amazing research group.

I would like to thank Prof. John Endler whose endless knowledge I was able to draw from throughout all these years. It is John's way of thinking that transpires many aspects of this thesis and if it wasn't for him and his scientific legacy, none of this work would look the way it does today. Thank you for everything!

I would like to thank Dr. Simone Blomberg for years of advice on how to crunch the numbers and so much inspiration for trying different avenues in comparative phylogenetics. Thank you for letting me be part of your research group.

Thank you, Dr. Jolyon Troscianko, for crossing my path and joining me on this challenging but rewarding trip. Thank you for lending an ear to my crazy ideas, fusing them with yours and turning things into the fantastic result our work has become. You're a wizard and an exceptionally kind person!

Thank you, Ian Tibbets, Chris Roelfsema, Sophie Dove, Janet Lanyon and Steve Salisbury, for supporting my strive to grow outside of my degree by welcoming me into the world of teaching, citizen science and science communication

I would like to thank my family at home for supporting me throughout all these years. Thank you for allowing me to grow into what I am today by nurturing my sense of curiosity and adventure at every instant and sorry for being so far away!

And finally, thank you to all my friends and co-workers who have been listening to my ideas, helping me to figure things out, celebrating my successes and lending me an ear in times of need. Nothing beats a drink surrounded by friends!

Financial support

A PhD scholarship was provided by a Living Allowance Stipend (50% funded by School of Biological Sciences and 50% funded by an ARC Discovery Grant) and a UQ Tuition Fee Offset Scholarship. Research costs were provided by an ARC Discovery Grant awarded to supervisors Karen Cheney, John Endler and Justin Marshall.

Over the course of this PhD, Cedric van den Berg was awarded two Holsworth Wildlife Research Endowments, a research grant from Conchologists of America and a student research grant from the Australasian Society for the Study of Animal Behaviour.

Keywords

Defensive animal colouration, visual modelling, psychophysics, aposematism, camouflage, colour vision, spatial acuity

Australian and New Zealand Standard Research Classifications (ANZSRC)

060303 Biological Adaptation (25%)

060201 Behavioural Ecology (25%)

110906 Sensory Systems (50%)

Fields of Research (FoR) Classification

0602 Ecology (30%)

1109 Neurosciences (50%)

0603 Evolutionary Biology (20%)

List of Tables

List of Figures

List of Abbreviations

BSA	Boundary strength analysis
CAA	Colour adjacency analysis
CV	Coefficient of variance
dbl	Double cone
FFT	Fast Fourier transform
Glmm	Generalized linear mixed model
LED	Light emitting diode
LEIA	Local edge intensity analysis
lw	longwave sensitive cone
MC	Michelson contrast
MCMC	Markhov chain Monte Carlo
MDS	Multi-dimensional scaling
ML	Maximum likelihood
MMDS	Metric multi-dimensional scaling
MICA	Multispectral image calibration and analysis toolbox
mw	mediumwave sensitive cone
NMDS	Non-metric multi-dimensional scaling
PC	Principal component
PCA	Principal component analysis
QCPA	Quantitative colour pattern analysis
RGB	Red-Green-Blue
RNL	Receptor noise limited
SIFT	Scale invariant feature transform
sw	shortwave sensitive cone

UV	Ultra-violet
VCA	Visual contrast analysis
WC	Weber contrast

For a detailed list of abbreviations for QCPA parameters, please see Appendix A

Table of Contents

Preface to the Thesis

When I started my PhD, my primary goal was to understand how colourful visual signals were perceived in complex visual scenes through the eyes of animals. However, suitable tools to do that did not exist. The literature and expert opinions at the time suggested to use either hyperspectral cameras or digital imaging. However, hyperspectral cameras, especially when taken underwater, were far too expensive, delicate, slow and of low resolution. On the other hand, the use of digital cameras, although accepted for modelling spatial acuity and describing achromatic patterns, was considered highly unsuitable and problematic for the modelling of colour vision.

During my Masters' thesis, I had started to use Prof. John Endler's pattern analyses and knew that this approach to the quantification of colour patterns posed powerful advantages over (and addition to) alternative tools being used by researchers at that time. The problem I saw was that John's pattern analyses, despite going back to the late 70s, had never really found their way into the mainstream visual ecology literature. This was largely due to a lack of accessibility and complex literature but also because these methods require segmented images. At the time, breaking an image down into its colour pattern elements was an incredibly tedious and subjective manual process that could not be applied to complex natural scenes.

This meant that my first approaches to the quantitative analysis of colour patterns involved the taking of digital images which were manually redrawn to reconstruct the shape, size and location of colour pattern elements. Extensive Matlab scripts developed in collaboration with John would then connect these pattern elements with a library of spectral reflectance measurements in order to allow the implementation of spatiochromatic pattern analyses. This early stage of pattern analysis - in combination with a user input guided Matlab script that I had started to write - was the seed of what would become the QCPA.

The publication of the MICA toolbox in late 2015 proved to researchers that using calibrated photography to reliably obtain photoreceptor stimulation for entire visual scenes was possible and could allow for image segmentation using animal vision. This was the crucial step needed for the implementation of John's analyses at a quantitative scale. After about a year of development, a first prototype of the QCPA was functional and presented at international conferences in mid-2017. The framework

at that stage would complete colour vision modelling and image segmentation in ImageJ to produce input for a sophisticated graphical Matlab user interface that would perform spatial acuity modelling, region of interest (ROI) selection, colour pattern analysis and data visualisation. The Matlab side of QCPA ultimately became integrated into ImageJ while growing substantially, leading to the software presented in this thesis.

QCPA was first published as a pre-print at the end of March 2019, coinciding with the launch of an extensive online platform featuring hundreds of pages of user guides, articles, tutorials, video and a user forum followed by its eventual peer-reviewed publication in December 2019. However, I do not present that content in this thesis and neither do I present the roughly 300 A4 pages of carefully annotated code that make up the ImageJ and Matlab programmes. Despite having spent considerable time conducting behavioural experiments for chapter 3 and collecting data for chapter 4, a large part of my PhD has been dedicated to the development, testing and implementation of the QCPA. Was it worth it?

Feedback from the scientific community and the general public seems to support the notion that this work will have a significant impact in the field of visual ecology. The pre-print has been read and downloaded thousands of times, the website has been visited by thousands of people and the final publication has been covered by media throughout the world at an impressive level. The QCPA already has dozens of researchers around the world actively using it for their work and as such, I am confident that our work has left a mark in the scientific community.

The QCPA has implications beyond the final piece of code for ImageJ or the associated manuscript and supplementary material provided in this thesis. This project saw the revision of not just fundamental modelling aspects of animal colour, luminance and spatial vision but also colour pattern analyses which have been developed over the course of decades. However, it does significantly more than revise and comment on these tools: it provides a unified concept of how to combine these tools into a dynamic workflow, which supports our current understanding of animal vision. This process has been shaped by a long history of active communication across various international and national conferences and subsequent discussions with researchers across the field of visual ecology, for which I am extremely grateful.

The development of the QCPA falls into the context of a growing interest by the scientific community to pursue the development of tools for the investigation of spatiochromatic aspects of animal colouration at and beyond the retinal level. As a result, I have been engaging in efforts to develop community platforms, literature and collaborations across formerly ‘competing’ entities in the field of visual ecology in order to facilitate unified efforts and exchange of know-how.

The QCPA has opened many discussions and questions regarding the modelling of animal vision and the analysis of visual signals. A vast list of questions which await careful analysis across a range of visual systems and perceptual contexts. But QCPA didn’t just pose questions: we now have a valuable addition to a growing set of tools and methods that we can use to address some of these questions in ways which we previously couldn’t have.

Chapter 1
General Introduction

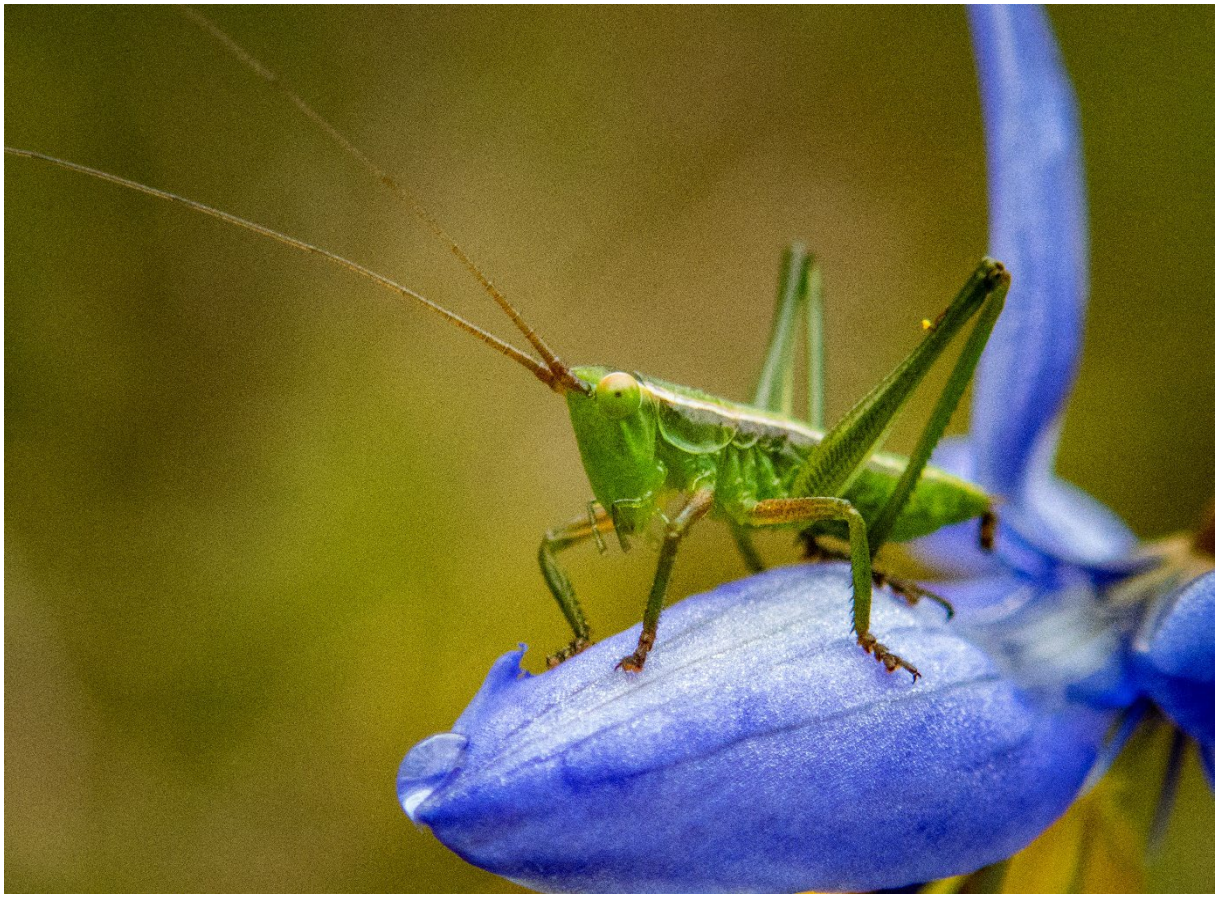

“For the rays, to speak properly, are not coloured”

- Newton, 1718

Chapter 1 - General Introduction

1.1 Preface

Animal colour patterns are complex and highly diverse morphological traits (Fig. 1.1A-F) that drive fundamental interactions between animals. They are used as signals in sexual selection, territorial defence, predator avoidance and social behaviour (Endler, 1978). The perception of colourful signals are influenced by the size and shape of colour pattern components, signaller behaviour, environmental parameters, as well as viewer physiology and psychology (Endler, 1978, 1990; Dawkins, 1993; Guilford & Dawkins, 1993; Renoult & Mendelson, 2019). The diversity of animal colour patterns are therefore thought to be the cumulative result of complex interactions and trade-offs, rather than a response to a single selective pressure (Endler, 1978; Merilaita, Lyytinen, & Mappes, 2001). Understanding these interactions and trade-offs is the key to understanding the design and evolution of animal colouration (Cott, 1940; Endler, 1978; Stevens & Merilaita, 2011; Stevens & Ruxton, 2012; Ruxton, Allen, Sherratt, & Speed, 2018). This thesis focuses primarily on fixed (permanently displayed and/or static) colour patterns and only secondarily on the perception of colour patterns in a temporal and/or motion context (but see Chapter 2). While not of primary concern in this thesis, colour patterns (pigments in general) can serve functions outside of visual signalling such as UV-protection (e.g. Tartarotti & Sommaruga, 2006), thermoregulation (e.g. Lindstedt, Lindström, & Mappes, 2009) or abrasion resistance (Cuthill et al., 2017), increasing the complexity of selective pressures acting on the evolution of colour patterns in nature.

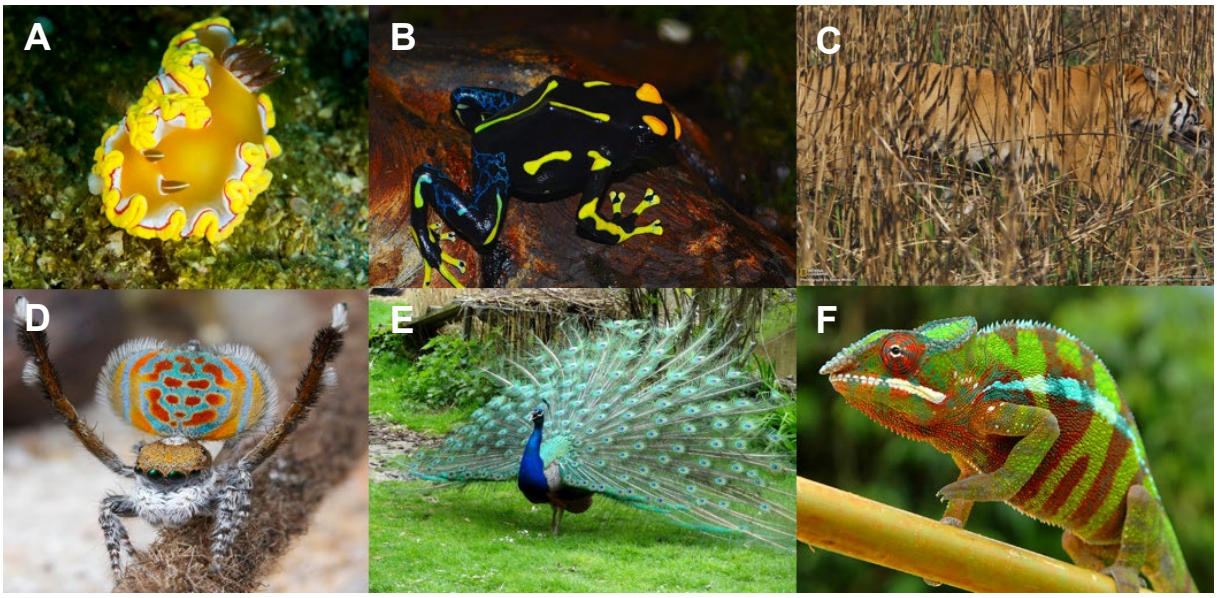

Figure 1.1: A) A nudibranch mollusc, and B) a poison dart frog displaying conspicuous warning colouration; C) A tiger using its stripes to hide in tall grass; D) A Peacock spider and E) a male peacock using conspicuous colour patterns for courtship displays; F) A chameleon, which can change colour for camouflage and signalling to conspecifics. Image credits: A) Cedric v. d. Berg, B) Christin Froehlich, C) Steve Winter, D) Juergen Otto, E) User 'Windydy' on deviantart.com, F) Thorsten Negro.

Colour patterns consist of multiple components: 1) brightness (Fig 1.2A), which refers to the perceived luminance of pattern elements; 2) chromatic properties such as hue (colour categories such as red or blue) (Fig 1.2B) and saturation (purity, or proximity to grey) (Figure 1.2D); and 3) the spatial alignment of colour pattern elements, which defines the geometry of the pattern (Fig 1.2C, E, F). All three components have strong implications for the functionality of an animal's colour pattern. I will first provide a brief review on colour, vertebrate colour vision, luminance, luminance vision and colour pattern geometry before discussing fundamental aspects of defensive animal colouration, as well as tools and methods available for their study.

1.2 Vertebrate Vision

To understand the selective forces shaping the evolution of animal colouration we require an understanding of animal visual systems. It is – with the exception of colours used in thermoregulation - these visual systems which signals emitted or obscured by animal colouration are targeting (Cronin, Johnsen, Marshall, & Warrant, 2014;

Stevens, 2016). All visual systems start the process of visual perception with the absorption of photons mediated by specialised neuronal cells, the photoreceptors (Land & Nilsson, 2012).

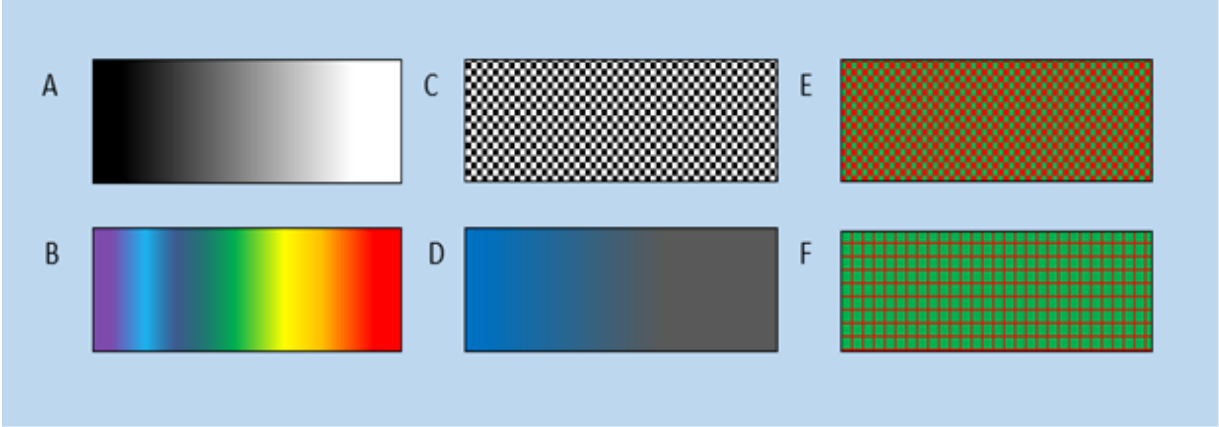

Figure 1.2: The four components of colour patterns. A) Luminance; B) hue; C) achromatic pattern; D) saturation; E) chromatic pattern; F) pattern with the same colours as E but different pattern. Note how the colours blend together to a different hue at distance despite identical colour composition.

There are two types of photoreceptor cells in vertebrate eyes: rods and cones. Most vertebrate eyes possess both in their retinas. Rods are designed for dim-light vision and extreme light sensitivity, and are often long and cylindrical (Cronin et al., 2014, Fig 1.3A). Cones are used in bright-light vision: they are relatively short with tapered sets of membrane (Fig. 1.3C) and are more finely tuned to a broader range of specific wavelengths than rods, which are usually maximally sensitive to light at around 500nm wavelength (Bowmaker, Heath, Wilkie, & Hunt, 1997; Hart, 2001b, 2001a; Cheney, Newport, McClure, & Marshall, 2013; Henze & Oakley, 2015; Marshall, Cortesi, de Busserolles, Siebeck, & Cheney, 2018). In vertebrates, rods and cones are usually distributed unequally across the retina leading to different visual properties in different parts of the visual field. A good example of this is the human retina with increased luminance contrast sensitivity in dim-light peripheral vision and peak colour contrast sensitivity and acuity at the fovea during daytime. These differences are due to a high abundance of cones at the fovea and rods at the periphery of the retina (Bruce, Green, Georgeson, & Dynan, 2010). However, similar retinal heterogeneity in rod and cone density can be found in many vertebrates (e.g. Hart, 2001; Dalton, de Busserolles, Marshall, & Carleton, 2017).

The absorption of photons is enabled by photopigments located in the outer segments of the photoreceptors (Fig. 1.3B & D). The photopigment itself is made up of the chromophore molecule and a covalently bound opsin protein, which determine the spectral sensitivity of a given photoreceptor (Loew, 1995; Yokoyama & Yokoyama, 1996). Initiated by a conformational change in the chromophore molecule a series of chemical processes is triggered, called the 'phototransduction cascade'. This process ultimately leads to the depolarisation of the photoreceptor cell and the subsequent emission of a neuronal signal (Pugh & Lamb, 2000).

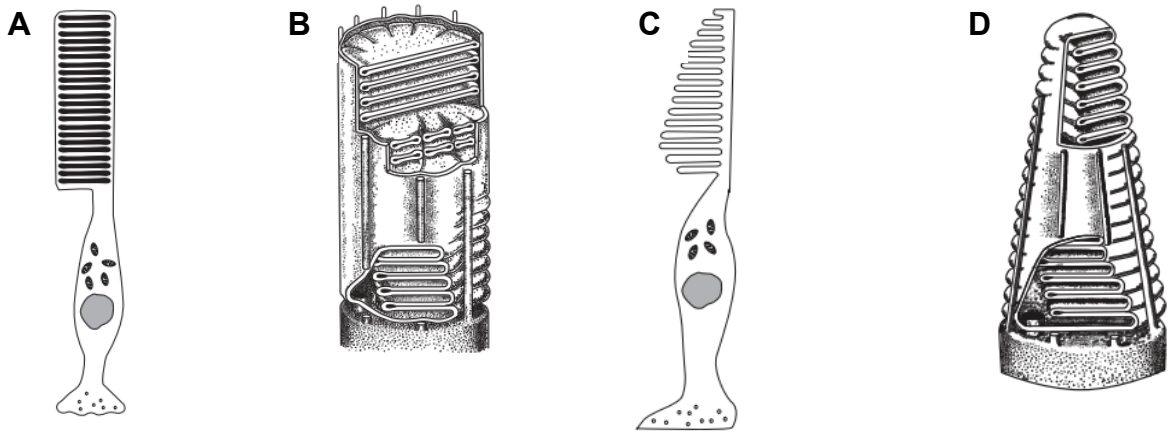

Figure 1.3: Schematic representations of a rod (A) and a cone (C) photoreceptor with their respective outer segments (B & D). Modified from Cronin et al., (2014).

1.2.1 Colour Vision

Colour vision is the ability to detect differences in light spectra based on their wavelength distribution (how much light is there at each wavelength), independent of light intensity. Colour vision has convergently evolved in both vertebrates and invertebrates and the ability of animals to perceive colours varies considerably between taxa (e.g. Marshall, Land, King, & Cronin, 1991; Briscoe & Chittka, 2001; Arrese, Hart, Thomas, Beazley, & Shand, 2002; Osorio & Vorobyev, 2008; Jacobs, 2009). To detect colour, vertebrate eyes need to have at least two different cone photoreceptors with different spectral sensitivities (Fig. 1.4).

Absorbed photons produce a retinal response which in turn enters a complicated neuronal circuit and is ultimately processed by the brain. At the earliest level of colour vision, the relative stimulation of photoreceptors, mediated by ON and OFF bipolar cells, are integrated by retinal ganglion cells into 'receptive fields' which

underlie colour, luminance and spatial vision (Cronin et al., 2014). The integration of signals from a population of upstream neurons reflecting a specific special arrangement is a common neurophysiological design principle that enables refined signal interpretation and modulation which features repeatedly throughout visual processing pathways (Bruce et al., 2010). The perception of colour in vertebrates largely depends on opponent processing of photoreceptor outputs (Kelber, Vorobyev, & Osorio, 2003, but see Shapley & Hawken, 2011). Opponent processing refers to the antagonistic (opponent) processing of separate colour pairs in distinct neural channels (Jameson & Hurvich, 1955; Wyszecki & Stiles, 2000, Fig. 1.5). The stimulation of opponent channels relative to each other subsequently determines the perceived hue & saturation of an object. However, photoreceptors have an intrinsic level of noise generated by stochastic excitation of the photopigments. Only when the stimulation of a photoreceptor is higher than the noise present is a signal leading to colour perception transmitted (Vorobyev & Osorio, 1998).

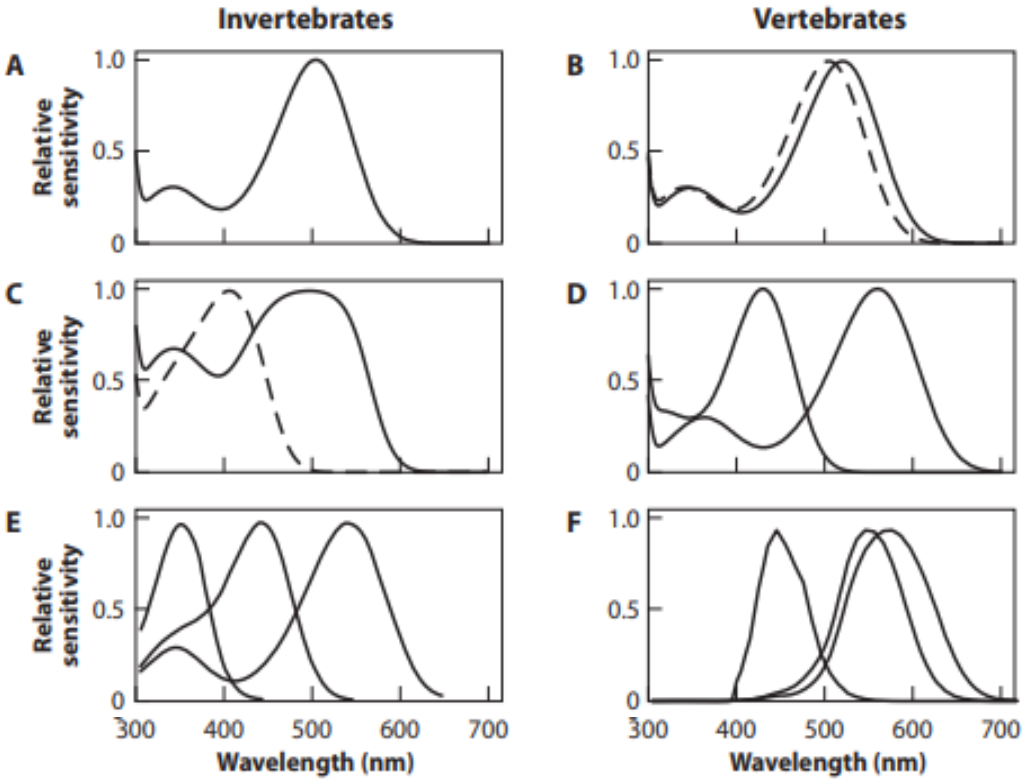

Figure 1.4: Varied spectral sensitivities of vertebrates and invertebrates. (A) Cuttlefish, *Sepia lessoniana*. (B) Dolphin, *Tursiops truncates* including the rod spectral sensitivity (dotted line), as this may be involved in color vision. (C) Shrimp, *Systellaspis debilis*. (D) Dog, *Canis familiaris*. (E) Honeybee, *Apis mellifera*. (F) Human, *Homo sapiens*. (modified from Cronin et al., 2014).

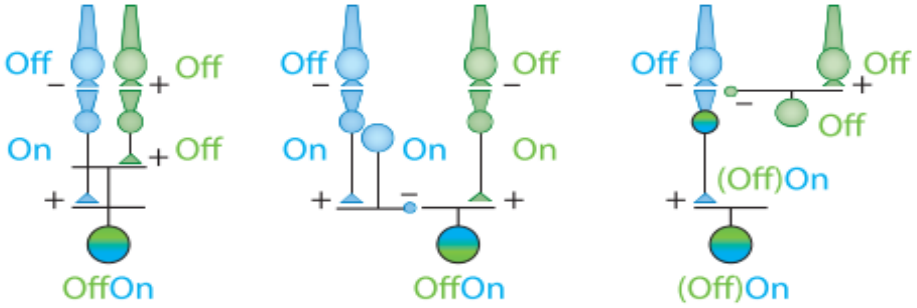

Figure 1.5: Three possible opponent processing circuit schema for a blue-green opponent circuit in mammal receptive fields. Modified from Baden & Osorio, (2019).

1.2.2 Luminance Perception

A significant amount of visual information is encoded by light intensity (luminance), irrespective of relative wavelength distribution (Fig. 1.6). Brightness refers to the perceived luminance of objects and surfaces whereas lightness refers to their perceived reflectance (for a review see Kingdom, 2011). Vertebrate eyes are thought to perceive brightness & lightness using either one or the cumulative output of single, as well as double cones (Macuda & Timney, 1999; Osorio & Vorobyev, 2005; Siebeck, Wallis, Litherland, Ganeshina, & Vorobyev, 2014). It is thought that luminance is widely used by animals to perceive spatial information and motion (Osorio, Mikló, & Gonda, 1999; Willis & Anderson, 2002; Osorio & Vorobyev, 2005). For example, primates use achromatic signals to identify the location, shape and motion of objects, as opposed to chromatic information, which is used to infer surface quality (Livingstone & Hubel, 1988). Evidence from across different vertebrates such as primates, birds and fish suggests that detection of fine spatial detail relies primarily on achromatic signals (Livingstone & Hubel, 1988; Osorio, Mikló, et al., 1999; Newport et al., 2017). Luminance contrast has been shown to constitute important parts of defensive animal colouration by modulating within-animal pattern contrast as well as animal-background contrast (Siddiqi, Cronin, Loew, Vorobyev, & Summers, 2004; Prudic, Skemp, & Papaj, 2007; Bradburry & Vehrencamp, 2011; Stevens & Merilaita, 2011; Ruxton et al., 2018).

Figure 1.6: A koala sitting on a tree: A) picture in colour, and B) picture with only luminance information (black and white). Note how much spatial information is still encoded when removing colour. Image by Cedric v. d. Berg.

The perception of achromatic information can be achieved by all visual systems and in photopic conditions is usually mediated by a specific class of photoreceptors, such as the medium or longwave sensitive cones (Whittle, 1986; Osorio & Vorobyev, 2008). In bees, the long-wavelength photoreceptors are thought to be responsible for luminance vision (Backhaus, 1991; Giurfa et al., 1997; but see Ng et al., 2018), while primates sum the output of the medium and long-wavelength sensitive cones (Whittle, 1986; Osorio & Vorobyev, 2008). Birds segregate achromatic and chromatic signals by allocating single cones to colour perception and use double cones in luminance perception (v. Campenhausen, Kirschfeld, Campenhausen, & Kirschfeld, 1998; Osorio, Mikló, et al., 1999; Osorio & Vorobyev, 2005). Fish may use individual or summed output of the medium or long-wavelength cones (Neumeyer, Wietsma, & Spekreijse, 1991; Siebeck et al., 2014); however, this is not clear.

1.3 Defensive Animal Colouration

The ability to see chromatic and achromatic visual information has led to visually guided predation being one of the key ecological processes in any given ecosystem. To reduce predatory attacks, prey species have evolved physical and behavioural defence mechanisms to reduce the likelihood of being preyed upon. Primary defences act before a predator initiates any interaction with the prey, whereas secondary defences act once a predator-prey interaction has commenced (Ruxton et al., 2018). Animal colour patterns can reduce the likelihood of detection (camouflage, e.g. Fig. 1.1C) or warn potential predators of the unprofitability of the prey (aposematism, e.g. Fig. 1.1A & B, Poulton, 1890). However, how the design of such colour patterns decreases the chances of predatory recognition (crypsis) or improves avoidance learning (aposematism) remains relatively unclear (Ruxton et al., 2018). Crypsis is a broad term that encompasses various functional sub-categories, and it is important to differentiate between the strategies that aim to avoid detection (camouflage) (e.g. Fig. 1.8), and the ones aiming at avoiding recognition, namely masquerade and mimicry (Fig. 1.7, Stevens & Merilaita, 2011).

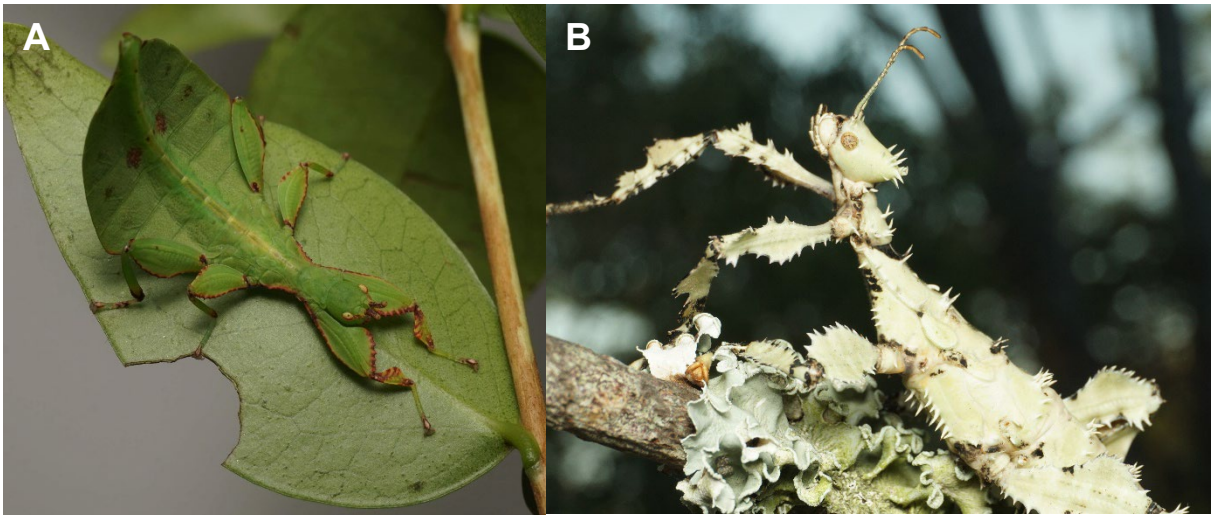

Figure 1.7: A) An Australian leaf insect (*Phyllum monteithi*) masquerading as a leaf. B) A spiny stick insect (*Extatosoma tiaratum*) masquerading as lichen on a stick. Images courtesy of Jessa Haley Thurman.

1.3.1 Crypsis through Background Matching

A color pattern is cryptic if it 'resembles a random sample of the background perceived by predators at the time and age, and in the microhabitat where the prey is most vulnerable to visually hunting predators' (Endler, 1978). This general need for similarity between animal and background holds for pattern, chromatic and luminance contrast, as any one of them can be used to set an object apart from its background and make it detectable (Endler, 1978). The need for a general resemblance to a visual background is intuitive, for example when looking at a moth (*Hypomecis roboraria*) camouflaging against tree bark (Fig. 1.8A) or a southern leaf-tailed gecko *(Phyllurus platurus)* (Fig. 1.8B). While explaining a key functional element of camouflage, Endler's definition of crypsis holds true for background matching, however it does not adequately incorporate the importance of additional cryptic colouration design principles which I briefly introduce in subsequent sections.

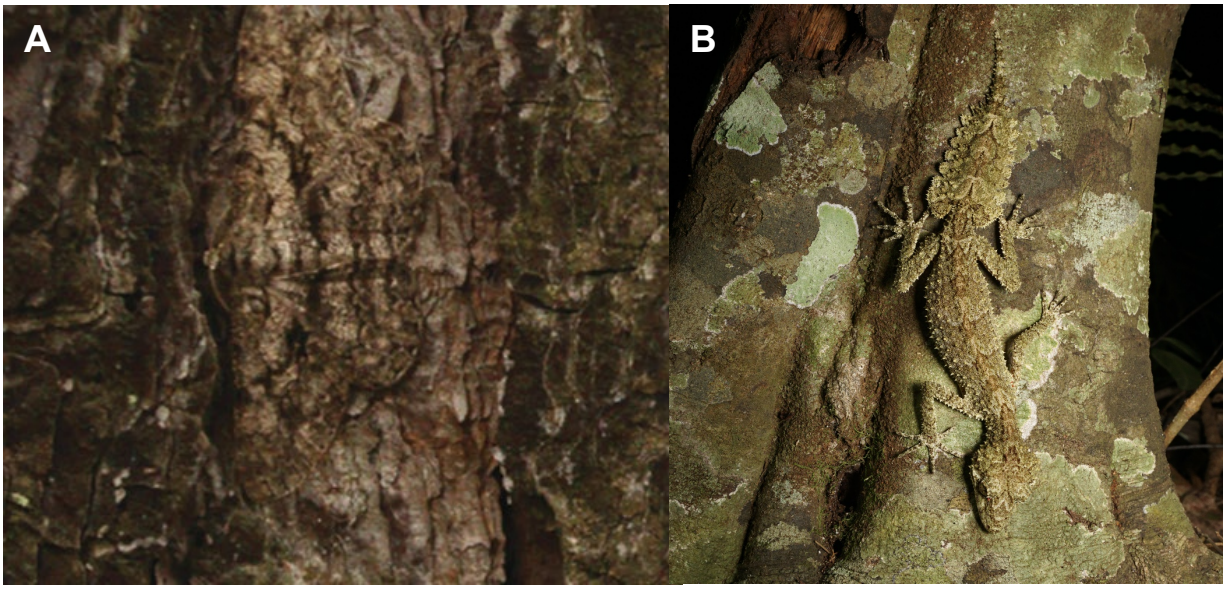

Figure 1.8: A) A moth (*Hypomecis roboraria*) resting on tree bark. The animal is almost perfectly camouflaged, largely due to its pattern, luminance and colour matching the visual background. Modified from Kang, Stevens, Moon, Lee, & Jablonski, (2015). B) A southern leaf-tailed gecko (*Phyllurus platurus*) matching the colour and pattern of a tree it camouflages against. Image courtesy of Jessa Haley Thurman.

1.3.2 Disruptive Colouration

Background matching through average resemblance to a background (Fig. 1.8) does not necessarily increase the protective value of an animal colour pattern because the

outline of an animal could set it apart from its background (Thayer, 1909; Cott, 1940). Edge detection plays a crucial role in object detection and recognition; therefore, patterns that break up the outline of the general animal body shape or body parts (Fig. 1.9) help in achieving camouflage. Disruptive colouration is especially effective if:

(i) pattern elements are more contrasting inside the animal than between the animal and its background;
(ii) contrast between animal pattern elements bordering the background is minimised;
(iii) pattern elements randomly create a sense of continuation between background and animal by being disrupted by the edge of an animal's body shape (Stevens & Cuthill, 2006; Endler, 2012).

Despite compelling theoretical arguments for the function of disruptive colouration in nature, only recently have studies provided empirical evidence to highlight its role in protective animal colouration (reviewed by Ruxton et al., 2018). There is supporting evidence that most animals, including insects, birds, mammals, fish, reptiles, amphibians, crustaceans and cephalopods use disruptive colouration to reduce predation risk (Cott, 1940; Cuthill & Székely, 2009; Stevens & Merilaita, 2011; Stevens, 2016; Ruxton et al., 2018).

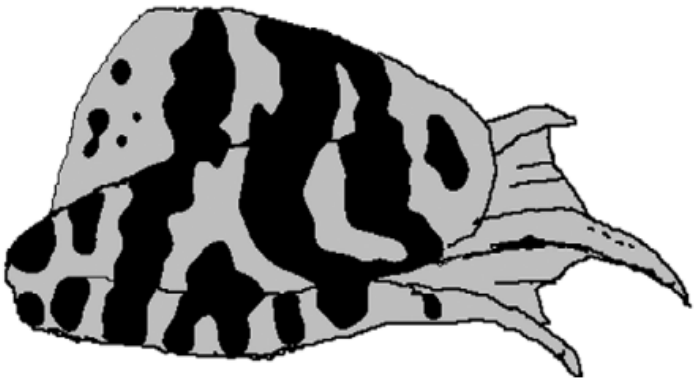

Figure 1.9: The leg of a frog (*Rana temporaria*) displaying disruptive patterning to obscure the outline of the limb (modified from Cuthill & Székely, 2009; originally drawn by Cott, 1940)

1.3.3 Aposematism

Aposematism describes the use of conspicuous signals by animals to advertise some form of secondary defence, such as toxicity or distastefulness (Poulton, 1890). For example, nudibranch molluscs have been shown to use highly conspicuous colour patterns in combination with potent chemical defences to defend themselves (Fig. 1.10). Other prominent examples of aposematic animals include frogs (e.g Summers & Clough, 2001; Dugas, Halbrook, Killius, del Sol, & Richards-Zawacki, 2015), moths (e.g. Honma, Mappes, & Valkonen, 2015; Henze, Lind, Mappes, Rojas, & Kelber, 2018) and snakes (e.g. Mochida, Zhang, & Toda, 2015; Rajabizadeh, Adriaens, Kaboli, Sarafraz, & Ahmadi, 2015). To what extent different components of a colour pattern contribute to the protective value of an aposematic signal remains largely unclear. While experiments using birds and fish seem to indicate that colour seems to play a more important role in the learning of aposematic signalling than pattern or luminance (Roper & Wistow, 1986; Cook & Roper, 1989; Osorio, Jones, & Vorobyev, 1999; Newport et al., 2017), there is still little empirical knowledge on how colour, pattern and luminance contribute to aposematism in its ecological context (Stevens, 2015). Most of the work done in this area makes use of comparably simple stimuli in experimental setups focusing on individual pattern components such as colour contrast or highly simplified artificial patterns (Osorio, Jones, et al., 1999; Dimitrova & Merilaita, 2010; Aronsson & Gamberale-Stille, 2013) but very few studies investigate complex multicomponent animal colour patterns in a complex natural or nature-like context.

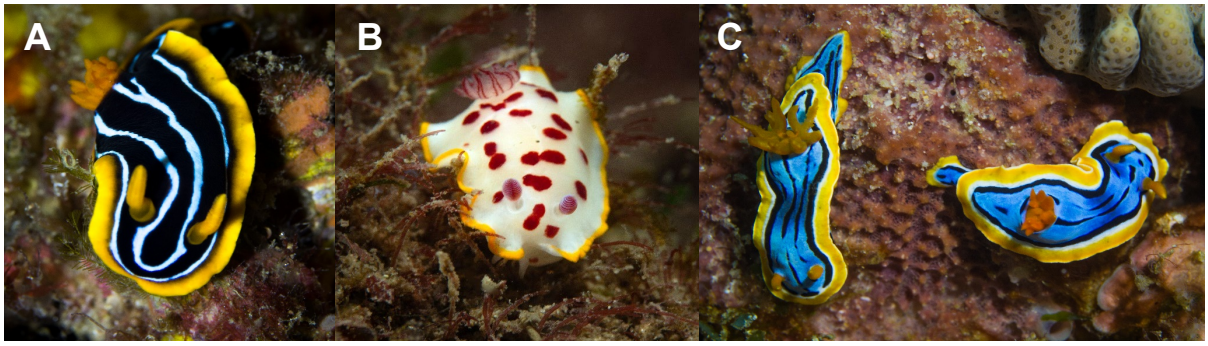

Figure 1.10: Various sympatric nudibranch molluscs from south-east Queensland, Australia, displaying bright colour patterns in combination with storing defensive chemicals. Note the commonly shared yellow rim across species. A) *Chromodoris kuiteri*, B) *Goniobranchus splendidus*, C) *Chromodoris elisabethina*. Images by Cedric v.d.Berg.

1.4 Considering Defensive Colouration in an Ecological Context

The signalling properties of animal colour patterns depend on the viewing conditions and the properties of a viewer's visual system (Endler, 1978). Visual signals are modulated by environmental factors such as the background against which they are displayed (Fig. 1.11) and the lighting conditions as well as the transmission properties of the medium (Endler, 1990; Dimitrova & Merilaita, 2010). Therefore, understanding the evolution and design of animal colour patterns requires careful consideration of both the conditions under which visual signals are displayed, and the vision of the intended signal receiver (Endler, 1990, 1993; Endler & Mielke, 2005; Johnsen & Mobley, 2012).

Most publications on the ecology and evolution of animal colour patterns acknowledge the importance of the ecological context under which colour patterns are displayed. However, very few simultaneously analyse colour, luminance and geometry contrast within animals and between animals and the background they are viewed against (but see Troscianko *et al.*, 2016) while also considering the physiology of a viewer under natural light conditions. This likely leads to a lack of understanding of the ecological function of animal colour patterns and subsequently their design and evolution.

Figure 1.11: *Bitis rhinoceros*, West African Gaboon viper: (a) the snake partly on white background and (b) partly on background similar to the natural habitat. Note how the cryptic colour pattern only works in the context of the background. From Spinner et al., (2013).

For example, while camouflage and aposematism represent somewhat opposing principles of animal colouration by either promoting or avoiding conspicuousness, there is increasing evidence that they can co-occur within a single colour pattern. In fact, animal colouration can often appear both highly conspicuous as well as cryptic, depending on the context (Caro, Sherratt, & Stevens, 2016). For example, a parrot fish -a very common and colourful reef fish - appears highly conspicuous at close range, displaying a variety of bright and highly saturated colour patches. However, when disappearing into the distance, those colour patches merge together to produce a perfect match to the blue background of the more distant reef (Marshall, 2000). Distance dependant switching from aposematism to crypsis was also shown in swallowtail butterfly larvae (*Papilio machaon*) (Tullberg, Merilaita, & Wiklund, 2005).

Another example highlighting the context dependence of defensive animal colouration was found in the tiger moth (*Parasemia plantaginis*). The animal usually displays black white and orange wings which are conspicuous when viewed against its natural background. However, when attacked the moths feign death by dropping to the ground and against this new background, the same colour pattern now provides camouflage (Honma et al., 2015). Similarly, Barnett and Cuthill (2015) demonstrated that such distance-dependent or dual function patterns improved the survival rate of artificial prey (Barnett & Cuthill, 2015; Barnett, Scott-Samuel, Cuthill, & Barnett, 2016).

1.5 Tools & Methods for the Study of Colour Patterns

The development of technology used to study how animals perceive visual information over the last three decades, including the use of spectrophotometry, digital photography, high-end computation, visual modelling and innovative behavioural experiments, has improved our capacity to investigate selective pressures driving the design of animal colouration (Endler, 1978, 1990; Alatalo & Mappes, 1996; Vorobyev & Osorio, 1998; Stevens, Parraga, Cuthill, Partridge, & Troscianko, 2007). However, many mechanisms shaping the evolution of animal colour patterns remain comparably understudied. Indeed, this is attributable to the lack of suitable analytical frameworks for comprehensive and thorough animal colour pattern analysis (Stevens & Merilaita, 2011; Endler, 2012; Stevens & Ruxton, 2012; Ruxton et al., 2018).I will give a brief

summary of commonly used methodology for the analysis of animal colour patterns to outline key properties and limitations of current analytical frameworks.

1.5.1 Colour Contrast

Measurements of spectral reflectance, obtained via a spectrophotometer, are used to determine colour contrast. There are two forms of colour contrast measured: that within an animal's own colour pattern (for example, the contrast between a black and blue stripe) and that between an animal and its background (such as the substrate). Spectral reflectance measurements are then used to calculate the Euclidian distance between the modelled perceived colours in perceptual colour spaces (Renoult, Kelber, & Schaefer, 2017, Fig. 1.12). The "Receptor Noise Limited" (RNL) model (Vorobyev & Osorio, 1998) is the most commonly used visual model for the measurement of colour contrast in vertebrates. It has been shown to accurately model colour contrast and associated colour discrimination thresholds in a range of organisms such as insects, birds, fish and reptiles (Endler & Mielke, 2005; Martin Schaefer et al., 2007; Spottiswoode & Stevens, 2010; Chen, Stuart-Fox, Hugall, & Symonds, 2012; Champ, Vorobyev, & Marshall, 2016).

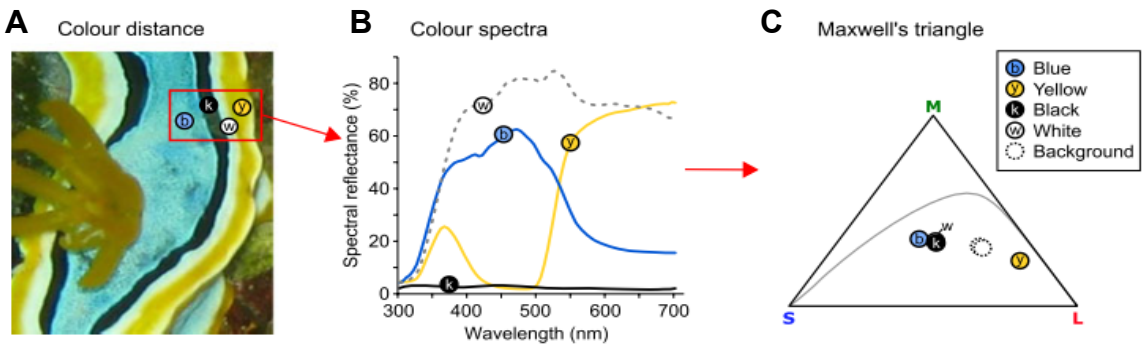

Figure 1.12: A) The colour pattern on a nudibranch mollusc B) Spectral reflectance curves obtained using a spectrophotometer C) The corresponding colours plotted in colour space. The background measurement refers to the substrate. The perceptual distance is then calculated using the RNL model (figure from Cheney et al., 2014).

1.5.2 Luminance Contrast

Increasingly, the RNL model is also being used to measure luminance discrimination contrasts (Siddiqi et al., 2004). However, the RNL model was originally developed to

estimate colour discrimination thresholds. Its common use in the literature to also estimate luminance discrimination thresholds has not been verified behaviourally, with the exception of birds (Spottiswoode & Stevens, 2010). Traditional methods of describing pairwise luminance contrasts such as the Michelson and Weber contrast indices, describe luminance contrast in the context of absolute brightness of a scene (Bex & Makous, 2002; Chiao, Chubb, & Hanlon, 2007). However, unlike the RNL model, they do not imply discrimination thresholds based on associated receptor noise and receptor abundance in the retina of a viewer.

1.5.3 Pattern Analysis

There are a variety of techniques to quantify spatial pattern contrast, although Fourier transform based approaches are most often seen in the literature (Godfrey, Lythgoe, & Rumball, 1987; Stoddard & Stevens, 2010; Cheney et al., 2014). Fourier transform analysis transforms the spatial frequencies of colour patterns into power spectrum curves (Fig. 1.13). This determines the difference between images, or components of images according to the relative distribution of spatial frequencies (Field, 1987). This method incorporates mechanisms of early post-retinal neuronal processing and has been widely used to quantify pattern contrast in terms of spatial frequencies (Stevens & Merilaita, 2011). There are a few alternative examples of colour pattern analyses such as ‘distance transform’ (Taylor, Gilbert, & Reader, 2013), adaptations of feature congestion analyses (Xiao & Cuthill, 2016) or variants of ‘Scale Invariant Feature Transform’ (SIFT) (Lowe, 1999). However, Fourier transform based approaches remain by far the most frequently used in the study of animal colour patterns.

Studies using spatial frequency analyses often do not filter the visual information in the image according to the visual limitations of ecologically relevant viewers, such as predators. Furthermore, Fourier transform based pattern analyses have a limited ability to differentiate and parameterise colour patterns and their components. This is because they are designed to quantify the similarity of spatial frequency distributions but not to parameterise colour pattern geometry such as describing the shape and relative position of elements inside patterns. Furthermore, a recent study found that Fourier transform based pattern contrast analysis did not predict detection rates in human subjects viewing artificial prey on complex backgrounds, suggesting that it may not be an effective predictor of pattern contrast (Troscianko, Skelhorn, & Stevens,

2017). However, these drawbacks do not mean that Fourier transform based pattern analyses do not have their purpose in the analysis of spatial properties of visual signals, but rather that there are substantial limitations to them.

To date, the study of animal visual signals has been limited by the absence of a comprehensive 'spatiochromatic' analysis. Such an analytical framework is required to provide an all-inclusive description of a signal by accounting for luminance contrast, colour contrast, pattern geometry, the environment of the animal and the visual systems of relevant viewers. In this way, the analysis produced would provide a more complete measure of the conspicuousness or inconspicuousness of a signal as well as a differentiated description and measure of colour patterns and their components, as perceived by ecologically relevant signal receivers (Endler, 1991, 2012; Endler & Mielke, 2005; Stevens & Merilaita, 2011; Veale, Hafed, & Yoshida, 2017).

1.5.4 Visual Contrast and Colour Adjacency Analysis

The concept of a spatiochromatic analytical framework for the analysis of colour patterns in nature goes back almost 40 years (Endler, 1978). Endler's visual contrast analysis (Endler, 1991; Endler & Mielke, 2005) and the "Colour Adjacency Analysis" (Endler, 2012) represent an important step towards the development of such comprehensive parametric colour pattern analyses.

1.5.5 Visual Contrast Analysis

To quantify the conspicuousness of animal colour patterns, Endler combined the measurement of spatial and chromatic, as well as achromatic components of animal colour patterns into parameters approximating their contribution to the potential conspicuousness of an animal. The contribution of a colour pattern element towards the average hue, saturation and brightness is proportional to the relative area of the pattern element and its contrast to the other colour pattern elements inside the animal (Endler, 1991). In a first step, the mean brightness of an animal colour pattern can be calculated by summing the individual cone capture quanta of each pattern element. Mean hue and saturation of a colour pattern can be expressed by summing the respective property of each colour pattern element after weighting by relative spatial abundance.

The visual contrast of a colour pattern is proportional to the absolute level of variation for a given pattern component (hue, saturation, brightness) considering the relative spatial abundance and chromatic as well as achromatic properties of the individual colour patches within the pattern (Endler, 1991; Bex & Makous, 2002; Endler & Mielke, 2005; Arenas, Troscianko, & Stevens, 2014; Shepard, Swanson, McCarthy, & Eskew, 2016). Thus, by calculating the standard deviation for the weighted colour pattern elements proxies for visual colour pattern contrast can be obtained regarding hue, saturation and brightness. For example, these statistics have been shown to be able to explain up to 70% of female guppy mate choice variance (Endler & Houde, 1995).

1.5.6 Colour Adjacency Analysis

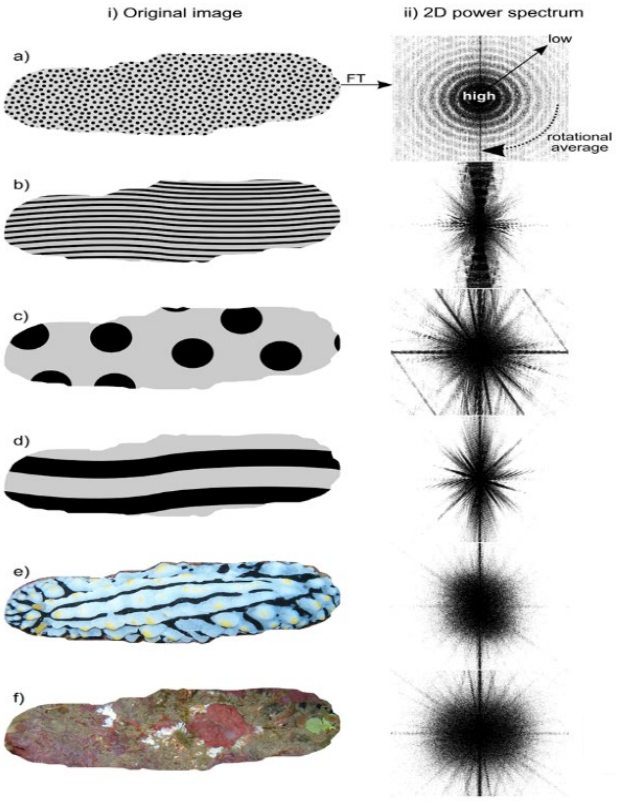

Figure 1.13: The spatial frequency analysis of 6 simulated and real example images. Each image (i) is analyzed using a two-dimensional Fourier transform (ii), which is then rotationally averaged to produce a one-dimensional power spectrum. The simulated images (a-d) contain strict periodic patterns, which produce clear peaks and troughs in the frequency analysis. In contrast, more natural scenes (e-f) contain a wider distribution of frequencies, and therefore exhibit smoother power spectrum relationships. Modified from (Cheney et al., 2014)

The colour adjacency analysis accounts for colour pattern adjacency while providing highly differentiated parametric colour pattern geometry analysis based on the distribution of colour and luminance in two dimensional space (Endler, 2012). The

fundamental principle of the colour adjacency analysis is the sampling of digital images along vertical and horizontal transects. Prior to the sampling process a digital image gets clustered into colour and luminance classes based on their RGB values. Along a sampling transect the identity of a sampled pixel is registered and the transitions between pixel classes summarized in a matrix. Statistical sampling of the transition matrix then allows the derivation of parameters such as pattern complexity, average colour patch size, aspect ratio and many more, describing the detailed geometrical properties of the colour pattern (Fig. 1.14 A-F).

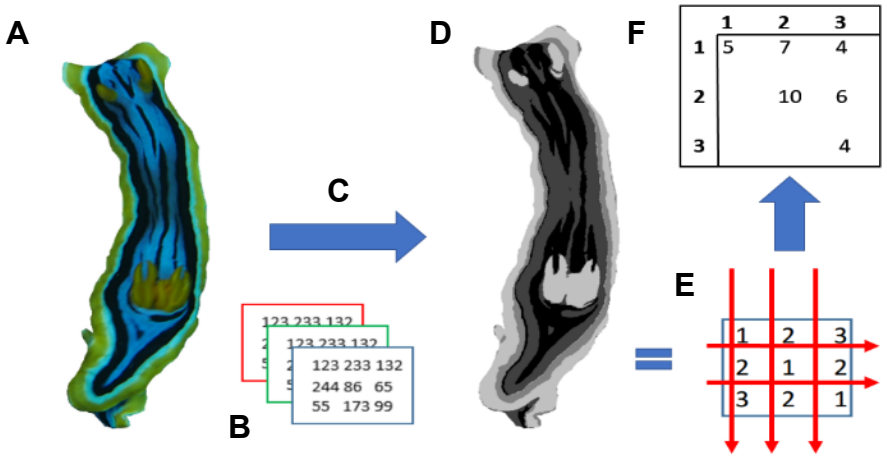

Figure 1.14: Schematic process of the adjacency analysis. A) An 8-bit RGB image of a nudibranch mollusc; B) Schematic representation of 8-bit 3D RGB image matrix; C) Clustering of pixels per proximity of RGB triplets into zone map D) Grey scale representation of the resulting zone map; E) Schematic of the zone map showing cluster IDs. Red arrows indicate the sampling of the zone map; F) Resulting transition matrix.

1.5.7 Quantitative Limitations

To determine how a colour pattern will appear to a viewer, the spatial acuity of species, and both their colour and luminance discrimination thresholds, should be incorporated in the pattern analysis, as well as ecologically relevant viewing conditions (distance, turbidity, light, angle, etc.). Furthermore, the analysis should measure the contrast of the animal's signal against natural backgrounds.

This has been limited by the availability of suitable technology for determining colour and luminance contrast on a quantitatively suitable level. Spectrophotometry has been, traditionally speaking (before early 2016, the start of this thesis), the most

common method of acquiring measures of colour and luminance contrast as perceived by non-human observers. However, spectrophotometry is unsuitable for quantitatively sampling complex visual scenes which requires thousands or hundreds of thousands of point samples (Stevens et al., 2007; Stoddard & Stevens, 2010; Troscianko & Stevens, 2015). However, a spectrophotometer can only ever acquire a single point measurement at a time, making the acquisition of suitably large sampling efforts near impossible. Therefore, colour pattern analysis incorporating animal vision has long been limited to simple animal colour patterns and backgrounds. Another solution is the use of hyperspectral cameras (cameras able to resolve narrow bandwidth data, i.e. taking a pixel measurement every 5nm, as opposed to multispectral imaging using digital cameras, which is only taking a few measurements across the electromagnetic spectrum) (Long & Sweet, 2006; Russell & Dierssen, 2015). However, hyperspectral cameras are extremely expensive and suffer from several drawbacks for the study of animal colouration, such as temporal and spatial resolution as well as weight and lack of robustness.

Some studies have tried to overcome this obstacle by using digital photography to estimate spectral reflectance curves in natural scenes using software like “Colourworker” (Osorio & Anderson, 2007). However, this approach is not widely used and suffers from the comparably poor quality of estimated spectral reflectance curves. The use of digital photography for visual modelling goes back more than a decade (Párraga, Troscianko, & Tolhurst, 2002; Stevens et al., 2007). However, the quality and affordability of digital cameras have increased significantly within the last decade. Troscianko & Stevens (2015) subsequently published an open-source ImageJ package which incorporated an intuitive software suite, the “Multispectral Image Calibration and Analysis Toolbox” (MICA) allowing for the reliable estimation of photoreceptor stimulation from calibrated digital images.

1.6 Specific Aims and Thesis Outline

The overarching aim of this thesis was to overcome current limitations in the study of defensive animal colouration. Over the past few years, I have developed a comprehensive methodology for the study of colour patterns (Chapter 2). The newly developed methodology and insights from behavioural experiments was then applied to the study of defensive colouration in nudibranch molluscs with the aim to increase

our understanding of the selective pressures shaping the design, function and evolution of defensive animal colouration (Chapter 3). I subsequently wanted to deepen our understanding of animal vision, calibrate parameter choices for colour pattern analysis and test the suitability of currently available tools and methods for visual modelling by conducting a series of behavioural experiments with trichromatic reef fish, the Picasso or lagoon triggerfish (*Rhinecanthus aculeatus*) (Chapter 4).

1.7 Significance

I have spent a large part of my time as a PhD student developing the Quantitative Colour Pattern Analysis (QCPA). The QCPA is of significance for a variety of reasons. First, it provides the first unified framework for the quantitative study of animal colouration. QCPA creates a coherent workflow merging the modelling of formerly independent aspects of animal vision, the detailed analysis of visual information and its visualisation. This allows researchers to approach the study of colour patterns in nature at an unprecedented quantitative and qualitative scale. Second, the framework introduces a range of novel tools and methods which provide exciting solutions to vision modelling as well as the analysis and visualisation of visual data. These new tools provide a range of future research directions aiming at increasing our understanding of animal vision and subsequent vision modelling.

Second, the QCPA is designed to bring down barriers for researchers in multiple ways. The framework is entirely open-source and free while being designed to use readily accessible and cheap hardware. Furthermore, the QCPA has been seamlessly integrated into the MICA toolbox, providing a user-friendly and dynamic work environment while profiting from synergies with - and access to - an already existing range of powerful tools and analyses in both the ImageJ and the MICA toolbox. The QCPA also provides a detailed discussion of currently existing tools for the modelling of animal vision and colour pattern analyses further assisting researchers to find the right methods for their research questions. It is further supplemented by an exceptional amount of supporting information as well as user and community support in the form of an interactive online platform.

Third, the development of the framework has greatly contributed to a growing sense of community and collaboration across research groups and institutes in the

field. It has significantly contributed to discussions and research focusing on the study of colour patterns in nature and will likely continue to do so, especially since its publication in December 2019.

The study of the defensive colouration of nudibranch molluscs (Chapter 3) has seen the first case of visual modelling using an underwater application of calibrated digital photography to obtain images of animals in their natural habitat, while highlighting the powerful abilities of the QCPA for the first time. This study has greatly contributed to the growing importance of nudibranch molluscs as a key model organism for the study of defensive animal colouration while providing important insights into the selective pressures underlying the evolution of nudibranch colour patterns.

Behavioural experiments conducted for Chapter 4 have significantly contributed to our understanding of luminance contrast perception by trichromatic reef fish while greatly informing the use of currently available methodology in visual modelling, including the QCPA and some of its components. It has also produced a broad range of questions and future research aiming at investigating the importance of perceptual context on animal vision and the development of new approaches for adjusting visual modelling to these insights while revealing crucial considerations for the design of behavioural studies aiming at investigating psychophysical properties of animal vision.

Chapter 2

Quantitative Colour Pattern Analysis (QCPA): A Comprehensive Framework for the Analysis of Colour Patterns in Nature

“Pattern recognition algorithms revolutionizing analyses of pattern and motion should be the next target of investigation”

The Biology of Color - Cuthill et al., (2017)

Chapter 2 - Quantitative Colour Pattern Analysis (QCPA): A Comprehensive Framework for the Analysis of Colour Patterns in Nature

2.1 Abstract

To understand the function of colour signals in nature, we require robust quantitative analytical frameworks to enable us to estimate how animal and plant colour patterns appear against their natural background as viewed by ecologically relevant species. Due to the quantitative limitations of existing methods, colour and pattern are rarely analysed in conjunction with one another, despite a large body of literature and decades of research on the importance of spatiochromatic colour pattern analyses. Furthermore, key physiological limitations of animal visual systems such as spatial acuity, spectral sensitivities, photoreceptor abundances and receptor noise levels are rarely considered together in colour pattern analyses.

In this chapter, a novel analytical framework is presented, called the 'Quantitative Colour Pattern Analysis' (QCPA). Many quantitative and qualitative limitations of existing colour pattern analyses have been overcome by combining calibrated digital photography and visual modelling. This work has integrated and updated existing spatiochromatic colour pattern analyses, including adjacency, visual contrast and boundary strength analysis, to be implemented using calibrated digital photography through the 'Multispectral Image Analysis and Calibration' (MICA) Toolbox. This combination of calibrated photography and spatiochromatic colour pattern analyses is enabled by the inclusion of psychophysical colour and luminance discrimination thresholds for image segmentation, which we call 'Receptor Noise Limited Clustering', used here for the first time. Furthermore, QCPA provides a novel psycho-physiological approach to the modelling of spatial acuity using convolution in the spatial or frequency domains, followed by 'Receptor Noise Limited Ranked Filtering' to eliminate intermediate edge artefacts and recover sharp boundaries following smoothing. A new type of colour pattern analysis is presented, the 'Local Edge Intensity Analysis' as well as a range of novel psycho-physiological approaches to the visualisation of spatiochromatic data. QCPA combines novel and existing pattern analysis frameworks into a unified, free and open source toolbox and introduces a range of novel analytical and data-visualisation approaches. These analyses and tools

have been seamlessly integrated into the MICA toolbox providing a dynamic and user-friendly workflow.

Keywords: animal colouration, colour pattern analysis, colour perception, colour space, image analysis, receptor noise limited model, visual modelling

2.2 Introduction

Animal colour patterns are complex traits which serve a multitude of purposes, including defence against predators (such as camouflage and aposematism), social signalling and thermoregulation (Cott, 1940). How colour patterns are perceived by animals is unique to a given visual system in a specific context. It depends on the visual background against which they are viewed, the visual capabilities of the signal receiver, the distance from which the pattern is viewed and the ambient light environment (Endler, 1978; Lythgoe, 1979; Endler, 1990; Merilaita, Lyytinen, & Mappes, 2001; Cuthill et al., 2017). Animal visual systems are diverse, and vary in eye shape and size, visual pigment number and absorbance maxima, photoreceptor type and number, and retinal and post-retinal processing (Lythgoe, 1979; Cronin et al., 2014). When determining the perception of colour patterns in other animals, it is therefore essential to consider spatial acuity (and viewing distance) as well as colour and luminance discrimination abilities (Endler, 1978). Humans have greater spatial acuity and contrast sensitivity than most vertebrates, except for some birds (da Silva Souza, Gomes, & Silveira, 2011; Caves, Frank, & Johnsen, 2016). We also have a different number of receptor classes, and different spectral sensitivity ranges compared to many animals (Cronin et al., 2014). For example, most other mammals are dichromats (i.e. they have only 2 compared to our 3 cone types), while most birds, reptiles and some amphibians, spiders and fish possess an ultraviolet cone sensitivity and are probably tetrachromats (Osorio & Vorobyev, 2005, 2008; Cronin & Bok, 2016). Among invertebrates the number of receptor classes may exceed 10 (Cronin et al., 2014).

To examine the perception of visual signals by animals, studies generally measure colour, luminance and pattern characteristics (e.g. Marshall, Vorobyev, & Siebeck, 2006; Cortesi & Cheney, 2010; Zylinski, How, Osorio, Hanlon, & Marshall, 2011; Allen & Higham, 2013; Xiao & Cuthill, 2016). For example, colour (chromatic)

and luminance (achromatic) contrast is measured between colour patches within an animal, or between an animal and its background, and is calculated in terms of perceptual distances in colour space often using the Receptor Noise Limited Model (RNL) (Vorobyev & Osorio, 1998). This model assumes that the noise inside a given class of photoreceptors, in combination with their relative abundance and opponent colour processing mechanisms, is the fundamental limit of colour and luminance contrast perception. The relative stimulation of photoreceptors can then be used to map the perceptual distances between colour patches in colour space (reviewed by Renoult, Kelber, & Schaefer, 2017). These Euclidean, or geometric distances are expressed in terms of ΔS values (Vorobyev, Brandt, Peitsch, Laughlin, & Menzel, 2001; Siddiqi, Cronin, Loew, Vorobyev, & Summers, 2004). The model predicts that a 'Just Noticeable Difference' (JND) should be equivalent to ΔS = 1 if model conditions and assumptions are met (Vorobyev & Osorio, 1998). For quantifying the spatial properties of patterns, Fast Fourier Transform (FFT) analyses of pixel intensity in digital images (Switkes, Mayer, & Sloan, 1978), pixel or location dependent transition matrices (Endler, 2012) or landmark based pattern metrics are often used (Lowe, 1999; Troscianko et al., 2017; Van Belleghem et al., 2018).

These types of analyses aim to computationally reproduce the retinal (and early post-retinal) processing of visual information, but often investigate colour, luminance or pattern contrast in isolation. For example, Cheney et al. (2014) quantified the conspicuousness of nudibranch molluscs (marine gastropods) by measuring pattern contrast against their natural backgrounds using FFT on digital images. They then measured chromatic contrast (ΔS) between animal and background using point measurements obtained by a spectrophotometer. While useful for many studies of animal colouration, these individual analyses ignore the interaction of visual information at various perceptual stages, both at lower (i.e. ganglion cells) and higher level (i.e. visual cortex) stages of information processing (for discussion see Gegenfurtner & Kiper, 1992; Shapley & Hawken, 2011; Stevens & Merilaita, 2011; Rowe, 2013; Endler & Mappes, 2017; Ng et al., 2018; Ruxton et al., 2018). However, recent publications continue to highlight the need to use an integrated approach to consider visual information when investigating the perception, and therefore the design, function and evolution, of complex visual signals (Endler, 1978, 1984, 2012; Rowe & Guilford, 1999; Rowe, 1999, 2013; Osorio, Smith, Vorobyev, & Buchanan-Smith, 2004; Hebets & Papaj, 2005; Shapley & Hawken, 2011; Stevens & Merilaita,

2011; Dalziell & Welbergen, 2016; Endler & Mappes, 2017; Ruxton et al., 2018; Endler, Cole, & Kranz, 2018). For example, not only is the efficiency of visual signals dependent on the presence or absence of colours, but also how those colours are arranged in patterns (e.g. Endler & Houde, 1995; Troscianko et al., 2017; Green, Urquhart, van den Berg, Marshall, & Cheney, 2018; Sibeaux, Cole, & Endler, 2019b).

Existing methods for spatiochromatic colour pattern analysis (Endler & Mielke, 2005; Endler, 2012; Endler et al., 2018), which have recently been implemented by PAVO 2 (Maia, Gruson, Endler, & White, 2019), parameterise geometric or chromatic properties of colour patterns such as geometric complexity, regularity, hue and saturation. They also provide parameters which themselves are simultaneously shaped by both spatial and chromatic properties of a colour pattern, such as abundance weighted chromatic contrast measures. However, such analyses require segmented images, meaning images in which the individual colour patches are delineated. Therefore, they are only suitable for processing colour patterns and visual scenes which have very clear colour differences (sharp boundaries with high chromatic and/or achromatic contrast), so that spectral data can be collected easily from each colour patch. Alternatively, these methods would require a prohibitively large number of spectral measurements to be made from a scene containing typical levels of natural variation; even the lowest acuity receivers would require many thousands of points to be measured. Digital imaging is therefore ideally suited to this type of analysis, because each image can rapidly and non-invasively capture millions of point samples which can provide the necessary chromatic and spatial information. However, currently available image segmentation and processing techniques do not incorporate physiological and cognitive limitations of ecologically relevant viewers. Indeed, many approaches rely on manually drawing the outlines of colour pattern elements by a human observer or clustering algorithms using uninterpreted RGB information inside a digital image (Endler & Houde, 1995; Isaac & Gregory, 2013; Winters et al., 2017). Such approaches inevitably introduce some degree of anthropocentric (qualitative) as well as quantitative bias in interpreting animal colouration, unless the colours fall in clear classes and they have been checked and calibrated with a spectrometer or calibrated digital photography.

In this chapter, we offer a method to overcome these problems and present a user-friendly, open-source framework is presented, which is called ‘Quantitative Colour

Pattern Analysis' (QCPA). QCPA is a comprehensive approach to the study of the design and function of colour patterns in nature. It combines calibrated digital photography (Stevens et al., 2007), visual modelling and colour pattern analysis into an analytical framework that is seamlessly integrated into the 'Multispectral Image Calibration and Analysis Toolbox' (MICA) (Troscianko & Stevens, 2015). QCPA enables the use of existing, revised and newly developed colour pattern analyses on an unprecedented quantitative and qualitative scale. This is enabled by image segmentation using combined colour and luminance discrimination thresholds (RNL clustering) or naïve Bayes clustering (Appendix A, page 168) as well as improved modelling of visual acuity (RNL ranked filtering). Pattern analyses included in QCPA are colour adjacency analysis, visual contrast analysis and boundary strength analysis (Endler & Mielke, 2005; Endler, 2012; Endler et al., 2018), which we have expanded, adapted and revised. For example, local edge intensity analysis (LEIA), an extension to boundary strength analysis (Endler et al., 2018), is introduced, which allows for colour pattern edge intensity analysis approximating the scale of receptive fields (Marr & Hildreth, 1980; Cronin et al., 2014) of a visual system while not requiring a segmented image. QCPA provides the user with a freely adjustable network of image processing tools which can convert visual information into a highly descriptive array of numbers and representative figures which may be used to examine a variety of evolutionary, behavioural and ecological questions (Fig. 2.1). Potential applications of QCPA include (but are not limited to): background matching, disruptive colouration, polymorphism, mimicry, aposematism, sexual signalling, territorial signalling, thermoregulation and landscape analysis.

2.3 Materials and Methods

First, a brief description of the acquisition of calibrated digital images and theoretical visual modelling of the viewer is presented and then individual tools of the QCPA in more detail are described, including:

- **Modelling of spatial acuity**: using an adaptation of Fast Fourier transform or Gaussian filters;
- **Image smoothing and edge reconstruction**: using the receptor noise limited ranked filter;
- **Image segmentation**: using receptor noise limited clustering and naïve Bayes clustering;
- **Pattern analysis:** using adjacency, boundary strength, visual contrast analysis, local edge intensity analysis and particle analysis;
- **Data visualisation:** using ΔS edge intensity images, XYZ chromaticity images, RNL saturation images and colour maps in RNL chromaticity space.

Finally, the rich numerical output of QCPA is described that can be used to investigate the design, function and evolution of colour patterns in nature. Extensive additional technical details, a glossary are provided, including worked examples inAppendix A.

2.3.1 Step 1: Acquisition of calibrated digital images

Acquiring data suitable for analysing the spatiochromatic properties of a scene is the first requirement for implementing QCPA. The open-source and user-friendly MICA toolbox can be used to generate calibrated multispectral images and cone-catch images from almost any digital camera (Troscianko & Stevens, 2015). Cone-catch images model the photoreceptor stimulation of an animal for every pixel within an image, with additional support for ultraviolet (UV)-sensitive cameras when modelling the vision of species with UV sensitivity (Fig. 2.1 & 2.2) (Troscianko & Stevens, 2015). While hyperspectral cameras are, theoretically, also well-suited to this task (e.g. Long & Sweet, 2006; Russell & Dierssen, 2015), there are a number of limitations in their use including cost and image resolution. However, the QCPA framework can also be

used for the analysis of hyperspectral images. Precise instructions on how to obtain high quality calibrated image data are outlined in Troscianko & Stevens (2015).

The MICA toolbox provides its own growing set of image analysis tools (e.g. Troscianko et al., 2017) to which QCPA contributes. Importantly, MICA allows the user to model cone captures in response to any possible light environment. This is very useful as it allows one to observe visual scenes in one light environment (e.g. a flower in a field at noon on a cloudy day) and translate them to another light environment (e.g. the same flower but under a long-wavelength enriched clear-sky sunrise light spectrum). MICA also lets the user switch between spectral sensitivities and cone channels of different species if that information is available (e.g. the same flower observed by a bee in comparison to a bird). This function is increasingly used by a range of researchers to introduce animal colour vision to their colour pattern studies (e.g. Chan, Chang, Huang, & Todd, 2019). Species-specific information on spectral sensitivities is often hard to obtain. However, in many cases it is possible to overcome this by estimating spectral sensitivities using information from closely-related species (Kemp et al., 2015; Olsson, Lind, & Kelber, 2018).

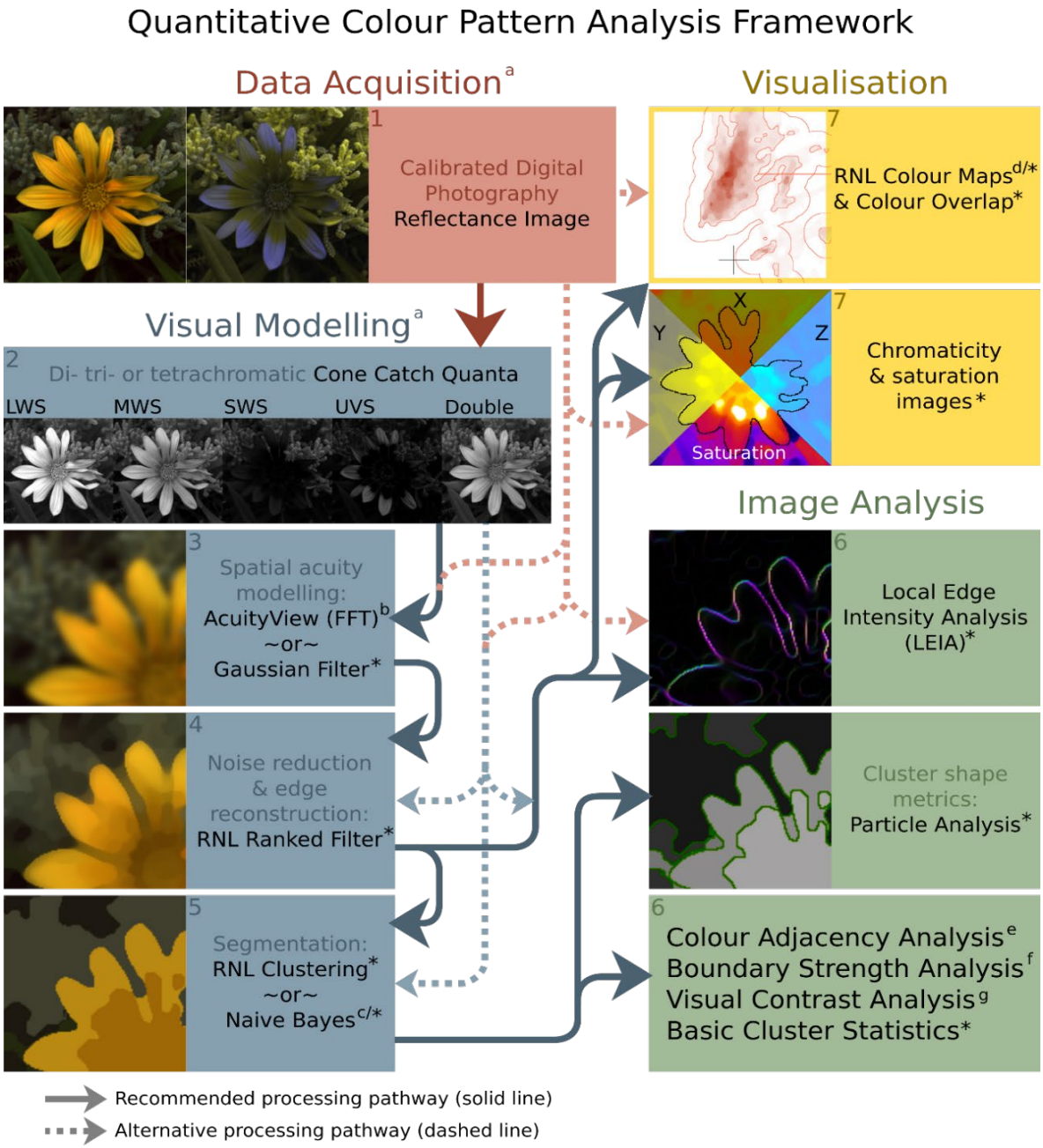

Figure 2.1: Schematic of the 'Quantitative Colour Pattern Analysis' QCPA framework. Asterisks (*) show steps in the framework which are novel or have been heavily adapted for use in this framework, while numbers refer to existing techniques. Cone-catch images are the input into the framework, which can be generated with the MICA toolbox (a Troscianko & Stevens 2015). Spatial acuity modelling is then used to remove visual information which would not be visible given the acuity and viewing distance (using either AcuityView 2.0, b Caves & Johnsen 2017, or a Gaussian convolution-based approach*). Acuity correction generates blurred images with intermediate colours that are not likely to be perceived by the receiver. The RNL ranked filter* is therefore used to recreate sharp boundaries. These images are ideal input for the local edge intensity analysis (LEIA)*, and for generating colour maps in RNL chromaticity space (*/d, Hempel De Ibarra et al., 2001; Kelber et al., 2003; Renoult et al., 2017). RNL clustering* or Naive Bayes clustering (*/c, Koleček et al., 2019) are then used to segment the image prior to colour adjacency analysis (e Endler 2012), boundary strength analysis (f Endler et al. 2018), visual contrast analysis (g Endler 1991; Endler & Mielke 2005), and particle shape analysis*. Numbers (1-7) indicate the corresponding sections (steps) in this document.

Figure 2.2: Example of multispectral image stacks as an output of MICA. Note that each image stack has a designated luminance channel layer needed for QCPA to allow inferences based on luminance discrimination thresholds.

2.3.2 Step 2: Defining discrimination thresholds

The chromatic (ΔS_C) and achromatic contrast (ΔS_L) within an image can be calculated as perceptual distance between any two pixels in 1 to *n*-dimensional colour space (Clark, Santer, & Brebner, 2017) using the RNL model (Vorobyev & Osorio, 1998) (as per Hempel de Ibarra, Giurfa, & Vorobyev, 2001 for chromatic contrast, and Siddiqi et al., 2004 for achromatic contrast). In its current state, QCPA uses the RNL equations for bright light (photopic) conditions (see discussion section of this paper for variations of the RNL). These contrasts can then be used to remove pixel noise (fluctuations in pixel intensity due to noise in the camera sensor) from a digital image, as well as for its segmentation into colour patterns. Species specific data on visual systems (particularly receptor noise) can be difficult to obtain (But see Olsson, Lind, & Kelber, 2015). This often results in model parameters being estimated. In combination with deviations from assumptions of the RNL model (Vorobyev & Osorio, 1998) this emphasizes the need to validate discrimination thresholds and model parameter choices using behavioural experiments or choosing conservative thresholds (Olsson et al., 2018).

QCPA tools using the RNL model should be used with caution for animals that may lack colour opponent processing (Thoen, How, Chiou, & Marshall, 2014) or opponent processing that potentially differs substantially from RNL model assumptions (e.g. Rocha, Saito, Silveira, De Souza, & Ventura, 2008). However, QCPA provides alternative image segmentation tools and pattern statistics particularly designed for these instances (pages 129 -154 and page 164 in Appendix A).

2.3.3 Step 3: Modelling of spatial acuity

The ability of an animal to resolve patterns depends on the spatial acuity of its vision, which may be determined through anatomical, behavioural or physiological measurements (Champ, Wallis, Vorobyev, Siebeck, & Marshall, 2014), in addition to the distance at which objects are viewed. To understand why animals display particular colour patterns, it is important to investigate if a colour pattern element is visible to an animal from a certain distance (Endler, 1978;Marshall, 2000). For example, a worker bee does not perceive the intricate UV patterns of a flower that guide the bee to its nectar storage until it is close due to the limitations of its visual acuity (Fig. 2.3). QCPA adapts and expands upon existing tools for modelling spatial acuity by using an adaptation of AcuityView (Caves & Johnsen, 2017) and Gaussian filter mediated blurring.

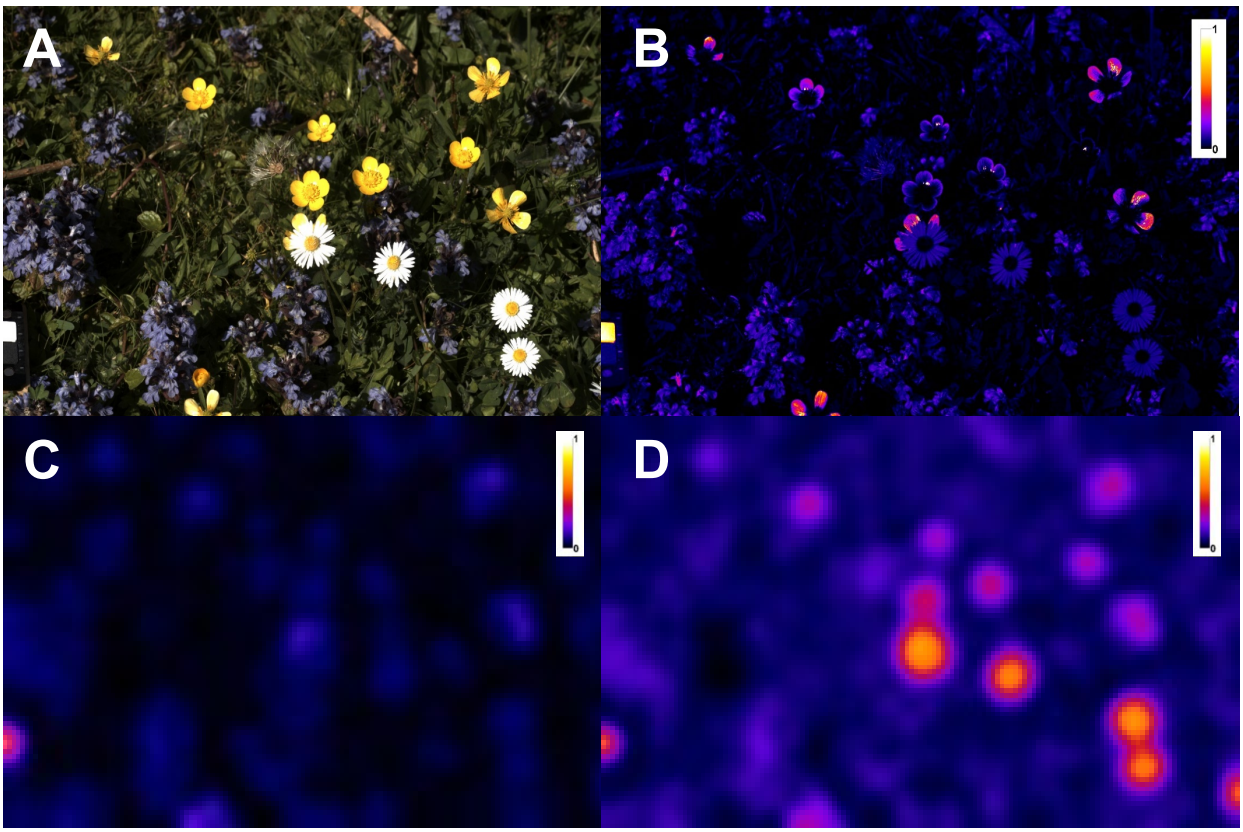

Figure 2.3: A) A flower meadow as seen by a human observer. B) UV intensity as detected by a worker bee with superior spatial acuity, which may lead to the false assumption of the UV information being available to the bee from a distance. C) UV intensity as detected by a worker bee with a spatial acuity of 0.5 cycles/degree at 1m distance. D) Medium-wavelength sensitive photoreceptor stimulation (used for luminance detection) of a worker bee at 1m distance. Note: the white standard (bottom left) remains detectable in all pictures. The scale in the top right of each image shows the relative stimulation of the given receptor channel. Note that the UV signal contributes to the perception of chromaticity as part of a colour opponency channel in the bee's visual system and is not interpreted individually.

2.3.4 Step 4: Eliminating problems in acuity-related processing using the RNL Ranked Filter

As noted by Caves & Johnsen (2017), the blurring of images to model visual acuity (Step 3) is not intended to manipulate images to represent how the scene would be perceived by the receiver; instead, it eliminates details which the specific visual system cannot resolve (Caves & Johnsen, 2017). It is likely that many animals perceive clearly delineated spatial information as the available visual information is integrated in retinal or post-retinal processing. Blurred edges are also problematic for clustering techniques or boundary comparison techniques and may create artefacts of processing that are likely irrelevant to the animal. Pixel noise fluctuation in the sensor of a digital camera

can also interfere with the clustering process, creating false edges, artificial colour pattern elements or influencing edge structure of colour pattern elements.

To overcome these issues, we have developed a filter that can be applied to an image prior to clustering, which we call the 'RNL Ranked Filter'. The filter resembles the 'Smart Blur' used in photo editing software (such as the 'Adobe Creative Cloud') and other rank selection filters, which rank the pixels in a kernel and modify them based on that ranking. However, our custom written algorithm uses an estimate of an animal's psychophysical ability (Using the RNL model) to discriminate between colours and luminance to recreate sharp edges and reduce pixel noise in a cone catch image (Fig. 2.4C, pages 157 – 159 in Appendix A). While the RNL ranked filter provides a possible solution to reconstruct sharp edges, the extent to which it reflects the perception of spatial information in a given species should be validated with behavioural experimentation.

2.3.5 Step 5: Psychophysical image segmentation using RNL Clustering

A range of pattern analyses, including granularity analysis (Stoddard & Stevens, 2010) or NaturePatternMatch (Stoddard, Kilner, & Town, 2014) can be applied to an unsegmented picture (Steps 1-4). Other pattern analyses, such as Patternize (Van Belleghem et al., 2018) or most analyses in QCPA require an image segmented into colour pattern elements. However, image segmentation is often created subjectively using human perception: for example, a researcher estimating how many colour elements there are within a pattern. This may be sufficient for simple patterns but is likely to introduce significant anthropocentric bias when analysing complex patterns and when the visual system of the animal differs dramatically from a human visual system. Here, we present an agglomerative hierarchical clustering approach (Day & Edelsbrunner, 1984) which uses colour and luminance discrimination thresholds of an animal, either in combination with each other or separately. By comparing each pixel to its neighbours, we can use the log-transformed RNL model to determine whether any two pixels could be discriminated based on colour and/or luminance contrast perceived by an animal. Once completed across an entire sample, this process results in an image that is segmented according to an animal's psychophysiological discrimination thresholds (Fig. 2.4D). This approach shares similarities with image

segmentation techniques in computer vision such as statistical region merging (Nock & Nielsen, 2004). Given the variability in previous investigations examining the relationship between the perception of spatial, chromatic and achromatic information (e.g. Shevell & Kingdom, 2008; Shapley & Hawken, 2011; Clery et al., 2013; Miquilini et al., 2017), we recommend such combined thresholds be confirmed using contextualised behavioural experiments. For more information on the mechanism of the RNL clustering as well as the combination and weighting of chromatic and achromatic thresholds seepages 159 – 161 in Appendix A.

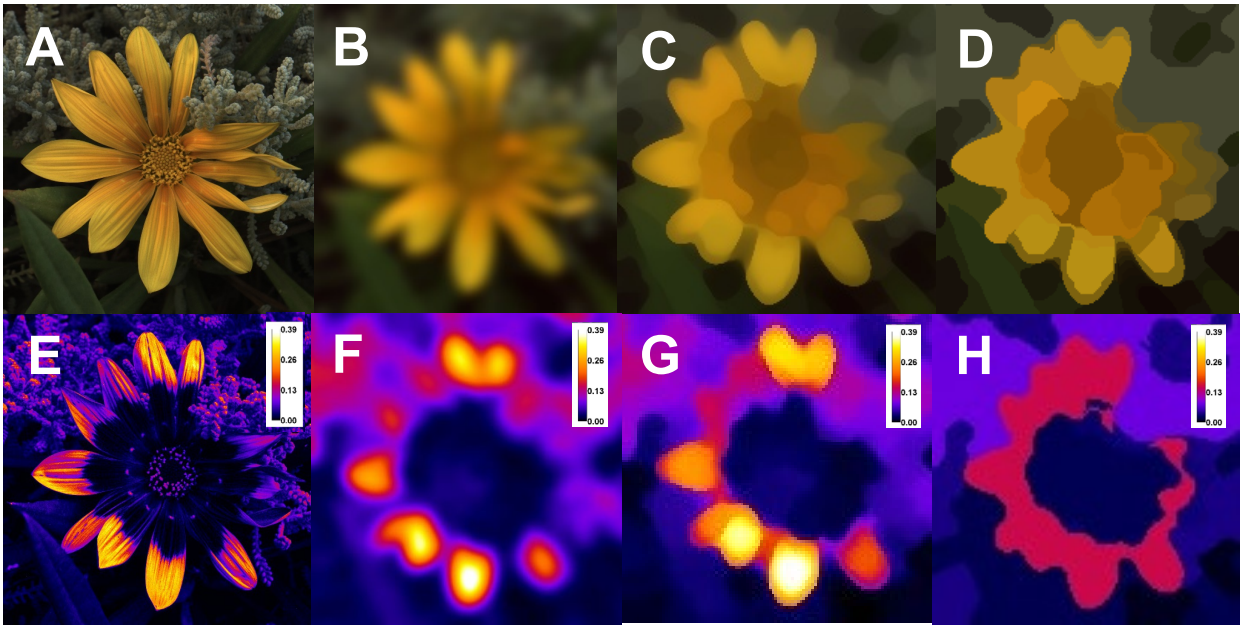

Figure 2.4: A) Reconstructed RGB image of a daisy using cone stimulation of the short, medium and long-wavelength sensitive photoreceptor channels of a blue tit (*Cyanistes caeruleus*). The UV photoreceptor is not shown for simplicity. B) The image after FFT filtering using a spatial acuity of 4.8 cycles/degree and a viewing distance of 2m. C) Recreation of sharp edges using RNL ranked filtering. D) Clustering the image into colour pattern elements with RNL clustering. C & D assume a conservative cone receptor noise of 0.05 and a cone ratio of 1:2:3:3 (Hart, Partridge, Cuthill, & Bennett, 2000). Clustered using a colour discrimination threshold of 3 ΔS and a luminance discrimination threshold of 4 ΔS. See Step 1 (Fig. 2.1) for details on multispectral imaging. E) UV information without acuity modelling as perceived by a worker bee (*Apis melifera*). F) Acuity modelled at 15cm viewing distance and 0.5 cycles/degree. G) RNL ranked filtered with uv receptor noise of 0.13 (Vorobyev & Osorio, 1998). H) RNL clustered UV layer using a chromatic threshold of 3 ΔS and an achromatic threshold of 4 ΔS. The scale on the top right of the images indicates the stimulation of the uv receptor channel.

2.3.6 Step 6: Colour pattern analysis

At this point of the QCPA workflow (Fig. 2.1), the user has an image which has been filtered and modified according to the physiological and psychophysical limitations of

an animal visual system, in the context of the physical environment. This information can now be quantified to investigate questions on the design and function of a colour pattern.

In this section, a range of secondary image statistics is presented that can be derived from unclustered (not using the RNL clustering or alternative image segmentation), filtered (using the RNL Rank Filter) as well as clustered images. We have, for this purpose, adapted and interpreted analytical frameworks such as colour adjacency analysis (Endler, 2012), visual contrast analysis (Endler, 1991; Endler & Mielke, 2005) and boundary strength analysis (Endler et al., 2018). We also present new parameters and alternative outputs of these frameworks, new types of pattern analysis as well as various ways of visualising and plotting image and pattern properties (Table 2.1, Fig. 2.1).

6.1: Colour Adjacency Analysis (CAA)

Colour adjacency analysis (CAA) provides an approach for measuring the geometric properties of colour patterns and entire visual scenes (Endler, 2012). The concept is based on measuring the frequencies of transitions along transects across an image parallel and perpendicular to an animal's body axis. The information is captured in a transition matrix which can then be used to derive pattern parameters relative to pattern geometry and potential function. While comparably novel to visual ecology, the use of transition matrices for the quantification of patterns and their emerging properties is well established in landscape ecology (McGarigal & Marks, 1994; Wickham, Riitters, O'Neill, Jones, & Wade, 1996). In addition to providing frequently used metrics describing pattern geometry (e.g. aspect ratio and patch size), CAA enables the quantification of the specific spatial arrangement (adjacency) of colour pattern elements (Fig. 2.5).

CAA can be used for (but is not limited to) the quantification of mimicry and colour pattern polymorphism, aposematism, camouflage, sexual signalling and studies on evolutionary genetics and evolutionary development of colour patterns (see Endler, 2012 for detailed discussion). For example, in many cases of mimicry, the mimic only replicates the presence or absence of model colours in their patterning, without precisely matching the model's spatial arrangement (e.g. Winters et al., 2018). To

human observers this imperfect mimicry might be immediately apparent, but the intended receiver is unable to distinguish between model and mimic (Mallet & Joron, 1999; Chittka & Osorio, 2007; Dalziell & Welbergen, 2016). In a hypothetical case, CAA could be used to quantify imperfect sexual mimicry of orchids (Fig. 2.5) where the plant mimics the visual and chemical appearance of a potential mate (e.g. Vereecken, 2008; Gaskett & Herberstein, 2010). For further discussion of the biological relevance, worked examples, potential future investigations, and guidance on parameter choices see Endler (2012), Rojas, Devillechabrolle, & Endler (2014), Ligon et al., (2018) and Winters et al. (2018). For details on CAA parameters available in QCPA see pages 133 -137 in Appendix A.

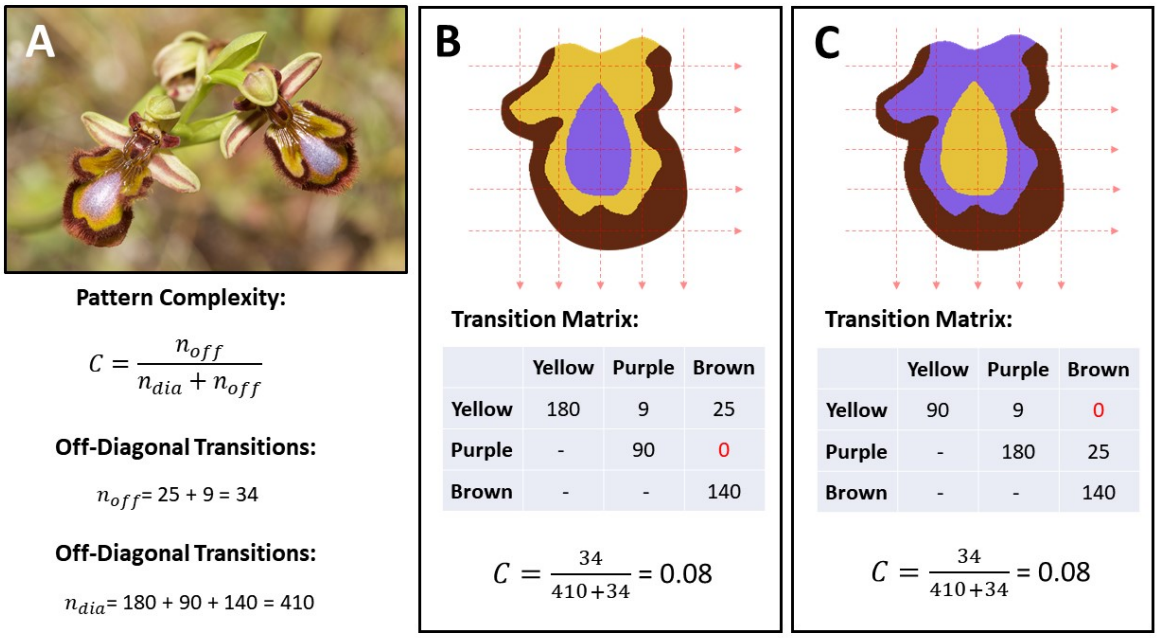

Figure 2.5: A) *Ophrys ciliata,* a bee mimicking orchid (Vereecken, 2008). B) Measuring colour pattern complexity as the proportion of off-diagonal transitions in the transition matrix resulting from horizontal and vertical transects (red dotted lines) across the segmented central flower pattern as seen in A. The diagonal transitions (synonymous) are proportional to the relative size of the colour pattern elements whereas the off-diagonals are proportional to the amount of border colour pattern elements share. C) Measuring colour pattern complexity of a hypothetical mimic. While the transition matrix clearly captures the difference between colour pattern B and C, the complexity of the two patterns is identical. Image credit Fig. 1.5A: Nicolas Vereecken.

6.2: Visual Contrast Analysis (VCA)

Visual contrast analysis (VCA) is designed to investigate colour, pattern and luminance simultaneously by providing pattern statistics which combine spatial and chromatic

properties of colour patterns such as abundance weighted chromaticity measures (Endler & Mielke, 2005,). The perception of visual contrast is a combination of spatial (relative size and position of colour pattern elements), chromatic (hue and saturation), and achromatic (luminance) properties of a colour pattern due to lower and higher level neuronal processing of visual information (e.g. Pearson & Kingdom, 2002; Simmons & Kingdom, 2002; Willis & Anderson, 2002; Shapley & Hawken, 2011; White et al., 2017). Furthermore, interactions between the absolute and relative size of colour pattern elements and their chromatic and achromatic properties includes simultaneous colour contrast and colour constancy mechanisms that are understood in very few visual systems (e.g. Simpson, Marshall, & Cheney, 2016). VCA provides a set of metrics that are designed to capture some of these effects. We have adapted some of these metrics to use known or assumed colour opponency mechanisms to measure chromaticity (pages 138 – 145 in Appendix A). Using the previous orchid example, VCA could be used to investigate how polymorphism in our hypothetical population interacts with pollinator learning or differences in attractiveness to pollinators (Fig. 2.6). SeeAppendix A (pages 127 – 128 and 138 – 145), original publications (Endler, 1991; Endler & Mielke, 2005) and empirical studies (Endler & Houde, 1995; Sibeaux, Cole, et al., 2019b) for further information.

6.3: Boundary Strength Analysis (BSA)

Boundary strength analysis (BSA, Endler et al., 2018) is an extension of CAA (Endler, 2012). The transition matrices generated in the process of adjacency analysis can be used to measure properties of boundaries between colour pattern elements. The underlying argument for this type of analysis is that the relative size, abundance, colour, brightness and adjacency of the patches within a colour pattern, and the chromatic or achromatic contrast of the boundaries between adjacent patches, influence its signalling properties (Shapley & Hawken, 2011; Endler et al., 2018; Green et al., 2018). These parameters also define the properties of the edges between and within parts of visual scenes and textures. BSA (as well as CAA and VCA) is also capable of quantifying possible effects of viewer perspective and movement (Endler et al., 2018). For a detailed introduction to BSA, possible future research, and guidance on parameter choices, please refer to the original publication (Endler et al., 2018) and empirical studies using BSA (e.g. Sibeaux, Cole, et al., 2019b). For detailed equations

and information on modifications of parameters since original publication, see pages 129 – 154 in Appendix A.

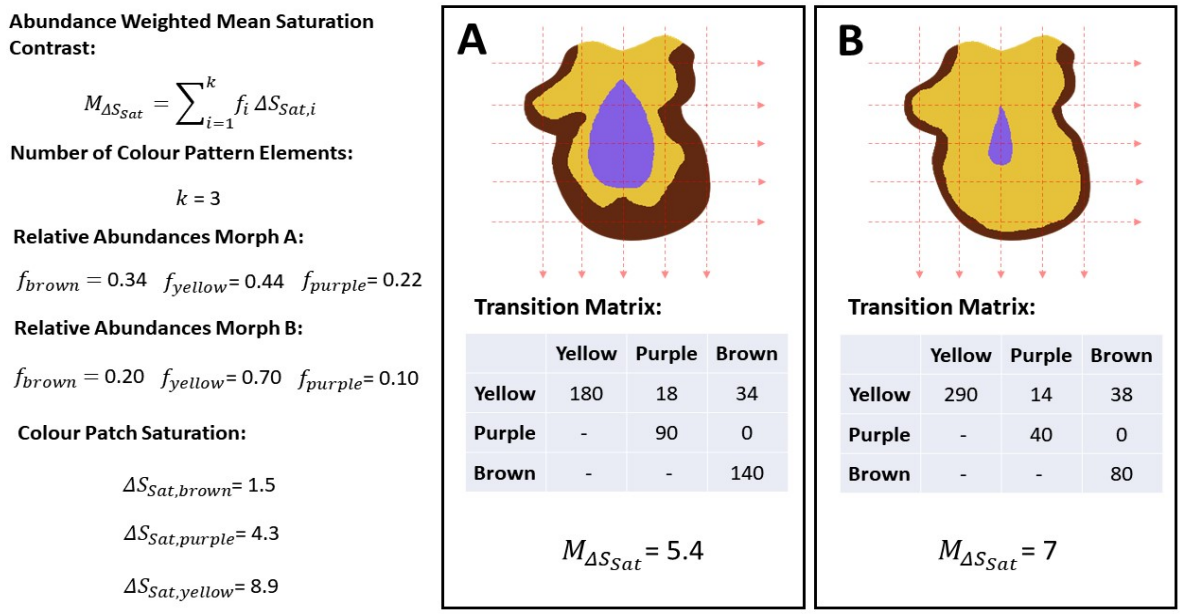

Figure 2.6: Using visual contrast analysis to quantify differences in appearance of a hypothetical polymorphism in *O.ciliata* (Fig. 2.5A). Average saturation (distance from the achromatic point in the log-transformed RNL colour space, ΔS_{sat}) in the colour pattern can be expressed as an abundance weighted mean. The relative abundance of each colour pattern element can be calculated as the proportion of diagonal transitions compared to the sum of all diagonal transitions (f_i). Note how the off-diagonal transitions between morphs change marginally in comparison to Figure 2.5, however, the level of overall colour pattern saturation for this kind of polymorphism differs substantially due to the increased relative abundance of saturated yellow.

6.4: Local Edge Intensity Analysis (LEIA) and ΔS Edge Maps

BSA depends on a segmented image with clearly delineated (clustered) colour pattern elements (Endler et al., 2018). However, the segmentation process removes a large degree of subthreshold information, particularly smooth gradients of brightness and colour which the viewer may perceive. For this purpose, we provide 'Local Edge Intensity Analysis' (LEIA), as a way of quantifying edge properties in an image or ROI (Region of interest) that does not rely on a segmented input. By comparing each pixel to its horizontal, vertical and diagonal neighbours LEIA quantifies edge intensities in

terms of colour and luminance contrast in log-linear RNL opponent space (Renoult et al., 2017). The result can be visualised as 'ΔS Edge Images' (Fig. 2.7). BSA weights the strength of boundary classes according to their global (across an entire image or ROI) relative abundance, whereas LEIA provides a local measurement of edge intensity on roughly the scale of an edge detecting receptive field. This approach allows one to consider edge contrast at the scale of the functional units (receptive fields) at which low level edge and feature detection are thought to take place (Marr & Hildreth, 1980; Marr, 2010). While LEIA is suited to the investigation of similar aspects of colour pattern design and function as BSA, it can do this without the need for clustering an image, while using a more neurophysiological approach than BSA. We recommend that LEIA should be used on images which have first been controlled for acuity (to remove imperceptible edge/gradient information) and images which have also been through the RNL ranked filter, so that local chromatic and luminance edges have been reconstructed to their maximal values. LEIA also provides numerical output describing the distribution of edge intensities across an image. These parameters are specifically designed to be robust in the case of non-normally distributed edge intensities in an image (e.g. a small conspicuous object on a homogeneous background). Local edge contrast can be visualised as ΔS edge intensity images (Fig. 2.7 B & C).

Figure 2.7: A) The RNL filtered flower from Fig. 2.4C. B) Edge intensities of chromatic ΔS contrast. Different colours indicate different angles of hypothetical edge detecting receptive fields, the intensity reflects the contrast. C) Edge intensities of achromatic (luminance) ΔS contrast. Colours show edge angle whereas intensity shows edge strength.

2.3.7 Step 7: Data visualisation

A range of novel approaches for data visualisation is provided. Calibrated digital photography and the coupled transformation of image data into psychophysical colour spaces provides a challenge but also an opportunity for visualisation. We have already introduced the ΔS edge intensity images and extend that selection with colour maps, XYZ opponency images and saturation images.

7.1 'Colour Maps' and 'XYZ Chromaticity & Saturation Images

The representation of chromatic information in colour spaces is a useful tool for data visualisation in visual ecology (Endler & Mielke, 2005; Maia, Eliason, Bitton, Doucet, & Shawkey, 2013; Renoult et al., 2017; Gawryszewski, 2018). To date, most studies present their data as a scattering of points, which are either discrete measurements taken with spectrometers, or the mean centroids of image ROI cone-catch values. Techniques such as area or volume overlap between point clouds, or permutation analysis are then used to determine how dissimilar two colour patches are (e.g. Endler & Mielke, 2005; Stoddard & Prum, 2008; Kemp et al., 2015; Maia & White, 2018).

Colour space data visualisations generally do not incorporate any spatial (colour pattern) information. The use of calibrated digital imaging provides thousands, or even millions of colour measurements within each ROI, capturing the entire range of chromatic gradients present in any natural pattern. Using the log transformed opponent colour space (Hempel de Ibarra et al., 2001; Kelber et al., 2003; Renoult et al., 2017) we provide representations of spatiochromatic information in a perceptually calibrated colour space. 'Colour Maps' allow for the representation of entire visual scenes in a chromaticity diagram, in addition to the abundance of colours across part of the image (Fig. 2.8). Among other purposes, colour maps may be used for visualisations and investigations of chromatic background matching. The overlap of ROIs in colour space can be expressed as an abundance weighted percentage. QCPA integrates tools which enable colour maps to be flexibly combined and compared between image sections, or measurements taken from multiple images.

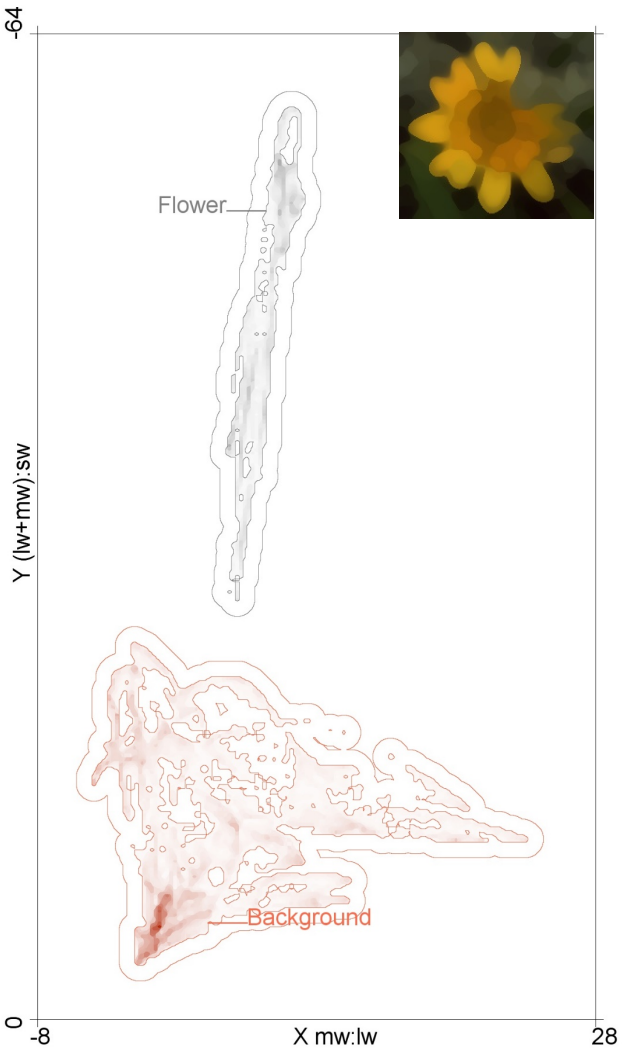

Figure 2.8: Colour map in a log-transformed RNL chromaticity space of the non-UV information in figure 5c. The axes are automatically labelled based on the names of the receptor channels used to create each dimension of colour, for example the X-axis (RNL X dimension) is mw:lw, showing that mw-dominant colours are on the left, and lw-dominant colours are on the right of the plot. X and Y are defined in equation 4 of Hempel de Ibarra et al. (2001). Darker parts of the cloud indicate more pixels in that ROI are located at that coordinate. The boundary around each ROI pixel cloud reflects 1 ΔS. In this case, the flower and its background do not overlap. For tetra-chromatic colour maps the Z-axis is represented as a stack of X&Y maps (see Supplementary Material).

We also introduce the ability to convert cone-catch images to RNL XYZ chromaticity & saturation images, allowing visualisation and measurement of the independent axes of colour in a di- tri- or tetra-chromatic image (showing the Euclidean distance of each pixel's RNL XYZ axes coordinates), in addition to generating a saturation image (Euclidean distance of each pixel to the achromatic point) (Fig. 2.9).

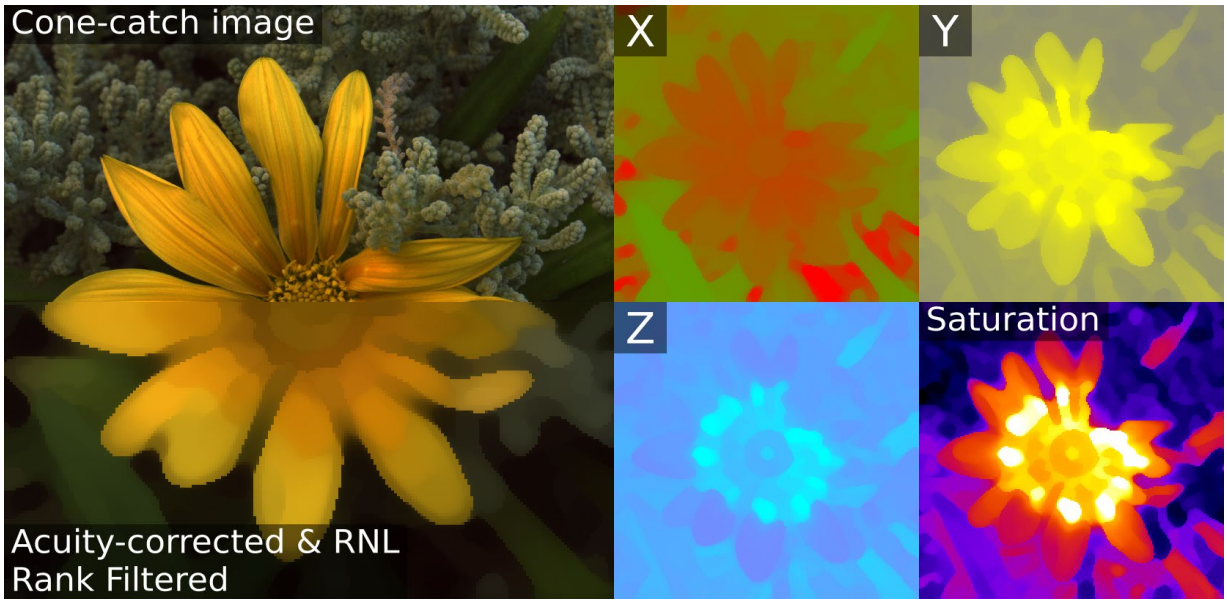

Figure 2.9: An example of the red-green (lw:mw) opponent channel (X), blue-yellow ((lw+mw):sw) channel (Y) and the UV channel (Z) where the colour indicates the position of a pixel along that axis. The saturation map shows the Euclidean distance of each pixel to the achromatic point.

2.3.8 Step 8: Interpreting QCPA output

QCPA provides a huge range of metrics from each image (currently 181 parameters). Some of these parameters likely correlate well with aspects of animal evolution, behaviour and neurophysiology, while others are likely to show no signal. Likewise, some parameters will operate synergistically with each other, while others are independent or antagonistic. Moreover, these relationships could be fundamentally different between taxa, meaning caution should be used when comparing results between highly divergent taxa (such as vertebrate versus invertebrate systems). QCPA can be used to address specific hypotheses linking one or a small subset of parameters (e.g. mean animal vs. background luminance contrast) to a response variable (e.g. predator attack rates) based on the context of the task. Such experiments require highly calibrated environments and stimuli where confounding influences on

the perception of specific spatial, chromatic or temporal properties of a visual stimulus are controlled for (reviewed in Shapley & Hawken, 2011). However, colour patterns can be quantified in a great number of parameters, all of them capturing different aspects of chromatic, achromatic and spatial properties or combinations thereof (of which QCPA only captures a few).

Commonly used terms such as ‘Complexity’, ‘Conspicuousness’ or ‘Similarity’ should be considered as umbrella terms describing perceptual consequences caused by the variation of physical properties of colour patterns and their visual backgrounds (which often cannot be described by a single parameter). The lack of empirical testing of many QCPA parameters (and those of most other pattern analyses) makes it hard to offer broad recommendations for parameter choice across the huge diversity of possible contexts, especially when making observations in natural or nature-like levels of spatiochromatic complexity. The ‘simpler’ the research question and the more controlled the experiment, the more adequate it is to consider one or a few pattern parameters in isolation.

Therefore, when there is no *a priori* reason to choose specific parameters, we recommend the use of multidimensional data analyses, such as principal component analysis (PCA), metric- and non-metric multidimensional scaling (MMDS/NMDS) or similar multivariate approaches such as factor analysis to identify correlations between pattern analysis output and animal behaviour (e.g. Sibeaux, Cole, et al., 2019b) or to distinguish between taxa (e.g. Ligon et al., 2018; Winters et al., 2018; Chan et al., 2019). Doing so can be thought of as operating in a multidimensional pattern space (for discussion see Cuthill, 2019 and Stoddard & Osorio, 2019). Such a pattern space can include categorical data (e.g. presence/absence), data from other pattern analyses (table 1) as well as environmental data. Such dimensionality reduction may then be used to identify latent colour pattern parameters or combinations thereof (e.g. a principal component) that could be used to obtain scores for each species or individual.

Reducing the dimensionality of such data comes with considerable statistical challenges. However, it is possible to avoid many issues such as bias from the structure of datasets or false positives. For example, by adjusting statistical tests for the likelihood of false-positives (Benjamini & Hochberg, 1995) or by aiming for suitable observation to number of parameter ratios to increase the accuracy of dimensionality reduction approaches (Osborne, Osborne, Costello, & Kellow, 2011). While obvious

for the use of QCPA, interpreting many potentially interacting pattern parameters is of increasing importance given a steadily growing diversity of analytical methods (Table 2.1) and the desire to incorporate effects of higher-level processing of visual information into the analysis of visual signals.

2.4 Discussion

Quantitative Colour Pattern Analysis (QCPA) is a framework for the analysis of colour patterns in nature at an unprecedented quantitative and qualitative level. At its core, QCPA uses the advantages offered by calibrated digital photography to enable the use of existing spatiochromatic colour pattern analyses (Fig. 2.1). It also improves existing methodologies used in visual ecology by introducing a user-friendly and open-source framework which incorporates the ability to contextualise visual scenes according to photoreceptor spectral sensitivities, receptor noise levels and abundances, natural light environments, complex natural backgrounds, spatial acuity and viewing distance.

The individual modelling components of QCPA rely on approximations and assumptions, which are based on our best current understanding of the underlying biological processes. As such, it is important to be aware of the limitations and underlying assumptions of the individual components of QCPA, some of which we discuss. QCPA makes extensive use of the receptor noise limited model (RNL) which has been behaviourally validated in various species including: humans, honeybees, birds, lizards, reef fish and freshwater fish (e.g. Vorobyev & Osorio, 1998; Vorobyev et al., 2001; Champ, Vorobyev, & Marshall, 2016; Escobar-Camacho, Marshall, & Carleton, 2017). However, the RNL model and RNL colour space is one of various available visual models and colour spaces that have also considered behavioural context to some degree and which may be considered as alternatives (reviewed in Renoult et al., 2017; Gawryszewski, 2018).

The RNL model (or any other visual model) is unlikely to represent the perceptual complexity of natural visual scenes for all species across all light regimes. To avoid making false assumptions it is necessary to consider the perceptual context in which it is applied and how this context may violate model assumptions (Lind, 2016; Olsson et al., 2018; Kelber, 2019; Price, Stoddard, Shevell, & Bloch, 2019). For example, behavioural experiments have shown varying sensitivity to differences in colour in specific quadrants of colour space relevant to the behavioural ecology of

species (Caves et al., 2018; Sibeaux, Cole, & Endler, 2019a). Another aspect that needs further investigation is the question of how distances in RNL colour space scale with behavioural thresholds across a wide range of visual systems and perceptual contexts (e.g. Fleishman et al., 2016). QCPA applies the log-transformed RNL colour space to minimize, but not remove, the impact of such threshold distortions (Vorobyev & Osorio, 1998; Vorobyev et al., 2001; Gawryszewski, 2018). Overall, the less validated model parameters are, and the more profound assumption violations may be, the more likely deviations from the assumption that 1 ΔS equates to a behavioural threshold (e.g. a 75% success rate in a pairwise choice paradigm) will occur. Furthermore, the photopic version of the RNL, which is used here, was developed to model colour discrimination near the achromatic point under photopic conditions (Vorobyev & Osorio, 1998; Vorobyev et al., 2001). However, when visual systems operate in crepuscular or scotopic conditions, the retinal stimulation to visual information becomes the result of both cone and rod stimulation or rod stimulation only (Vorobyev & Osorio, 1998; Kelber, Balkenius, & Warrant, 2002; Osorio et al., 2004; Veilleux & Cummings, 2012; Olsson et al., 2015). Another example highlighting context specific threshold modelling is the distinction between detection and discrimination thresholds which has direct implications on the application of the RNL (Lind, 2016; Price et al., 2019).

QCPA enables the application of known sensory limitations to filter the information that is subsequently processed by low-level vision. While a range of parameters provided by the QCPA have been shown to be of importance in some species (e.g. Endler & Houde, 1995; Rojas et al., 2014; Winters et al., 2018), many remain to be applied and investigated in a broad range of behavioural contexts and visual systems. To what extent the observed parameterisation of visual information bears ecological or behavioural significance subsequently must be inferred and calibrated using behavioural experimentation (Olsson et al., 2018). QCPA provides numerous parameters based on concepts shown to be relevant to a range of natural contexts (Endler, 1991, 2012; Endler & Houde, 1995; Rojas & Endler, 2013; Rojas et al., 2014; Endler et al., 2018; Winters et al., 2018; Sibeaux, Cole, et al., 2019b). However, it also provides parameters which are yet to be validated, particularly on a quantitative scale. This provides great potential for future research as well as parameter calibration using behavioural experiments and highlights the importance and feasibility of a reductionist approach to the quantification of colour patterns and

their function (*sensu* Stoddard & Osorio, 2019). Given the ability to link QCPA parameters and animal behaviour we encourage the use of QCPA to design carefully calibrated behavioural experiments in the context of complex colour patterns and visual backgrounds.

There is considerable potential to improve QCPA by continuing to refine, test and develop its components. For example, we currently have not considered the loss of spatial and chromatic information due to light scattering or absorption, particularly in aquatic or dusty environments (e.g. Nilsson, Warrant, & Johnsen, 2014). Furthermore, many animal eyes do not have uniform retinas which, in combination with diversity in eye movements and eye shapes, leads to a little investigated diversity of visual perception in addition to the already discussed perceptual diversity in animal visual systems (Wiener, 1957; Land, 1999; Willis & Anderson, 2002; Daly, How, Partridge, & Roberts, 2018; Hughes, 2018; Sibeaux, Keser, Cole, Kranz, & Endler, 2019). QCPA could also be adapted to investigate moving patterns (e.g. Endler, 2012; Endler et al., 2018), given recent advances in the understanding of colour pattern functionality in the context of motion (Fleishman, 1986; Hughes, Troscianko, & Stevens, 2014; Ramos & Peters, 2017; Murali, 2018; Nityananda et al., 2018; Cuthill, Matchette, & Scott-Samuel, 2019; Umeton, Tarawneh, Fezza, Read, & Rowe, 2019). There are types of visual information we have barely begun understanding, such as polarisation vision, the use of fluorescence as well as their interaction with an animal's perception of colour and brightness (Foster et al., 2017; Marshall & Johnsen, 2017; Marshall et al., 2018; Smithers, Roberts, & How, 2019).

Recent years have seen growing diversity of colour pattern analyses (Table 2.1). While some use conceptually similar pattern statistics to QCPA, others provide alternative approaches such as scale invariant feature (SIFT) analysis based metrics (Lowe, 1999) and combinations with models to describe cognitive aspects of attention (Rosenholtz, Li, Jin, & Mansfield, 2010). The concept of QCPA based pattern analysis is entirely compatible with any of these methods. In fact, QCPA does not currently include any computer vision mediated object recognition or figure-ground segregation. However, QCPA provides a promising platform for future implementations of computational approaches to higher level neuronal processing of visual information (e.g. Serre, 2014).

	QCPA	MICA	Patternize	PAT-GEOM	PAVO 2.0	Colourvision	NaturePatternMatch
Modelling of non-human Photoreceptor stimulation	✓	✓			✓	✓	
Modelling of visual acuity	+						
Visual Contrast Analysis	+						
Local Edge Intensity Analysis (LEIA)	★						
Adjacency Analysis	+				✓		
Boundary Strength Analysis	✓				✓		
Bandpass based pattern analysis		+					
Alternative pattern metrics	★	★✓+	✓	+			
Landmark based pattern analysis			+				+
Image segementation using perceptual thresholds	★						
Alternative image segmentation tools	+	+	✓		✓		
Plotting colours in colour space	+				+	+	
Plotting of spatiochromatic information in colour space	★						
Graphical user interface							
Software / Language	ImageJ	ImageJ	R	ImageJ	R	R	C++ (Matlab)

✓ Adapted as per original scientific publications + Substantially modified ★ Novel concept or methodology

Table 2.1: A comparison of the QCPA framework to other existing pattern analyses and frameworks. For patternize see Belleghem et al. (2018). For PAT-GEOM see Chan et al. (2018). For PAVO see Maia et al. (2019). For NaturePatternMatch see Stoddard et al. (2014). For Colourvision see Gawryszewski (2018). We would also like to point out an approach by Pike (2018) which shares similarities with NaturePatternMatch.

QCPA provides an unprecedented level of accessibility and user-friendliness by being free, open-source, graphical user interface mediated and accompanied by a vast body of support material. QCPA presents a comprehensive, dynamic and coherent work process starting with the acquisition of calibrated digital images and ending with the extraction of behaviourally and neurophysiologically contextualised pattern space. ImageJ has been the software platform of choice for image analysis for decades. Its architecture minimises the risk of non-compatibilities due to future patches of co-dependant packages (Often seen in R or Matlab) making QCPA (and MICA) well equipped for the future. ImageJ and MICA provide their own, rich, sets of image and pattern analysis and manipulation tools that QCPA profits from and can interact with. For example, GabRat (Troscianko et al., 2017) can be used in combination with QCPA to investigate chromatic aspects of disruptive colouration in the context of spatial

acuity. Furthermore, it is possible to use QCPA and MICA with a simple smartphone or cheap digital camera and a colour chart for calibration. While it is advantageous to have access to spectrophotometry for comparison of modelling output, this is no longer a requirement and reduces the cost for equipment drastically.

In conclusion, there are many theories and predictions regarding the design, function and evolution of colour patterns in nature which, if at all, have only been investigated in comparably simplistic or qualitative ways. QCPA provides a powerful framework to investigate these theories in a novel quantitative and qualitative context.

Data accessibility

The latest version of QCPA and its open source code (JAVA script) are available for download as part of the MICA toolbox at www.empiricalimaging.com. The website provides detailed manuals, tutorials, FAQs, a dedicated forum and updates. If you intend to use QCPA and/or the micaToolbox, please use the website to familiarise yourself with the latest updates. We do encourage users to use the website and Appendix Aas their primary source of information on how to use QCPA. The version of the code used at the time of publication can be found at: https://doi.org/10.5281/zenodo.3517896.

A fully functional MATLAB based precursor of QCPA can be accessed at https://doi.org/10.5281/zenodo.3518682.

Chapter 3

The Effects of Diel Activity on the Defensive Colouration of Nudibranch Molluscs

"In all works on Natural History, we constantly find details of the marvelous adaptation of animals to their food, their habits, and the localities in which they are found."

- Alfred Russel Wallace, 1853

Chapter 3 - The Effects of Diel Activity on the Defensive Colouration of Nudibranch Molluscs

3.1 Abstract

Empirical evidence linking defensive colour pattern morphology with visual predation is rare due to many factors confounding the function of animal colouration such as thermoregulation and intraspecific signalling. Nudibranch molluscs are a promising model organism for the study of defensive animal colouration as, unlike other systems, their poor visual capabilities and marine habitat remove many such confounding factors. Visual predation is therefore likely to be the predominant force of selection for colour pattern morphology. However, there is little empirical evidence to support this assumption. Recent research has identified distinct daytime specific nudibranch species assemblages occurring off the coast of Nelson Bay, NSW, Australia. Given the assumed importance of visual predation, I hypothesized that species occurring exclusively during the night would differ in their appearance from those found during the day. I modelled the visual perception of triggerfish (*Rhinecanthus aculeatus*), a trichromatic generalist feeder, using quantitative colour pattern analysis (QCPA) and have quantified the appearance of colour pattern morphology in 23 species of dorid nudibranchs found either exclusively during the night, day or both. Using quantitative colour pattern analysis (QCPA), we show that the morphology of dorid nudibranchs found during night-time is significantly different from that of species found exclusively during the day, supporting the hypothesis that visual predation indeed may act as a key selective force shaping defensive colouration in nudibranch molluscs.

Keywords: Quantitative colour pattern analysis, aposematism, mimicry, colour pattern analysis, animal colouration, visual modelling

3.2 Introduction

Camouflage and aposematism are two key strategies of visual defence that are used by animals in their fight for survival (Ruxton et al., 2018). However, how such defensive mechanisms have evolved has puzzled scientists for over 100 years: whilst many pivotal theories exist, empirical studies of such hypotheses with real prey species are severely lacking (for review see Endler & Mappes, 2017; Ruxton et al., 2018). Visually

hunting predators are considered the main selective force shaping the evolution of defensive animal colouration (Cott, 1940; Endler, 1978; Ruxton et al., 2018). While strong evidence for this exists from studies of post-industrial melanisation of moths (see Majerus, 2009 for a detailed review), more recent empirical examples linking specific defensive colour pattern design and survival in a natural context (i.e. using real predators and real prey animals in their natural environment) remain rare (but see Troscianko et al., 2016b) and as such, observations of the effects of selection on colour pattern morphology are much more common (e.g. Allen, Moreno, Gamble, & Chiari, 2019).However, as covered in detail in Chapter 2, until recently such studies would analyse colour and pattern in isolation and often without a comprehensive analysis of the ecological context which shapes the evolution of defensive animal colour patterns (van den Berg & Troscianko et al. 2020).

There is little empirical knowledge on how profound and prolonged changes in terrestrial light environments that go along with diurnal and nocturnal activity correlate with general adaptations in defensive colouration (but see Kamilar, 2009; Allen et al., 2019; Galván, Vargas-Mena, & Rodríguez-Herrera, 2020). However, the aquatic, and especially the marine environment, seems to be a particularly good environment to observe adaptations both in colouration and visual systems to permanent and fundamental changes in the light environment (Lythgoe, 1979; Marshall, Jennings, McFarland, Loew, & Losey, 2003; Marshall et al., 2018; Cronin et al., 2014; Price, 2017). Examples of evolutionary responses to changes in selective pressures associated to such changes in the light environment can be found in many deep-sea marine fish species which have repeatedly evolved red, orange or black colouration as a response to the lack of long-wavelength light (Douglas & Partridge, 1997; Johnsen, 2005) or animals which spend their entire life time in the absence of light such as cave dwelling animals which have evolved to be completely white or translucent (Poulson & White, 1969).

Within most light environments, transient changes also occur due to seasons, weather, changes in habitat growth and diurnal rhythms. As a result, many animals have adapted their daily activity patterns to avoid visual predation. For example, billions of animals, such as planktonic crustaceans and other zooplankton, migrate daily from the depths of the ocean to feed under the cover of darkness, avoiding visually guided predators (Enright, 1977). This is considered to be the largest animal migration on the planet (Stich & Lampert, 1981; Wiebe, Copley, & Boyd, 1992). Surprisingly, despite

drastic changes in the light environment between day and night-time, the impacts this has on the design of defensive animal colouration remains a largely unstudied area (Hanlon et al., 2007 but see Endler, 1987). Most of the animals many people would naturally associate with elaborate chromatic visual defences (particularly warning colouration), such as bees, are active, at least partially, during the day. In contrast, strictly nocturnal animals often lack permanently displayed distinct coloured patterning, and defence mechanisms associated with them. This seems intuitive, as the lack of illumination at night prevents the perception of colour in the vast majority of predators capable of colour vision (Cronin et al., 2014). Hence, why evolving colourful defences in the first place?

However, many examples of sophisticated (albeit predominantly achromatic) patterning for the purpose of crypsis (but also aposematism, e.g. with skunks) can be found in nocturnal and crepuscular animals, most likely to avoid predation by visual predators during daytime periods of rest or protection from nocturnal visual predators. For example, Hanlon et al. (2007) demonstrated that a significantly larger proportion of cuttlefish showed background matching camouflage during night-time as opposed to daytime. Following this finding, Warrant (2007) suggested that visual ecologists studying the evolution of defensive colouration might underestimate the importance of visual predation during night-time, while also suggesting the likely existence of various potential predators with visual systems well developed for visual hunting during the night such as fish or cephalopods. Indeed, visual processes (such as colour vision), which were previously thought to be limited to daylight conditions, are now known to be used by animals at night (Warrant, 1999, 2017, 2019; Kelber et al., 2002). Such findings could alter our understanding of selective pressures acting on visual defences of nocturnal species.

Finding a suitable model organism for the study of defensive colouration is difficult due to animal colouration often serving multiple purposes aside from visual defence, such as sexual signalling, territorial displays and thermoregulation (Cott, 1940; Caro, Merilaita, & Stevens, 2008; Cuthill et al., 2017). This makes it difficult to isolate the effect of visual predation, particularly in non-laboratory conditions (but see Troscianko et al., 2016). For example, poison dart frogs are considered a flagship species for the study of aposematic colouration (e.g. Darst et al., 2006), yet it remains unclear to what extent their colouration is confounded by thermoregulation, in addition

to sexual and territorial signalling. Similar constrains apply to moths and butterflies, (e.g. Lindstedt et al., 2009; Honma et al., 2015).

Many of these constraints do not apply to marine invertebrates, such as nudibranchs, due to their rudimentary vision (basic phototaxis) and their aquatic habitat (Barth, 1964; Eakin, Westfall, & Dennis, 1967; Purchon, 1977; Tabata & Alkon, 1982; Behrens, Petrinos, & Schrurs, 2005). Therefore, predation by visually hunting predators is deemed the main selective pressure on nudibranch colouration (Edmunds, 1987, 1991). Nudibranch molluscs are a highly diverse and colourful marine group, with more than 3000 described species world-wide (Wägele & Willan, 2000). While being increasingly important indicators of ecosystem health (Smith, 2005), nudibranchs are an intriguing model organism for the study of defensive animal colouration, particularly camouflage and warning colouration (e.g. Cortesi & Cheney, 2010; Cheney et al., 2014; Winters et al., 2017). Recent studies have provided empirical evidence that some species of nudibranchs are nocturnal while others are active either only during the day or in both day and night, leading to distinct species assemblages present at either day or night with substantial seasonal variation (Chang, Chen, Willan, Mok, & Yu, 2013; Larkin, Smith, Willan, & Davis, 2017). However, to what extent the activity patterns of these species correlate with their morphology remains unknown.

In this chapter, I hypothesized that there would be differences in colour pattern morphology between diurnal, cathemeral (active during both, day and night) and nocturnal species assemblages as perceived by an ecologically relevant observer. Specifically, I hypothesized a lack of highly contrasting colour patterns and signs of mimicry in nocturnal species. To test this, I conducted analysis on dorid nudibranchs (Suborder: Doridina, Bouchet et al., 2017) as these are among the best studied clade of nudibranch molluscs in terms of phylogenetics (e.g. Valdés, 2002; Hausdorf & Bouchet, 2005; Johnson & Gosliner, 2012), chemical defences and feeding ecology (e.g. Faulkner & Ghiselin, 1983; Okuda & Scheuer, 1985; Rudman & Bergquist, 2007; Haber et al., 2010; Carbone et al., 2013; Cheney et al., 2016), but are also known for their highly diverse colouration (e.g. Rudman, 1986; Ortea, Valdes, & Espinosa, 1994; Haber et al., 2010; Layton, Gosliner, & Wilson, 2018).

Using the ‘Quantitative Colour Pattern Analysis’ (QCPA) presented in Chapter 2 (van den Berg et al., 2020) we quantified the colour pattern design of daytime specific

assemblages of dorid nudibranchs in Nelson Bay, New South Wales, Australia (Larkin et al., 2017). Here, for the first time, the design and function of defensive colouration in nudibranchs was investigated using calibrated digital photography (Troscianko & Stevens, 2015). Using QCPA, the visual system of a trichromatic triggerfish (*Rhinecanthus aculeatus*) was used as a model predator, to understand how nudibranchs would be perceived in their natural context. I examined how 29 QCPA pattern parameters were related to daytime activity of 23 dorid nudibranch species (Fig. 3.1, Table 3.2) using comparative phylogenetic regression analysis (Grafen, 1989).

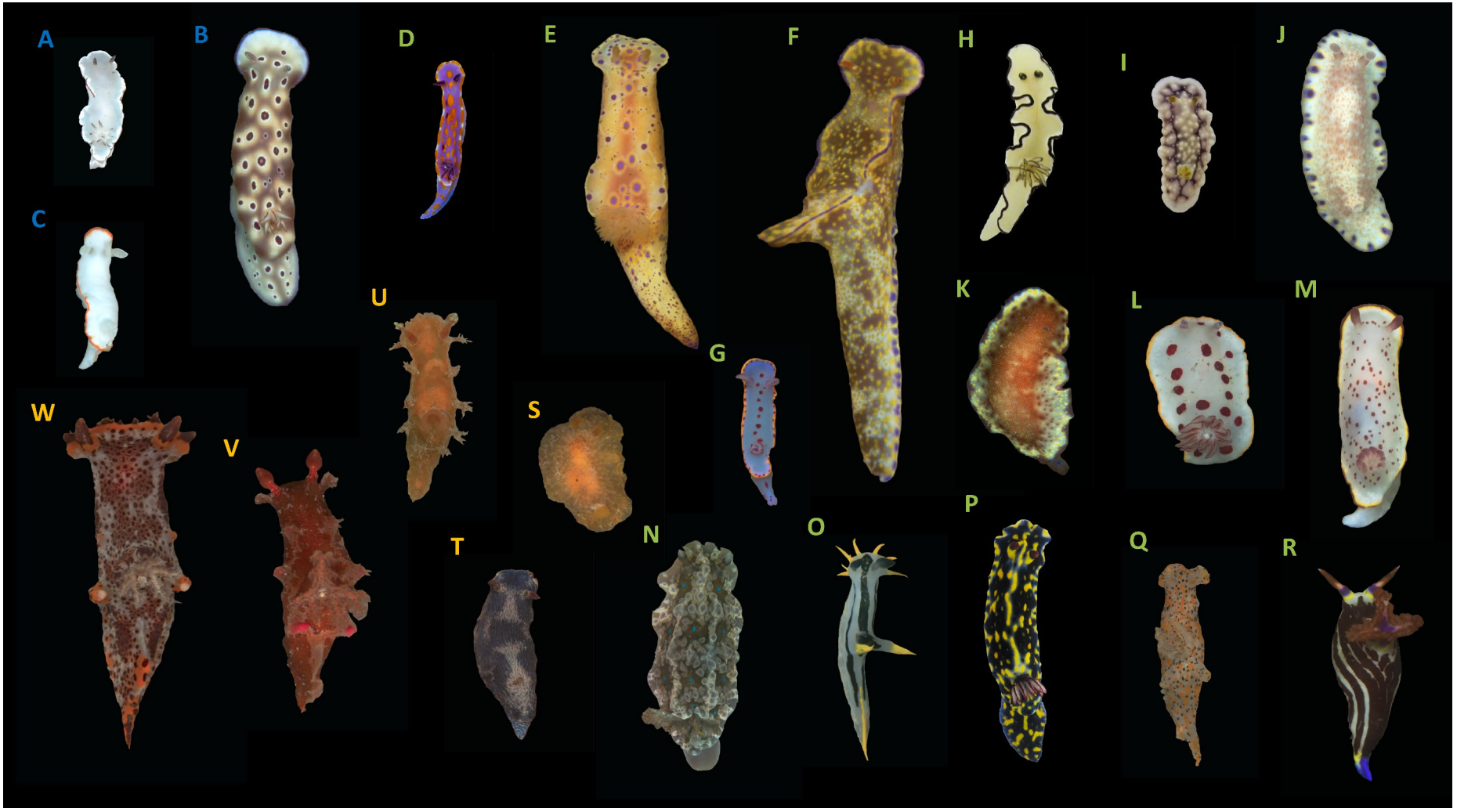

Figure 3.1: All 23 species of dorid nudibranchs as observed by the camera. A) *Glossodoris angasi* B) *Hypselodoris tryoni* C) *Goniobranchus albonares* D) *Ceratosoma amoenum* E) *Ceratosoma brevicaudatum* F) *Ceratosoma tenue* G) *Hypselodoris bennetti** H) *Doriprismatica atromarginata* I) *Goniobranchus geometricus* J) *Goniobranchus aureopurpureus* K) *Goniobranchus collingwoodi* L) *Goniobranchus splendidus** M) *Goniobranchus daphne* N) *Dendrodoris krusensterni* O) *Polycera capensis* P) *Hypselodoris obscura* Q) *Thecacera pennigera* R) *Nembrotha purpureolineata* S) *Doriopsilla miniata* T) *Chromodoris cf striatella* U) *Kaloplocamus ramosus* V) *Plocamopherus imperialis* W) *Plocamopherus tilesii*. Species found exclusively during daytime denoted in blue, species found during the night in orange, both (cathemeral) in green. Members of the putative red-spot mimicry ring are denoted with an asterix.

3.3 Materials and Methods

3.3.1 Sampling

I acquired calibrated images (Troscianko & Stevens, 2015, Chapter 2) on SCUBA during three consecutive fieldtrips to Nelson Bay, NSW (32°42'53.0"S 152°09'00.7"E), (Trip 1: 16.3.2016 – 21.3.2016, Trip 2: 17.3.2018 – 24.3.2018, Trip 3: 2.6.2019 – 11.6.2019) at the following dive sites: Little Beach, Fly Point, Pipeline and Seahorse Garden. Sampling effort was conducted during 38 dives, distributed roughly equally between sites and different times of the day (18 night / 20 day) depending on tides (low and high) and weather conditions. Night dives were conducted after sunset or before sunrise (6pm-6am). We captured images of 369 individuals from 54 species of sea slugs, of which 49 were identified as nudibranchs. This equates to about 25% of all known sea slugs in the area and possibly as much as 50% of all nudibranch species (Nimbs & Smith, 2017). Of these 49 species 23 were identified as dorids (Suborder: Doridina) for which phylogenetic information was available and were used in this analysis (Table 3.2, Fig. 3.6). 12 species of dorid nudibranch could not be used due to a lack of phylogenetic data. Of these species, 3 were cathemeral and 9 were nocturnal. Post-dive species identification was achieved using various identification books as well as the expertise of nudibranch taxonomists and local experts. All images were taken at depths between 1-18 meters. Dives were performed in groups of 2-4 divers, with one dedicated photographer taking images and other divers searching the environment haphazardly for individuals to sample.

3.3.2 Photography

All images contained a custom-made resin cast colour & grey standard (Fig. S3.1) to allow for image linearization and normalisation (Troscianko & Stevens, 2015). The standard was crafted from a Tiffen Color Separation Guide and Gray Scale (small) (Q-13) (Tiffen, NY, USA) which was cast into clear resin and dried in a vacuum to remove any trapped air (detailed instructions can be found on www.empiricalimaging.com). We calibrated an Olympus E-PL5 PEN camera with a 60mm macro lens (Fig. S3.2) in the corresponding Olympus PT-EP10 housing. The camera was equipped with two 12,000 lumen VK6 Pro Scubalamp and two 6,500 lumen PV6S Scubalamp video lights providing a total of 37,000 lumen of white LED light (Fig. S3.2). All pictures were taken in RAW format using manual aperture and shutter speed with automatic white balancing and a fixed ISO of 200.

3.3.3 Colour Pattern Analysis

Images were analysed using the QCPA framework (van den Berg et al., 2020, Chapter 2). Images were linearised and normalised using the 'estimate black point' option in MICA with a grey standard tile, which was calibrated against a 99% Spectralon (Ocean Insight, FL, USA) white standard to control for eventual staining of the resin. The images where then transformed into cone catch images as per the photoreceptor stimulation of a Picasso triggerfish (*Rhinecanthus aculeatus*) (spectral sensitivities of photoreceptors from Cheney et al., 2013) at a slightly greenish illumination (typical for NSW coastal waters) as measured at 5m depth (Fig S3.2). *R. aculeatus* was chosen as a representative for an ecologically relevant observer as they are abundant, are omnivorous and have a comparatively well studied trichromatic visual system representative of many fish in shallow coastal waters (Losey et al., 2003). The amount of spatial information perceived by the fish was modelled using a combination of Gaussian acuity filtering followed by image smoothing using the RNL ranked filter, both implemented in QCPA (Chapter 2). Images were rendered assuming a spatial acuity of 2.75 cycles/degree (Champ et al., 2014), a 10cm viewing distance and weber fractions of 0.07:0.05:0.05:0.05 (sw:mw:lw:dbl) derived from a relative receptor abundance of 1:2:2 (sw:mw:lw) (Cheney et al., 2013), with luminance contrast perception mediated by the double cone receptors measured as (mw+lw)/2 (Pignatelli, Champ, Marshall, & Vorobyev, 2010). The nudibranchs were manually isolated from their visual backgrounds prior to acuity modelling using 'Region of Interest' (ROI) selection tools in ImageJ, which was followed by image segmentation into colour pattern elements using RNL clustering with a chromatic threshold of 2 ΔS and an achromatic threshold of 4 ΔS, which were based on behavioural experiments (Chapter 4, Cheney *et al.*, (2019)). Each animal ROI was then analysed using QCPA's modified versions of the 'Colour Adjacency Analysis' (CAA) (Endler, 2012), 'Visual Contrast Analysis' (VCA) (Endler & Mielke, 2005) and the 'Boundary Strength Analysis' (Endler et al., 2018) as described in Chapter 2. A total of 29 pattern parameters containing no missing data (as some statistics can only be calculated with complex colour patterns) were selected from the QCPA output (Table 3.1). Species averages were calculated using between 1 and 8 individuals per species, depending on availability of suitable pictures (Table 3.2).

Parameter Abbreviation	Parameter Description
CAA.Sc (Simpson colour diversity)	How evenly all (*k*) available colours are distributed across a pattern. Based on inverse Simpson diversity index. Range: 0-*k*
CAA.Jc (Normalised Simpson colour diversity)	Normalised CAA.Sc. Range: 0-1
CAA.St (Simpson transition diversity)	How regularly all possible boundaries (*n*) between colour patches are distributed across a pattern. Based on inverse Simpson diversity index. Range: 0-*n*
CAA.Jt (Normalised Simpson transition diversity)	Normalised CAA.St. Range: 0-1
CAA.Hc (Shannon colour diversity)	How evenly all (*k*) available colours are distributed across a pattern. Based on inverse Shannon diversity index. Range: 0-ln(*k*)
CAA.Qc (Normalised Shannon colour diversity)	Normalised CAA.Qc. Range 0-1
CAA.Ht (Shannon transition diversity)	How regularly all possible boundaries (*n*) between colour patches are distributed across a pattern. Based on Shannon diversity index. Range: 0-ln(*n*)
CAA.Scpl (Colour complexity)	Assuming highest complexity if CAA.Jt and CAA.Jc are highest. Range 0-1
CAA.C (Pattern complexity)	Amount of borders between patches (patchiness). Range: 0-1
VCA.ML (Mean luminance contrast)	Relative abundance weighted mean luminance channel stimulation. Range: 0-1
VCA.sL (Standard deviation of ML)	Standard deviation of abundance weighted luminance channel stimulation.
VCA.CVL (Coefficient of variation luminance)	Coefficient of variation of abundance weighted luminance channel stimulation
VCA.MSL (Mean RNL luminance)	Relative abundance weighted mean luminance contrast measured in ΔS using the RNL model
VCA.sSL (Standard deviation of MSL)	Standard deviation of abundance weighted RNL luminance contrast
VCA.CVSL (Coefficient of variation RNL luminance)	Coefficient of variation of abundance weighted RNL luminance contrast
VCA.MS (Mean colour contrast)	Abundance weighted RNL chromaticity contrast as colour contrast between all colour pattern elements in ΔS
VCA.sS (Standard deviation of colour contrast)	Standard deviation of abundance weighted colour contrast
VCA.CVS (Coefficient of variation colour contrast)	Coefficient of variation of abundance weighted colour contrast
VCA.MSsat (Mean saturation contrast)	Abundance weighted mean RNL saturation. Measured as Euclidean distance to the achromatic point in ΔS.
VCA.sSsat (Standard deviation of saturation contrast)	Standard deviation of abundance weighted saturation contrast
VCA.CVSsat (Coefficient of variation saturation contrast)	Coefficient of variation of abundance weighted saturation contrast
VCA.MDmax (Mean Dmax contrast)	Abundance weighted Dmax contrast (assuming most contrasting possible opponent processing)
VCA.sDmax (Standard deviation Dmax contrast)	Standard deviation of abundance weighted Dmax contrast
VCA.CVDmax (Coefficient of variation Dmax contrast)	Coefficient of variation of abundance weighted Dmax contrast
BSA.BML (Mean luminance contrast)	Relative abundance weighted mean luminance channel stimulation of boundary contrasts.
BSA.BMSL (Mean RNL luminance contrast)	Relative abundance weighted mean RNL luminance contrast of boundaries.
BSA.BMS (Mean boundary colour contrast)	Relative abundance weighted mean RNL colour contrast of boundaries.
BSA.BMSsat (mean boundary saturation contrast)	Relative abundance weighted mean RNL saturation contrast of boundaries.
BSA.BMDmax (mean boundary Dmax contrast)	Relative abundance weighted mean Dmax contrast of boundaries.

Table 3.1: Summary of the 29 QCPA pattern parameters used. Colour adjacency analysis (CAA) parameters in light blue, visual contrast analysis (VCA) parameters in yellow, boundary strength analysis parameters in light green. For a detailed description and equations of the parameters see Appendix A.

Species (n=23)	Daytime activity (Larkin et al. 2017)	Numbers of individuals
Glossodoris angasi	Day	2
Goniobranchus albonares	Day*	1
Hypselodoris tryoni	Day*	2
Ceratosoma amoenum	Both	7
Ceratosoma brevicaudatum	Both	6
Ceratosoma tenue	Both	3
Doriprismatica atromarginata	Both	5
Goniobranchus daphne	Both	3
Goniobranchus splendidus	Both	8
Hypselodoris bennetti	Both	3
Hypselodoris obscura	Both	6
Goniobranchus aureopurpureus	Both	8
Nembrotha purpureolineata	Both	2
Goniobranchus collingwoodi	Both	5
Goniobranchus geometricus	Both	6
Dendrodoris krusensterni	Both	4
Polycera capensis	Both	4
Thecacera pennigera	Both	1
Kaloplocamus ramosus	Night	2
Plocamopherus imperialis	Night	3
Plocamopherus tilesii	Night	3
Chromodoris cf striatella	Night	2
Doriopsilla miniata	Night	1

Table 3.2: Summary of all species, daytime activity and number of individuals available for calculating species means. Activity marked with an asterix were not observed by Larkin et al. (2017) but categorised from when observed in this study.

3.3.4 Nudibranch Phylogeny

To create a phylogeny for our focal species, data for COI and 16S were taken from GenBank and aligned in Geneious V11 (Biomatters, Kearse et al., 2012) using the plug in for MAFFT (Katoh & Standley, 2013). Auto options were used for aligning COI and 16S was aligned with the iterative algorithm FFT-NS-I x1000 using default scoring matrix 200PAM. Primer regions were removed and both datasets were concatenated and analysed with maximum-likelihood in IQ-tree (Trifinopoulos, Nguyen, von Haeseler, & Minh, 2016). The resulting tree was rooted, made ultrametric and basal polytomies were resolved using the *ape* package (Paradis & Schliep, 2019) in R software (R Core Team, 2015).

3.3.5 Statistical Analysis

The resulting data was then mean-centered, normalised ((parameter-min(parameter)) / (max(parameter) - min(parameter))) and analysed using a centered and scaled phylogenetic PCA analysis (phyl.pca) in the *phytools* package in R (Revell, 2009, 2012). The first five PCA component scores (>90% cumulatively explained variance) were analysed using a Bayesian approach with a MCMC GLMM (Markov chain Monte Carlo Sampler for Multivariate Generalised Linear Mixed Models) (formula = daytime activity ~ PC1 + PC2 + PC3 + PC4 + PC5 -1) from the *MCMCglmm* package (Hadfield, 2010) and convergence diagnostics using the 'Gelman and Rubin's convergence diagnostic' (Gelman & Rubin, 1992; Brooks & Gelman, 1998) to deal with the comparably strong level of uncertainty in the phylogenetic tree (Fig. 3.6). The model was run with 24'000 iterations, a burnin of 40'000 and a thinning interval of 100. Priors were set as R/G: (V = 1, nu = 0.002) and B left at default. Daytime activity was determined using data from Larkin *et al.*, (2017) with missing values filled-in according to when specific species were found during sampling (Table 3.2). Species where determined either nocturnal or diurnal if only a small minority of animals in Larkin *et al.*, (2017) would be found at the opposite daytime. If substantial proportions of a species were found at both, night and day, the species was determined to be cathemeral. Post hoc analysis was done using pairwise permutation tests on pattern parameters (daytime activity ~ parameter) (Mangiafico, 2016) to allow for non-parametric analysis with a Benjamini & Hochberg adjusted p-value (Benjamini & Hochberg, 1995). Differences in variance were tested using a Kruskal-Wallis rank sum test (Hollander & Wolfe, 1973) from the *stats* package (R Core Team) (daytime activity ~ parameter). Colour maps were produced by creating pixel weighted species and community averages using the 'Colour Map' tool in QCPA (van den Berg et al., 2020).

3.4 Results

The first five PCA components explained 93.35% of the variance in the dataset (PC1: 62.02%, PC2:12.78%, PC3: 10.50%, PC4: 4.62%, PC5: 3.43%) (Fig. 3.2, 3.3 & 3.4). MCMC GLMM analysis shows that PC3 (post. mean (95% CI) = -0.52 (-0.97 – 0.00), p=0.041) and PC 4 (post. mean (95% CI) = 0.80 (0.18 – 1.55), p=0.026) significantly correlate with daytime activity (Fig. 3.5). The phylogenetic signal using the MCMglmm approach was strong (H = 0.88, Fig. 3.6). PC1 seems mostly linked to describing variation in colour pattern geometry, whereas subsequent PCs capture mostly variation concerning the brightness and saturation of the average animal (Fig. 3.3). Thus, PC3 & 4 mostly describe differences in animal saturation and luminance. While not significant in explaining the differences between daytime activity, PC2 shows that animals with a high level of average saturation among colour pattern elements (VCA.MDmax & VCA.MSsat) tend to have weakly contrasting borders between colour pattern elements with regard to both, luminance and saturation (BSA parameters) (Fig. 3.3). PC3 shows that bright animals (VCA.ML & VCA.MSL) tend to have a lot of variation in luminance among their colour pattern elements (VCA.sL & VCA.sSL) but tend to be overall less saturated (VCA.MDmax & VCA.MSsat) with very little saturation contrast between patches (BSA.BMS) (Fig. 3.3). PC4 shows that dark animals (VCA.ML & VCA.MSL) tend to have a comparably strong variation in luminance among colour pattern elements relative to the mean luminance of the animal (VCA.CVL) while also having a more regular pattern (CAA.Jc & CAA.Qc) with comparably little variation in saturation among patches (VCA.sSsat & VCA.sS) (Fig. 3.3).

Post hoc analysis using pairwise permutation testing showed night-time species had a significantly lower VCA.MSL (mean abundance weighted patch contrast measured in RNL luminance contrast) than both daytime species and those active during both day and night (adjusted p=0.049). BSA.BMSL (mean abundance weighted border contrast measured in RNL luminance contrast) was also significantly lower in night-time species than it was in both, diurnal and cathemeral species (adjusted p=0.05) (Fig. 3.5). None of the other parameters were significantly correlated with daytime activity and no parameter showed significant differences in variance across daytime groups, although general trends towards differences in luminance and saturation are apparent (Table 3.3).

Notable differences in chromaticity, particularly saturation (distance to the achromatic point), can be visualised on colour maps (Fig. 3.7), with the centre of colour density being closest to the achromatic point for the daytime species average and furthest for the night-time species. The daytime species have the most restricted spread in RNL colour space while species found at both day and night-time cover a substantially larger diversity of colours. Night-time species on the other hand have a much more even spread across colour space, indicating more solid colouration as opposed to colour patterns with smaller highly chromatic (i.e. ‘blue’ or ‘yellow’) colour patches (Fig. 3.7).

Pattern Parameter	Pairw. Permut. Adjusted P-value	Fligner-Killeen Test P-value (df =2)	Pattern Parameter	Pairw. Permut. Adjusted P-value	Fligner-Killeen Test P-value (df =2)
CAA.Sc	0.662	0.510	**VCA.MSsat**	**0.075**	**0.430**
CAA.Jc	**0.051**	**0.933**	**VCA.sSsat**	**0.071**	**0.108**
CAA.St	0.482	0.690	VCA.CVSsat	0.446	0.500
CAA.Jt	0.737	0.925	**VCA.MSL**	**0.049**	**0.144**
CAA.Hc	0.624	0.548	VCA.sSL	0.305	0.918
CAA.Qc	**0.192**	**0.100**	VCA.CVSL	0.705	0.916
CAA.Ht	0.447	0.846	**VCA.MS**	**0.092**	**0.069**
CAA.Scpl	0.514	0.777	VCA.sS	0.240	0.427
CAA.C	0.647	0.530	VCA.CVS	0.420	0.715
VCA.ML	**0.551**	**0.080**	**BSA.BML**	**0.051**	**0.924**
VCA.sL	0.109	0.109	BSA.BMDmax	0.738	0.841
VCA.CVL	0.624	0.372	BSA.BMSsat	0.733	0.925
VCA.MDmax	**0.073**	**0.651**	**BSA.BMSL**	**0.050**	**0.866**
VCA.sDmax	**0.064**	**0.135**	**BSA.BMS**	**0.086**	**0.146**
VCA.CVDmax	0.380	0.229			

Table 3.3: Summary of all pairwise permutation and homoscedasticity tests. Parameters with values below or equal to p=0.1 are highlighted in bold. Blue = CAA parameters, yellow = VCA parameters, green = BSA parameters.

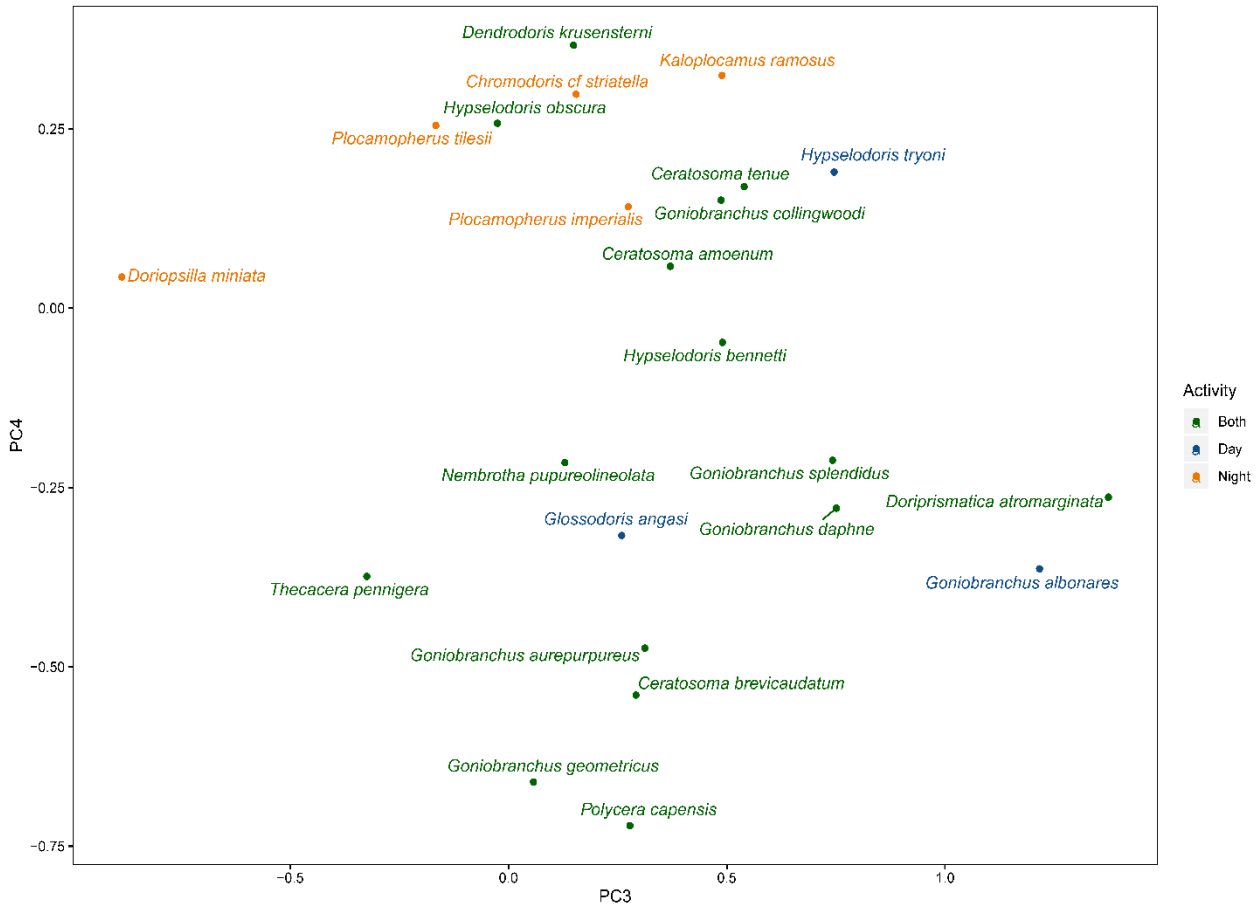

Figure 3.2: A scatterplot of all 23 species of dorid nudibranchs using PC3 and PC4.

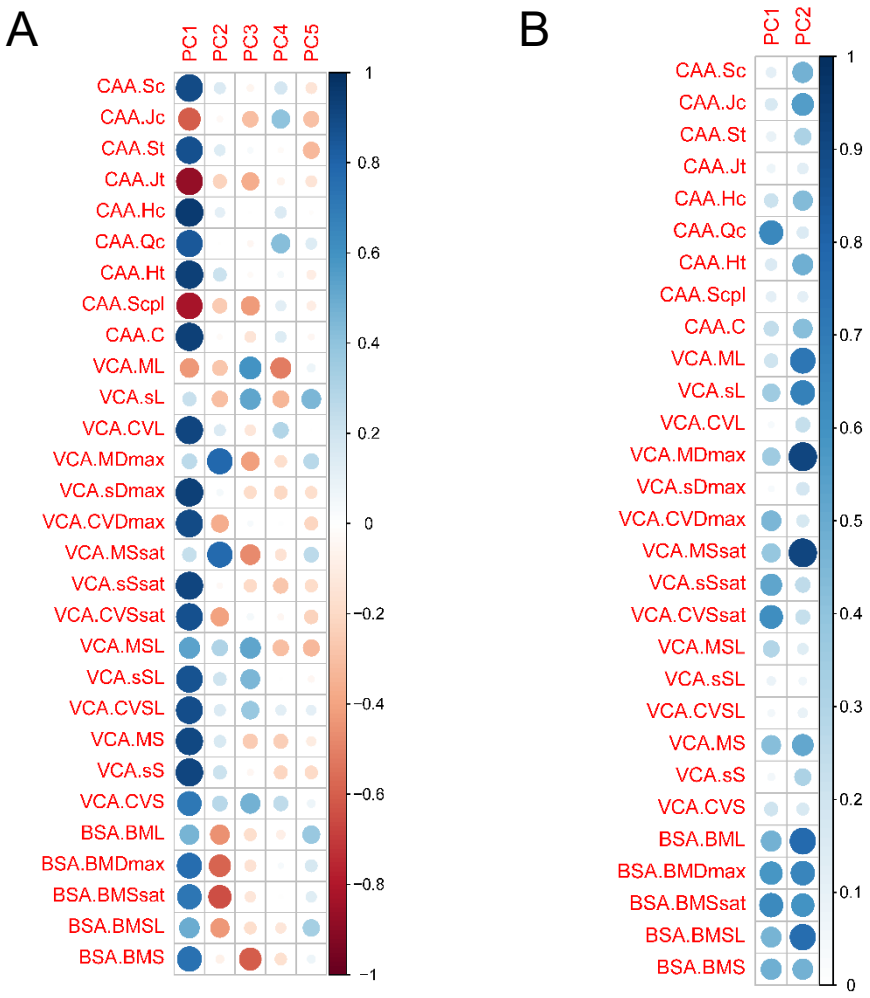

Figure 3.3: Relative contribution (loadings) of each colour pattern parameter. A) Loadings of the first 4 principal components of the dataset. B) Mean of the sum of absolute differences of the first two principal components within each group to the first two principal components of the entire dataset. Values close to 1 mean that there is a strong average difference of the PC between the within group variance and the variance in the entire dataset. Note how PC1 is comparably similar between the entire dataset (PC1 in A) and each of the daytime groups, whereas PC2 is not.

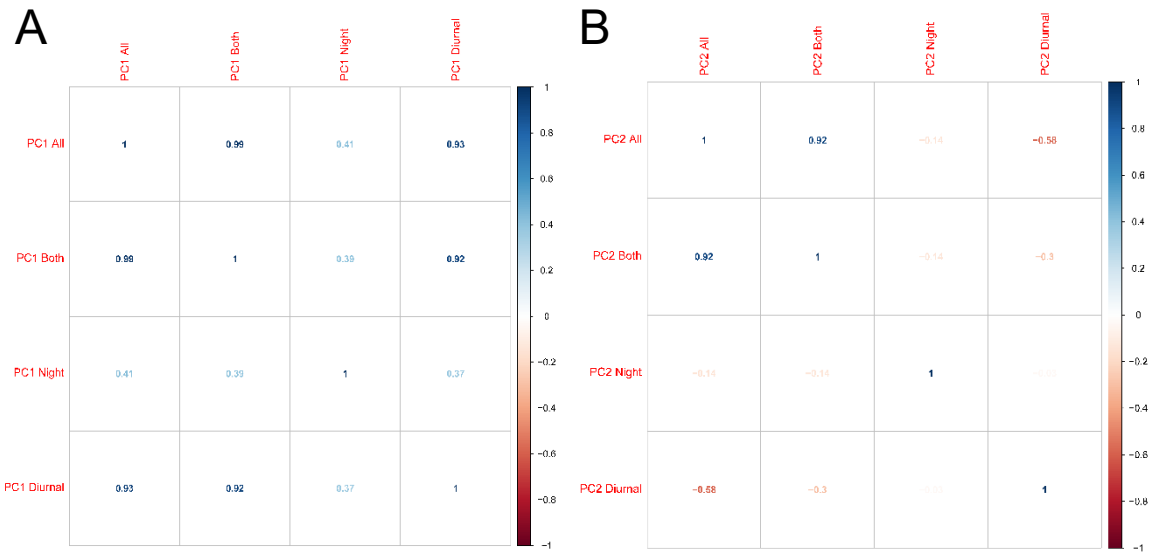

Figure 3.4: Correlation plot of the principle components 1 (A) and 2 (B) of each daytime group compared against the first two principal components for the entire dataset.

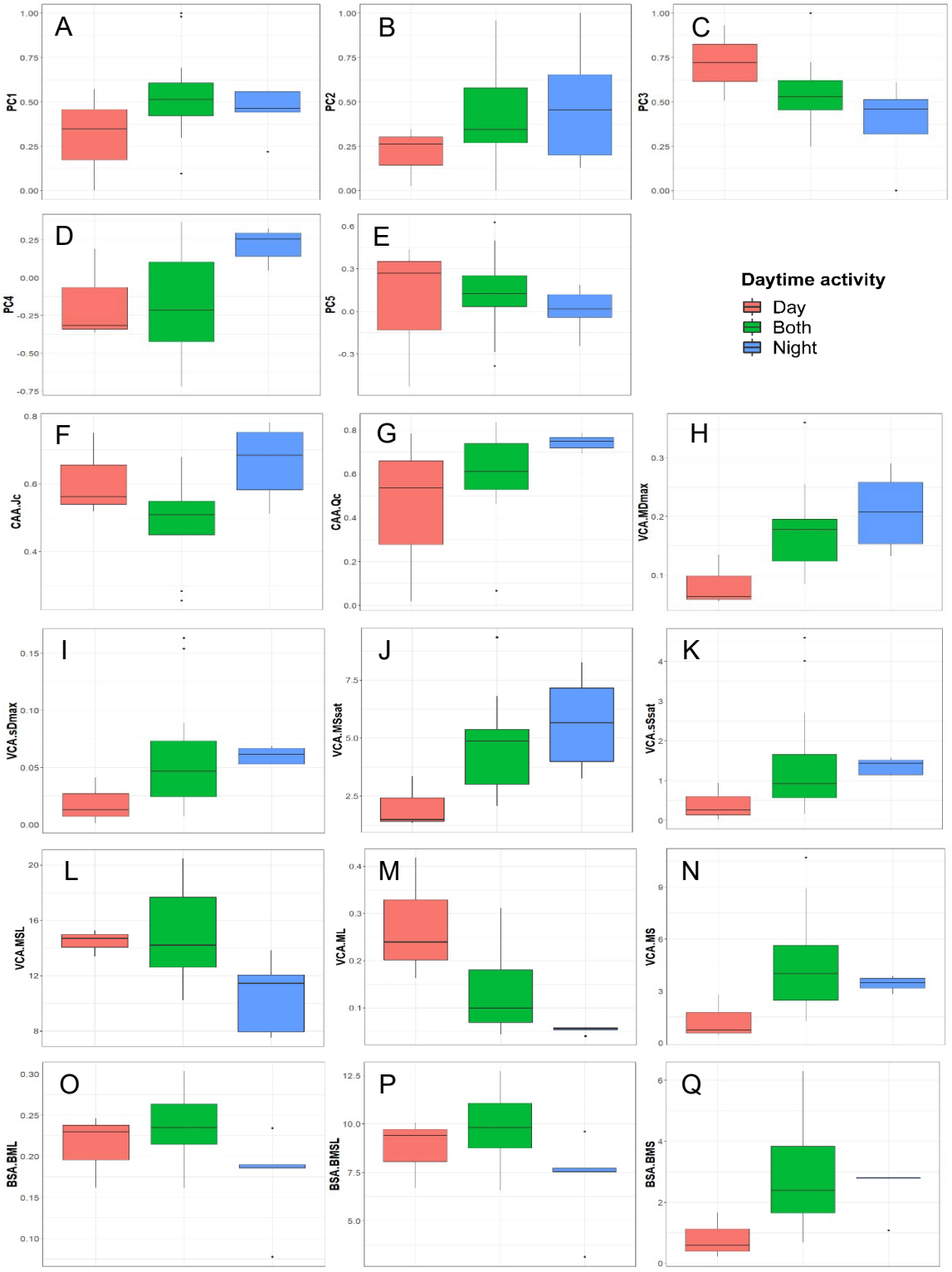

Figure 3.5: Boxplot of PC1 – PC5 (A-E) and pattern parameters highlighted in Figure 3.3. F) Normalised Simpson colour diversity G) Normalised Shannon colour diversity H) Mean abundance weighted Dmax colour patch contrast I) Standard deviation of abundance weighted Dmax colour patch contrast J) Mean abundance weighted RNL saturation patch contrast K) Standard deviation of abundance weighted RNL saturation patch contrast L) Mean abundance weighted RNL luminance patch contrast M) Mean abundance weighted luminance patch contrast N) Mean abundance weighted patch RNL colour contrast O) Mean abundance weighted boundary luminance contrast P) Mean abundance weighted RNL luminance contrast Q) Mean abundance weighted RNL colour contrast boundary contrast.

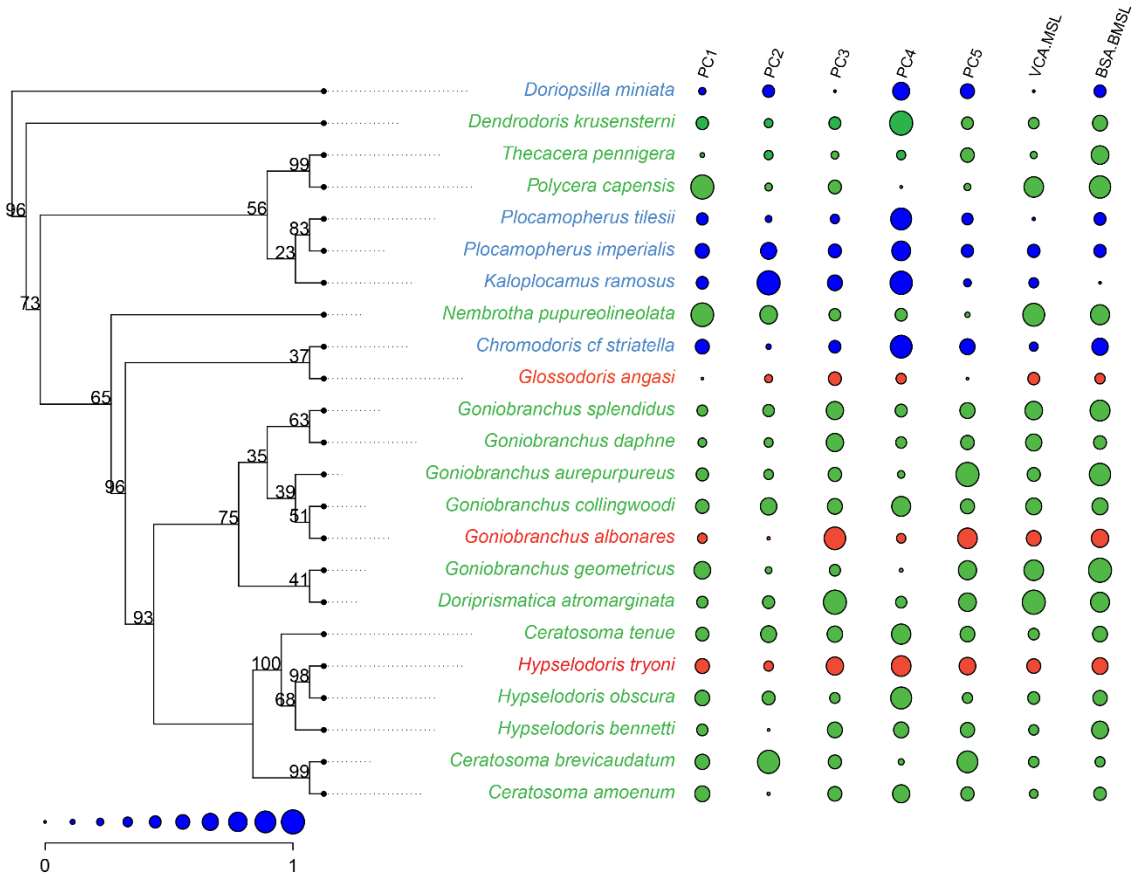

Figure 3.6: Normalised parameters plotted against the phylogeny of the 23 species. Circle size indicates relative strength of parameter contribution. Bootstrap values are presented for node support. VCA.MSL and BSA.BMSL are plotted as they are representative for the key differences between the assemblages (i.e. key contributors to PC2). Night-time species are highlighted in blue, daytime species in red and cathemeral (both) species in green.

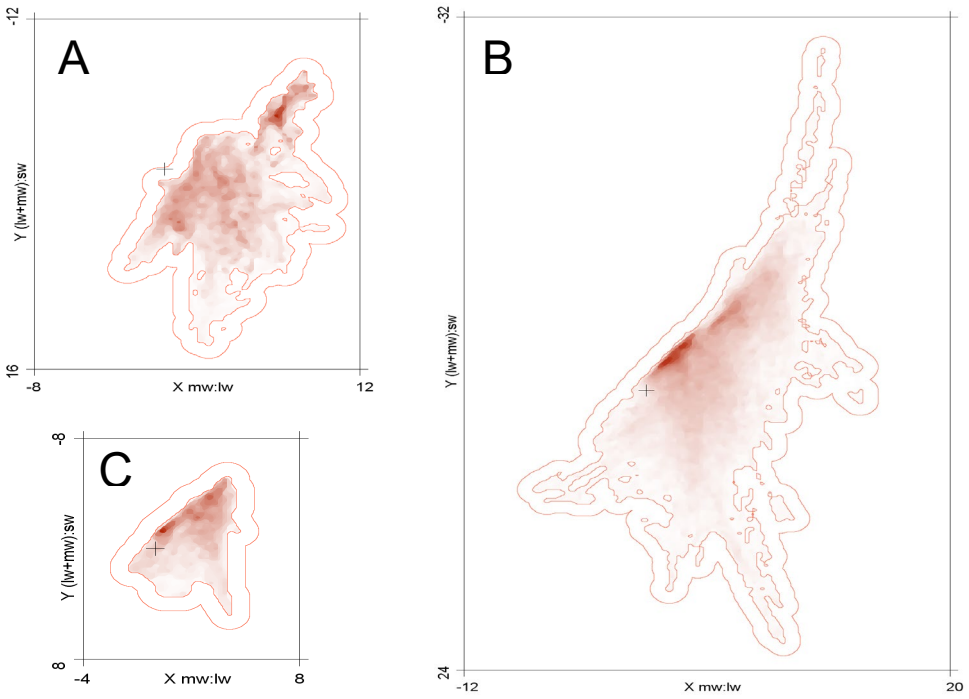

Figure 3.7: Colour maps of species assemblages calculated as the mean of all species in a given assemblage. A: Night-time assemblage, B: Both (cathemeral), C: Daytime assemblage

3.5 Discussion

3.5.1 Summary of results

We show that dorid nudibranch species assemblages varied significantly in colour pattern characteristics according to time of the day, as perceived by a trichromatic reef fish (*Rhinecanthus aculeatus*). Specifically, species found exclusively during night-time differed significantly from those exclusively found during the day. Species found during both day and night did not differ from exclusively nocturnal or diurnal species. Differences in appearance between the communities can be characterized by significant contributions from parameters including overall animal luminance (VCA.MSL), luminance contrast within a colour pattern (VCA.sL & BSA.BML) and overall saturation (VCA.MSsat & VCA.MDmax). Species found during the night tend to be significantly darker and more saturated than those found exclusively during the day, while generally lacking vividly contrasting markings in terms of luminance (e.g. black and white/yellow markings, Fig. 3.1). The strong phylogenetic signal supports the notion of correlated evolution between colour and activity time.

PC1 predominantly described variation within the assemblages, and as such, it seems intuitive to find parameters linked to describing the geometry of colour patterns equally contributing to PC1 (Fig. 3.3 & 3.4) given the predictable degree of correlation between colour pattern parameters (e.g. if a colour pattern gets more complex, pattern elements tend to get smaller etc.). Considering unequal sample sizes between assemblages it is also not surprising that most of the variation in appearance (PC1) is attributed to parameters capable of describing differences within the largest group, i.e. nudibranchs found both during day and night-time, which display a considerable degree of variability in colour pattern morphology (Fig. 3.1 & 3.3).

The observed differences in colour pattern morphology and behaviour, in combination with a strong phylogenetic signal, can partially be explained by what is currently known about the evolution of nudibranch molluscs. First, assuming visual predation to be the predominant selective pressure shaping nudibranch colouration (Rudman, 1986, 1991; Cortesi & Cheney, 2010; Cheney et al., 2014) matches our finding that species found during the night lack vivid patterning. Furthermore, none of the species identified by Winters et al., (2018) as belonging to the red-spot mimicry group in Nelson Bay (Rudman, 1991) were found to be active during the night, neither in this study nor Larkin et al., (2017). This further supports the notion of nudibranch

colour patterns being predominantly shaped by visual predation and a therefore probable absence of aposematism and mimicry in nocturnal species.

3.5.2 Daytime activity and nudibranch evolution

Nudibranchs are assumed to have undergone a transition from an ancestral state with a shell (lacking sophisticated defences or aposematic colouration) to the currently present radiation in chemical defences and associated aposematic colouration (Wägele & Klussmann-Kolb, 2005). Being (or becoming) nocturnal could be a formidable way of reducing the need for investing into producing costly shells, especially when there is no need for daylight given the absence of dedicated visual capabilities. In other words, light is not needed for foraging or finding mates. The switch to nocturnality as a precursor to losing the shell (or vice versa) not only bears the benefit of reduced metabolic investment in a shell, it provides the benefit of not needing to adapt to specific visual backgrounds for camouflage, thus providing facilitated access to a broad range of resources and mating opportunities in the environment, hypothetically laying the foundation for the adaptive radiation observed in dorid nudibranchs (and nudibranchs in general) today. Given ongoing efforts to resolve the evolutionary tree of nudibranchs (e.g. Wägele & Willan, 2000; Grande et al., 2004; Wilson & Lee, 2005; Layton et al., 2018) this study thus provides a rationale for increasing sampling and DNA sequencing efforts targeting nocturnal species. Subsequently improved phylogenies could then be used for more reliable ancestral state reconstructions.

The increase in saturation (VCA.MSsat) for nocturnal species seems counter-intuitive in the light of the previous arguments, given that many aposematic colour patterns use highly saturated colours to convey their warning signal, such as poison dart frogs (Maan & Cummings, 2012) or insects (Briolat, Zagrobelny, Olsen, Blount, & Stevens, 2018). However, VCA.MSsat describes an abundance weighted mean of colour pattern saturation. This means that a species with intricate but highly saturated markings (i.e. a rim or stripes) displayed on a comparatively achromatic body will generally score very low (but high on the standard deviation of saturation contrast). This is further amplified by the loss of spatial detail, preventing such small markings to be detected at a distance (in this case 10cm). However, most of the nocturnal species in this study are dominated by highly saturated longwave dominated hues, such as orange or red. The shortwave-shifted visual systems of many trichromatic fish (such

as *R. aculeatus* used in this study) tends to perceive pure reds, such as seen in the red-spot mimicry group in Winters et al., (2018) as dull browns, as their receptors are not sensitive to long wavelengths. However, many of the more orange ('shortwave shifted red') hues closer to the spectral sensitivity of the longwave-sensitive photoreceptor remain highly chromatic, albeit considerably darker than how they appear to us humans. These two arguments together likely explain the observed difference between the communities in terms of colour saturation (and overall luminance, VCA.ML) and is further supported by the distribution of the species-assemblage-specific relative abundance of hue and saturation in colour space (Fig. 3.6).

In fact, assuming that shortwave-shifted visual systems are the norm, rather than the exception in marine ecosystems (Lythgoe, 1979; Losey et al., 2003; Marshall et al., 2018), displaying long-wavelength shifted body colouration (often observed in deep sea fish (Johnsen, 2005)) is a parsimonious way of appearing dark and achromatic while blending in with ubiquitous amounts of red macro algae (common in Nelson Bay) as well as red-encrusting algae often dominating rocky reefs and cracks and crevices across the benthic environment. Being red is furthermore energetically less expensive, given that less pigmentation is needed to obtain a red colouration as opposed to a truly black one, especially given the abundance (Bandaranayake, 2006) of red pigment in the marine environment. It would therefore be interesting to investigate these species assemblages using a variety of predator visual systems.

In summary, there is ample variation in luminance, colour and pattern across the three communities. However, the species analysed in this study tend to be brighter and less saturated if active exclusively during the day as opposed to their nocturnal counterparts. Species active during both, day and night (cathemeral) made up most of the dataset and can be characterised by a huge diversity of colours and patterns, featuring the most contrastingly coloured species. The cathemeral group also had the strongest sings of colour patterns that might serve aposematic or mimicking purposes which can only be explained by visual predation. However, nocturnal species tended to be the most saturated in terms of colours, many featuring regular or uniform dark red and/or orange colouring.

3.5.3 Limitations & future research

Despite providing intriguing insights into the ecology and evolution of nudibranch colouration, this study was subject to several limitations. First, the amount of species for which phylogenetic information was available had a strong influence on the resulting species featured in this study. Unfortunately, nocturnal species of dorid nudibranchs were comparatively poorly represented. This could reflect a systematic bias in that there is a strong interest in diurnal aposematic nudibranch species for their ecotoxicology, or investigations of mimicry and aposematism (e.g. Cheney et al., 2016; Layton et al., 2018; Winters et al., 2018). Sampling by researchers also occurs more frequently during the day. Given the strong trends observed regarding differences in daytime assemblages, chances are that an increased availability of nocturnal species for comparative phylogenetic analysis will help to further differentiate and accentuate these differences while allowing for more sophisticated statistical methods to be applied.

Second, in order to comment on the presence or absence, let alone relative strength, of aposematism in the respective species assemblages, it is crucial to investigate the strength of chemical defences (e.g. Tullrot, 2013; Winters et al., 2018) as well as the function of colour patterns relative to the visual background against which they are presented (e.g. Michalis et al., 2017). Neither of these aspects have been investigated at this point and are likely to provide further insights into the adaptive properties of colour patterns in dorid nudibranchs. Furthermore, a recent study has demonstrated considerable phenotypic plasticity present within each species (Layton et al., 2018), which, in combination with the need to adequately sample the diversity of visual backgrounds, warrants the need for a substantial increase of sample sizes per species. Increasing sample size is also key to a third limitation, the use of statistical methods to infer on morphological differences between species assemblages.

The present dataset is over-parameterised (29 pattern parameters for 23 observations) which makes detailed investigations problematic due to a lack of statistical power as well as non-parametric properties of such a dataset such as the prominent lack of normality and heteroscedasticity. Specifically, limitations of such over-parametrisation and lack of parametric properties impair the adequate use of multivariate regression models such as GLMs, especially when interactions between variables need to be considered without prior dimension reduction (see discussion

Chapter 2). The best way of overcoming these limitations is to substantially increase sample sizes in terms of number of species (to have a more even representation of taxonomic levels such as families and genera across daytime assemblages) but also in terms of individuals per species. This would then facilitate to analyse communities at the level of individuals animals, rather than using species averages. Most importantly it would allow to apply more sophisticated methods to identify key parameters (or combinations thereof) capable of best describing morphological differences between daytime assemblages. This said, it is important to distinguish between the identification of individual pattern parameters and the identification of latent variables which can be explained by a partial contribution of individual parameters (see Chapter 2).

Nevertheless, dimensionality reduction remains key. PCA is designed to find vectors describing the maximum amount of variation within a dataset. Alternatively, Multi-Dimensional-Scaling (MDS) allows a similar approach by compressing a distance matrix into *n* dimensions resulting in the biggest distance between observation. However, similar to a PCA, this approach is not guided by the goal to maximise the ability to differentiate between two pre-defined subgroups of a dataset but rather 'blindly' identifies principal components or dimensions. Chan *et al.*, (2019) have elegantly described how to achieve that goal by using a linear discriminant analysis (LDA). Alternatively, a discriminant function analysis (DFA) could be used (e.g. Breitman *et al.*, 2013). However, in order to train an LDA model or apply a traditional DFA, a much larger number of individuals per species is necessary. Amey et al., (2018) show an elegant solution to deal with the issue of an over-parameterised dataset containing substantial amount of autocorrelation, using a regularised discriminant analysis (Friedman, 1989). This approach certainly seems promising, especially given that we have used but 29 out of more than 181 parameters available in QCPA.

This study has identified significant differences in the perceived morphology of colour patterns in dorid nudibranch assemblages. However, this study has only observed differences at an observed distance of 10cm. While being a realistic distance at which a fish might decide on whether to take a bite out of a slug, a substantial amount of spatial information is no longer perceivable. This indicates that a large amount of colour pattern geometry is potentially designed to deliver a signal upon closer distance, possibly upon actual physical contact. This warrants the analysis of the image data at closer distance which might lead to additional differences between assemblages and

potentially a stronger contribution of parameters designed to capture differences in colour pattern geometry.

This study presents the first application of the QCPA framework in order to investigate a biological question. The presented findings highlight the formidable descriptive ability of the QCPA while showcasing the framework's unique ability to obtain a large amount of highly contextualised quantitative data. It is important to keep in mind that this study does not just simply describe morphological differences between species assemblages, it comprehensibly describes the visual perception of morphological differences between them. While certainly providing a satisfying proof of concept, this study has also highlighted issues that need addressing. First, using the RNL clustering algorithm has proven highly efficient for handling the segmentation of complex visual information. However, applying a uniform luminance discrimination threshold of $\Delta S = 4$ across an entire image irrespective of local and global contrast as well as spatial frequency (discussed in detail in Chapter 4) leads to a suboptimal degree of object and pattern coherence, likely misrepresenting the actual perception of colour pattern geometry and thus influencing many spatiochromatic parameters in the QCPA output. Applying a more context sensitive algorithm for luminance contrast perception would certainly help as a range of solutions would available (discussed in Chapter 4, but also see Marr, 2010). Alternatively (and to investigate the potential impact of this issue) it would be meaningful to analyse images using QCPA's naïve Bayes clustering algorithm and use a post-clustering confirmation of colour and luminance contrast among colour pattern elements *sensu* Maia et al., (2019).

Second, given the high dynamic contrast in many images, very dark colour pattern elements are in danger of being calculated as highly chromatic due to small absolute (but strong relative) differences in camera receptor stimulation resulting from dark noise. Future versions of the QCPA will be equipped to deal with this problem by preventing chromaticity calculations below a certain luminance threshold. However, the currently analysed data still potentially suffer from this issue. Third, throughout the three years of taking calibrated images it has become clear that the search for a Lambertian underwater standard will be crucial to further increase the quality of obtained image data (due to viewing angle restrictions) as well as to facilitate the taking of pictures in the first place.

Chapter 4

Context dependant luminance contrast sensitivity in a coral reef fish (*Rhinecanthus aculeatus*)

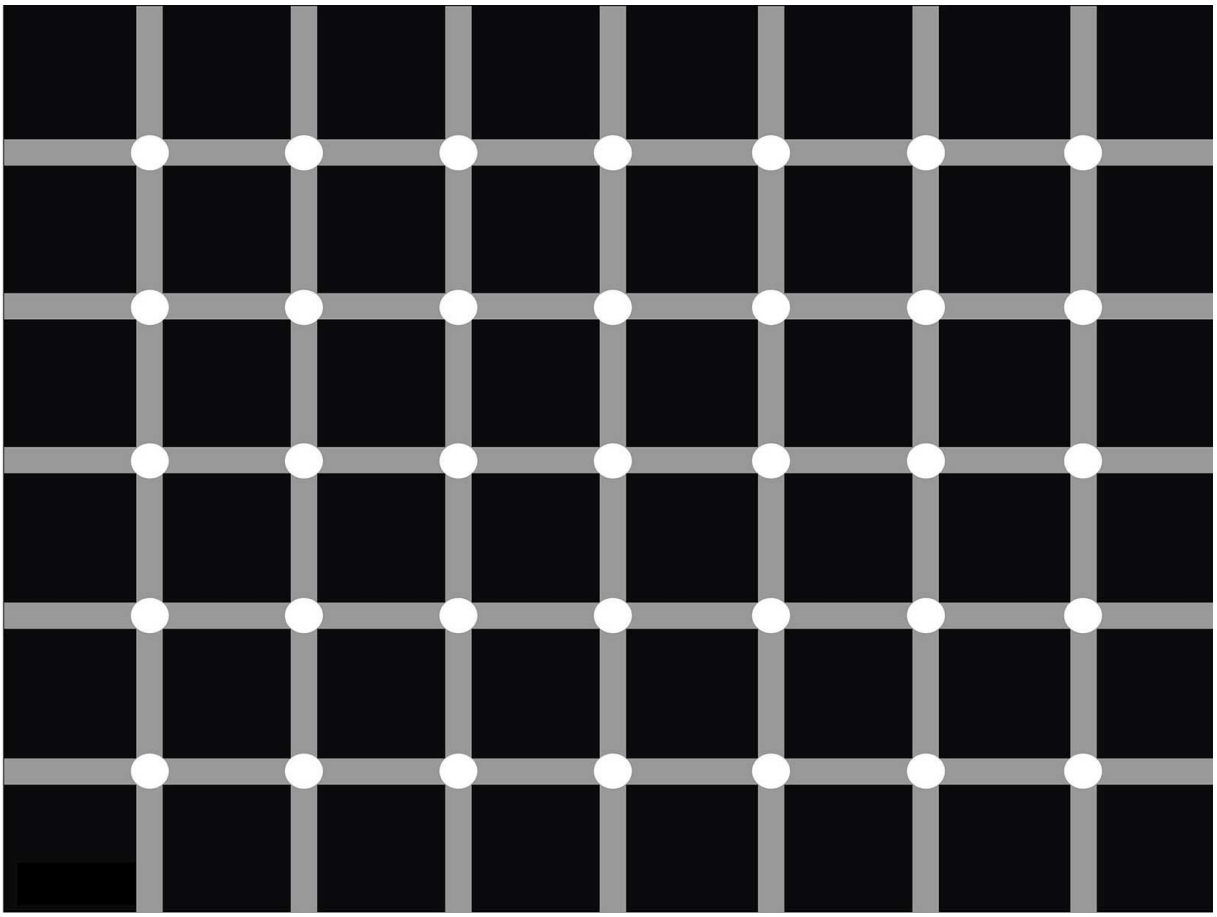

"Thus, studying only photon flux and ignoring perception cannot lead us to an understanding of how camouflage works"

How Camouflage Works - Merilaita, Scott-Samuel, & Cuthill, (2017)

Chapter 4 - Context dependant luminance contrast sensitivity in a coral reef fish (*Rhinecanthus aculeatus*)

4.1 Abstract

Achromatic (luminance) vision is used by animals to perceive motion, pattern, space and texture. The perception of luminance contrast is complex and is affected by contextual changes in spatiotemporal and spatiochromatic aspects. However, studies investigating how such changes influence perception in non-human animals are limited. Luminance contrast sensitivity thresholds obtained from a variety of behavioural contexts are often poorly standardised, and then applied uniformly across a diverse range of perceptual contexts and visual systems to make conclusions on the ecology of visual signals. However, the use of such a single threshold ignores the influence of the perceptual context on luminance contrast perception. Furthermore, luminance contrast sensitivity thresholds are often estimated solely based on the quantum catch and noise levels of photoreceptors using colour vision modelling, such as the Receptor Noise Limited model (RNL). However, the suitability of the RNL model to describe luminance contrast perception remains poorly tested, despite its increasing use in studies on the design, function and evolution of visual signals.

We investigated the ability of the RNL model to describe luminance discrimination thresholds of triggerfish (*Rhinecanthus aculeatus)* discriminating relatively large achromatic stimuli (spots) against uniform achromatic visual backgrounds of varying absolute and relative luminance contrasts in both a detection (detect a spot) context and a 'discrimination' (odd one out) context using a noisy achromatic background. The RNL model was not able to reflect threshold scaling across scenarios as predicted by the Weber-Fechner law, highlighting limitations in the use of the RNL model to quantify luminance contrast perception. Our results suggest there are differences in psychophysical thresholds between the discrimination of objects that are darker or brighter than their visual background (detection) or identically shaped distractors (discrimination), largely agreeing with the Weber-Fechner law regarding threshold scaling as a result to overall luminance of a visual scene. Thus, our results confirm that luminance contrast perception is complex, and luminance discrimination thresholds obtained in one context may not be applicable to others.

Keywords: Receptor Noise Limited Model, experimental psychophysics, perceptual thresholds, visual ecology.

4.2 Introduction

The perception of chromatic (colour) and achromatic (luminance) information from the surrounding environment enables animals to perform complex behaviours such as navigation, mate choice, territorial defence, foraging and predator avoidance. Chromatic information is largely used to assess the spectral composition and quality of objects or other organisms (Osorio & Vorobyev, 2008; Lotto, Clarke, Corney, & Purves, 2011), whereas achromatic information is predominantly used for object grouping, pattern and texture detection, figure-ground segregation, and the perception of motion and depth (Elder & Sachs, 2004; Gilchrist, 2008; Elder & Velisavljević, 2009; Gilchrist & Radonjić, 2009; Anderson, 2011; Brooks, 2014).

Behavioural experiments to examine colour and luminance discrimination thresholds are important to enable inferences on the perception of visual information by non-human observers. However, such thresholds are impacted by spatiochromatic and spatiotemporal properties of a visual scene, as the perception of colour, pattern, luminance and motion interact when low-level retinal information is processed along pathways in the visual cortex (Monnier & Shevell, 2003; Shevell & Kingdom, 2008; Shapley & Hawken, 2011). For example, the perception of luminance contrast in animals is influenced by absolute and relative brightness (perceived illumination) and lightness (perceived reflectance), in addition to various spatial and temporal properties, such as depth perception, adaptation, stimulus geometry, viewer expectation of stimulus position, and shape of a stimulus (Craik, 1938; Hochberg & Beck, 1954; Adelson, 1993; Heinemann & Chase, 1995; Eagleman, Jacobson, & Sejnowski, 2004; Corney & Lotto, 2007; Gilchrist & Radonjić, 2009; Kurki, Peromaa, Hyvärinen, & Saarinen, 2009; Kingdom, 2011; Lind, Sunesson, Mitkus, & Kelber, 2012; Pelli & Bex, 2013). The influence of post-photoreceptor and particularly post-retinal neuronal processing on luminance perception are often illustrated by visual illusions. In simultaneous contrast illusions, squares of equal intensity appear to differ in brightness due to the surrounding intensity: a square surrounded by a darker grey appears

brighter, whereas a square surrounded by a lighter achromatic background appears darker (Adelson, 2000; Shapiro & Todorovic, 2017, Fig. 4.1). We must understand the influence of such perceptual context sensitivity to the perception of visual information to investigate the design, function and evolution of animal visual signals.

The perception of achromatic information may follow different processing pathways depending on the task. For example, detection tasks require an animal to identify the mere presence or absence of a stimulus, while a discrimination task might require an individual to perceive a difference between identically shaped stimuli of differing intensity, either from memory or adjacent contrast (Sagi & Julesz, 1984; Laming, 1988; Gescheider, 1997; Straube & Fahle, 2011). Detection is thought to be perceptually simpler, mediated by pre-attentive, parallel processing and perceptual learning. Whereas discrimination can be a serial process requiring attention (Sagi & Julesz, 1984; Laming, 1988; Gescheider, 1997; Straube & Fahle, 2011) and conceptual learning (Gordon, 2004). However, the terms discrimination and detection are often used interchangeably with a moderate level of confusion in the literature. Problems can arise from both a mix-up of terminology (referring to discrimination when actually meaning detection) or using discrimination thresholds to assess the detectability of objects (e.g. Rodriguez-Morales et al., 2018). In this study, we refer to the task of discriminating a stimulus from its background as a detection task, as this reflects a common use of the achromatic contrast modelling in visual ecology, most prominently when quantifying the efficiency of animal camouflage (e.g. Troscianko et al., 2016).

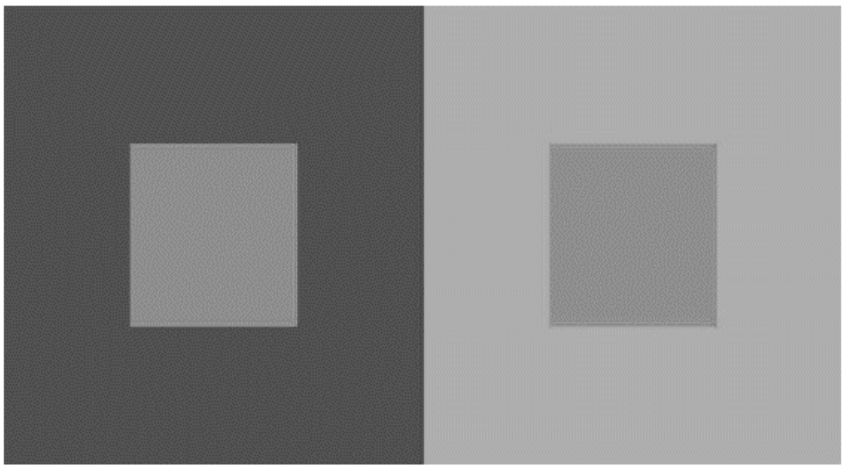

Figure 4.1: The simultaneous contrast effect. The left square appears brighter than the right one as a result of the background contrast against which they are viewed. From Adelson, 2000.

The impact of such context dependant processing on psychophysical thresholds remains largely unstudied in non-human animals (but see Lind, 2016 and Price et al., 2019). However, evidence from human studies suggests that luminance thresholds for detection are often, although not always, lower than those for more complex discrimination tasks (Furchner, Thomas, & Campbell, 1977; Bradley & Ohzawa, 1986; Gescheider, 1997; Purves, Lotto, Williams, Nundy, & Yang, 2001; Monnier & Shevell, 2003; Straube & Fahle, 2011).

Luminance contrast of objects against their visual background or between objects can be measured in a number of different ways, including Michelson contrast (MC), Weber contrast (WC) and Root Mean Square (RMS) (Moulden, Kingdom, & Gatley, 1990; Vorobyev & Osorio, 1998; Bex & Makous, 2002). While MC is commonly used to describe the contrast between two comparably sized objects or sine gratings (Bex & Makous, 2002; Pelli & Bex, 2013), the WC, particularly popular is psychophysics, is designed to describe the contrast of an object against a dominating background, accounting for the Weber-Fechner law which states that psychometric thresholds scale with stimulus intensity at a constant ratio, the so-called Weber fraction (Treisman, 1964; Norwich, 1987; Dzhafarov & Colonius, 1999). In animals, luminance discrimination thresholds have traditionally been determined using MC (e.g. Scholtyssek *et al.*, 2008; Lind et al., 2013) and (more interestingly) WC by using behavioural experiments. Human discrimination thresholds are between 0.11 and 0.14 WC (Cornsweet & Pinsker, 1965), which is similar to seals (0.11-0.14 WC) (Scholtyssek et al., 2008; Scholtyssek & Dehnhardt, 2013). Other animals have poorer discrimination capabilities, such as birds (0.18-0.22 WC) (Lind et al., 2013), dogs (0.22-0.27 WC) (Pretterer, Bubna-Littitz, Windischbauer, Gabler, & Griebel, 2004), manatees 0.35 WC (Griebel & Schmid, 1997) and horses (0.42- 0.45 WC) (Geisbauer, Griebel, Schmid, & Timney, 2004).

Behavioural experiments to validate perceived intensity of the luminance contrast by an animal viewer are often not possible, especially when studying non-model organisms. This can be due to logistic restrictions, i.e. inability to obtain and/or keep the animal of interest in captivity, as well as behavioural restrictions, i.e. inability of getting a specific animal to perform tasks. Therefore, the ‘Receptor Noise Limited’ (RNL) model (Vorobyev & Osorio, 1998) has been adopted as a means of estimating whether luminance contrast is perceivable to a signal receiver, both within and between animal colour patterns, or between animals and their backgrounds (Siddiqi et al.,

2004). The RNL model assumes that signal discrimination is limited by noise originating in the receptors (Vorobyev & Osorio, 1998; Vorobyev et al., 2001). It was originally designed to estimate when a signal receiver could discriminate between two colours that were spectrally similar, adjacent, of fixed size and luminance, and close to the achromatic point. To do so, the model calculates the responses of colour opponent channels in the context of relative photoreceptor abundance in the retina and corresponding photoreceptor noise while disregarding the stimulation and confounding effects of luminance contrast perception. The point at which the contrast between two stimuli surpasses a behaviourally determined threshold (e.g. 75% correct choice in a pairwise choice paradigm) is then expressed as a 'Just Noticeable Difference' (JND) corresponding to a Euclidian distance (ΔS) in an *n*-dimensional space, where *n* is the number of colour or luminance processing channels (Hempel de Ibarra et al., 2001). The model predicts a JND is equal to 1 ΔS if all model assumptions are met (Vorobyev & Osorio, 1998; Vorobyev et al., 2001).

The RNL model has been used to assess luminance contrast in a large number of studies, expanding on its initial purpose of colour contrast modelling (e.g. Spottiswoode & Stevens, 2010; Stoddard & Stevens, 2010; Troscianko & Stevens, 2015; Marshall, Philpot, & Stevens, 2016). However, the neuronal pathways leading to the perception of luminance contrast vary significantly from those involved in the perception of colour contrast. For example, the pronounced context sensitivity of luminance contrast perception is partly due to the fact that achromatic vision in vertebrates lacks a process as potent as colour constancy (Wallach, 1948; Land, 1986; Kelber et al., 2003; Osorio & Vorobyev, 2008), which enables the perceived color of objects to remain relatively constant under varying illumination conditions (but see Lotto & Purves, 2000; Simpson *et al.*, 2016).

Therefore, assuming receptor noise levels to be the limiting factor shaping both chromatic and achromatic contrast perception, behavioural validations of perceptual distances calculated using the RNL model are required in various visual contexts (e.g. Olsson, Lind, & Kelber, 2018 but see Skorupski & Chittka, 2011; Vasas, Brebner, & Chittka, 2018). Furthermore, Olsson et al. (2018) have suggested a conservative threshold of up to 1JND = 3ΔS for colour discrimination, as both parameter choice and behavioural threshold validation are often difficult. The use of such conservative chromatic discrimination thresholds in perceptually complex contexts has recently been supported by empirical work (Cheney et al., 2019; Escobar-Camacho et al., 2019;

Sibeaux, Cole, et al., 2019a). However, no empirical evidence exists for choosing conservative luminance (achromatic) contrast thresholds using the RNL model.

In this study, we performed behavioural experiments with triggerfish, *Rhinecanthus aculeatus*, to determine luminance discrimination thresholds in a foraging task using large stimuli (spot 1.6 cm diameter) under well-illuminated conditions. We trained fish to both a detection and a discrimination task. For the detection task fish were required to locate a target spot randomly placed on an A4 sized homogenous, achromatic background from which the spot differed only in luminance and peck it to receive a food reward. The discrimination task required the animals to discriminate the odd-one-out among four identically shaped achromatic, non-adjacent stimuli presented against a noisy achromatic background. Luminance discrimination and detection thresholds were measured for both increasing and decreasing luminance, on both a relatively bright and a dark background. We report thresholds in terms of Michelson and Weber contrast, but then translate these thresholds into achromatic ΔS using the log transformed RNL model, as per Siddiqi et al. (2004).

4.3 Materials and Methods

4.3.1 Study Species

We used triggerfish *Rhinecanthus aculeatus* (n = 15), which ranged in size from 6 to 16 cm (standard length, SL). This species inhabits shallow tropical reefs and temperate habitats throughout the Indo-Pacific and feeds on algae, detritus and invertebrates (Randall, Allen, & Steene, 1997). They are relatively easy to train for behavioural studies (e.g. Green et al., 2018), and their visual system has been well-studied (Pignatelli et al., 2010; Cheney et al., 2013; Champ et al., 2014, 2016). They have trichromatic vision based on one single cone, containing short-wavelength visual pigment (photoreceptor λ_{max} = 413 nm); and a double cone, which houses the medium-wavelength pigment (photoreceptor λ_{max} = 480 nm) and long-wavelength pigment (photoreceptor λ_{max} = 528 nm) (Cheney et al., 2013). The double cone members are used independently in colour vision (Pignatelli et al., 2010), but are also thought to be used in luminance vision (Siebeck et al., 2014), as per other animals such as birds and lizards (Lythgoe, 1979).

Fish were obtained from an aquarium supplier (Cairns Marine Pty Ltd, Cairns), shipped to The University of Queensland, Brisbane and housed in individual tanks of 120L (W: 40cm; L: 80 cm, H: 40cm). They were allowed to acclimatise for at least one week before training commenced. Experiment 1 was conducted in September-November 2017 and Experiment 2 was conducted in March-April 2018. All experimental procedures for this study were approved by the University of Queensland Animal Ethics Committee (SBS/077/17).

Aquaria were divided in two halves by a removable grey, opaque PVC partition. This enabled the fish to be separated from the testing arena while the stimuli were set up. Stimuli were displayed on vertical, grey, PVC boards and placed against one end of the aquaria. Tanks were illuminated using the same white LED lights (EcoLight KR96 30W) used for stimulus calibration. To ensure equal light levels in all tanks, sidewelling absolute irradiance was measured using a calibrated OceanOptics USB2000 spectrophotometer, a 180˚ cosine corrector and a 400nm optic fibre cable fixed horizontally in the tank (Fig. S4.4, Appendix C).

We randomly allocated fish into two groups prior to training. For the detection scenarios (Experiment 1), group 1 (n = 7) had to find and peck at target spots that were brighter (T_{bd}) or darker (T_{dd}) than a relatively dark background (Fig. 4.2A, table 4.1); group 2 (n = 8) had to find and peck target spots that were brighter (T_{bb}) or darker (T_{db}) than a relatively bright background (Fig. 4.2B, Table 4.1). These groups (the same fish) were then subsequently used for the discrimination experiment (Experiment 2) where group 1 (n = 7) had to find and peck at target spots that were brighter (D_{bd}) or darker (D_{dd}) than relatively dark distractors (Fig. 4.2C, table 4.1); group 2 (n = 7) had to find and peck target spots that were brighter (D_{bb}) or darker (D_{db}) than relatively bright distractors (Figure 4.2D, Table 4.1). The fish were kept in the same groups to maximise the potential for the fish to associate a specific grey level (background for detection = distractors for discrimination) as unrewarded and therefore facilitate training. Fish were not trained for the discrimination task first (resulting in a truly crossed experimental design) due to the natural succession in task complexity from detection to discrimination and training.

4.3.2 Stimulus Creation and Calibration

We used a custom programme in Matlab (MathWorks, 2000) to create the stimuli (Fig. 4.2, Table 4.1) for both the detection and the discrimination experiments. This programme allowed us to specify the RGB values of the background and target spot, and randomly allocate the target spot (1.6cm diam) to a position on the background. The size of spot was chosen to be well within the spatial acuity of *R. aculeatus* (Champ et al., 2014) and could be easily resolved by the fish from anywhere in their aquaria. Stimuli, distractors and backgrounds were printed on TrendWhite ISO 80 A4 recycled paper using a HP Laserjet Pro 400 color M451dn printer. This specific type of paper was used to ensure greys were as close to the achromatic point as possible as bleached paper is whitened, causing a reflectance peak at around 350-450nm. For the detection task (Experiment 1), stimuli were then laminated using matte laminating pouches to try to reduce specular reflection (Fig. 4.2 A & B). Variation in stimulus contrast is a result of variation in print outs as well as a consequence of the method used to identify suitable RGB values.

For the discrimination experiment (Experiment 2), we used an 'odd one out' paradigm (Fig. 4.2 C & D), in which fish were required to locate the spot which differed from three distractors. This was chosen over a traditional pairwise choice contrast (e.g. Goldsmith & Butler, 2003; Olsson, Lind, & Kelber, 2015) to simulate a level of complexity found in nature and allow simultaneous testing of multiple target stimuli without re-training (Cheney et al., 2019). The four choices were displayed against a noisy background (Fig. 4.2 C & D) formed by randomising pixel intensity (pixel size of 1mm^2; resolvable by the fish from 16cm away), to be one of 255 (8-bit) RGB grey levels, ranging from 0/0/0 (black) to 255/255/255 (white). Target and distractor stimuli were printed using the previously described Matlab programme, laminated, cut and glued onto the noisy background. This ensured that the edge of any given stimulus or distractor could be easily detected by the fish while simulating achromatic noise comparable to that found in a shallow underwater environment (Matchette, Cuthill, & Scott-Samuel, 2019). Any stimuli with detectable scratches or damage were replaced.

To ensure all stimuli were achromatic, reflectance measurements were plotted in colour space as per Cheney et al. (2019). Target and background colours were < 1 ΔS from the achromatic locus in the RNL colour space as per equations 1-4 in Hempel de Ibarra et al. (2001). Photoreceptor stimulation was calculated using spectral

sensitivities of triggerfish from Cheney et al. (2013). Measures of photoreceptor noise are not available in this species, therefore we assumed a cone ratio of 1:2:2 (SW:MW:LW) with a standard deviation of cone noise (univariant Weber fraction) of 0.05 as per (Champ et al., 2016; Cheney et al., 2019). The cone abundance was normalised relative to the LW cone, which resulted in channel noise levels of 0.07:0.05:0.05 (SW:MW:LW).

We quantified luminance contrast using calibrated digital photography (Stevens et al., 2007), taking pictures of each stimulus combination with an Olympus E-PL5 Penlight camera fitted with a 60mm macro lens (see page 188 in Appendix C). Two EcoLight KR96 30W white LED lights were used to provide even illumination between 400-700nm wavelength (page 187 in Appendix C). Pictures were analysed using the 'Multispectral Image Calibration and Analysis' (MICA) Toolbox (Troscianko & Stevens, 2015) to calculate cone capture quanta of the double cone. The double cone stimulation was calculated as the average stimulation of the medium-wavelength (MW) and long-wavelength (LW) cone as per Pignatelli *et al.* (2010). We used a spatial acuity estimation of 2.75 cycles per degree (Champ et al., 2014) at 15cm viewing distance using AcuityView (Caves & Johnsen, 2017) implemented in MICA's QCPA package (van den Berg et al., 2020).

Stimulus contrast was measured as Michelson contrast using the MICA derived cone catch values of the double cones. The stimuli contrasts were evenly spaced around an area of interest in which the threshold was expected to lie, according to pilot trials (van den Berg, unpublished data). Weber contrast of the thresholds was calculated as $\Delta I_t/I_s$ (where ΔI_t is the stimulus contrast at threshold and I_s is the intensity of the distractor or background respectively) as per Lind et al., 2013. Achromatic ΔS values were calculated according to equation 7 in Siddiqi et. al (2004) (Eq. 4.1).

$$\Delta S = |\Delta f_{dbl}/\omega| \qquad \textbf{Equation 4.1}$$

Where Δf_{dbl} describes the contrast in von Kries corrected double cone stimulation between the stimulus (f_t) and its background/distractors (f_b), calculated as

per equation 4 in Siddiqi *et. al* (2004) (Eq. 4.2) in relation to the weber fraction (ω) of the double cone channel.

$$\Delta f_{dbl} = ln(f_t) - ln(f_b). \qquad \textbf{Equation 4.2}$$

Each scenario (e.g. T_{bb} or D_{db}) consisted of 6 stimuli ranging from very easy (positive control) to very hard (negative control) contrast detectability (Table 4.1). Each of these stimuli would then be tested as specified below for each experiment.

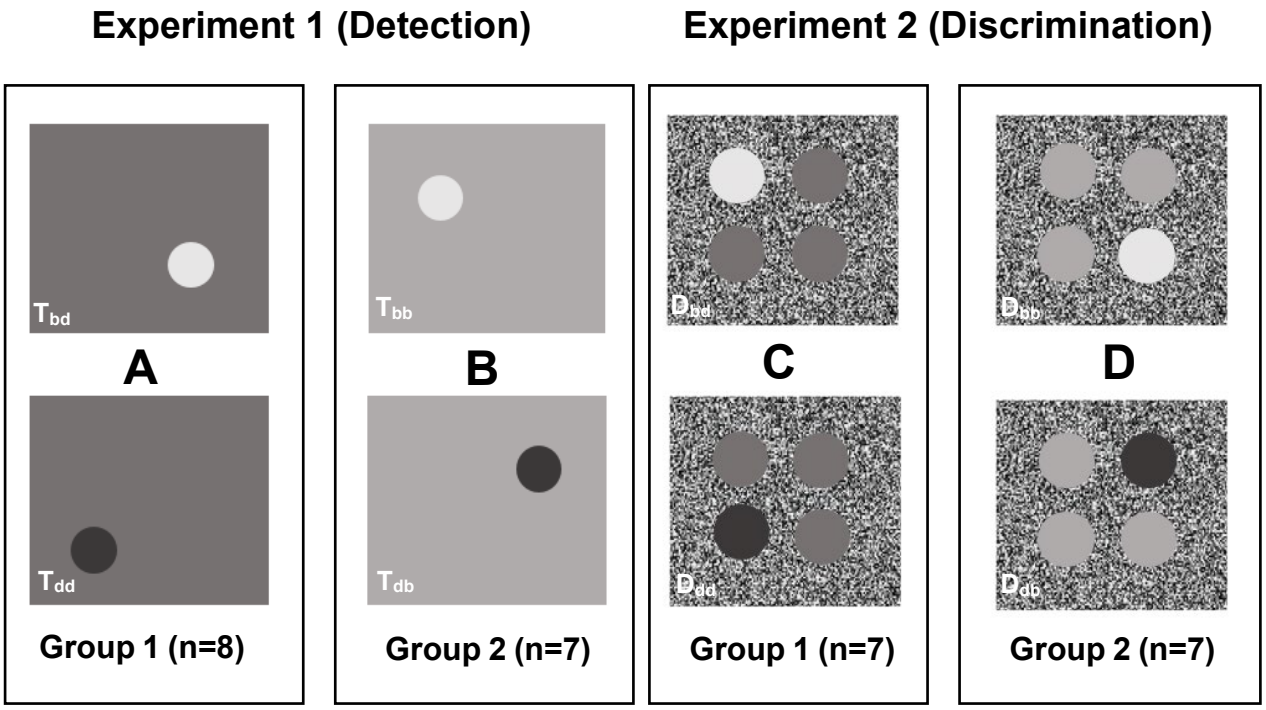

Figure 4.2: Schematic representation of stimulus for experiment 1: Detection scenarios (A&B) and experiment 2: Discrimination scenarios (C&D) treatment groups. Figures are not to scale. The contrasts displayed here are the maximum contrast for each scenario. The number of fish used for each scenario are indicated in brackets.

	Dark Background (Group 1) [ΔS] / [Michelson Contrast]		Bright Background (Group 2) [ΔS] / [Michelson Contrast]	
	Detection ($n=8$, T_{bd})	**Discrimination ($n=7$, D_{bd})**	**Detection ($n=7$, T_{bb})**	**Discrimination ($n=7$, D_{bb})**
Bright Spot	15.34 / 0.37*	14.28 / 0.34*	17.87 / 0.42*	17.36 / 0.41*
	5.98 / 0.15	7.18 / 0.18*	8.84 / 0.22	7.74 / 0.20*
	4.82 / 0.12	5.83 / 0.14	5.19 / 0.13	6.92 / 0.19
	3.94 / 0.10	5.12 / 0.13	3.98 / 0.10	3.29 / 0.08
	2.34 / 0.06	4.76 / 0.12	1.82 / 0.05	1.47 / 0.04
	0.58 / 0.01	3.80 / 0.09	0.84 / 0.02	1.31 / 0.03
Dark Spot	9.26 / 0.23*	10.23 / 0.25*	15.51 / 0.37*	21.78 / 0.50*
	6.55 / 0.16	8.70 / 0.21*	7.99 / 0.20	8.60 / 0.21*
	5.04 / 0.13	4.59 / 0.11	5.92 / 0.15	6.42 / 0.16
	3.03 / 0.08	3.69 / 0.09	4.65 / 0.12	6.05 / 0.15
	1.24 / 0.03	1.70 / 0.04	2.46 / 0.06	5.64 / 0.14
	0.89 / 0.02	0.61 / 0.02	1.58 / 0.04	2.87 / 0.07

Table 4.1: Summary of the contrasts used for training (*) and trials for both groups in ΔS and Michelson contrast. Contrasts were calculated as per equations 4.1 & 4.2.

4.3.3 Experiment 1: Detection scenario

Fish were trained to peck at the target dot using a classic conditioning approach. First, fish were trained to pick a small piece of squid off a black or white (randomly chosen) spot (1.6 cm diam) on the grey background corresponding to the treatment group ('bright' background/distractor or 'dark' background/distractor, Table 4.1). We trained the fish to detect target spots on both brighter and darker backgrounds/distractors to reduce hypersensitivity through anticipation by applying the principle of 'constant stimuli' thresholds (Laming & Laming, 1992; Colman, 2008; Pelli & Bex, 2013). This approach intended to produce thresholds more closely related to a natural context as prey items in the natural environments can be both brighter or darker than their natural background. Second, once fish consistently removed the food reward from the black and white target spots, a second food reward was immediately presented from above using forceps. Once fish were confident with this, the final stage of training was a food reward given from above once they had tapped at the target stimulus (without food). For both experiments, training consisted of up to two sessions per day, with six to ten trials per fish/session. Fish moved to the testing phase when fish were successful in performing the task in > 80% trials over at least 6 consecutive sessions. A trial was considered unsuccessful if the fish took longer than 90 seconds (timeout) to make a choice or if it pecked at the background more than twice. Testing was suspended for the day if the fish showed multiple timeouts for training contrasts, assuming the fish was not motivated.

As with the training of the animals, the target spots were presented in a random position against an A4 sized achromatic background in two sessions per day consisting of 6-10 trials per session and fish, depending on the appetite of the fish. The trials for each session were chosen pseudo-randomly from all possible contrasts, thus fish were presented with both darker and brighter spots compared to their background/distractor in each session. For the 'detection' scenarios each stimulus was presented a minimum of 6 times with higher levels of replication for intermediate levels of contrast. For both, detection and discrimination, motivation was considered low when the animal did not engage in the trial immediately (>10s) and, if this occurred, trials were ceased for that fish until the next session. A trial was considered unsuccessful if the fish took longer than 90 seconds (timeout) to make a choice or if it pecked at the background more than twice ('detection') or once ('discrimination'). Wrong pecks were recorded and time

to detection was recorded as the time between the moment the fish moved past the divider and the successful peck at the target spot.

4.3.4 Experiment 2: Discrimination scenario

Following the detection scenario trials, seven out of the eight fish from group 1 (dark background, Table 4.1) and all seven fish from group 2 (bright background, Table 4.1) were retrained to complete the discrimination experiment. Retraining was conducted by first habituating the fish to the noisy background and then, following the same stepwise approach from the detection experiment, training the fish to find the odd one out using black and white target stimuli against the grey distractors for the respective scenarios (Table 4.1). Habituation to the noisy background was achieved by placing a noisy background into the tanks for several hours at a time and gradually switching a uniform background with the new noisy background in training. Fish easily adapted to the new task and continued to peck the odd spot to receive a food reward. To ensure fish did not learn specific contrast but instead learnt that the task was an odd-one-out scenario, an easy intermediate contrast was added to the training stimuli resulting in each fish being trained with two easy-to-discriminate bright spots and two dark spots (Table 4.1).

For the discrimination scenarios each target intensity level was presented between 9 and 25 times per fish. We carried out more trials for target intensity levels close to the threshold, and fewer towards the asymptotes accounting for a higher variability in success rates closer to threshold. Using four possible choices reduced the chance of the animals randomly locating the target spot from 50% compared with a paired choice test, therefore we allowed fish one wrong peck (2/4= 50%), as per Pelli & Bex (2013).

4.3.5 Statistical Analysis

Psychometric curves were fitted to the data (% correct choice per stimulus vs. stimulus contrast measured in Michelson contrast) using the R package *quickpsy* (Linares & Lopez-Moliner, 2015; R Core Team, 2015). Using these curves, we interpolated the 50% correct choice thresholds with a 95% confidence interval. We also provide a 30% (less conservative) correct choice threshold for the detection task because the chance

of selecting the correct location by chance, was extremely low (<2%) which makes a 50% correct choice threshold very conservative (pages 186 to 187 in Appendix C).

The best model fit was determined using AIC as per Yssaad-Fesselier & Knoblauch (2006) and Linares & Lopez-Moliner (2015). Thresholds between summed graphs for each scenario were compared as per Jörges et al. (2018) using the Bootstrap (Boos, 2003) implemented in *quickpsy* (100 permutations). The Bonferroni method (Bland & Altman, 1995) was used to adjust the significance level of the confidence intervals to 1-0.05/n, with n corresponding to the number of comparisons.

4.4 Results

4.4.1 Experiment 1: Detection Scenarios

We conducted a total of 1365 detection trials across all fish and scenarios, resulting in a mean number of 7.6 trials/fish/stimulus. The total success rate was 68.5% across all 24 stimuli with a median (±sd) time to detection of 3.1±12.6 seconds with the fastest success at 0.3 seconds and the slowest at 90.0 seconds. The median time for successful detection was similar across all scenarios (±sd): T_{dd} = 2.9±12.9 seconds, T_{bd} = 2.8±10.8 seconds, T_{db} = 3.1±13.5 seconds, T_{bb} = 3.22±12.58 seconds. Detection thresholds (50% correct choice) for all scenarios are presented in Figure 4.3 and Table 4.2. The sum of AIC across all four detection scenarios (fit=cumulative normal) was 162.4 (T_{dd}=24.2, T_{bd}=50.8, T_{bb}=50.1, T_{db}=37.3). When comparing thresholds within groups, the detection thresholds for group 1 (dark background) were not significantly different from each other (T_{bd} - T_{dd} = 0.01 MC, CI_{diff} [0 - 0.02]) whereas the detection thresholds for group 2 (bright background) were significantly different from each other (T_{db} - T_{bb} = -0.03 MC, CI_{diff} [0.02 – 0.04]).

When comparing between groups 1 and 2, thresholds for detecting a dark spot differed significantly between a dark and a bright background (T_{db} - T_{dd} = 0.01 MC, CI_{diff} [0-0.02]) as did the threshold for detecting a bright spot (T_{db} - T_{dd} = 0.03 MC, CI_{diff} [0.02-0.04]). However, the threshold for detecting a bright spot on a bright background was not significantly different from detecting a dark spot on a dark background (T_{bb} - T_{dd} = 0.04 MC, CI_{diff} [0.03-0.05]). Finally, the thresholds for the exact inverse of the scenarios, detecting a bright spot on a dark background and vice versa, are not

significantly different from each other (T_{bd} - T_{db} = 0 MC, CI_{diff} [-0.01-0.01]) (Fig. 4.3 – 4.5, Table 4.2).

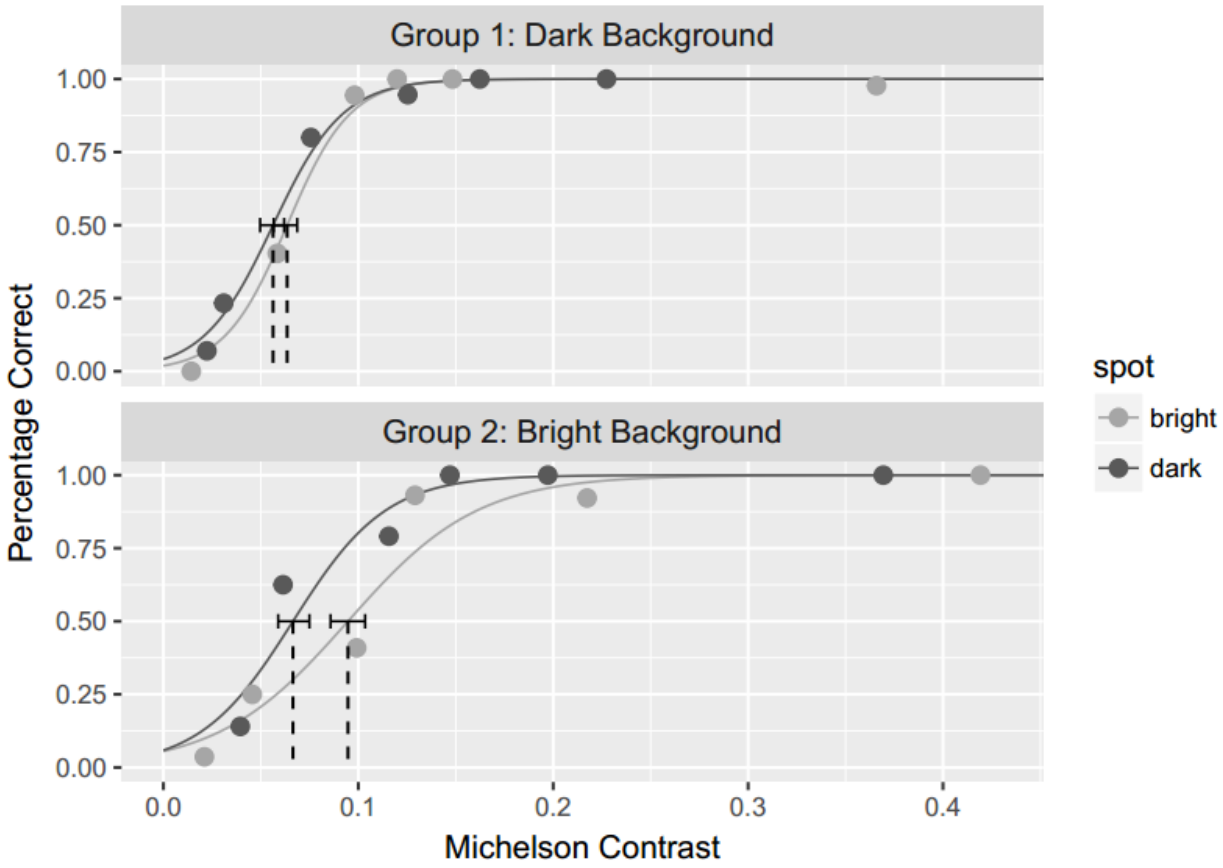

Figure 4.3: Logistic regression fitted to the detection data. Thresholds for each scenario in Michelson contrast, error bars represent the 95% confidence intervals.

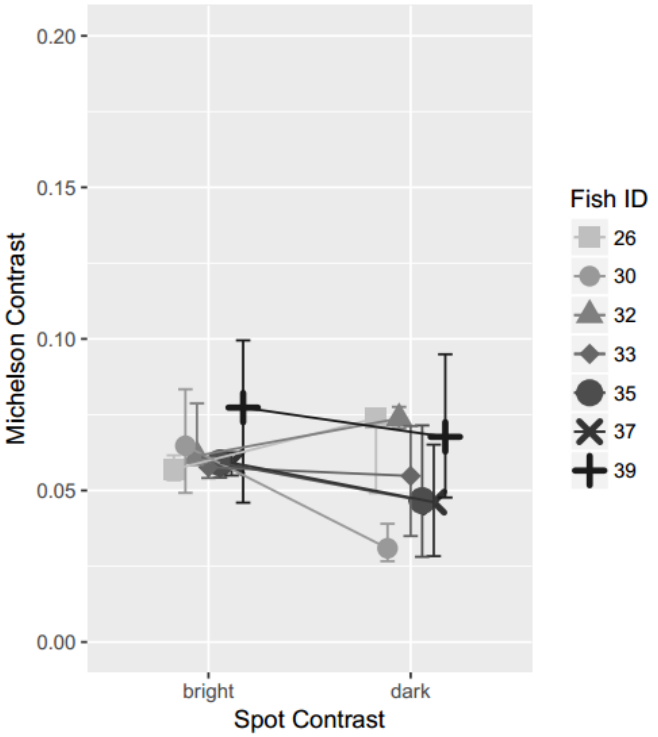

Figure 4.4: Individual detection thresholds of the dark background scenarios (group 1). Error bars represent the 95% confidence intervals.

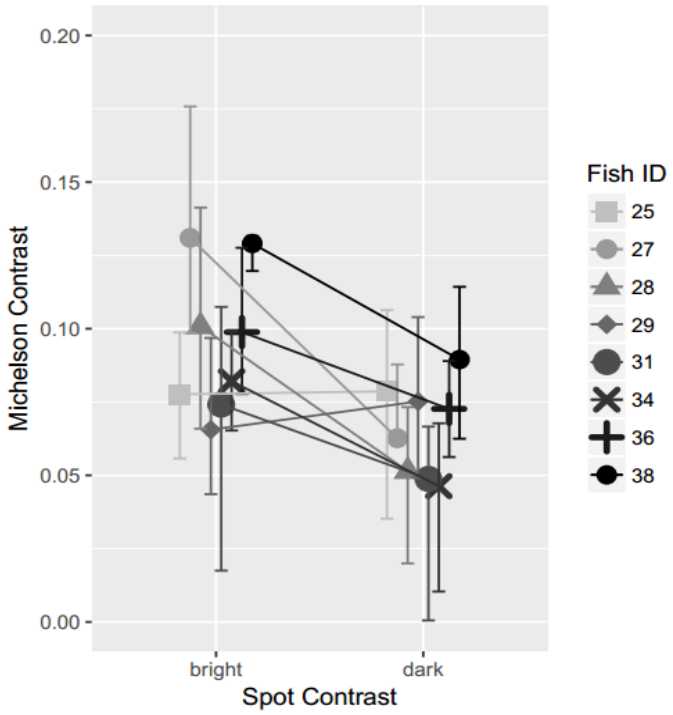

Figure 4.5: Individual detection thresholds of the bright background scenarios (group 2). Error bars represent the 95% confidence intervals.

Scenario	Michelson Contrast (95% CI)	Weber Contrast (95% CI)	ΔS (95% CI)
	0.06 (0.06-0.07)	0.31 (0.28-0.35)	2.54 (2.29-2.83)
	0.06 (0.05-0.06)	0.28 (0.24-0.31)	2.25 (1.96-2.51)
	0.09 (0.08-0.10)	0.32 (0.29-0.35)	3.80 (3.38-4.18)
	0.07 (0.06-0.07)	0.23 (0.20-0.25)	2.66 (2.32-2.98)

Table 4.2: Summary of results for the 50% correct choice threshold contrasts. Group 1 & 2 (dark & bright background) are indicated by bold borders.

4.4.2 Experiment 2: Discrimination Scenarios

At total of 3230 trials were conducted combined across group 1 (n=7) and 2 (n=7). Each stimulus was tested between 9 and 31 times per fish. The sum of AIC across all four detection scenarios (fit=cumulative normal) was 314.1 (D_{dd}=95.6, D_{bd}=62.8, D_{bb}=48.2, D_{db}=107). The results are shown and summarized in Figure 4.6 and Table 4.3. The threshold for discriminating a dark spot (D_{dd} & D_{db}) was not different between the different groups, nor was the threshold for discrimination a bright spot (D_{bd} & D_{bb}). All other threshold comparisons are significant (Fig. 4.6 – 4.8, Table 4.3).

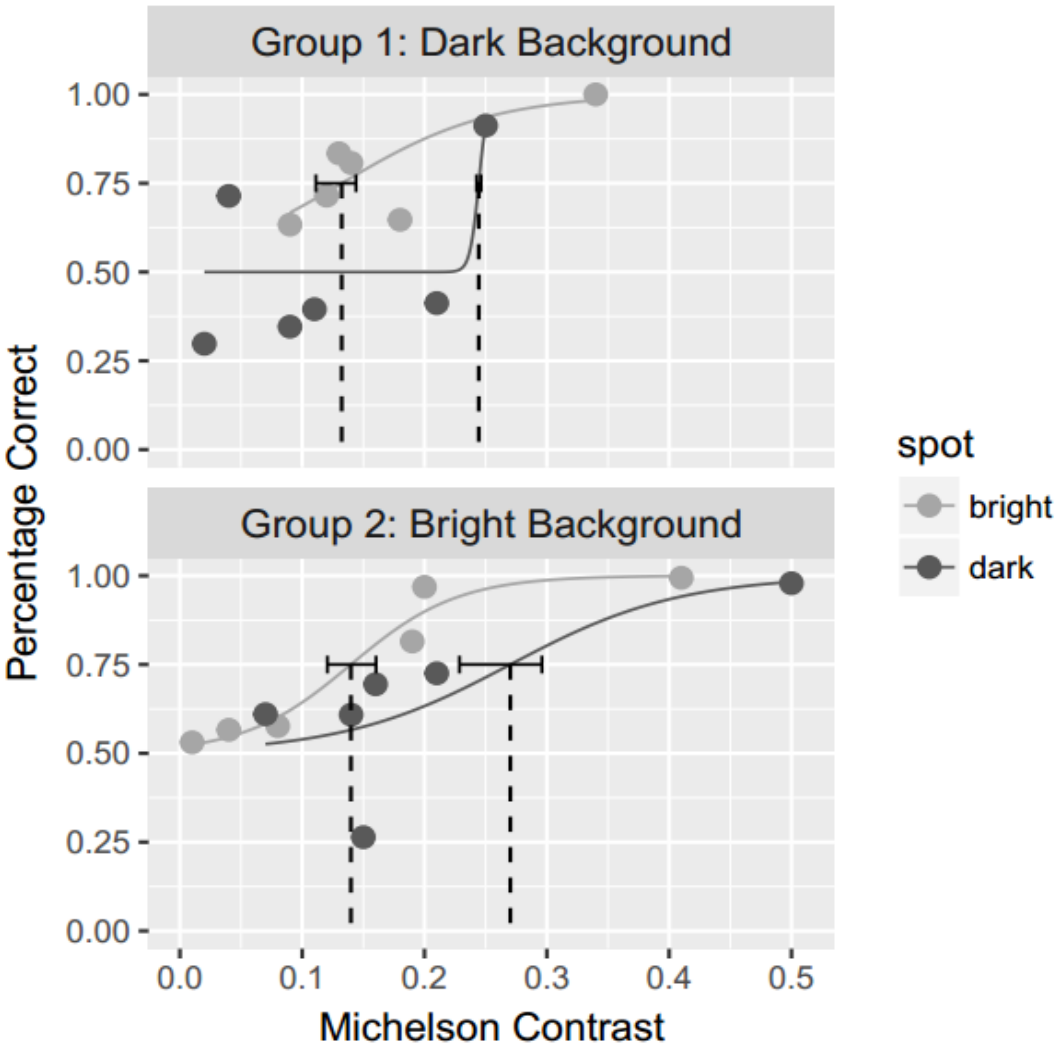

Figure 4.6: Logistic regression fitted to the discrimination data. Thresholds for each scenario in Michelson contrast, error bars represent the 95% confidence intervals. Note that the fit for these graphs is possibly not meaningful in case of the dark spot against a dark background due to poor fit.

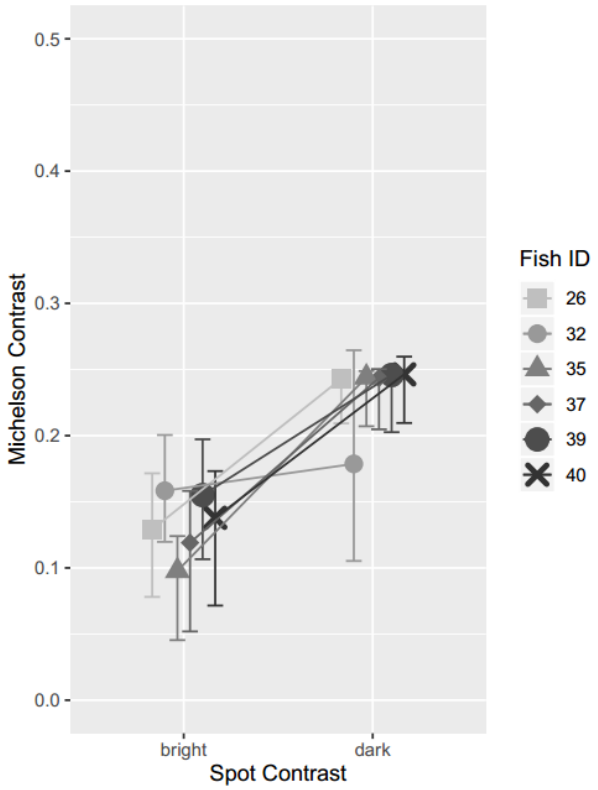

Figure 4.7: Individual discrimination thresholds of the dark background scenarios (group 1). Error bars represent the 95% confidence intervals.

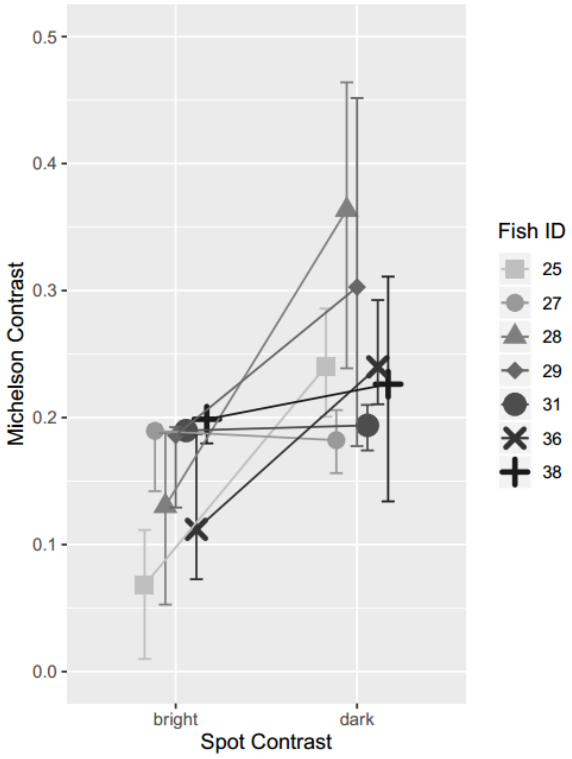

Figure 4.8: Individual discrimination thresholds of the bright background scenarios (group 2). Error bars represent the 95% confidence intervals.

Scenario	Michelson Contrast (95% CI)	Weber Contrast (95% CI)	ΔS (95% CI)
	0.13 (0.11-0.15)	0.67 (0.55-0.76)	5.35 (4.44 – 6.07)
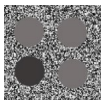	0.24 (0.23-0.25)	1.23 (1.14-1.23)	10.00 (9.20-10.01)
	0.14 (0.12-0.16)	0.46 (0.40-0.53)	5.48 (4.71-6.33)
	0.28 (0.24-0.31)	0.94 (0.8-1.04)	11.47 (9.99–12.73)

Table 4.3: Summary of the discrimination thresholds across the 'discrimination' experiments. Values are calculated relative to the luminance of the corresponding distractors.

4.5 Discussion

4.5.1 Preface

The results of this study suggest that there is a range of fundamental issues which need to be addressed prior to a detailed discussion. While the detection scenarios do not suffer from any major issues, this is not at all the case for the discrimination scenarios. For example, it seems as if only the 'bright spot against bright distractors' discrimination scenario has truly worked as intended (Fig. 4.6). However, its counterpart ('dark spot against bright distractors'), tested with the same animals at the same time (see Materials & Methods), shows a clear outlier (Fig. 4.6). The guess ratio of close to 25% suggests that all animals of group 2 have perceived the stimulus as different to its distractors and, as a result, pecking the distractors more often than it would be the case if the stimulus was not discriminable to them. However, we were not able to find out why the animals developed a systematic avoidance of that stimulus, despite vigorous re-testing and repeated replacements of the stimulus to exclude the possibility of any scratches or other distractions. The overall guess ratio of close to 50% suggests that all fish in group 2 have truly learned the concept of being rewarded for finding the odd one out. This proves that the concept of this study, in principle, is feasible. Furthermore, the data also suggests that the animals might have indeed remembered the position of a non-rewarded stimulus after a wrong first peck, making the overall guess rate slightly higher than 50%. To show this being the case could be an interesting future investigation into the cognitive abilities (e.g. counting, spatial and temporal memory capacities and decision making) of *R. aculeatus* in the context of variable reward and punishment contexts sensu Aurorès-Weber et al., (2010) and Howard et al., (2019).

The results from group 1 warrant far more caution than those from group 2 (Fig. 4.6). Despite having trained the fish to learn to identify the odd one out for the two most contrasting stimuli (Table 4.3) of each scenario, the results show that this did not lead to reliable stimulus discrimination under trial conditions. In fact, detailed analysis of our data suggests that this was the case right from the beginning of trials (rather than a gradual extinction of the learned behaviour). The 'dark spot against dark distractors' scenario suggests that the animals almost showed a preference for the distractors or possibly were even avoiding the rewarded stimulus, except for the most contrasting stimulus which was clearly preferred. This could suggest that the animals did not in

fact learn an ‘odd one out’ scenario but rather remembered that the most contrasting stimulus (or certain levels of grey) was always rewarded. This might have been influenced by interactions on contrast perception by the noisy background, i.e. if the fish used cues relative to the background intensity. Given the high numbers of trials, it could also hint at the fish not being hungry or motivated enough to make careful choices i.e. they got sloppy. Personal observations suggest this to be the case at least for some individuals. This could be prevented by reducing the amount of trials in combination with the introduction of punishing wrong choices using distasteful food rewards. Furthermore, the scenario shows a clear outlier for the second lowest contrast (Fig. 4.6). As this contrast is far too low to be readily detected by the animals this can only be explained by some systematic cue from the target stimulus other than its relative contrast to the distractors. This, in addition to issues with conceptual learning, could have been due to the way the stimuli were printed, laminated or glued, possibly hinting at issues with the general experimental design.

The ‘bright sport against dark distractors’ (D_{bd}) scenario seems to further hint at issues with experimental design. Given that the grey (RGB) values chosen for the scenarios were identical to the ones used in the ‘detection’ experiments it is surprising to see clear differences between the stimulus contrasts when comparing the discrimination and the detection stimulus contrasts, particularly the clumping of stimulus contrasts for the ‘bright spot against dark distractors’ (D_{bd}) scenario. This could be due to variation in prints. However, while that certainly might have been the case, deviations and variation is stimulus contrast could have been introduced by variation in lamination. Furthermore, despite extreme levels of care, the cutting, laminating and gluing of stimuli to the noisy backgrounds could have introduced cues or distractions such as variation in the amount of glue underneath or adjacent to stimuli, minute differences in the shape of the stimuli or differences in angle magnified by specular reflection when viewed underwater. Thus, given the tedious venture of calibrating luminance in a behavioural setup (as opposed to randomising luminance noise as if often done in colour vision experiments) we thoroughly discourage the use of printers for future studies and recommended to conduct research on luminance discrimination and detection thresholds using calibrated screens or projectors (e.g. Smithers, Roberts, & How, 2019). The use of calibrated screens would further help to truly randomise stimulus positioning. This could further be aided using more than just 3 distractors, i.e. by using an achromatic ishihara stimulus sensu Cheney et al., (2019).

4.5.2 'Detection' Scenarios

Our study demonstrates that for *Rhinecanthus aculeatus*, RNL luminance discrimination thresholds in a 'detection' scenario vary significantly (ΔS 2.25 - 3.80) according to the perceptual context in which they are measured. We found effects of both the background luminance as well as the target luminance on the ability of our animals to detect a large uniform achromatic stimulus on a uniform achromatic background. The magnitude of these effects agrees with the Weber-Fechner law with thresholds falling in a comparable range of Weber contrasts with a noticeable effect of the absolute target stimulus contrast, i.e. both bright spot scenarios have a more similar WC compared to each other (WC 0.23 – 0.28) in comparison to the dark spot scenarios (0.31 – 0.32), indicating both global (absolute luminance contrast) and local influences (relative luminance contrast) on luminance contrast perception.

The relationship of absolute (background + stimulus) and relative luminance (background vs. stimulus) contrast is not reflected when expressing thresholds as ΔS. This is a result of the equations used in Siddiqi et al. (2004). The exclusion of signal intensity is a fundamental assumption when calculating chromatic contrasts using the RNL (Vorobyev & Osorio, 1998) which has been designed to quantify contrast perception between two weakly chromatic stimuli viewed against an achromatic background. As a result, the RNL equations used by Siddiqi et al. (2004) calculate a relative comparison of two background adapted receptor responses without scaling the difference in photoreceptor stimulation between stimulus and background in relation to the overall brightness of a scene. Therefore, the commonly used RNL equations in Siddiqi *et al.* (2004) fail to reflect the Weber-Fechner law for the discrimination of a stimulus from its background, often described as a detection threshold. This directly contradicts Olsson et al. (2018) who clearly state that the achromatic RNL equations in Siddiqi et al. (2004) conform with the weber-Fechner law despite not showing any empirical proof for it (neither do the authors of the original study).

A possible approach to this problem is to use the Weber contrast as a guide as to what is detectable by a visual system. Thus, if the contrast of a stimulus against the average luminance response to its visual background (WC_S) is smaller than the WC at a conservative threshold (WC_T), then the stimulus is likely not detectable by a visual system (Eq. 4.3):

$$\Delta WC = \left|\frac{WC_S}{WC_T}\right| \qquad \textbf{Equation 4.3}$$

This approach could provide an elegant solution to the need to quantify luminance contrast detectability of large stimuli against varying levels of background luminance without the need for knowledge on photoreceptor abundances or noise. In fact, introducing receptor noise seems like an unnecessary complication given that the WC simply describes the behavioural proof of what an animal can do in a specific perceptual context. However, this implicitly requires behavioural validation of a threshold and therefore does not fulfil the function of the RNL model, which allows to draw conclusions without the need for such threshold validation. However, as we show, neither does the achromatic RNL model in the way it is currently used. Furthermore, while this solves the problem of scaling contrast sensitivity with absolute luminance, it does not account for the difference in detection between the dark spot and the bright spot scenarios, independently of background intensity i.e. the relative importance of local scaling at the level of a receptive field.

The difference in WC between dark and bright spots (Table 4.2) suggests intensity mediated luminance contrast sensitivity scaling at smaller spatial scales, i.e. edge detecting receptive fields. This would explain why the MC thresholds for the completely inverse scenarios (T_{bd} vs. T_{db}) are almost identical to each other despite having different WC (Which only accounts for the background intensity). To a receptive field which spans only a fraction of the stimulus surface these two scenarios would not be discriminable in terms of relative intensity contrast (MC). Furthermore, our results match findings that humans are consistently better at detecting darker stimuli (decrements) (e.g. Bowen, Pokorny, & Smith, 1989; Emran et al., 2007; Lu & Sperling, 2012), and has also been shown in non-human vertebrate (e.g. Baylor, Hodgkin, & Lamb, (1974) using turtles) and invertebrate visual systems (e.g. Smithers, Roberts, & How, (2019) using fiddler crabs). Research suggests that increasing and decreasing luminance changes are processed differently. Decrements are detected by off-centre ganglion cells, while increments are detected by on-centre ganglion cells (Schiller, Sandell, & Maunsell, 1986). Decrements are indicated by the depolarization of photoreceptors, whereas increments are detected as hyperpolarization (Baylor et al., 1974). For example, investigation of turtle photoreceptors has shown that decrements

result in much greater depolarization of photoreceptors, than the magnitude of hyperpolarization resulting from increments (Baylor et al., 1974).

However, any guesses on the specific mechanisms causing the observed difference in WC between the detection of a dark spot and a bright spot (or mathematical approximations thereof) are speculative. Further investigations will require substantial advances in the understanding of neurophysiological mechanisms underlying luminance contrast perception in *R. aculeatus*. These include knowledge on the detailed anatomy and receptor noise of double cone photoreceptors in *R. aculeatus,* the relative contribution of each double-cone member to luminance contrast sensitivity (Siebeck et al., 2014) as well as the precise mechanism by which photoreceptor stimulation is integrated in post-receptor structures such as edge detecting receptive fields. Behavioural experiments with closely related species with different retinal morphologies would be of interest to further investigate e.g. the role of retinal neuroanatomy on luminance contrast perception.

For now, we propose using the highest WC as a conservative threshold choice as the difference in WC seems constant across varying background luminance. However, this is a superficial (although efficient) fix and does not account for the effects of spatial frequency on luminance contrast sensitivity when discriminating objects against visual backgrounds. This is probably the most notable confounding effect on low-level processing of luminance contrast as a result of post-receptor lateral-inhibition (Veale et al., 2017). One possible approach would be the use of contrast sensitivity functions (CSF) to scale Weber fractions as a function of spatial frequency in a visual scene. However, given that these are determined using a perceptually different experimental setup (da Silva Souza et al., 2011) this should be investigated using context specific behavioural experimentation.

4.5.3 ‘Discrimination’ Scenarios

As with the ‘detection’ experiments presented in the main manuscript, this study shows distinct effects of the perceptual context on luminance discrimination thresholds of non-adjacent stimuli. However, while there are systematic similarities to the ‘detection’ scenarios, there also are clear differences. Importantly, there are obvious issues regarding outliers in the data as well as the seemingly large differences in performance across scenarios. I will first discuss what the data indeed could be showing us and will

then discuss possible explanations for the observed irregularities, flaws of experimental design and possible future improvements and further research.

We must assume that luminance contrast perception scales with the overall level of luminance of a scene. However, the variation across Weber contrasts (if scaled according to the luminance of the distractors (Table 4.3)) as well as their impossibly high contrast value suggest that the contrast perception of the animals is probably not, or only partially, influenced the luminance of the distractors. This makes sense, as most of the visual scene is now made up by the noisy background (blurred at a distance or resolved close up) rather than the distractors. Indeed, if we scale the Michelson contrast at threshold of each scenario (Table 4.3) in relation to the luminance of the noisy background (I_n) we can establish almost identical Weber fractions across the different relative intensity contrasts (dark on dark = 1.05, bright on dark = 0.57, dark on bright = 1.20, bright on bright = 0.58). This shows that indeed, contrast perception is likely subject to the overall luminance of a visual scene. These discrimination Weber fractions are still substantially larger than those of the detection thresholds. However, this is in line with the literature discussed in the introduction (Furchner et al., 1977; Bradley & Ohzawa, 1986; Gescheider, 1997; Purves et al., 2001; Shevell, 2003; Straube & Fahle, 2011). These Weber contrasts relative to the noisy background are also more uniform than their distractor scaled equivalents. Despite the suspiciously high values, this shows that the discrimination thresholds likely scale with absolute intensity, just like the detection scenarios. Therefore, again, we must exclude the suitability of the RNL model for luminance discrimination due to its inability to adequately scale with global intensity (Table 4.2, discussion in Chapter 2).

As with the detection scenarios, there seems to be a systematic difference between the fish having to find a dark spot or a bright spot. However, the Weber fractions for the dark spots are worse than for the bright spots which contradicts the findings and discussion from Chapter 2 which agreed with the literature suggesting increased sensitivity for decreasing (‘darker than’) contrasts. However, the double cone stimulation that corresponds to a given discrimination threshold is always lower than the average double stimulation from the noisy background (b1…4-n). This might hint at the influence of the noisy background luminance on the discrimination thresholds. Interestingly, this difference in double cone catch is in the range of 5-10% cone stimulation across all scenarios, precisely the range of contrasts determined as the detection thresholds (Table 4.2).

Our findings therefore suggest interactions between both, the relative contrast of target stimuli against the distractors, in addition to influences of the luminance of the background against which they are compared. If we assume the perception of the threshold contrast (relative to the distractors) to be scaled with the intensity of the noisy background, we can express the perceptual distance of the Michelson contrast of each scenario to the distractors at threshold in relation to its distance to the luminance of the noisy background as:

$$Q_{i=|\Delta I_t - I_n|} \qquad \textbf{Equation 4.4}$$

Where Q_i is the absolute difference between the Michelson contrast at threshold of a given scenario (ΔI_t) and the average luminance of the noisy background (I_n). This is not to be confused with the Weber scaling introduced in the next paragraph. It simply expresses how 'close' to the background luminance that comparison is being made, assuming that: the further the distance between that relative contrast (target vs. distractor) and the luminance of the background, the stronger the contrast perception.

Based on our previous observation we can assume that this relative contrast perception is then scaled by the global luminance which is dominated by the noisy background. This adjusted Weber contrast for the discrimination threshold of a given scenario *i* ($W_{disc,i}$) can be expressed as:

$$W_{disc,i} = Q_i / I_n \qquad \textbf{Equation 4.5}$$

Surprisingly, this yields Weber fractions which seem very reasonable ($W_{disc,dd}$ = 0.05, $W_{disc,bd}$ = 0.43, $W_{disc,db}$ = 0.20, $W_{disc,bb}$ = 0.41) and suggests the notion of increased salience of stimuli which are darker than their distractors in relation to the visual background against which the comparison is being made. This holds especially true if we assume the Michelson contrast for the 'dark spot with dark distractors' scenario to be slightly higher (i.e. identical to the dark on bright scenario), which our data suggests being possible (Table 4.3). Therefore, this approach might be able to

capture subtle interactions between the absolute and relative luminance contrast when discriminating non-adjacent stimuli against an achromatic background.

4.5.4 Summary

Despite some profound experimental issues with the discrimination scenario, our study shows both significant differences and similarities between luminance contrast perception in various perceptual contexts. Similar findings have been made for the use of the chromatic RNL model in contexts which deviate from model assumptions (e.g. Caves et al., 2018; Sibeaux, Cole, et al., 2019a). A commonly stated solution to these threshold deviations is to 'behaviourally calibrate' the RNL model for a given species and a given perceptual context (e.g. Olsson et al., 2018). However, as various researchers have repeatedly pointed out (particularly those studying human & bee vision), our perception of colour and luminance contrast are highly context dependent and co-dependant and in most natural contexts subject to various degrees of post-retinal neuronal processing. In fact, some researchers openly doubt that such a 'behavioural calibration' of the RNL to natural contexts is impossible as the model is not capable (and certainly not designed) to reflect these higher-level aspects of visual perception (Skorupski & Chittka, 2011; Vasas et al., 2018). The standard reply from many researchers using the RNL model is twofold. Firstly, the RNL model was never developed to precisely quantify colour vision across all sorts of perceptual contexts. Visual ecologists therefore ought to only use it very conservatively (i.e. assuming thresholds of 3 ΔS) to give an initial guess at how likely it is a certain colour contrast is perceivable in the first place. Secondly, the RNL model, at least for colour vision, has been shown to do a fairly good job across various visual systems, largely independent of the perceptual context in which it has been applied. Thus, it is fair to attribute biological effect to RNL contrast measurements.

However, our research seems to (at least regarding the use for achromatic contrast perception in a trichromatic visual system) contradict this notion. My data suggest fundamental incompatibility of the RNL model for achromatic contrast perception in natural perceptual contexts be it for detection or discrimination. Given the potentially profound impact on a popular tool in visual ecology (The RNL model) we strongly advise further investigation of context dependant contrast perception in conjunction with efforts to further understand the neurophysiology of both lower and

higher-level pathways of the visual system of *R. aculeatus*. The study (and its shortcomings) presented in this chapter can and should be used to guide these efforts.

The discrimination experiment also produced a surprising result. After multiple weeks of training and testing we started noticing that about 5 of our 14 fish would start doing complete rotations before picking the stimuli whereas most of the other fish would perform partial rotations. Initial discussions with other researchers in the field started to hint towards a visual 'illusion' i.e. some level of interference with the depth or 3D shape recognition of the fish in relation to the noisy background. The appearance of our stimuli shares surprisingly strong similarities with several vivid motion and shape illusions (e.g. Nguyen-Tri & Faubert, 2003) which might explain some of the underlying perceptual mechanisms involved. Indeed, unpublished research in *R.aculeatus* shows that the fish use optic flow for distance estimation (Karlsson, unpublished). Furthermore, when peeling the stimuli off the noisy background and re-attaching them with a couple of millimetres of distance (using blue tack) to create shadows and other cues for 3D shape estimation, the rotating behaviour would stop in 100% of the cases. This behaviour potentially shows a key mechanism of visual perception in *R. aculeatus* worth investigating in future research.

Despite having investigated luminance contrast sensitivity using two different levels of background luminance, our study only considered but two specific and highly calibrated contexts: the discrimination of a large, uniform and achromatic circular target stimulus against a uniform grey background and the discrimination of an achromatic circular target stimulus against identically shaped achromatic distractors. However, we know that a variety of factors can fundamentally influence luminance contrast perception in most, if not all, animals. If luminance thresholds are determined simply by the intensity detected by the receptors, we would expect thresholds to be determined solely by the difference in quantum catch in relation to the channel specific noise. However, as discussed in the introduction, luminance perception is rarely a direct outcome of the intensity, as the judgement of brightness and lightness is a complex, poorly understood, multistage process (Gilchrist et al., 1999; Gilchrist & Radonjić, 2009; Kingdom, 2011; Gilchrist, 2014; Maniatis, 2014). Unsurprisingly then, there is ample evidence that luminance contrast modulates the salience of objects at stages well beyond the retina (Einhäuser & König, 2003).

As such we would like to highlight the importance to quantify the context sensitivity of visual discrimination and detection thresholds. This should be done by continuing to adapt insights from studies on human psychophysics but equally important by conducting species and context specific behavioural experiments to obtain parameters by which models of contrast perception can be fine-tuned. For example: How does achromatic and chromatic noise contribute to such behaviourally determined thresholds (Gegenfurtner & Kiper, 1992; Whittle, 1992; Solomon, 2009)? To what extent can the context dependant processing of luminance contrast be generalised between different taxa (Olsson et al., 2018)? How do interactions between chromatic and achromatic information processing influence such species-specific contrast sensitivity thresholds in various spatial and temporal contexts (Gegenfurtner & Kiper, 1992; Syrkin & Gur, 1997; Vingrys & Mahon, 1998; Párraga et al., 2002; Willis & Anderson, 2002; Kachinsky, Smith, & Pokorny, 2003; Shapley & Hawken, 2011; Clery et al., 2013; Kelley & Kelley, 2014; Ng et al., 2018)? How does the mental state (e.g. motivation) of an animal contribute to behaviourally determined thresholds (Hanson, 1959; Aurorès-Weber, de Brito Sanchez, Giurfa, & Dyer, 2010; Webber, Chambers, Kostek, Mankin, & Cromwell, 2015; Chirimuuta, 2016; Howard, Avarguès-Weber, Garcia, Greentree, & Dyer, 2019)? To what extent is this confounded by the degree of cognitive complexity of a task (Eskew, 2009)? To what degree is luminance contrast detection and discrimination determined by neural noise at various stages of cognitive context and complexity (e.g. Garcia *et al.*, 2018)?

The list of questions (and necessary future behavioural experiments) appears as endless as empirical evidence seems scarce and our understanding of luminance contrast perception in humans is certainly far more advanced than in non-human vertebrates, let alone invertebrates. This warrants caution in the use of uniform contrast sensitivity thresholds (be it achromatic or chromatic) across widely diverse perceptual contexts, independently of which models are used to describe them. Luminance discrimination, as expected, is not just limited by photoreceptor noise and therefore cannot be adequately represented by the use of a singular detection or discrimination threshold determined using the equations in Siddiqi et al. (2004) as it currently is widely done in visual ecology. This realisation shares many parallels with ongoing discussions regarding the use of the RNL model outside of model assumptions (e.g. Olsson *et al.*, 2018 and comments). Our results suggest the use of a conservative achromatic RNL threshold assumption of 3ΔS (e.g. Spottiswoode & Stevens, 2010) to be far from a

conservative threshold assumption, despite the possibly simplest perceptual context in which they could be applied, let alone the comparatively well-known visual system and corresponding parameter choice for *R.aculeatus* in this study.

To our knowledge, this is the first time that achromatic discrimination thresholds have been quantified in a marine vertebrate. Furthermore, this is the first time discrimination thresholds have been determined using a detection and a 'discrimination' task as well as doing so using animals which have been trained to detect and discriminate both randomly placed 'brighter' and 'darker' stimuli simultaneously. Finally, our findings provide important insights to the processing of achromatic information as well as the use of the RNL model to quantify achromatic discrimination and detection by non-human observers. Our study shows that the current use of the RNL model for the quantification of luminance contrast sensitivity thresholds warrants caution, due to its seeming inability to adequately reflect consequences of the neurophysiological differences between achromatic and chromatic contrast perception at both retinal and post-retinal levels. More specifically, our study suggests the lack of adequate scaling of thresholds by the RNL model to the average luminance of a scene. Furthermore, our study highlights currently unresolved issues of the consideration of context and species-specific differences of not just where those thresholds are located for a given context, but which models or parameters mathematically best represent them.

We conclude that our results warrant a wide range of future investigations using behavioural experimentation, literature reviews as well as investigations of neurophysiology across a wide range of taxa. Methodological advances which facilitate behavioural threshold testing for more complex cognitive contexts (such as the adaptation of Ishihara colour tests presented in Cheney et al. (2018)) will greatly contribute to our ability to investigate these barely investigated aspects of animal vision using a combination of bottom-up and top-down approaches. Furthermore, given the vast range of contexts in which luminance discrimination thresholds are obtained, calculated and applied we ask for a fundamental increase in the standard and level of caution applied for the choice of context and species-specific luminance discrimination and detection thresholds as well as behavioural estimates thereof.

Chapter 5
General Discussion

“Exactly!" said Deep Thought. "So, once you do know what the question actually is, you'll know what the answer means.”

- Douglas Adams, 1981

Chapter 5 - General Discussion

5.1 Preface

In this thesis I have developed, tested and applied a novel framework for the study of colour patterns in order to increase our understanding of the design, function and evolution of defensive colouration in nudibranch molluscs. In Chapter 2, I developed the 'Quantitative Colour Pattern Analysis' (QCPA), an analytical framework for the study of colour patterns in nature which contributes to concepts and methods available in visual ecology. Chapter 3 saw the application of the QCPA to study the ecology and evolution of defensive colouration in nudibranch molluscs. Finally, Chapter 4 focused on the behavioural validation of luminance discrimination and detection thresholds in Picasso Triggerfish (*Rhinecanthus aculeatus*) to inform parameter choice and as a general investigation into limitations of visual models implemented in QCPA. I will briefly discuss the context of each of these chapters and will spend a more substantial amount of time on future research.

5.2 Chapter 2 – Development of the Quantitative Colour Pattern Analysis (QCPA)

QCPA unifies a broad range of visual modelling tools into a coherent conceptual framework. The idea of a unified framework is the most important aspect of the QCPA and meant combining a variety of currently separate methodological aspects:

1. Calibrated digital photography capable of capturing reliable quantitative data of visual scenes
2. Creating a workflow that links the modelling of spatial acuity, colour and luminance perception
3. Assembling an array of existing, modified and novel colour pattern analyses
4. Providing a range of existing and novel solutions for visualising spatiochromatic data

Current methodology in the field of visual ecology is diverse. Meaning that there is not just one 'correct' approach towards measuring chromatic contrast or spatial acuity, nor how to combine such individual tools. In fact, many of the visual modelling and pattern analysis tools that are currently used in visual ecology are still in the process of being applied and tested in various contexts, as well as validated using behavioural experimentation. For example, this applies to the receptor noise limited model for chromatic and achromatic contrast perception (e.g. Cheney et al., 2019;

Escobar-Camacho et al., 2019; Sibeaux, Cole, & Endler, 2019) or any kind of pattern analysis such as granularity analysis (e.g. Troscianko, Skelhorn, & Stevens, 2017; Ramírez-Delgado & Cueva del Castillo, 2020) or, in the case of QCPA, John Endler's approaches (Sibeaux, Cole, et al., 2019b). In order to provide a comprehensive collection of tools and methods (in addition to the pre-existing capabilities of MICA), the QCPA needed to provide a variety of tools for each of the four steps mentioned above. As a result, QCPA leaves the user the freedom to choose among a variety of curated options at each stage of image processing and analysis, including the option to skip whatever step the user deems unnecessary.

Many of the tools and methods implemented in QCPA did exist in some form prior to adaptation. For example, John Endler's colour pattern analyses have formed over decades (Endler, 1978) and continue to develop (Endler et al., 2018). However, in some cases software, having been written for multiple different software platforms such as R (e.g. AcuityView by Caves & Johnsen, (2017)) or Matlab (e.g. colour adjacency analysis (CAA) by Endler, (2012)) only possessed limited functionality. Furthermore others, such as the RNL model, had been adapted by multiple software platforms such as PAVO (Maia et al., 2013) or Colourvision (Gawryszewski, 2018) in forms which may vary in output.

Creating a well-curated framework whose specific mechanics and operation would be transparent and well documented was key. Increasing user-friendliness meant operating outside of paywalls using a single software platform. As a result we had decided to spend a lot of effort into re-writing and expanding the QCPA as a fully integrated part of the MICA toolbox while spending equally substantial amounts of effort into: A) writing a manuscript that would objectively explain the concepts, tools and principles underlying the QCPA. B) compiling a comprehensive supplement providing additional detail, explanations and worked examples C) creating the online platform of www.empiricalimaging.com to provide a support-platform containing user guides, tutorials, a community forum as well as news and updates on the framework.

QCPA, in many ways, is but proof of concept. Every component of the framework is subject to ongoing research and development, be it the modelling of animal colour vision, achromatic contrast perception, the combination of both or the modelling of spatial vision, to name a few. What we have done for QCPA is creating the scaffolding of the framework and placing a selection of components at each of the

crucial steps of the framework. At no point do we claim to have found the perfect solution of a given component or the conceptual approach of a unified framework itself. Our understanding of processes involved in the visual perception of complex visual information by animal observers will continue to evolve and so will our ability to translate these insights into computational solutions. The goal of QCPA was to provide a blueprint that could be used to add these insights to an adapting framework of tools and methods. To allow anyone access to and support for these tools and to invite contributions and modifications.

As outlined in the discussion of Chapter 2, such contributions and modifications can range in complexity and size from the simple addition of extra pattern analysis output (e.g. cohesiveness weighted visual contrast or additional colour map overlap metrics) as a small scale adaptation, the automatization of certain scripts, implementation of substantial improvement on existing modules of the QCPA such as context sensitive visual contrast thresholds (e.g. coinciding contrast (Lotto & Purves, 2000), retinex theory (E. H. Land, 1986)), threshold adjustments based on behavioural evidence (e.g. Cheney et al., 2019) and eye tracking weighted generation of transition matrices. Or, on the extreme end, the introduction of entirely novel capacities able to investigate aspects of visual perception, such as algorithms for the modelling of object and shape recognition beyond the level of the 'primal sketch' (Marr, 2010), thus capable of investigating higher level perceptual aspects of complex visual signals, such as more definite answers on the perception of shapes and elements in colour pattern elements, which in turn would allow for a more informed analysis of the perceptual importance of symmetry (Osorio, 1996; Forsman & Herretröm, 2004; Wagemans et al., 2012). However, the feasibility of species-specific computational approaches to such higher-level visual processing are discussed at the end of this chapter. For now, the integration of methods capable of approximating more basic levels of neuronal mechanisms involved in object and shape recognition could serve as an interesting addition to the capacities of QCPA. These could include SIFT based approaches (Lowe, 1999) or approaches incorporating concepts of attention (Rosenholtz et al., 2010).

5.3 Chapter 3 – Investigating Colour Pattern Morphology in Nudibranch Molluscs

This chapter saw the application of QCPA to investigate the perception of colour pattern morphology of daytime dependent nudibranch species assemblages in Nelson

Bay, NSW. This study provided intriguing preliminary results, supporting the assumption that visual predation is a driver of nudibranch colouration while applying the QCPA framework. However, due to the massive investment into Chapter 2 and substantial investment into Chapter 4 as well as substantial limitations on the extent of the dataset, the analysis of the data for this chapter has but scratched the surface.

How to deal with the many parameters resulting from QCPA is one of the main topics originating from this chapter and has already been discussed in both the discussion of Chapter 2 as well as that of Chapter 3. A first step of facilitating the analysis of such overparameterised datasets is the increase of sample size, i.e. an increase of the number of individuals per species as well as the number of species for a given taxonomic level. An increase in sample size will also be necessary to approach a core ability of QCPA, the quantification of complex natural visual backgrounds and how these relate to colour pattern morphology. Given the huge spread in commonality of nudibranch species, finding enough rare species individuals will remain an important obstacle for future sampling efforts but key, given the frequency dependence of selective pressures associated with the evolution of aposematic colouration (Servedio, 2000; Speed & Ruxton, 2005; Endler & Greenwood, 2006; Gray & McKinnon, 2007).

However, the study of nudibranch colour pattern morphology needs to be approached using comparative phylogenetic analysis in order to be capable of distinguishing between the effect of relatedness and the influence of environmental factors (such as daytime). The sequencing of nudibranch DNA is a challenging job which, over the course of the last 20 years, has steadily progressed. However, while the amount of species for which genetic markers are available is steadily growing, this remains a bottleneck in the study of nudibranch ecology and evolution. For example, the currently available calibrated image database contains some 130 species of which roughly 30% currently cannot be used for comparative phylogenetic analyses as genetic information is missing. As discussed in Chapter 3, this likely includes a sampling bias for nocturnal and particularly well camouflaged species. Furthermore, investigating the evolutionary origin of traits in nudibranchs at larger scales is currently hampered by poor resolution at the base of the phylogeny.

Nevertheless, Chapter 3 has demonstrated the application of QCPA in a challenging context. Taking calibrated images underwater in often turbid and turbulent environmental conditions over the course of years (2016-2017) has provided a steep

learning curve regarding the suitability and need for future development in procedure and hardware. This also includes investigating questions regarding the robustness of calibrated digital photography. Finding cheap and effective lambertian (or near-lambertian) underwater grey standards will remain a top priority as current polymer solutions (including my resin cast version or more conventional spectralon standards) remain potentially problematic with poorly quantified impacts on data quality (e.g. Voss & Zhang, 2006). Furthermore, given the cost and effort involved in achieving satisfactory image illumination (discussed in Chapter 2 and pages 124-126 in Appendix A), quantifying the impact of the light environment on cone-catch calculations is also a crucial topic in need of attention.

5.4 Chapter 4 - Investigating Luminance Detection and Discrimination Thresholds in *Rhinecanthus aculeatus*

This chapter saw the quantification of psychophysical luminance contrast detection and discrimination thresholds in one of the currently best studied coral reef visual systems (*Rhinecanthus aculeatus*). The visual system of *R. aculeatus* has been used in a range of studies to model the visual perception of animal colouration or visual stimuli (e.g. Cheney, Newport, McClure, & Marshall, 2013; Cheney et al., 2019; Newport et al., 2017; Green, Urquhart, van den Berg, Marshall, & Cheney, 2018) and features as the visual system of choice used in the analysis of nudibranch colouration in Chapter 3. Given the advanced stage of investigations into neuroanatomy, colour vision, spatial acuity and now luminance contrast perception (discussed in Chapter 4), in combination with the exquisite ability of this species to be trained for a vast range of behavioural tasks, makes it likely that *R.aculeatus* will remain one of the key visual systems for the investigation of vision in trichromatic coral reef fishes. Given the pivotal role of luminance contrast perception in animal vision, the importance of developing a contextualised understanding of thresholds associated with *R.aculeatus* is self-evident if we want to deepen our understanding of the perception of complex visual information in nature.

This chapter fulfils a broader purpose than just putting a number to the threshold entered into QCPA. It identifies a larger and more important issue that extends beyond the modality of luminance contrast perception. Many studies modelling aspects of animal vision are, and have been, unlikely to reflect the spatiochromatic (discussed in

Chapter 2) and spatiotemporal (discussed in Chapter 4) context and how post-photoreceptor processing of visual information can be influenced by this context. Regarding this chapter, it means that there is room for a more profound, context sensitive validation of currently used methodology in visual ecology regarding the modelling of luminance contrast perception.

5.5 Synthesis

Visual ecologists continue to face many unknowns regarding species and context specific processing of visual information at post-retinal stages. The extent of this unknown, and resulting potential inadequacy of applied tools, appear in contrast to conclusions reached regarding the ecological meaning of complex visual information. The cause of this discrepancy is manifold. The RNL model has been gradually adapted by many ecologists (currently cited more than 700 times) to investigate the significance of animal colouration. However, the RNL model had been designed to describe colour contrast perception under specific viewing conditions and assumptions which remove many constrains on colour vision from post-retinal processing of visual information (Vorobyev & Osorio, 1998). There are few commonly accepted alternatives to the use of the RNL model (see discussion Chapter 2).

Science is still very much in the process of learning to understand many aspects of vision and cognition, including the precise neuronal pathways underlying them or computational analogies to them (e.g. Griffiths, Chater, Kemp, Perfors, & Tenenbaum, 2010). That is in humans. And humans are the one animal for which we probably have the best understanding of cognition and higher-level neuronal processing. Understandably then, the road to an equivalent (incomplete) understanding of these aspects for a variety of non-human animals remains long (and exciting). And second, yes, the RNL model is (in many cases) pretty good at providing a first guess on the perception of colour contrast.

How do we adjust for the non-linearities and biases in colour contrast perception discussed in Chapter 2? The easiest approach, for now, seems to be the quantification of these departures from assumptions, to try to understand where and why they occur and use this information to reflect on the currently used models. QCPA is not designed to model the ultimate perception of visual information, but rather give an estimate on the amount and kind of information that is available to a non-human observer given the very fundamental physiological limitations of its visual system. It does this while

providing a modular and dynamic approach which allows the user to modify any component of the framework according to context specific constrains and resulting parameter choice.

Will we ever be able to fully describe the visual perception of animals in complex visual contexts? In my opinion probably not. Or at least, not in the foreseeable future and not for animals distantly related to humans. There is a key issue provided by the lack of species-specific bottom-up (neurophysiological) knowledge of higher-level aspects of visual perception and cognition. But what about the ability to translate these processes into generalist mathematical models?

What kicked off the development of bio-inspired computer vision (Marr, 2010) continues to develop into highly sophisticated computational representations of biological vision using the power of neuronal networks (Itti, Koch, & Niebur, 1998; Riesenhuber & Serre, 2004; Serre, 2014). However, such approaches are currently only capable of considering the first few milliseconds of visual processing, prior to any eye movements or any remotely conscious perception of visual information. These approaches provide a demonstration that what was originally considered as a fundamentally artificial and thus non-biological type of vision, is indeed capable of reproducing biologically validated functional principles of vision. Neuronal networks and artificial intelligence (AI) are increasingly used to make predictive estimates on visual perception (e.g. Fennell, Talas, Baddeley, Cuthill, & Scott-Samuel, 2019) or to perform detailed analyses of morphological similarities (e.g. Wu et al., 2019). An interesting use of AI will be the exploration of its predictive capabilities in combination with our ever-increasing ability to obtain large amounts of data in combination with agent based models predicting adaptive outcomes of animal interactions with other animals in the context of a given visual environment (e.g. Strannegård, Xu, Engsner, Endler, & Marshall, 2020; Talas et al., 2020). Such approaches are of great interest regarding the need of tools and methods with predictive abilities i.e. on the detectability or memorability of a given stimulus when designing ever more complex and nature-like behavioural experiments. However, artificial intelligence is a very recent addition to visual ecology, and it will continue to be an exciting process to explore its abilities and synergies with existing frameworks.

Appendix A – Supplementary Material: Chapter 2

QCPA

Quantitative Colour Pattern Analysis

micaToolbox

empirical imaging

empiricalimaging.com

Introduction

This document provides detailed information on the mechanics of the individual tools. Detailed equations to all output parameters can also be found here. It provides further discussion on important aspects of how to use QCPA and additional considerations. It also provides a range of applied examples to visualise the effect of different tools while also showing worked examples where QCPA (or parts of it) has been applied to a specific example.

Glossary

ΔS: The Euclidian distance between two points in the receptor noise limited opponent colour space (Vorobyev & Osorio, 1998; Hempel de Ibarra et al., 2001). ΔS is simply a distance and does not make any inference on discriminability. Therefore, describing distances in colour space in terms of ΔS is correct. In fact, ΔS is the Mahalanobis distance between two stimuli, a classical measure of multivariate distance (Clark et al., 2017; Endler et al., 2018). Describing distances in "Just Noticeable Differences" (JNDs) is not correct because the relationship between ΔS and perception is nonlinear. JND only applies near threshold, in other words when ΔS is close to 1 (Vorobyev & Osorio, 1998).

Weber Fraction: The Weber fraction describes the relation between the absolute intensity of a stimulus (e.g. cone stimulation) and the noise that underlies the perception (receptor noise). Weber fractions are a key concept of psychophysiology and apply to all our senses (weight discrimination, hearing, etc.). Weber fractions are a constant for a given sensory channel. It is crucial to point out that there is a moderate level of confusion about what constitutes a Weber fraction in visual ecology. We therefore recommend to

strictly adhere to the original equations of Vorobyev & Osorio (1998).

JND: A “Just Noticeable Difference” (JND) describes the psychometric discrimination threshold under specific conditions. This is an estimate of the point at which the contrast between two stimuli is detectable by a sensory system. While a JND conceptually should correspond to a distance of 1 ΔS, this often is not the case due to real-time higher-level processing of visual information and possible interactions between vision and prior experience. These thresholds need to be determined with behavioural experiments and are likely to be highly context dependent (e.g. Sibeaux, Cole, & Endler, 2019)

Receptor Noise: Photoreceptors have an inherent “dark noise”. Meaning, they constantly produce a weak signal, similar to the audio noise of a radio without a signal. A visual system can only detect a signal once the level of stimulation exceeds that level of receptor noise. These noise levels, in combination with the relative abundance of each photoreceptor type and the corresponding opponent channels fundamentally determine the ability of a visual system to perceive colour and luminance contrast. It is important to distinguish between the noise level in a single neuron and the channel specific noise level determined by receptor abundance.

Hue: Hue, in an anthropocentric meaning, describes the ‘kind’ of colour we perceive. E.g. ‘red’ or ‘blue’. Physically speaking, it refers to the location of the peaks and steps in the reflectance spectra of a surface and the illuminant spectra in relation to the spectral sensitivities and opponent channels of a given visual system (relative photoreceptor stimulation). In simplistic terms: hue is the photoreceptor stimulation relative to each other. This can be

graphically represented as the angle or angles of a colour relative to the achromatic point in a colour space (see discussions in Endler, 1990 and Endler & Mielke, 2005).

Saturation: Saturation describes how ‘pure’ a colour is. The more grey it contains (the less pronounced the peaks and steps of the reflectance spectra), the less saturated it will appear. The perception of saturation is possible due to the difference between high and low intensity parts of a spectrum being captured by at least two different cone classes. This can be graphically represented as the distance to the achromatic point in a colour space (see discussions in Endler, 1990 and Endler & Mielke, 2005)

Colour Space: The stimulation (or relative stimulation in case of opponent processing) of photoreceptors can be displayed on one or more axes. Thus, the photoreceptor stimulation a colour produces can be displayed in a n-dimensional colour space where n is defined by the number of receptors or opponent channels. For relative stimulation the dimensionality is n-1. For a detailed review of colour spaces see (Renoult et al., 2017).

Chromaticity Diagram: A specific type of colour space which only plots/considers photoreceptors or opponent channels contributing to colour vision. This term explicitly excludes any contributions from achromatic signals. Some publications use the term ‘colour space’ synonymously: ensure the correct usage to avoid vagueness.

Chromaticity: Chromaticity refers to “colourfulness”. As colour is defined by both hue and saturation, chromaticity is a term that refers to both simultaneously. Opponent channels can be calculated which eliminate the achromatic signal and describe chromaticity in a single dimension of colour (such as the red-green and blue-yellow

opponent systems described in humans). In some chromaticity diagrams each axis is a measure of a different chromaticity.

Luminance: In the context of visual ecology “luminance” encompasses both the perceived “lightness” and “brightness” of a given surface and is dependent on the spectral sensitivity of the receiver receptor classes involved in luminance perception, the intensity of the signal, and the context-dependent cues and cognitive processes.

Brightness: Brightness refers to the perceived amount of light a given surface seems to emit or reflect. As such it is confounded by viewer perception and highly context dependent due to cognitive processes. It is frequently used incorrectly and/or loosely in the literature to mean a combination of luminance and saturation and often is used instead of saturation. As a result, it is best avoided altogether if not used in its proper definition.

Lightness: Lightness refers to the perceived reflectance or intensity of a surface. Like brightness, it is a perceptual property of surfaces and highly confounded by the perceptual context.

Spatiochromatic: Spatiochromatic is a term that implies spatial (what is where) and chromatic (colour and luminance) properties of objects or scenes being considered within each other’s context.

Spectralon: A patented material consisting of sintered PTFE (Polytetrafluorethylene) powder. It is known for its near-Lambertian and spectrally flat reflectance properties because it has nearly the same reflectance at most wavelengths, no matter what angle you look at it from. This makes it a grey standard of

choice. It can be bought with various degrees of carbon in it which alters its grey value. While the Lambertian properties of Spectralon are undisputed in air, this is not the case for its use underwater. Without enough pressure from the surrounding water (e.g. in shallow water) the material's hydrophobic properties create an air-water barrier on the material's surface, which creates multiple reflections and renders the spectralon non-Lambertian. However, how this correlates with depth is poorly researched. In shallow water sand-blasted or acid-etched marine-grade stainless steel has been used as an alternative.

RAW: RAW refers to the unprocessed information a camera's sensory array has captured. Each manufacturer has its own RAW file format, e.g. .orf for Olympus and .nef for Nikon. It is the format of choice for calibrated photography. For detailed information see Troscianko & Stevens (2015).

JPEG: JPEG is the most commonly encountered image format. It refers to an image that has been compressed to save space, using a specific compression algorithm. However, as JPEG compression is a lossy format (e.g. it produces fringes), it is not recommended for calibrated digital photography.

Camera calibration: This refers to obtaining the spectral sensitivities of a camera's sensory array.

Calibrated image: An image where the pixel values are linear in respect of radiance measured at the sensor, and which has been normalised so that pixel values are represented as being relative to the reflectance of a reflectance standard (thereby controlling for variations in lighting

conditions and camera exposure). This is the type of image required for mapping to cone-catch images.

Cone-catch image: An image where pixel values are expressed as the predicted cone-catch quanta for a given visual system's receptor classes.

Aposematism: A type of defensive colouration that is defined as the use of conspicuous colouration in combination with unprofitability.

Crypsis: Any type of mechanism that prevents or minimises detection.

Camouflage: All forms of concealment, including those preventing recognition as well as detection.

Mimicry: An organism that has developed similarity to another organism as a result of fitness benefits of close resemblance.

Transition matrix: Cumulative count of transitions along transects across a segmented image. The basis for most QCPA pattern statistics. See Endler, 2012 for detailed discussion.

Minimum Resolvable Angle (MRA): The angular width of the narrowest black/white line pair that can be discerned by a visual system. This is similar to a cutoff defined in cycles/degree which describes how many square waves (black to white being one wave) can be resolved within a degree of the visual field.

Additional Considerations for Underwater Calibrated Photography

The QCPA is intended to be applied in both terrestrial and aquatic environments. While the acquisition of calibrated digital images in terrestrial environments is well documented, no studies have yet used calibrated digital photography underwater. The aquatic environment comes with its separate set of constraints, particularly regarding the light environment and physics of grey standards underwater. Ambient light underwater ranges from almost unaltered daylight in clear shallow water to a rapid loss of both short- and long-wavelength light in combination with decreasing light levels with depth, as well as the effects of particles an pigments in the water (Jerlov, 1976; Lythgoe, 1979). As a result, underwater photography in most cases relies on some form of artificial illumination such as strobes or video lights unless taken in shallow water. However, artificial illumination introduces three key issues. One, using a strong light source is likely to introduce artificial light gradients within an image if not carefully diffused. This can result in artificially cast shadows and general heterogeneity of light levels within an image that can significantly degrade further image analysis. Two, unless absolutely dominating over the ambient light, the resulting illuminant will likely be an unknown mixture of natural and artificial light which makes it hard to choose a suitable illuminant in subsequent visual modelling. Three, illuminating the image with artificial light removes the natural light conditions under which the scene would usually be viewed. Furthermore, an aquatic environment can pose problems regarding the use of suitable colour and grey standards for image calibration (Voss & Zhang, 2006). These issues need to be addressed and solved prior to engaging in data acquisition and may require substantial equipment costs and testing. If the user is generally unfamiliar with underwater photography, we strongly recommend getting advice from professionals. We would like to emphasise that the quality of the images on which the subsequent analyses are conducted fundamentally constrains the meaning and realistic interpretation of QCPA output.

Additional Considerations for Colour & Grey Standard Choice

Ideally, the grey scales should differ in luminance by the behaviourally validated discrimination or detection thresholds of the modelled viewer. This allows for adjusting and approximating the optimum luminance discrimination threshold for each image separately while making sure that the resulting clustering agrees with behaviourally

tested discrimination thresholds. Additional chromatic tiles in the colour standard allow for better adjustment and quality control of the clustering process and can also be chosen to correspond to key perceptual limits of the colour vision of a selected animal. However, the use of customised colour and grey standards can be regarded as an easy-to-implement failsafe but is not a necessary component of the RNL clustering as a lack of behavioural data is often the case when studying non-model organisms. CMOS and CCD camera sensors behave linearly with the radiance of light measured at each photosite (Maître, 2017) provided the camera has the appropriate aperture and exposure time, and linear image data can typically be extracted from RAW images produced by most consumer cameras using the appropriate software (DCRAW), or using the new linearisation modelling functions of the micaToolbox (Troscianko, unpublished) or others (Garcia, Dyer, Greentree, Spring, & Wilksch, 2013). Therefore as long as the grey standard is well exposed (i.e. not saturated or so close to zero that it's value is affected by sensor noise), there is no light "bleeding" onto the sensor (e.g. due to lens flare, which is very common in ultraviolet photography), and the scene is not being photographed through a transparent layer or through mist/haze/turbidity, then only a single standard is required for normalisation where none of the image channels are over-exposed (i.e. reaching saturation point of the sensor). Ideally this standard should have a reflectance value similar to the scene average to ensure appropriate exposure, e.g. a white standard risks being over-exposed in a scene which is otherwise very dark. Otherwise two or more (preferably three or more) standards should be used, in which case the standards should ideally have reflectance values at the higher and lower end of the scene's reflectance. A standard colour chart (e.g. X-Rite color checker) has a range of grey standards, so is ideal for covering all eventualities and exposures.

Additional Considerations for Image Illumination when using QCPA

Image analysis based on luminance discrimination thresholds is very sensitive to gradients of illumination; therefore, it is necessary to make sure that illumination is uniform inside an image (or represents natural variation in illumination). Using diffusers, taking images in a diffuse light environment or using diffuse artificial illumination can achieve this. There are post-processing techniques, such as local mean removal, which are able to mitigate the effect of illumination gradients inside an

image (Buades, Coll, & Morel, 2005). However, such post-processing may have profound effects on the results and must only be attempted with much caution and extensive calibration. Variances in both natural and artificial illumination can also lead to chromatic differences, which can have significant impacts on the perception of a visual scene (Endler, 1993). Therefore, careful consideration of illumination conditions is paramount to the use of calibrated digital photography.

How to Report Methodology using QCPA

QCPA provides a lot of functionality which goes along with many choices the user must make. To create reproducible research, the following information needs to be provided either in the main manuscript or in the supplement:

- Camera model & lens & Underwater housing (if applicable)
- Camera settings (Aperture, shutter speed and white balance)
- Image file type / compression (RAW, JPG, etc.)
- Camera calibration (How did you calibrate your camera)
- Illuminant (Give the spectrum AND its units)
- Colour & grey standard (What is it made of, what does it look like)
- Photoreceptor ratios and how you normalise them.
- Receptor noise (Of the single photoreceptor and the channel specific noise: Weber fraction or ω component value)
- Spectral sensitivities (Give the original citation)
- Spatial acuity
- Viewing distance
- Colour & luminance discrimination thresholds
- ANY settings you choose in QCPA and MICA (e.g. negative value replacement, etc.)

QCPA provides an automatic file renaming system that helps in keeping track of chosen settings. However, many choices the user makes are not recorded by the file renaming and must be kept track of. For additional guidance on good methods reporting in visual ecology see White et al. (2015).

Fundamental Mechanics of CAA, VCA & BSA

All three pattern analyses (Colour Adjacency Analysis/CAA, Visual Contrast Analysis/VCA and Boundary Strength Analysis/BSA) share a common baseline mechanism: they derive their information of pattern geometry from a transition matrix. This transition matrix is created by running horizontal and vertical sampling transects across every line and column in a pixel matrix and summing up the synonymous and non-synonymous transitions along each transect and storing the information (Fig. 2.1S). It is this transition matrix that is then used to calculate the relative and absolute abundance of colour pattern elements and boundaries. The strength of this approach is that it conserves the information of ‘What is touching what and how much’ which gives rise to unique parameters which can account for adjacency. This conserved information about the identity of each patch or border type is also the basis for the combination of the spatial and chromatic properties into spatiochromatic pattern parameters. As the horizontal and vertical transects can be used to create a separate horizontal and vertical transition matrix, this allows CAA, VCA and BSA to analyse horizontal pattern properties separately from vertical ones (The user can make this choice in the interface). This has some intriguing potential application i.e. in the context of motion and viewer perspective as is discussed in both Endler (2012) and Endler et al. (2018).

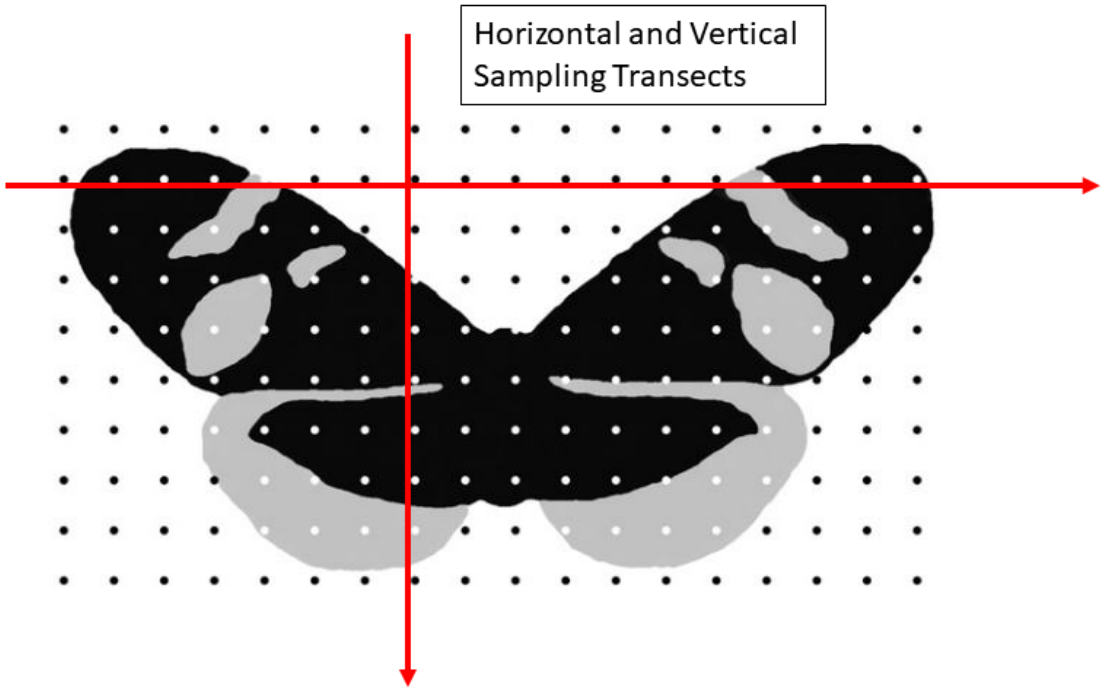

Figure S2.1: A schematic example of horizontal and vertical transects across a clustered image of a butterfly. There are 3 cluster classes present in this image: Black, grey and white. Modified from Endler (2012).

Variable Summary

Note: Blue text denotes parameters which are either entirely new or have been changed from their original publication or have never been written down as a specific equation despite having been mentioned in these publications. It is not advised to blindly assume identical numerical outcomes matching the original publications for these parameters.

General variables

k	Number of colour pattern elements inside a colour pattern
E	Number of all theoretically possible types of transitions inside a colour pattern. ($E=k*(k-1)/2$).
n	Number of observed types of non-zero transitions (types of non-zero upper or lower off-diagonal cells in the transition matrix)
$n_{off,i,j}$	Total number of non-synonymous transitions (e.g. red -> blue) of type (i,j) where $i \neq j$, sum of the off-diagonals of a transition matrix.
$n_{dia,i,j}$	Total number of synonymous transitions (e.g. red -> red) of type (i,j) where $i=j$, the diagonals of a transition matrix.
f_i / f_j	Relative abundance of a colour pattern element i or j (from the diagonal of a transition matrix)
t_{ij}	Relative abundance of a transition between patch i and patch j, i.e. the sum of instances in the image where a pixel of pattern element i is directly adjacent to pixel of pattern element j, divided by the total number of pattern element transitions (termed “off-diagonal” transitions) across the entire image.
$D_{max,i}$	Maximum possible opponency contrast of colour pattern element i

S_i or S_j Cone capture quanta or cone stimulation of colour pattern element *i* or *j* in a given class of photoreceptors

L_i or L_j Cone capture quanta or cone stimulation of colour pattern element *i* or *j* in the photoreceptor channel responsible for luminance contrast perception

$\Delta S_{Sat,i}$ Euclidian distance to the achromatic point in the log-transformed Receptor Noise Limited colour space of a colour pattern element *i.* This corresponds to the saturation of a colour pattern element.

$\Delta S_{i,j}$ Euclidian distance in the log-transformed Receptor Noise Limited colour space between two colour pattern elements *i* and *j*

$\Delta S_{L,i,j}$ Euclidian distance in the log-transformed Receptor Noise Limited colour space between two colour pattern elements *i* and *j* specific to the photoreceptor channel (S_i) responsible for luminance contrast perception

Output parameters of the Adjacency Analysis

S_c Simpson colour diversity

J_c Relative Simpson colour diversity

S_t Simpson transition diversity

J_t Relative Simpson transition diversity

H_c Shannon colour diversity

Q_c Relative Shannon colour diversity

H_t Shannon transition diversity

Q_t Relative Shannon transition diversity

S_{cpl} Simpson pattern complexity

Q_{cpl} Shannon pattern complexity

C Pattern Complexity

PT Average Patch size in pixels

A Aspect ratio

Output parameters Visual Contrast Analysis

M_L Weighted mean pattern L contrast

M_{Dmax} Weighted mean pattern D_{max} contrast

$M_{\Delta SSat}$ Mean weighted pattern ΔS_{Sat} contrast

$M_{\Delta SL}$ Mean weighted pattern ΔS_L contrast

$M_{\Delta S}$ Mean weighted pattern ΔS contrast

s_{Dmax} Weighted standard deviation pattern D_{max} contrast

s_L Weighted standard deviation pattern L contrast

s_{Dmax} Weighted mean pattern D_{max} contrast

$s_{\Delta SSat}$ Weighted standard deviation pattern ΔS_{Sat} contrast

$s_{\Delta SL}$ Weighted standard deviation pattern ΔS_{Lum} contrast

$s_{\Delta S}$ Weighted standard deviation pattern ΔS contrast

CV_L Weighted coefficient of variation pattern L contrast

CV_{Dmax} Weighted coefficient of variation pattern D_{max} contrast

$CV_{\Delta SSat}$ Weighted coefficient of variation pattern ΔS_{Sat} contrast

$CV_{\Delta SL}$ Weighted coefficient of variation pattern ΔS_{Lum} contrast

$CV_{\Delta S}$ Weighted coefficient of variation pattern ΔS contrast

Output parameters of the Boundary Strength Analysis

$BM_{\Delta S}$ Weighted mean of pattern boundary ΔS contrast

$BM_{\Delta SL}$ Weighted mean of pattern boundary ΔSL contrast

BM_{L} Weighted mean of pattern boundary L contrast

BM_{Dmax} Weighted mean of pattern boundary $Dmax$ contrast

$BM_{\Delta Ssat}$ Weighted mean of pattern boundary ΔS_{Sat} contrast

$Bs_{\Delta S}$ Weighted standard deviation pattern boundary ΔS contrast

$Bs_{\Delta SL}$ Weighted standard deviation pattern boundary ΔS_{L} contrast

Bs_{L} Weighted standard deviation of pattern boundary L contrast

Bs_{Dmax} Weighted standard deviation of pattern boundary $Dmax$ contrast

$Bs_{\Delta Ssat}$ Weighted standard deviation of pattern boundary ΔS_{Sat} contrast

$BCV_{\Delta S}$ Weighted coefficient of variation of pattern ΔS contrast

$BCV_{\Delta SL}$ Weighted coefficient of variation of pattern ΔS_{L} contrast

BCV_{L} Weighted coefficient of variation of pattern boundary L contrast

BCV_{Dmax} Weighted coefficient of variation of pattern boundary $Dmax$ contrast

$BCV_{\Delta Ssat}$ Weighted coefficient of variation of pattern boundary ΔS_{Sat} contrast

Output parameters of the Colour Adjacency Analysis (CAA)

Simpson Colour Diversity (S_c)

A measure called the colour diversity (S_c) can be obtained by calculating the inverse Simpson diversity index of the diagonal of the transition matrix (f_i representing the relative abundance of each colour/luminance class *i*). S_c ranges from 0 to *k* (k being the number of different colour pattern elements inside the pattern). It should only be used for dense pixel sampling (>5 samples per smallest colour pattern element dimension. See Endler (2012) for a detailed discussion). It describes how evenly the colour/luminance classes are represented inside a pattern. S_c=*k* when all classes are equally abundant. Therefore, the higher the number of different colour classes inside a pattern, the higher the potential maximum value of S_c.

$$S_c = \frac{1}{\sum_{i=1}^{k} f_i^2} \quad (1)$$

Relative Simpson Colour Diversity (J_c)

The range of S_c depends on *k* (the number of colour pattern elements inside a pattern) and as such it can be useful to express colour diversity in relative terms, therefore making patterns more comparable if they possess different *k*. This eliminates the information on how high *k* inside the animal is and simply shows how evenly the available colour classes are distributed

$$J_c = \frac{S_c}{k} \quad (2)$$

Simpson Transition Diversity (S_t)

The regularity of a colour pattern can be described by analysing the relative transition frequencies (t_{ij}) which show what is next to what and how much. As stated in Endler (2012), these transition frequencies must be transformed to add up to 1, e.g. relative transition frequencies (t_{ij}) and not the actual values from the off-diagonal in the transition matrix, therefore t_{ij} is divided by the sum of transitions in the matrix (n). As with S_c, the inverse Simpson diversity index of the transition frequencies is calculated resulting in S_t which is ranged between 0 and k. $S_t=k$ when all possible transitions are equally frequent.

$$S_t = \frac{1}{\sum_{i=1}^{k}\left[\sum_{j=i+1}^{k} t_{i,j}^2\right]} \quad (3)$$

Relative Simpson Transition Diversity (J_t)

To eliminate the differences in transition diversity between patterns due to different numbers of pattern elements (k), the transition diversity can be divided by the absolute number of possible transitions inside the pattern (n). This gives us the relative transition diversity which describes how evenly the available transitions inside the pattern are distributed independent of k.

$$J_t = \frac{S_t}{E} \quad (4)$$

Shannon Colour Diversity (H_c)

The diversity of colour pattern elements can alternatively be represented by calculating the Shannon diversity index (H_c) of the colour pattern elements. $H_c(max)$ = ln(k) when all colour pattern elements (k) are equally frequent. This is also referred to as entropy.

$$H_c = -\sum_{i=1}^{k} f_i ln(f_i) \quad (5)$$

Relative Shannon Colour Diversity (Qc)

H_c is confounded by the number of colour pattern elements (k) in the pattern. We can normalise it by dividing it by its maximum possible value, so it ranges from 0 to 1.

$$Q_c = \frac{H_c}{ln\,(k)} \quad (6)$$

Shannon transition diversity (H_t)

The diversity of transitions between colour pattern elements can be described using the Shannon index (H_t) of the relative transition frequencies (t_{ij}). $H_t(max)$ = ln(n) when all types of non-zero transitions (n) are equally frequent.

$$H_t = -\sum_{i=1}^{n} \left[\sum_{j=i+1}^{n} t_{i,j} \ln\left(t_{i,j}\right) \right] \quad (7)$$

Relative Shannon transition diversity (Q_t)

H_t is confounded by the number of non-zero transition types (n) in the pattern. We can normalise it by dividing it by its maximum possible value (ln(n)), so it ranges from 0 to 1 where 1 corresponds to a maximum diversity.

$$Q_t = \frac{H_t}{ln\,(n)} \tag{8}$$

Simpson colour pattern complexity (S_{cpl})

As per Endler (2012), a possible way of defining colour pattern complexity is to combine J_t (Relative Simpson Transition Diversity) and J_c (Relative Simpson Colour Diversity). This is based on the argument that the colour patterns possessing J_t and J_c closest to 1 would have the highest possible complexity. It is easy to imagine this by thinking of a perfectly regular chessboard like a pattern that makes use of all available colours in equal frequency. Consequently, a low S_{cpl} corresponds to a simple pattern whereas a value close to 1 would refer to a complex or even pattern.

$$S_{cpl} = (J_t + J_c)/2 \tag{9}$$

Shannon colour pattern complexity (Q_{cpl})

The Shannon equivalent to S_{cpl} is Q_{cpl}. A low Q_{cpl} corresponds to a simple pattern whereas a value close to 1 would refer to a complex or even pattern.

$$Q_{cpl} = (Q_t + Q_c)/2 \quad (10)$$

Pattern Complexity (*C*)

A simple way of describing the geometric complexity of a pattern is to count the ratio between the sum off the actual diagonal values in the transition matrix (n_{dia}) and the sum of all values in the off-diagonal (n_{dia}). *C*=1 if every single pixel is adjacent to a pixel belonging to a colour class other than itself. Therefore, a pattern with more complex structures will exhibit a higher *C.*

$$C = \frac{n_{off,i}}{n_{dia,i} + n_{off,i}} \quad (11)$$

Average Patch size (*PT*)

The average patch size (*PT*) in pixels in a pattern is calculated by averaging the mean number of sequential transitions across horizontal and vertical transects where no change of colour pattern element occurs; these are the diagonal entries in the transition matrix, which need to be divided by the sum of the diagonals (the trace). The average horizontal and average vertical patch size are then multiplied with each other to calculate the average patch size in pixels. To translate the patch size into an area metric *PT* can be divided by the pixel/distance ratio derived from a scale bar. For a precise measure of patch size, we recommend the particle analysis tool in imageJ and the dedicated particle analysis in QCPA.

Aspect Ratio (*A*)

The aspect ratio describes the relation between the horizontal (h) and vertical (v) average patch size (v/h+v). A value close to 0 corresponds to a horizontally elongated

pattern, whereas a value close to 1 refers to a vertically elongated pattern. A value close to 0.5 indicates circular or quadratic patterning.

Output parameters of the Visual Contrast Analysis (VCA)

Colour pattern element (Patch) specific parameters:

Patch maximum possible chromaticity (D_{max})

The maximum possible chromatic contrast (D_{max}) a colour patch can elicit in a hypothetical opponent process (for detailed rationale see cited literature in Endler & Mielke, 2005). Given that most opponent processing pathways are unknown in animals, this parameter calculates the cone catch contrast for each possible combination of photoreceptors in a visual system and lists the maximum. With photoreceptor stimulation $S_{i,n}$ and $S_{i,m,}$ corresponding to the patch specific photoreceptor stimulation of colour patch *i* in photoreceptor class *n* or *m*. The comparison of which photoreceptors D_{max} corresponds to is listed in the output summary under 'D_{max} *Channel*'.

$$D_{max} = max_i \left(\frac{S_{i,n} - S_{i,m}}{S_{i,n} + S_{i,m}} \right) \quad (12)$$

Patch Luminance (L_i)

Like the chromaticity of a patch, the perceived luminance of a patch (L_i) can be represented by the cone catch of the photoreceptor class responsible for luminance contrast detection (S_l). In most animals this is either a single class of photoreceptor such as the longwave (LWS) cone or the sum/mean of the cone captures of both members of the double cones.

Patch Receptor Noise Limited (RNL) Saturation (ΔS_{Sat})

The saturation of each colour pattern element can be expressed as the Euclidian distance from the achromatic point in the n-dimensional log-transformed RNL colour space (ΔS_{Sat}) (Vorobyev & Osorio, 1998; Hempel de Ibarra et al., 2001; Endler & Mielke, 2005; Renoult et al., 2017).

Pattern visual contrast parameters:

Weighted mean of pattern Luminance contrast (M_L)

The luminance contrast of a pattern can be expressed as the mean luminance of the pattern elements *(k)* weighted by their relative abundance (f_i).

$$M_L = \sum_{i=1}^{k} f_i \, L_i \tag{13}$$

Weighted standard deviation pattern *L* contrast (s_L)

Similarly, we can calculate the standard deviation of the luminance contrast inside a colour pattern, weighted by the relative abundance of each colour pattern element (f_i). Where k is the number of colour pattern elements in a pattern, f_i is the relative abundance of a given colour pattern element, L_i is the L value of a given (i) colour pattern element and M_L is the mean weighted luminance contrast of a colour pattern. Different to Endler & Mielke (2005) we make use of the standard deviation instead of the variance as proposed in Endler et al. (2018.)

$$s_L = \sqrt{\frac{k \sum_{i=1}^{k} f_i (L_i - M_L)^2}{(k-1) \sum_{i=1}^{k} f_i}} \tag{14}$$

Weighted coefficient of variation pattern *L* contrast (CV_L)

To express the variation of the luminance contrast inside a pattern we can calculate the weighted coefficient of variation relative to the weighted mean (Endler et al., 2018).

$$CV_{Dmax} = \frac{s_L}{M_L} \tag{15}$$

Weighted mean of pattern D_{max} Contrast (M_{Dmax})

Similarly, we can calculate the chromatic contrast in a colour pattern by calculating the mean maximum hypothetical chromaticity of the pattern elements (*k*) weighted by their relative abundance (f_i).

$$M_{Dmax} = \sum_{i=1}^{k} f_i \, D_{max,i} \tag{16}$$

Weighted standard deviation pattern D_{max} contrast (s_{Dmax})

We can also calculate the standard deviation of the D_{max} chromaticity contrast inside a colour pattern, weighted by the relative abundance of its colour pattern elements. Where *k* is the number of colour pattern elements in a pattern, f_i is the relative abundance of a given colour pattern element, $D_{max,i}$ is the D_{max} value of a given (*i*) colour pattern element and M_{Dmax} is the mean weighted D_{max} chromaticity contrast of a colour pattern. Different to Endler & Mielke 2005 we make use of the standard deviation instead of the variance as proposed in Endler et al 2018.

$$s_{Dmax} = \sqrt{\frac{k \sum_{i=1}^{k} f_i \left(D_{max,i} - M_{D_{max}}\right)^2}{(k-1) \sum_{i=1}^{k} f_i}} \quad (17)$$

Weighted coefficient of variation pattern *Dmax* contrast (CV_{Dmax})

To express the variation of the *Dmax* contrast inside a pattern we can calculate the weighted coefficient of variation relative to the weighted mean (Endler et al., 2018).

$$CV_{Dmax} = \frac{s_{Dmax}}{M_{Dmax}} \quad (18)$$

Weighted mean of pattern ΔS_{Sat} contrast ($M_{\Delta S_{Sat}}$)

And the same goes for the RNL Saturation. Note that this parameter measures saturation as the distance of each colour pattern element from the achromatic point in the log transformed RNL colour space and not a pairwise comparison inside a colour pattern as suggested by Endler & Mielke 2005.

$$M_{\Delta S_{Sat}} = \sum_{i=1}^{k} f_i \, \Delta S_{Sat,i} \quad (19)$$

Weighted standard deviation pattern ΔS_{Sat} contrast ($s_{\Delta S_{Sat}}$)

Similarly, we can calculate the standard deviation of the RNL saturation contrast inside a colour pattern, weighted by the relative abundance of each colour pattern element (f_i). Where k is the number of colour pattern elements in a pattern, f_i is the relative abundance of a given colour pattern element, $\Delta S_{Sat,i}$ is the ΔS_{Sat} value of a given (i) colour pattern element and $M_{\Delta S_{Sat}}$ is the weighted mean RNL saturation contrast of a

colour pattern. Different to Endler & Mielke 2005 we make use of the standard deviation instead of the variance as proposed in Endler et al. 2018.

$$s_{\Delta S_{Sat}} = \sqrt{\frac{k \sum_{i=1}^{k} f_i \left(\Delta S_{Sat,i} - M_{\Delta S_{Sat}}\right)^2}{(k-1) \sum_{i=1}^{k} f_i}} \quad (20)$$

Weighted coefficient of variation pattern ΔS_{Sat} contrast ($CV_{\Delta S_{Sat}}$)

To express the variation of the RNL saturation contrast inside a pattern we can calculate the weighted coefficient of variation relative to the weighted mean (Endler et al., 2018).

$$CV_{\Delta S_{Sat}} = \frac{s_{\Delta S_{Sat}}}{M_{\Delta S_{Sat}}} \quad (21)$$

Weighted mean of patternΔS_L contrast $\left(M_{\Delta S_L}\right)$

Similarly, the luminance contrast can be thought of as being limited by the receptor noise and photoreceptor abundance in the luminance channel (Siddiqi et al., 2004). Thus, the luminance contrast in a pattern can be expressed as the RNL luminance contrast between pattern elements *i* and *j* $\left(\Delta S_{L,i,j}\right)$ in response to their relative abundance of the cone class responsible for luminance contrast detection and the photoreceptor specific noise weighted by the mean relative abundance (f_i and f_j) of each colour pattern element combination ((f_i + f_j)/2) (Endler & Mielke, 2005). Note, this is different to the Boundary Strength Analysis (BSA) which looks at the edge contrast between adjacent colour pattern elements with respect to chromatic and luminance contrasts separately (Endler et al., 2018).

$$M_{\Delta S_L} = \frac{\sum_{i=1}^{k}\left[\sum_{j=i+1}^{k}\frac{f_i + f_j}{2}\Delta S_{L,i,j}\right]}{\sum_{i=1}^{k}\left[\sum_{j=i+1}^{k}\frac{f_i + f_j}{2}\right]} \quad (22)$$

Weighted standard deviation pattern ΔS_L contrast $s_{\Delta S_L}$

Similarly, we can calculate the standard deviation of the RNL luminance contrast inside a colour pattern, weighted by the relative abundance of each colour pattern element (f_i and f_j). Where k is the number of colour pattern elements in a pattern, f_i is the relative abundance of a given colour pattern element, $\Delta S_{L,i,j}$ is the ΔS_{Lum} value between two given (i, j) colour pattern elements and $M_{\Delta SLI}$ is the mean weighted luminance contrast of a colour pattern. Different to Endler & Mielke 2005 we make use of the standard deviation instead of the variance as proposed in Endler *et al.* 2018.

$$s_{\Delta S_L} = \sqrt{\frac{k\sum_{i=1}^{k}\left[\sum_{j=i+1}^{k}\frac{f_i + f_j}{2}\left(\Delta S_{L,i,j} - M_{\Delta S_L}\right)^2\right]}{(k-1)\sum_{i=1}^{k}\left[\sum_{j=i+1}^{k}\frac{f_i + f_j}{2}\right]}} \quad (23)$$

Weighted coefficient of variation of pattern ΔS_L contrast ($CV_{\Delta SL}$)

To express the variation of the RNL luminance contrast inside a pattern we can calculate the weighted coefficient of variation relative to the weighted mean (Endler et al., 2018).

$$CV_{\Delta S_L} = \frac{s_{\Delta S_L}}{M_{\Delta S_L}} \quad (24)$$

Weighted mean of ΔS pattern contrast ($M_{\Delta S}$)

Colour contrast inside a colour pattern can result from the pattern elements being comparably contrasting to each other as opposed to being very chromatic *per se*. Thus, the chromatic contrast in a pattern can be expressed as the mean RNL chromaticity contrast between pattern elements *i* and *j* $(\Delta S_{,i,j})$ weighted by the mean relative abundance of each colour pattern element combination ((f_I + f_j)/2) (Endler & Mielke, 2005). Note, this is different to the Boundary Strength Analysis (BSA) which does a similar computation for only adjacent (touching) pattern elements.

$$M_{\Delta S} = \frac{\sum_{i=1}^{k}\left[\sum_{j=i+1}^{k}\frac{f_i + f_j}{2}\Delta S_{i,j}\right]}{\sum_{i=1}^{k}\left[\sum_{j=i+1}^{k}\frac{f_i + f_j}{2}\right]} \quad (25)$$

Weighted standard deviation pattern ΔS contrast ($s_{\Delta S}$)

Similarly, we can calculate the standard deviation of the chromaticity contrast inside a colour pattern, weighted by the relative abundance of each colour pattern element (f_I and f_j). Where *k* is the number of colour pattern elements in a pattern, f_i is the relative abundance of a given colour pattern element, $\Delta S_{i,j}$ is the Euclidian distance in log-transformed RNL colour space between two given (*i, j*) colour pattern elements and $M_{\Delta S}$ is the mean weighted luminance contrast of a colour pattern. Different to Endler & Mielke 2005 we make use of the standard deviation instead of the variance as proposed in (Endler et al., 2018).

$$s_{\Delta S} = \sqrt{\frac{k \sum_{i=1}^{k} \left[\sum_{j=i+1}^{k} \frac{f_i + f_j}{2} \left(\Delta S_{i,j} - M_{\Delta S} \right)^2 \right]}{(k-1) \sum_{i=1}^{k} \left[\sum_{j=i+1}^{k} \frac{f_i + f_j}{2} \right]}} \quad (26)$$

Weighted coefficient of variation of pattern ΔS contrast ($CV_{\Delta S}$)

To express the variation of the RNL luminance contrast inside a pattern we can calculate the weighted coefficient of variation relative to the weighted mean (Endler et al., 2018).

$$CV_{\Delta S} = \frac{s_{\Delta S}}{M_{\Delta S}} \quad (27)$$

Output parameters of the Boundary Strength Analysis (BSA)

Weighted mean of luminance (*L)* boundary strength (BM_L)

Similar to Endler *et al.* 2018 we can calculate the mean boundary strength in a colour pattern in terms of luminance (*L*) contrast using the following formula. The number of colour pattern elements present in a colour pattern corresponds to *k* (The length of the diagonal of the transition matrix). $t_{i,j}$ corresponds to the relative proportion of the non-zero transition frequencies (the number of transitions of a boundary type divided by the sum of all transitions). The term $\left|\frac{L_i - L_j}{L_i + L_j}\right|$ corresponds to the absolute Michelson luminance contrast of that type of boundary ($t_{i,j}$).

$$BM_L = \frac{\sum_{i=1}^{k}\left[\sum_{j=i+1}^{k} t_{i,j}\left|\frac{L_i - L_j}{L_i + L_j}\right|\right]}{\sum_{i=1}^{k}\left[\sum_{j=i+1}^{k} t_{i,j}\right]} \quad (28)$$

Weighted standard deviation of luminance (*L*) boundary strength (Bs_L)

Similar to Endler *et al.* (2018) we can calculate the standard deviation of the boundary strength in a colour pattern in terms of luminance contrast using the following formula. The number of colour pattern elements present in a colour pattern corresponds to *k* (The length of the diagonal of the transition matrix). $t_{i,j}$ corresponds to the relative proportion of the non-zero transition frequency between pattern element *i* and *j*. The term $\left|\frac{L_i - L_j}{L_i + L_j}\right|$ corresponds to the absolute Michelson luminance (*L*) contrast of that type of boundary ($t_{i,j}$). The number of different types of non-zero entries in the off diagonal of the transition matrix (types of present types of boundaries) corresponds to *n*.

$$Bs_L = \sqrt{\frac{n\sum_{i=1}^{k}\left[\sum_{j=i+1}^{k} t_{i,j}\left(\left|\frac{L_i - L_j}{L_i + L_j}\right| - BM_L\right)^2\right]}{(n-1)\sum_{i=1}^{k}\left[\sum_{j=i+1}^{k} t_{i,j}\right]}} \quad (29)$$

Weighted coefficient of variation of luminance (*L*) boundary strength (BCV_L)

As in Endler *et al.* (2018) we can express the variation of the boundary intensities in a colour pattern relative to the mean by calculating the corresponding coefficient of variance.

$$BCV_L = \frac{Bs_L}{BM_L} \tag{30}$$

Weighted mean of *Dmax* boundary strength (BM_{Dmax})

Similar to Endler *et al.* 2018 we can calculate the mean boundary strength in a colour pattern in terms of *Dmax* contrast using the following formula. The number of colour pattern elements present in a colour pattern corresponds to *k* (The length of the diagonal of the transition matrix). $t_{i,j}$ corresponds to the relative proportion of the non-zero transition frequencies (the number of transitions of a boundary type divided by the sum of all transitions). The term $\left|\frac{Dmax_i - Dmax_j}{Dmax_i + Dmax_j}\right|$ corresponds to the absolute Michelson *Dmax* contrast of that type of boundary ($t_{i,j}$).

$$BM_{Dmax} = \frac{\sum_{i=1}^{k}\left[\sum_{j=i+1}^{k} t_{i,j}\left|\frac{Dmax_i - Dmax_j}{Dmax_i + Dmax_j}\right|\right]}{\sum_{i=1}^{k}\left[\sum_{j=i+1}^{k} t_{i,j}\right]} \tag{31}$$

Weighted standard deviation of *Dmax* boundary strength (Bs_{Dmax})

Similar to Endler *et al.* (2018) we can calculate the standard deviation of the boundary strength in a colour pattern in terms of *Dmax* contrast using the following formula. The number of colour pattern elements present in a colour pattern corresponds to *k* (The length of the diagonal of the transition matrix). $t_{i,j}$ corresponds to the relative proportion of the non-zero transition frequency between pattern element *i* and *j*. The term $\left|\frac{Dmax_i - Dmax_j}{Dmax_i + Dmax_j}\right|$ corresponds to the absolute Michelson *Dmax* contrast of that type of boundary ($t_{i,j}$). The number of different types of non-zero entries in the off diagonal of the transition matrix (types of present types of boundaries) corresponds to *n*.

$$Bs_{Dmax} = \sqrt{\frac{n\sum_{i=1}^{k}\left[\sum_{j=i+1}^{k} t_{i,j}\left(\left|\frac{Dmax_i - Dmax_j}{Dmax_i + Dmax_j}\right| - BM_{Dmax}\right)^2\right]}{(n-1)\sum_{i=1}^{k}\left[\sum_{j=i+1}^{k} t_{i,j}\right]}} \quad (32)$$

Weighted coefficient of variation of *Dmax* boundary strength (BCV_{Dmax})

As per Endler *et al.* (2018) we can express the variation of the boundary intensities in a colour pattern relative to the mean by calculating the corresponding coefficient of variance.

$$BCV_{Dmax} = \frac{Bs_{Dmax}}{BM_{Dmax}} \quad (33)$$

Weighted mean of ΔS_{sat} boundary strength ($BM_{\Delta S_{Sat}}$)

Similar to Endler *et al.* 2018 (but notably different) we can calculate the mean boundary strength in a colour pattern in terms of RNL saturation contrast using the following formula. The number of colour pattern elements present in a colour pattern corresponds to *k* (The length of the diagonal of the transition matrix). $t_{i,j}$ corresponds to the relative proportion of the non-zero transition frequencies (the number of transitions of a boundary type divided by the sum of all transitions). The term $\left|\frac{\Delta S_{Sat,i} - \Delta S_{Sat,j}}{\Delta S_{Sat,i} + \Delta S_{Sat,j}}\right|$ corresponds to the absolute Michelson RNL Saturation contrast of that type of boundary ($t_{i,j}$).

$$BM_{\Delta S_{Sat}} = \frac{\sum_{i=1}^{k}\left[\sum_{j=i+1}^{k} t_{i,j}\left|\frac{\Delta S_{Sat,i} - \Delta S_{Sat,j}}{\Delta S_{Sat,i} + \Delta S_{Sat,j}}\right|\right]}{\sum_{i=1}^{k}\left[\sum_{j=i+1}^{k} t_{i,j}\right]} \quad (34)$$

Weighted standard deviation of ΔS_{sat} boundary strength ($Bs_{\Delta S_{Sat}}$)

Similar to Endler et al (2018) we can calculate the standard deviation of the boundary strength in a colour pattern in terms of RNL saturation contrast using the following formula. The number of colour pattern elements present in a colour pattern corresponds to *k* (The length of the diagonal of the transition matrix). $t_{i,j}$ corresponds to the relative proportion of the non-zero transition frequency between pattern element *i* and *j*. The term $\left|\frac{\Delta S_{Sat,i} - \Delta S_{Sat,j}}{\Delta S_{Sat,i} + \Delta S_{Sat,j}}\right|$ corresponds to the absolute Michelson RNL Saturation contrast of that type of boundary ($t_{i,j}$). The number of different types of non-zero entries in the off diagonal of the transition matrix (types of present types of boundaries) corresponds to *n*.

$$Bs_{\Delta S_{Sat}} = \sqrt{\frac{n\sum_{i=1}^{k}\left[\sum_{j=i+1}^{k} t_{i,j}\left(\left|\frac{\Delta S_{Sat,i} - \Delta S_{Sat,j}}{\Delta S_{Sat,i} + \Delta S_{Sat,j}}\right| - BM_{\Delta S_{Sat}}\right)^2\right]}{(n-1)\sum_{i=1}^{k}\left[\sum_{j=i+1}^{k} t_{i,j}\right]}} \quad (35)$$

Weighted coefficient of variation of ΔS_{sat} boundary strength ($BCV_{\Delta S_{Sat}}$)

We can express the variation of the boundary intensities in a colour pattern relative to the mean by calculating the corresponding coefficient of variance.

$$BCV_{\Delta S_{Sat}} = \frac{Bs_{\Delta S_{Sat}}}{BM_{\Delta S_{Sat}}} \quad (36)$$

Weighted mean of ΔS_L boundary strength ($BM_{\Delta S_L}$)

As per Endler et al 2018 we can calculate the mean boundary strength in a colour pattern in terms of RNL luminance contrast using the following formula. The number of colour pattern elements present in a colour pattern corresponds to *k* (The length of the diagonal of the transition matrix). $t_{i,j}$ corresponds to the relative proportion of the non-zero transition frequencies (the number of transitions of a boundary type divided by the sum of all transitions). $\Delta S_{L,i,j}$ corresponds to the RNL Luminance contrast (ΔS_L) of that a given type of boundary ($t_{i,j}$).

$$BM_{\Delta S_L} = \frac{\sum_{i=1}^{k}\left[\sum_{j=i+1}^{k} t_{i,j} S_{L,i,j}\right]}{\sum_{i=1}^{k}\left[\sum_{j=i+1}^{k} t_{i,j}\right]} \quad (37)$$

Weighted standard deviation ΔS_L boundary strength ($Bs_{\Delta S_L}$)

As per Endler et al (2018) we can calculate the standard deviation of the boundary strength in a colour pattern in terms of RNL luminance contrast using the following formula. The number of colour pattern elements present in a colour pattern corresponds to *k* (The length of the diagonal of the transition matrix). $t_{i,j}$ corresponds to the relative proportion of the non-zero transition frequency between pattern element *i* and *j*. $S_{L,i,j}$ corresponds to the RNL luminance contrast (ΔS_L) of that a given boundary. The number of different types of non-zero entries in the off diagonal of the transition matrix (types of present types of boundaries) corresponds to *n*.

$$Bs_{\Delta S_L} = \sqrt{\frac{n\sum_{i=1}^{k}\left[\sum_{j=i+1}^{k} t_{i,j}\left(\Delta S_{L_{i,j}} - BM_{\Delta S_L}\right)^2\right]}{(n-1)\sum_{i=1}^{k}\left[\sum_{j=i+1}^{k} t_{i,j}\right]}} \quad (38)$$

Weighted coefficient of variation of ΔS_L boundary strength ($BCV_{\Delta S_L}$)

We can express the variation of the boundary intensities in a colour pattern relative to the mean by calculating the corresponding coefficient of variance.

$$BCV_{\Delta S_L} = \frac{Bs_{\Delta S_L}}{BM_{\Delta S_L}} \quad (39)$$

Weighted mean of ΔS boundary strength ($BM_{\Delta S}$)

As per Endler et al 2018 we can calculate the mean boundary strength in a colour pattern in terms of RNL chromaticity contrast using the following formula. The number of colour pattern elements present in a colour pattern corresponds to *k* (the length of the diagonal of the transition matrix). $t_{i,j}$ corresponds to the relative proportion of the non-zero transition frequencies between pattern element *i* and *j*. $\Delta S_{i,j}$ corresponds to the RNL chromaticity contrast (ΔS) of that a given boundary (between pattern element *i* and pattern element *j*).

$$BM_{\Delta S} = \sum_{i=1}^{k}\left[\sum_{j=i+1}^{k} t_{i,j}\Delta S_{i,j}\right] \quad (40)$$

Weighted standard deviation ΔS boundary strength ($Bs_{\Delta S}$)

As per Endler et al 2018 we can calculate the standard deviation of the boundary strength in a colour pattern in terms of RNL chromaticity contrast using the following formula. The number of colour pattern elements present in a colour pattern corresponds to *k* (The length of the diagonal of the transition matrix). $t_{i,j}$ corresponds to the relative proportion of the transition frequencies between pattern element *i* and *j*. $\Delta S_{i,j}$ corresponds to the RNL chromaticity contrast (ΔS) between pattern elements *i* and *j*. The number of different types of non-zero entries in the off diagonal of the transition matrix (types of present types of boundaries) corresponds to *n*.

$$Bs_{\Delta S} = \sqrt{\frac{n\sum_{i=1}^{k}\left[\sum_{j=i+1}^{k} t_{i,j}\left(\Delta S_{i,j} - BM_{\Delta S}\right)^2\right]}{(n-1)\sum_{i=1}^{k}\left[\sum_{j=i+1}^{k} t_{i,j}\right]}} \quad (41)$$

Weighted coefficient of variation of ΔS boundary strength ($BCV_{\Delta S}$)

We can express the variation of the chromatic boundary intensities in a colour pattern relative to the mean by calculating the corresponding coefficient of variance.

$$BCV_{\Delta S} = \frac{Bs_{\Delta S}}{BM_{\Delta S}} \quad (42)$$

Parameter Abbreviations for QCPA Results Output

To make the QCPA output file easier to navigate we have used a coded contraction of the parameters. We have divided the parameters into three families (Table 1). CAA for colour adjacency analysis, VCA for visual contrast analysis and BSA for border strength analysis.

Variable Name	Abbreviation
Simpson colour diversity - S_c (eq. 1)	CAA:Sc
Relative Simpson colour diversity - J_c (eq. 2)	CAA:Jc
Simpson transition diversity - S_t (eq. 3)	CAA:St
Relative Simpson transition diversity - J_t (eq. 4)	CAA:Jt
Shannon colour diversity - H_c (eq. 5)	CAA:Hc
Relative Shannon colour diversity - Qc (eq. 6)	CAA:Qc
Shannon transition diversity - H_t (eq. 7)	CAA:Ht
Relative Shannon transition diversity - Q_t (eq.8)	CAA:Qt
Simpson colour pattern complexity S_{cpl} (eq. 9)	CAA:Scpl
Shannon colour pattern complexity Q_{cpl} (eq. 10)	CAA:Qcpl
Pattern Complexity - C (eq. 11)	CAA:C
Average patch size – PT (no equation)	CAA:PT
Average horizontal patch size - PT_{Hrz} (no equation)	CAA:PT Hrz
Average vertical patch size - PT_{Vrt} (no equation)	CAA:PT Vrt
Aspect ratio – A (no equation)	CAA:Asp
Weighted mean of pattern **luminance** contrast - M_L (eq. 13)	VCA:ML
Weighted standard deviation of pattern **luminance** contrast - s_L (eq. 14)	VCA:sL
Weighted CoV of pattern **luminance** contrast - CV_L (eq. 15)	VCA:CVL
Weighted mean of pattern ***Dmax*** contrast - M_{Dmax} (eq. 16)	VCA:MDmax
Weighted standard deviation of pattern ***Dmax*** contrast - s_{Dmax} (eq. 17)	VCA:sDmax
Weighted CoV of pattern ***Dmax*** contrast - CV_{Dmax} (eq. 18)	VCA:CVDmax
Weighted mean of pattern **RNL saturation** contrast - ΔS_{Sat} (eq. 19)	VCA:MSsat
Weighted standard deviation of pattern **RNL saturation** contrast - $s_{\Delta S_{Sat}}$ (eq. 20)	VCA:sSsat
Weighted CoV of pattern **RNL saturation** - $CV_{\Delta S_{Sat}}$ (eq. 21)	VCA:CVSsat

Weighted mean of **RNL luminance** pattern contrast - $M_{\Delta S_L}$ (eq. 22)	VCA:MSL
Weighted standard deviation of **RNL luminance** pattern contrast - $s_{\Delta S_L}$ (eq. 23)	VCA:sSL
Weighted CoV of **RNL luminance** pattern contrast - $CV_{\Delta S_L}$ (eq. 24)	VCA:CVSL
Weighted mean of pattern **RNL chromaticity** contrast - $M_{\Delta S}$ (eq. 25)	VCA:MS
Weighted standard deviation of pattern **RNL chromaticity** contrast - $s_{\Delta S}$ (eq. 26)	VCA:sS
Weighted CoV of pattern **RNL chromaticity** contrast - $CV_{\Delta S}$ (eq. 27)	VCA:CVS
Weighted mean of **luminance** boundary strength - BM_L (eq. 28)	BSA:BML
Weighted standard deviation of **luminance** boundary strength - Bs_L (eq. 29)	BSA:BsL
Weighted CoV of **luminance** boundary strength - BCV_L (eq. 30)	BSA:BCVL
Weighted mean of ***Dmax*** boundary strength - BM_{Dmax} (eq. 31)	BSA:BMDmax
Weighted standard deviation of ***Dmax*** boundary strength - Bs_{Dmax} (eq. 32)	BSA:BsDmax
Weighted CoV of ***Dmax*** boundary strength - BCV_{Dmax} (eq. 33)	BSA:BCVDmax
Weighted mean of **RNL saturation** boundary strength - $BM_{\Delta S_{Sat}}$ (eq. 34)	BSA:BMSsat
Weighted standard deviation of **RNL saturation** boundary strength - $Bs_{\Delta S_{Sat}}$ (eq. 35)	BSA:BsSsat
Weighted CoV of **RNL saturation** boundary strength - $BCV_{\Delta S_{Sat}}$ (eq. 36)	BSA:BCVSsat
Weighted mean of **RNL luminance** boundary strength - $BM_{\Delta S_L}$ (eq. 37)	BSA:BMSL
Weighted standard deviation of **RNL luminance** boundary strength - $Bs_{\Delta S_L}$ (eq. 38)	BSA:BsSL
Weighted CoV of **RNL luminance** boundary strength - $BCV_{\Delta S_L}$ (eq. 39)	BSA:BCVSL
Weighted mean of **RNL chromaticity** boundary strength - $BM_{\Delta S}$ (eq. 40)	BSA:BMS
Weighted standard deviation of **RNL chromaticity** boundary strength - $Bs_{\Delta S}$ (eq. 41)	BSA:BsS
Weighted CoV of **RNL chromaticity** boundary strength - $BCV_{\Delta S}$ (eq. 42)	BSA:BCVS

Table S2.1: Summary of the parameter abbreviations in the QCPA output file

AcuityView 2.0 & Gaussian Convolution Filter

Using acuity parameters of an animal (morphological or behavioural), it is possible to simulate the loss-of-contrast in an image of known angular width by removing high-spatial frequency information, often performed using Fast Fourier Transform (FFT) techniques. The methodology behind this approach is described in detail in Caves et al. (2016) and has been thoroughly reviewed in Stoddard & Osorio (2019). Caves and Johnsen (2017) have compiled this approach into an R package called *AcuityView* which we have re-written to be used in ImageJ. However, among other modifications attempting to increase user friendliness, for QCPA the input is no longer required to be in square format (Fig. S2.2). However, due to the computational nature of FFT the image still needs to be rectangular. Therefore, we introduce the ability to blur irregular regions of interest (ROI) using a Gaussian filter kernel convolution (Marr, 2010). Standard Gaussian filters (e.g. those used by MATLAB or ImageJ) use separable convolutions, which require rectangular images or the use of edge padding to mitigate for non-independence of selection surroundings. This padding can introduce new (potentially misleading) pattern details. Our technique uses a custom-written non-separable convolution which ignores out-of-kernel pixels and adjusts the convolution denominator appropriately. This is more computationally intensive than applying separable convolutions in the spatial or frequency domains but can process irregularly shaped image sections completely independently of their backgrounds. At this stage the image can also be scaled to a specified number of pixels per minimum resolvable angle (MRA) to eliminate unnecessary spatial detail and increase the efficiency of subsequent processing steps. We recommend using 5 pixels per MRA to ensure no loss of spatial information.

Prior to applying acuity-control image blurring it makes sense to reduce the resolution of the image, thereby making subsequent processing steps faster without any loss of spatial information. We have determined the lowest pixel per the viewing animal's minimal resolvable angle (MRA) ratio to be approximately 5 pixels/MRA. If an image is resized to a lower resolution it will result in a loss of spatial information following acuity control, greater than 2%.

AcuityView (Caves & Johnsen, 2017) uses FFT-based processing, which requires square or rectangular images. We therefore wrote our own acuity control method which uses a Gaussian convolution, and is unlike FFT or standard Gaussian

blur filters which use a separable convolution (vertical and horizontal pixels convolved separately, which also requires square/rectangular images). Our Gaussian convolution is therefore more computationally intensive but is capable of acuity-control smoothing in an ROI of any shape without being affected by the ROI's surrounds or using potentially inappropriate surround manipulation (as used with separable Gaussian filters in programs such as MATLAB). The sigma of the Gaussian kernel is used to specify the desired level of blurring, and we therefore needed to determine which sigma values to use in order to reduce spatial information to a given MRA. We wrote a script which searched for the sigma level required to reduce a sine-wave image's amplitude to 2% of the original amplitude at the specified MRA given the number of pixels per MRA in the image. There was a near-perfect linear relationship between these values, and we used the model (shown in Fig. S2.3) to determine the sigma level required given the user's specified pixels/MRA value.

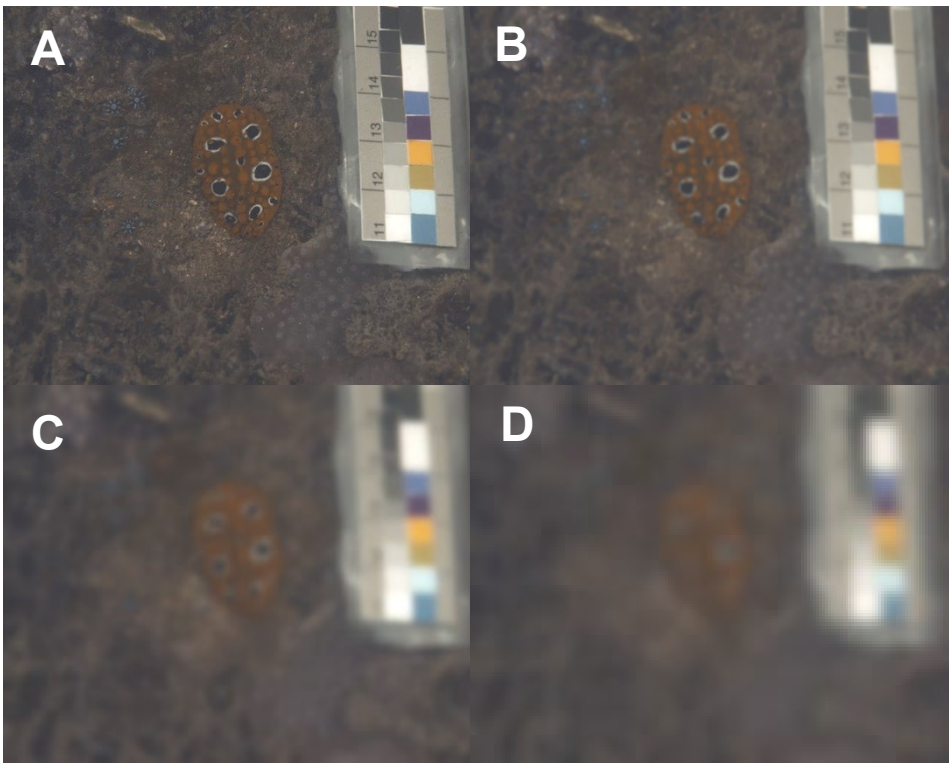

Figure S2.2: Examples of a nudibranch, modelled as seen by a triggerfish (*R. aculeatus*) in 5m depth at various viewing distances modelled using AcuityView. A: No acuity modelling B: 10cm C: 30cm D: 50cm

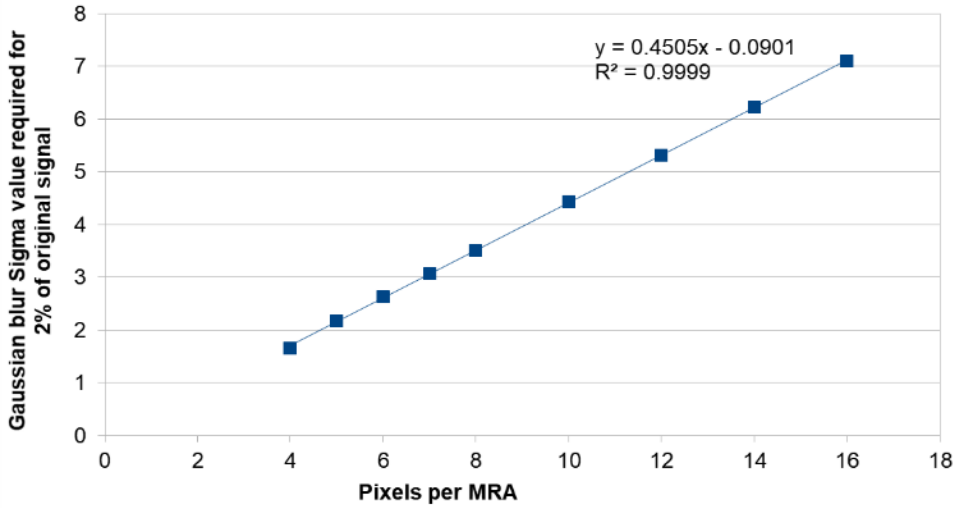

Figure S2.3: Modelling the sigma value required to reduce a sine-wave amplitude to 2% of its original across a range of pixels/MRA values.

Receptor Noise Limited (RNL) Ranked Filter

The filter first compares each focal pixel's colour and luminance contrast to each of its neighbouring pixels within a given pixel scale radius selected by the user. The chromatic (ΔS_C) and achromatic (ΔS_L) discrimination threshold is used to rank the neighbouring pixels from those with the most to the least similar colour and luminance. Next, the focal pixel's equivalent cone-catch value is averaged with its neighbours using weighting which follows an exponential decay curve across the rankings, meaning the focal pixel is blended most with neighbours which share similar colours and brightness, and least with dissimilar neighbours. The fall-off of that smoothing curve can be specified by the user. The result is a colour and luminance discrimination threshold-based filter that reduces noise while preserving (when applied on a non-blurred image) or recovering (when applied on a blurred image) chromatic and achromatic edges.

By setting the radius of the 'RNL Ranked Filter' to equal or just above the pixel/MRA ratio the filter spans the scale of the 'blurriness' and uses appropriate Weber fractions for each receptor to remove artificial intermediate areas in the image. This restores sharp boundaries between blurred parts of the image without altering its spatial information content (Fig. S2.4, S2.5 & S2.6). While this tool is not intended to directly mimic any particular stage of biological image processing, the resulting

recovered sharp edges support the phenomenon of “hyperacuity”, whereby visual systems are capable of interpolating the location of edges at a scale which exceeds the theoretical resolution offered by the retinal arrangement of photoreceptors (Hering, 1861).

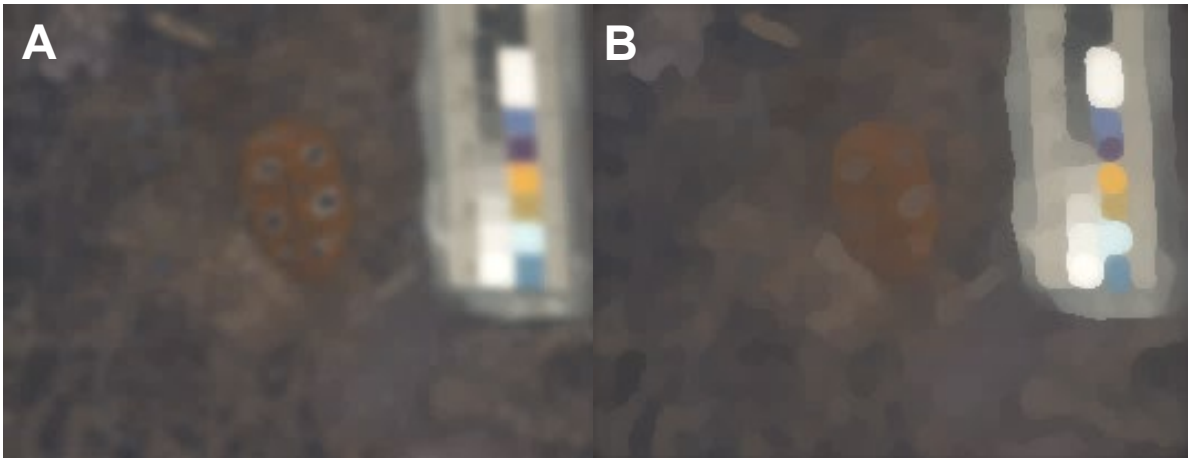

Figure S2.4: Example of an image modelled as viewed by a triggerfish from 30cm distance (A) and application of the ‘RNL Filter’ to restore sharp edges.

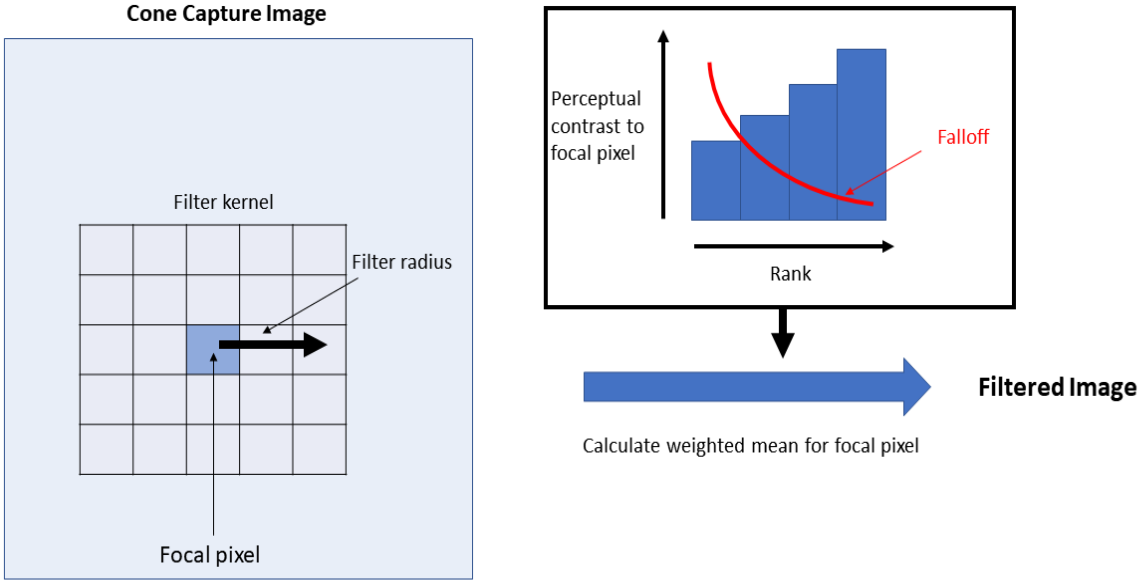

Figure S2.5 Schematic representation of the RNL ranked filter. This specific example shows a 3x3 pixel filter kernel (Filter radius = 3) and a falloff close to 5. The bars in the right panel go in the opposite direction of the falloff because pixels with more similarity to the focal pixel get a rank closer to 1 which in return results in a higher weighting from the falloff curve.

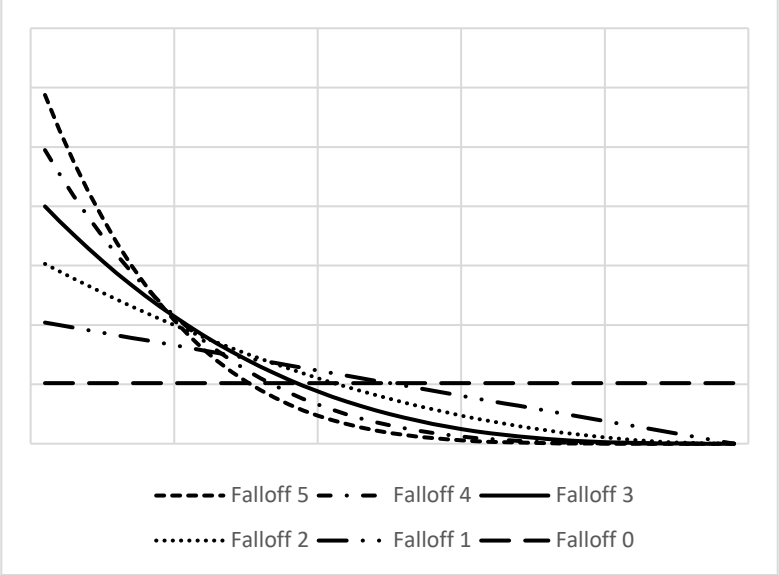

Figure S2.6 Visualisation of different falloff intensities. 0 corresponds to equal weighting across the ranks within the filter kernel. 5 leads to a much more distinct weighting of the highest ranks. The area underneath all the curves = 1.

Receptor Noise Limited Clustering

Segmentation of cone-catch images is performed using an agglomerative hierarchical clustering approach, which is formally presented here for the first time. Initially, each pixel in the cone-catch image stack is assigned as a unique cluster with corresponding cone-catch values. The algorithm then calculates the colour and luminance distance between neighbouring clusters, pairing the most similarly coloured clusters (Fig. S2.7). This distance is based on both colour and luminance contrast values (ΔS), creating a single distance weighted contrast measure (ΔS_T) weighted by the user defined thresholds as shown in equation S2.1 (below) where ΔS_C is the colour contrast between two clusters, ΔS_L the luminance contrast, S_C the colour discrimination threshold and S_L the luminance discrimination threshold. In this example chromatic and achromatic information is weighted based on our experience of optimal clustering output. However, users may find alternative weighting to be more suitable. This is subject to ongoing research and likely highly context dependant (e.g. Kelber et al., 2003).

$$\Delta S_T = \sqrt{\left(\frac{\Delta S_C}{S_C}\right)^2 + \left(\frac{\Delta S_L}{S_L}\right)^2}$$ Equation S2.1

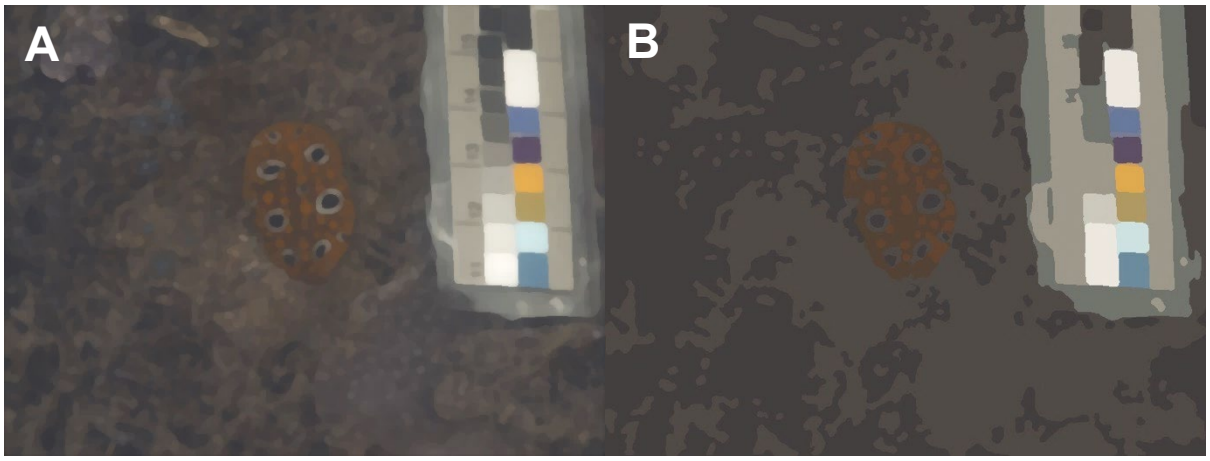

Figure S2.7: A: Example of an image as viewed by a triggerfish from 10cm at 5m depth, treated with RNL Filtering (but no clustering). B: Image A after being clustered with conservative threshold assumptions of the colour ΔS=2 and the luminance ΔS =5

If a cluster and its nearest neighbour are similar enough in colour and luminance (result in $\Delta S_T \leq k$, where k is a threshold such as 1 ΔS), then the pixels are combined into the same cluster. Combined clusters have their mean cone-catch values recalculated, weighted by the number of pixels in each cluster. The clustering algorithm repeats this process over several sequential passes. Within each pass, each cluster can be combined with one other cluster if they meet the threshold criteria. So, for example, if cluster 'A' is closest in colour to cluster 'B', and cluster 'B' is closest to cluster 'C', all three are combined into a single cluster in that pass. This method is therefore a 'single-linkage', or 'nearest neighbour' approach, which lends itself to the pairwise RNL colour comparison techniques.

The radius (or 'receptive field') over which clusters are compared is initially small (e.g. 2 pixels), however over successive passes this radius can be set to increase so that as the number of clusters decreases with each pass, the radius, and therefore number of cluster comparisons increases. The user can specify the rate at which the radius of this receptive field increases with each pass. This keeps the processing load to manageable levels (e.g. it would be computationally impractical to compare every

cluster with every other cluster in a large image). This is not the same radius as the one used for the RNL ranked filter and these processes run separately and sequentially. After approximately 5 to 6 clustering passes the total number of clusters in the image have typically reduced to the thousands or hundreds, at which point it becomes more computationally efficient to compare every cluster to every other cluster. The user can specify the point at which this switch occurs, and in larger images it may be more efficient to switch to whole-image comparisons after a larger number of initial passes.

The concept of the RNL clustering resembles a graph-cut image segmentation (Greig, Porteous, Seheult, & Seheultt, 1989) and mimics basic principles of a multi-layer neural network whose inputs have small receptive fields, and increasing receptive field size in subsequent layers, so that after a number of layers inputs from the entire image can be combined. The resulting clustering mechanism allows for segmentation of an image using only colour discrimination thresholds ($\Delta S_C \leq k$), only luminance discrimination thresholds ($\Delta S_L \leq k$) or both ($\Delta S_T \leq k$) in combination, depending on the purpose of the segmentation and the relative importance of colour and luminance to a species. To achieve the best clustering results for colour and luminance discrimination we recommend k between 1 and 3 which also fits most critical ΔS values used in the literature (e.g. Osorio, Smith, Vorobyev, & Buchanan-Smith, 2004; Martin Schaefer et al., 2007; Stevens, Lown, & Wood, 2014; Stevens et al., 2015; Kemp et al., 2015). Using thresholds higher than 1 ΔS reflects a conservative assumption of k for an animal for which the RNL model has not been tested or underlying parameters such as noise levels and photoreceptor abundances are not precisely known (Vorobyev & Osorio, 1998; Vorobyev et al., 2001; Garcia, Spaethe, & Dyer, 2017); this applies to almost all species to date. However, we emphasise that discrimination and detection thresholds are known to be highly context dependant (e.g. Furchner, Thomas, & Campbell, 1977; Heinemann & Chase, 1995; Smith, Pokorny, & Sun, 2000; Purves, Lotto, & Nundy, 2002; Garcia et al., 2017) and may extend well beyond the assumed conservative threshold of k=3 and may furthermore be subject to non-linearities across colour space (e.g. Mullen & Kulikowski, 1990; Sankeralli, Mullen, & Hine, 2002; Cheney et al., 2019). Therefore, considering perceptual and cognitive constraints that may influence the choice of suitable discrimination and detection thresholds is crucial. These thresholds should ideally be determined using behavioural experiments (e.g. Olsson, Lind, & Kelber, 2018; Sibeaux et al., 2019).

Local Edge Intensity Analysis: LEIA

The BSA uses the coefficient of variation (CoV) to describe the heterogeneity and intensity of edges in a scene. However, when a typical natural scene is processed into any kind of edge intensity image, the distribution of these edges is bounded at zero, with an intense skew (somewhat like a Poisson or gamma distribution) due to the low frequency of high-contrast edges. This means the CoV – which assumes a normal distribution – does not adequately capture the level of variation in the scene. We therefore introduce the option for log or square root transforming the ΔS values to create normal distributions, and additionally we include parameters which can capture this higher order deviation in ΔS distribution: skewness and kurtosis. These describe the shape of this non-normal edge intensity distribution using standardised moment measures on top of the standard deviation and CoV. An edge intensity distribution with a large right-hand tail would have a higher skewness value, while a distribution with a long tail of extreme outliers would have a higher kurtosis value. A pattern with high edge contrast skewness would therefore be more complex (including both high and low-contrast edges), while a high kurtosis might indicate the pattern is more salient (characterised by predominantly low-contrast edges, but with a large number of extreme-contrast edges). However, we provide the user with the option to log and sqrt transform the edge intensity values as well as ignore sub-threshold values prior to analysis which has profound impact on these output parameters and their meaning in a given context. We currently do not provide numerical examples (i.e. example distributions) but will certainly update these to the website and/or a later stage of the manuscript.

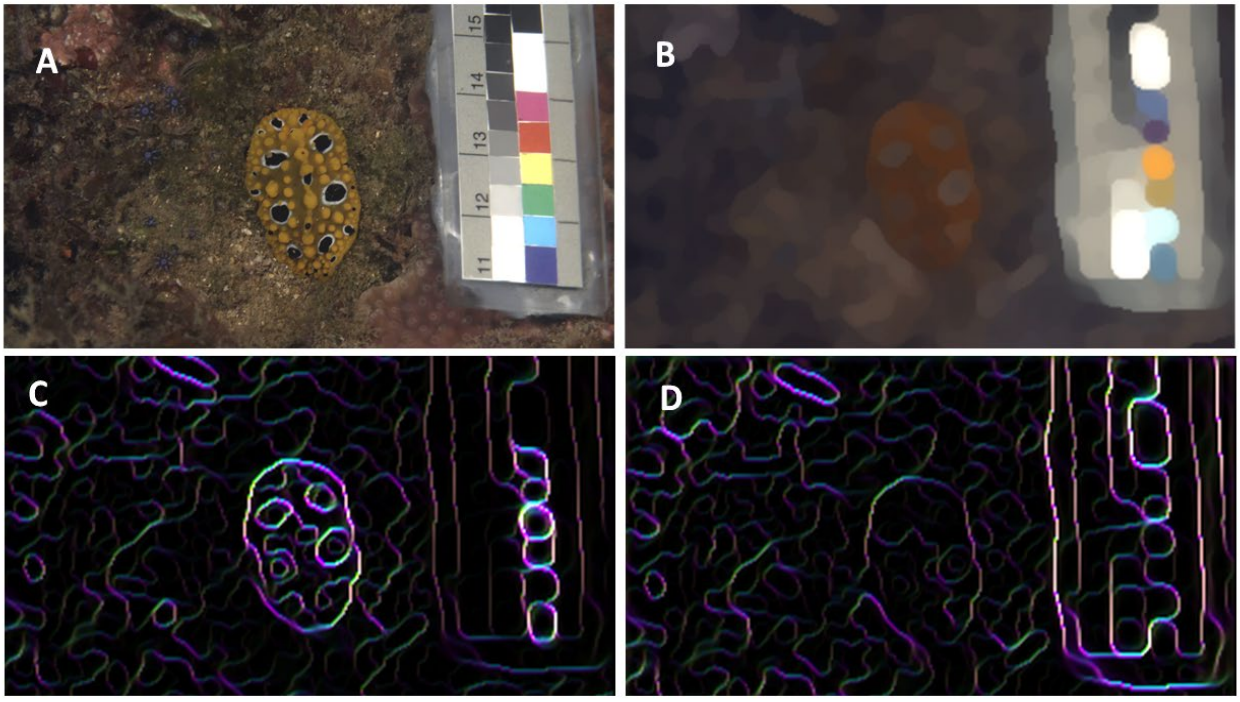

Figure S2.8: Example of an unclustered image (A), treated with RNL Filtering and subsequent extraction of the chromatic ΔS Edge Maps. B shows a RGB reconstruction of the image after modelling of triggerfish (*R. aculeatus*) colour and spatial vison at 30cm distance in a greenish natural light environment. C shows a composite image of all 4 directions of the chromatic edge contrast, each indicated with a different colour. Blue=horizontal, Yellow=vertical, Green=diagonal top left to bottom right, Magenta= diagonal top right to bottom left. The brightness corresponds to the edge intensity (See suppl. Material for details). D is the equivalent of C but using the luminance contrast in ΔS.

XYZ Chromaticity and Saturation Images

XYZ coordinates can be calculated for each pixel using the RNL equations provided by Renoult et al. (2017). The saturation image shows $\Delta S_{Sat,i}$ values (i.e. the distance of each pixel's colour to the achromatic point, equivalent to saturation).

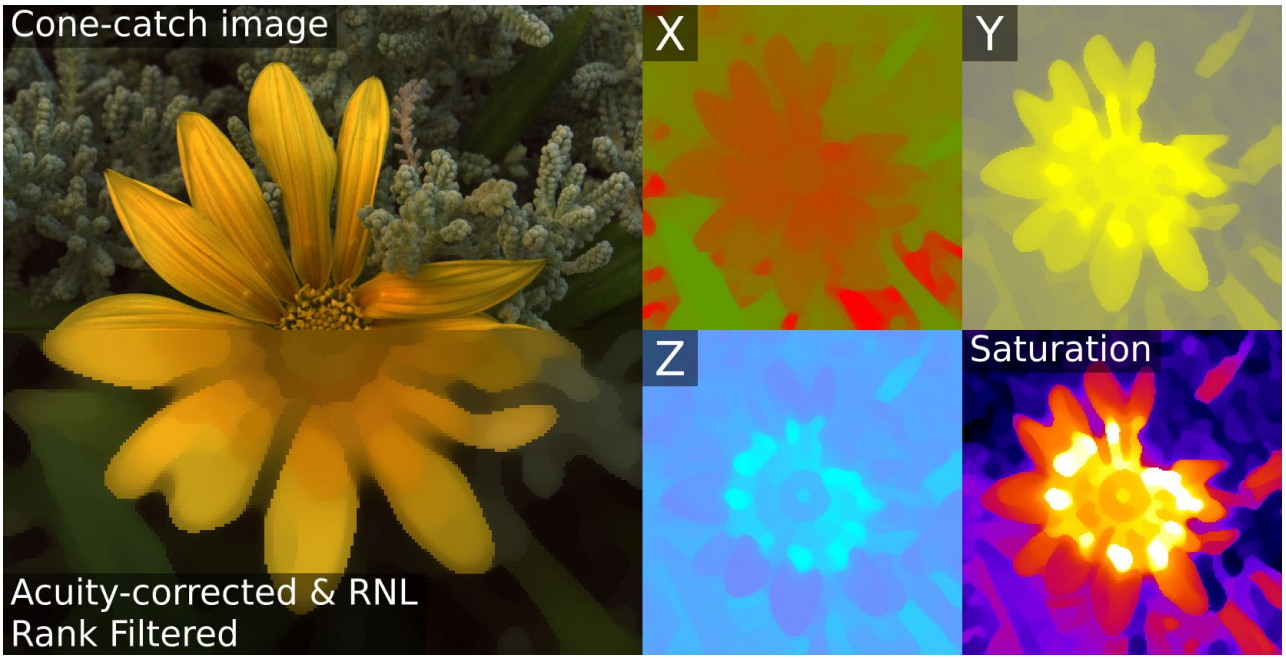

Figure S2.9 An example of the red-green (lw:mw) opponent channel (X), blue-yellow ((lw+mw):sw) channel (Y) and the UV channel (Z) where the colour indicates the position of a pixel along that axis. The saturation image shows the distance of each pixel to the achromatic point.

Naïve Bayes Clustering

If a pattern consists of very distinctly coloured elements or vision parameters are unknown, QCPA provides an alternative image segmentation technique, Naïve Bayes Clustering. The user can define a set of clusters by selecting corresponding pixels from a given pattern element (e.g. the yellow petal of a flower). Using a Naïve Bayes classifier (Domingos & Pazzani, 1997) the rest of the pixels in a pattern can be attributed to each of the user defined categories based on the probability of belonging to each of the categories. This approach is similar to the frequently used k-means clustering (Hartigan & Wong, 1979). However, Naïve Bayes Clustering allows the user to pre-define the clusters by making active selections in a pattern whereas k-mean clustering segments an image simply based on the similarity of each pixel in an image to each other and a pre-defined number of clusters. Thus, naïve Bayes clustering is a lot more interactive and allows a more tailored segmentation than k-means.

Impact of RNL Ranked Filter: Falloff

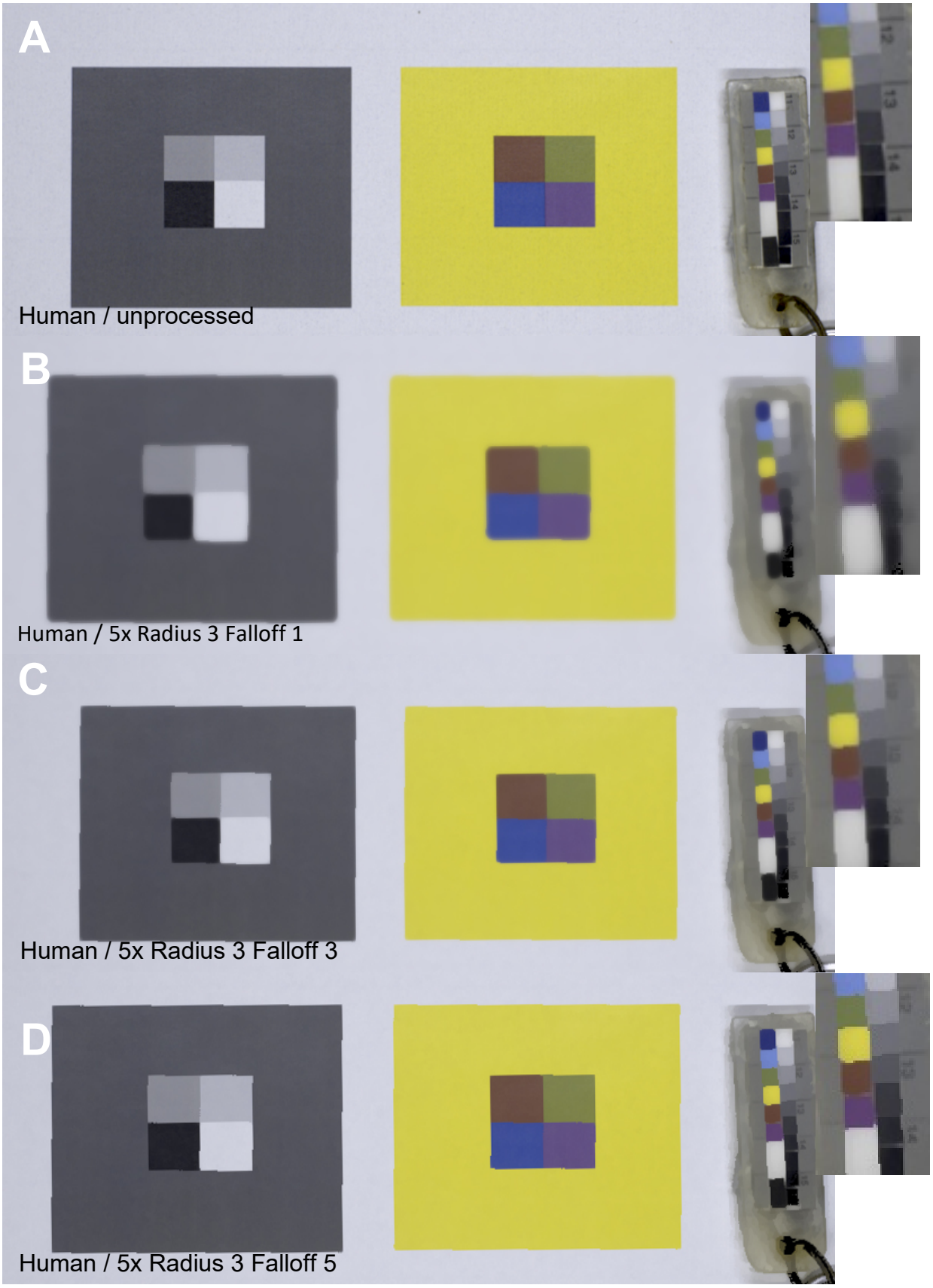

Figure S2.10 Examples showing the impact of varying the falloff intensity

Impact of RNL Ranked Filter: Radius

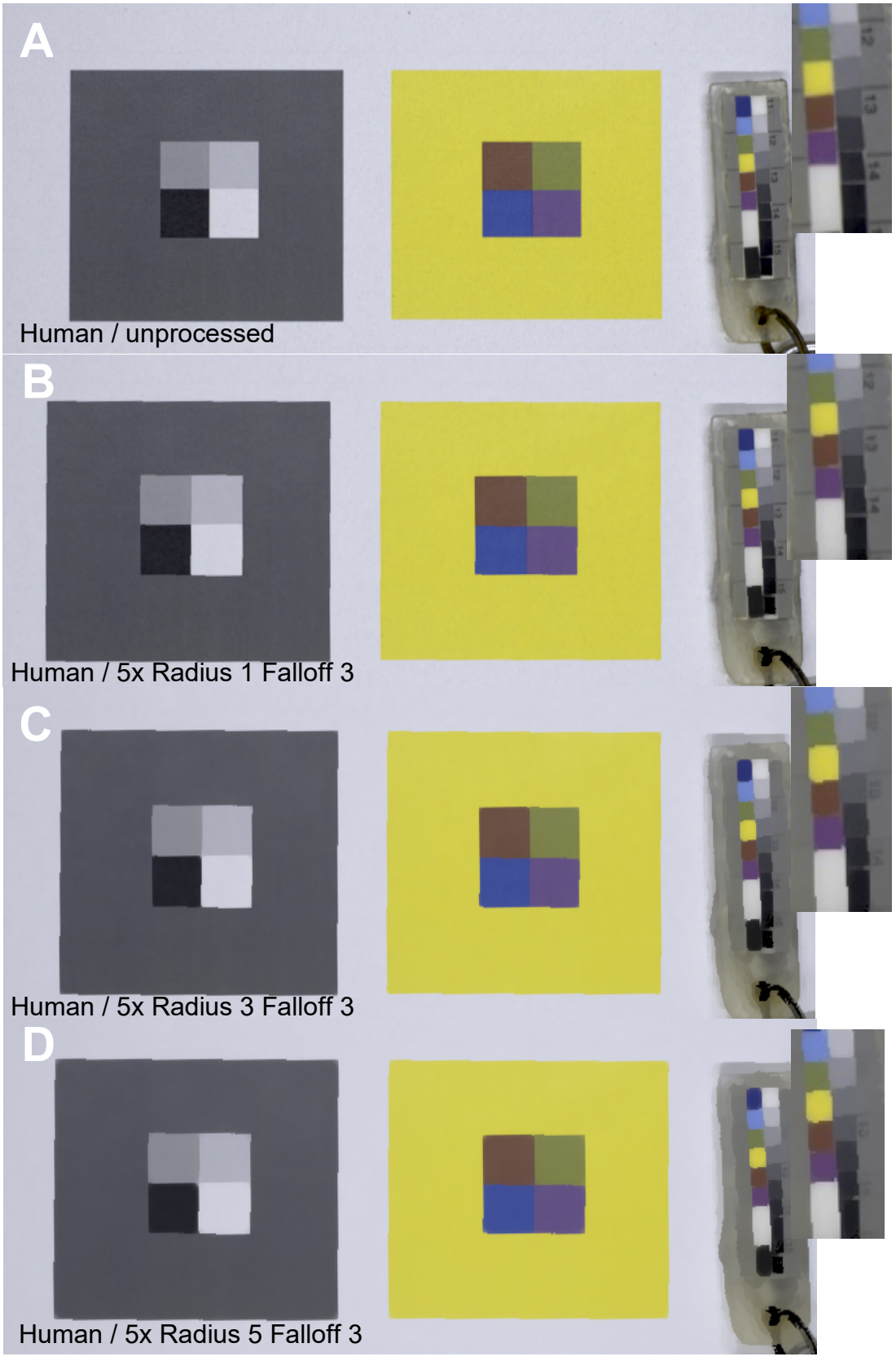

Figure S2.11 Examples showing the impact of varying the filter radius.

RNL Clustering and RNL Ranked Filter in Combination

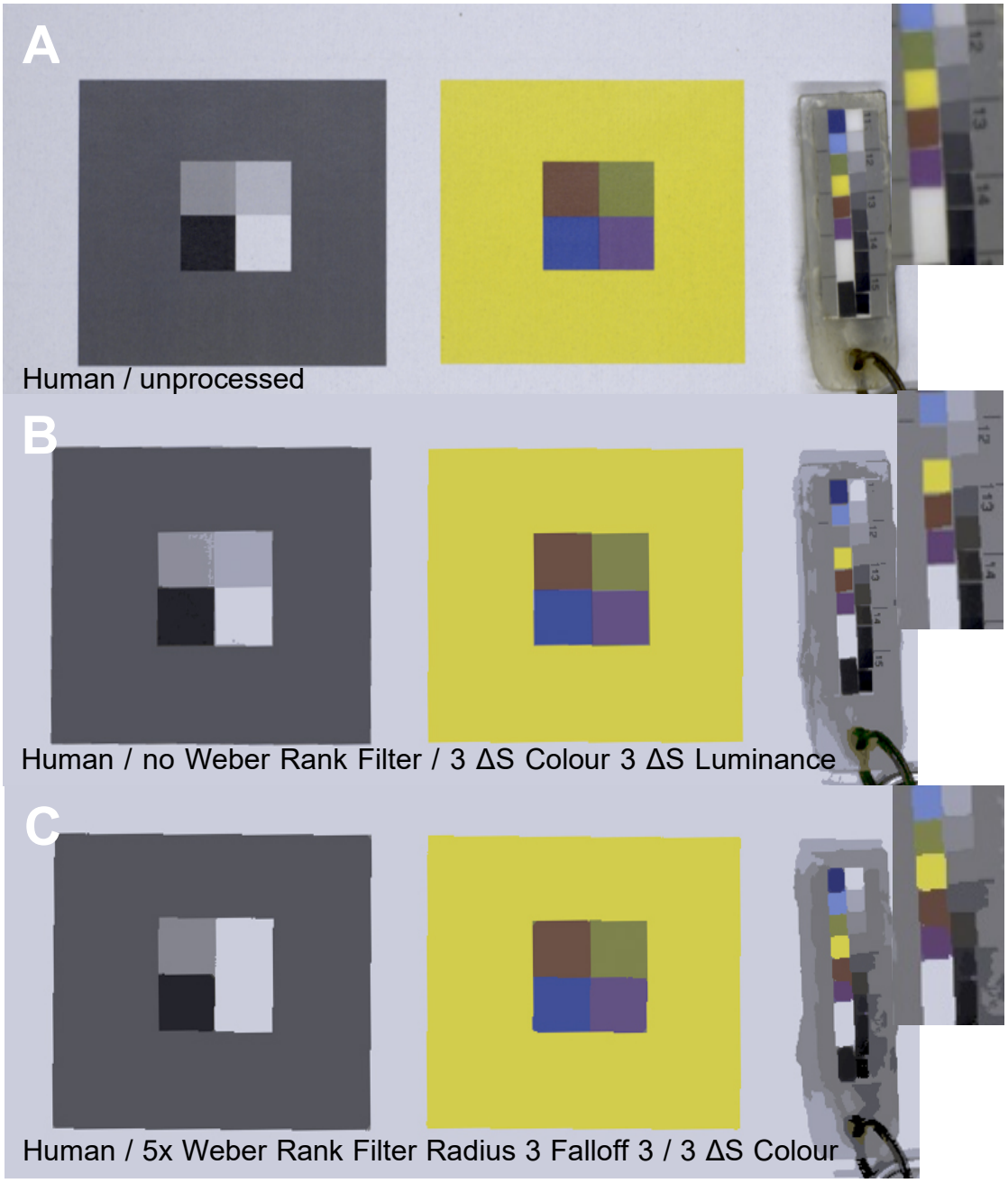

Figure S2.12 Example showing the impact of the RNL Ranked Filter on the RNL Clustering. Note the loss of small spatial detail between B & C but the increase in 'smoothness'. However, this can be modulated by choosing different filter settings to suit the best outcome.

RNL Clustering: Colour vs. Luminance Clustering

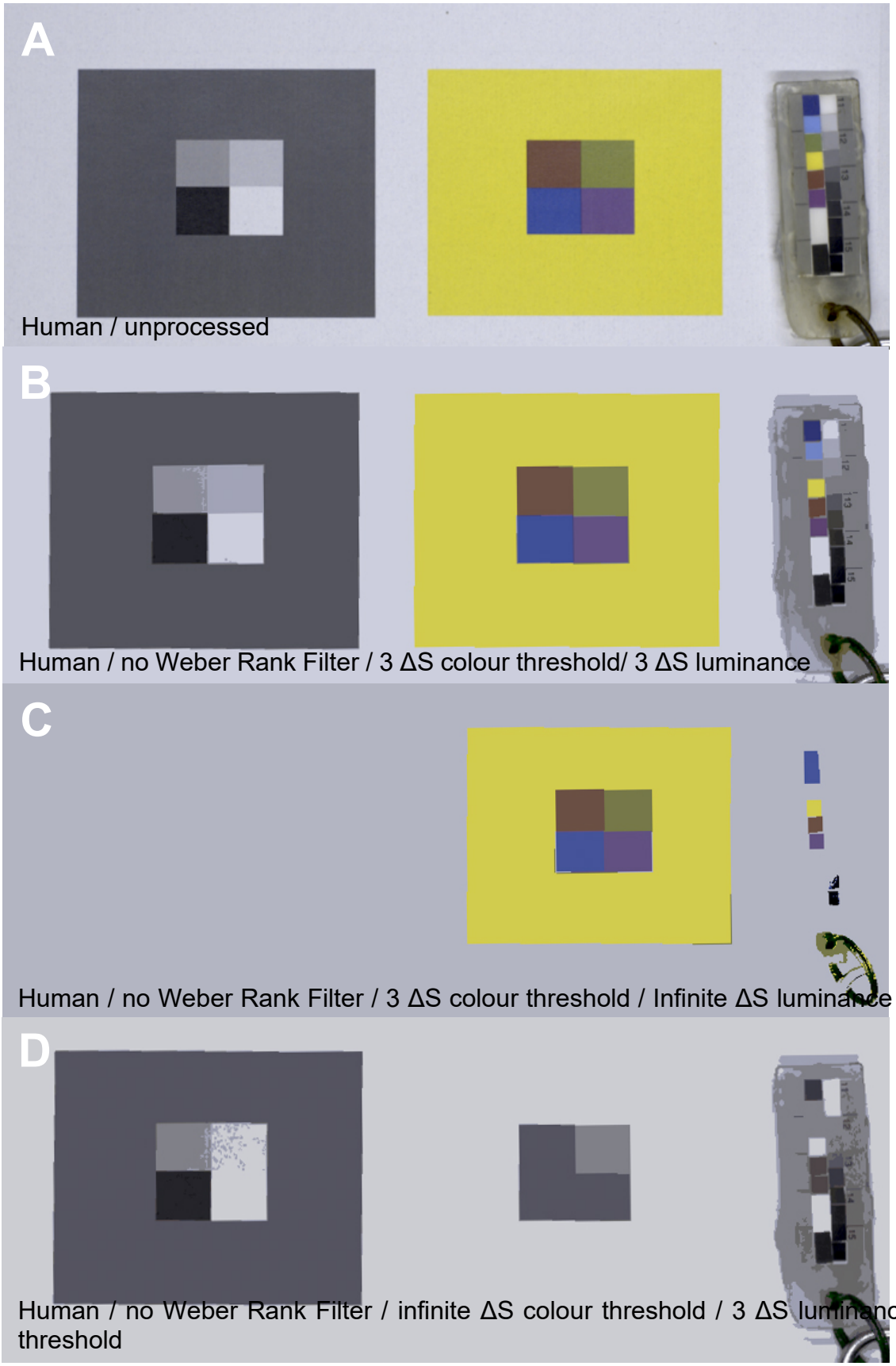

Figure S2.13 Example showing the impact of clustering with both an achromatic and chromatic threshold (B), only a chromatic threshold (C) and only an achromatic threshold (D).

AcuityView, RNL Ranked Filter and RNL Clustering in Combination

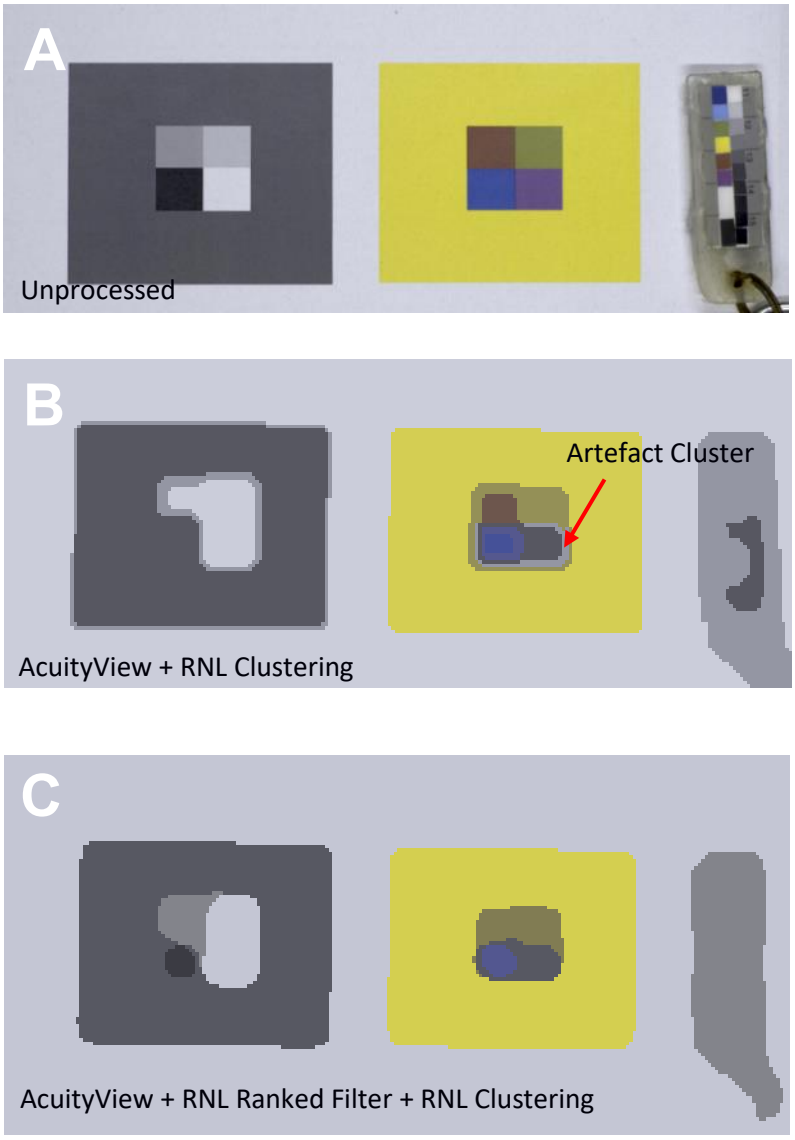

Human / unprocessed

Human / 3 cycles/degree from 0.5m distance/ 3 ΔS Colour / 3 ΔS Luminance threshold / no Weber Filter

Human / 3 cycles/degree from 0.5m distance/ 3 ΔS Colour / 3 ΔS Luminance threshold / 5x radius=MRA (5) Falloff 3 Weber Filter

Figure S2.14. Example showing the difference between using (C) and not using (B) the RNL Ranked Filter after modelling spatial acuity. Note the resulting artefact clusters in B.

Worked Example 1: Visual Defences in Nudibranchs Through the Eyes of a Triggerfish

Nudibranch molluscs are a diverse family of shell-less marine gastropods. Many of them are thought to be highly aposematic using vivid colour patterns together with chemical and mechanical defences to deter predators (Tullrot & Sundberg, 1991; Haber et al., 2010; Carbone et al., 2013). They have become an increasingly popular model organism for the study of the design, function and evolution of aposematic colouration (Cortesi & Cheney, 2010; Cheney et al., 2014; Winters et al., 2017). In this example we show the use of QCPA and its components to compare the colour pattern of two individual nudibranchs through the eyes of a potential predator, the lagoon triggerfish (*Rhinecanthus aculeatus*). The first one is an individual of the species *Phyllidia ocellata*, an assumedly aposematic species with high levels of chemical defence (Cheney et al. unpublished data). The second animal belongs to the species *Dendrodoris krusensternii*, an assumedly camouflaged species with no known chemical defences.

We first show the spectral sensitivities of the camera that was used, the visual system of the triggerfish as well as the light spectra under which the images had been taken and finally the light spectra for which we used the MICA toolbox to calculate the triggerfish's photoreceptor stimulation. We show the original image captured by the camera and the reconstructed RGB image based on the photoreceptor stimulation of a triggerfish at 5m depth in clear water.

We then estimate the spatial information available to our triggerfish viewer as per a given viewing distance and known visual acuity (Champ et al., 2014) using Fast Fourier Transform (FFT) based acuity modelling. We then recreate distinct boundaries in the image (as the fish is unlikely to perceive a blurred image). This is done by using the RNL Ranked Filter. We set the Filter so that its radius equals the Minimum Resolvable Angle to which the image has been rescaled (In this case, 5 pixels per MRA). This prevents the creation of artificial clusters when we then continue to segment the image into its colour pattern elements using the RNL Clustering. We can use both the clustered and the unclustered image to derive secondary image statistics and data visualisations. These steps can be done at multiple simulated viewing distances or light environments, which we do not do here in this example.

Similarly, we can analyse the second individual from the species *Dendrodoris krusensternii*. We can then compare some selected image statistics to quantify the degree of background matching in either one of the animals. We can also quantify the salience of each animal colour pattern.

Spectra and Sensitivities

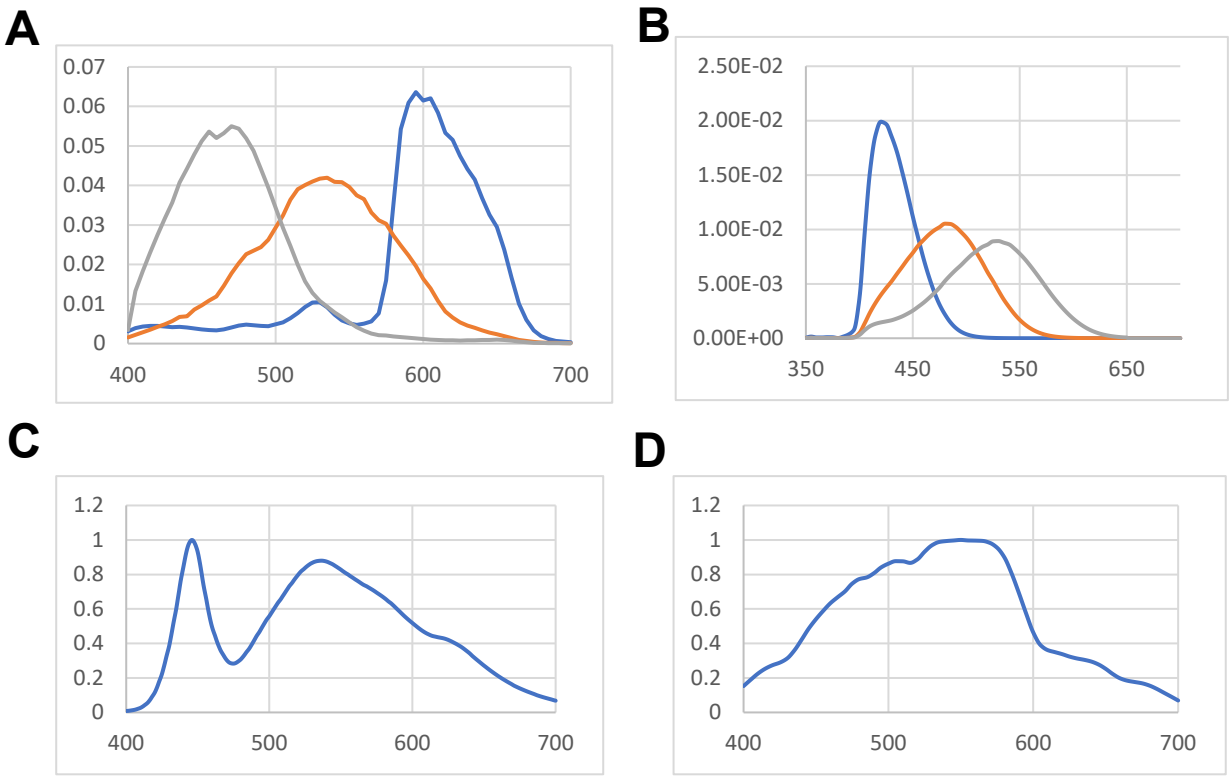

Figure S2.15: A: Spectral sensitivity of the camera used in this example (Olympus PEN-EPL5). The spectral sensitivity is available in the micaToolbox. Grey: blue channel sensitivity, orange: green channel sensitivity, blue: red channel sensitivity. B: Spectral sensitivity of the lagoon triggerfish (R. aculeatus). Blue: sw cone sensitivity, orange: mw cone sensitivity, grey: lw cone sensitivity. C: Light spectrum of the white LED video lights used for photography D: Light spectrum at 5m depth with a moderate amount of green algae in the water column.

Phyllidia ocellata (aposematic nudibranch)

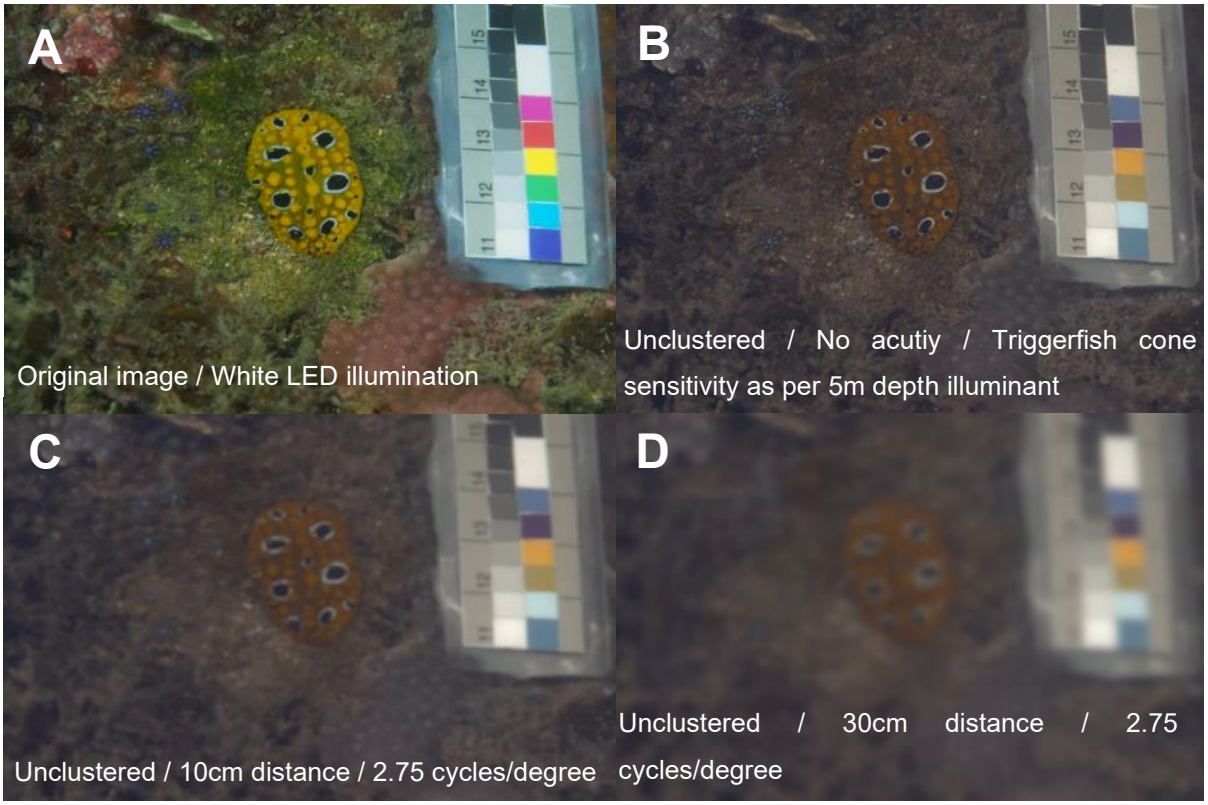

Figure S2.16: Modelling cone capture quanta (B) and spatial acuity (C&D).

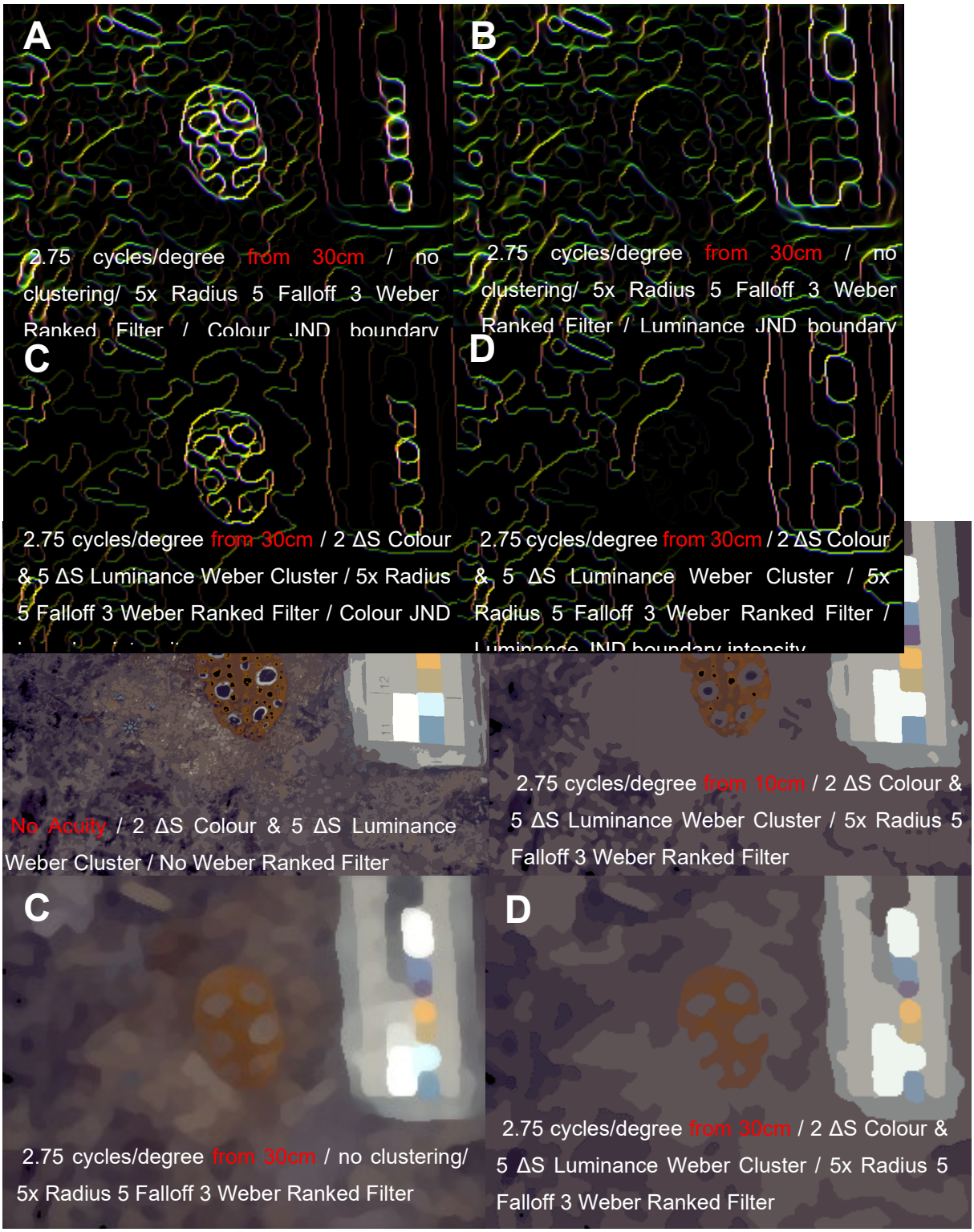

Figure S2.17: Clustering the image and recreating distinct pattern boundaries

Figure S2.18: Using the unclustered image (Fig S2.17C) to visualise local edge contrast with LEIA. These images can be quantified using the LEIA output parameters.

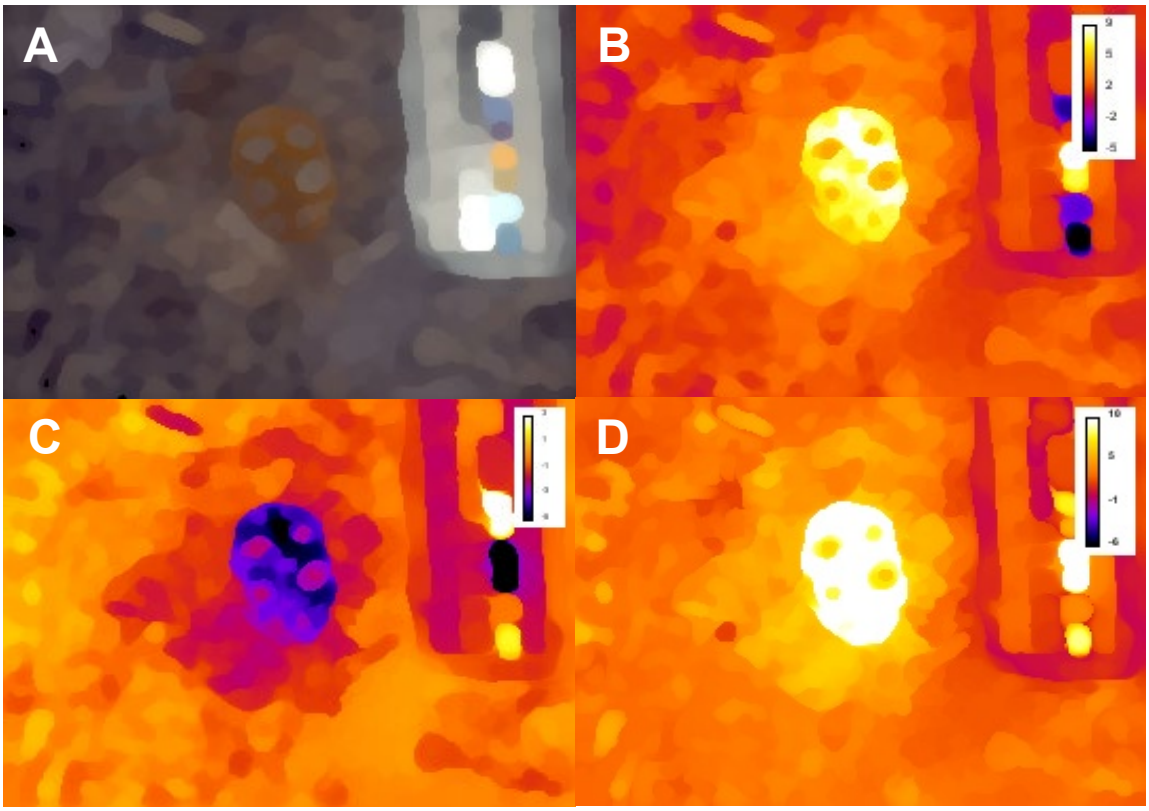

Figure S2.19: Using the unclustered image (A) to visualise opponent channel stimulation in 'XYZ Chromaticity Images'. B: The X-axis of colour space. C: The Y-axis of colour space. Note that there is no Y-axis as we are using a tri-chromatic visual system. D: Saturation Image. The user may want to quantify these images using pattern analysis or image analysis tools provided in ImageJ and MICA.

***Dendrodoris krusensternii* (cryptic nudibranch)**

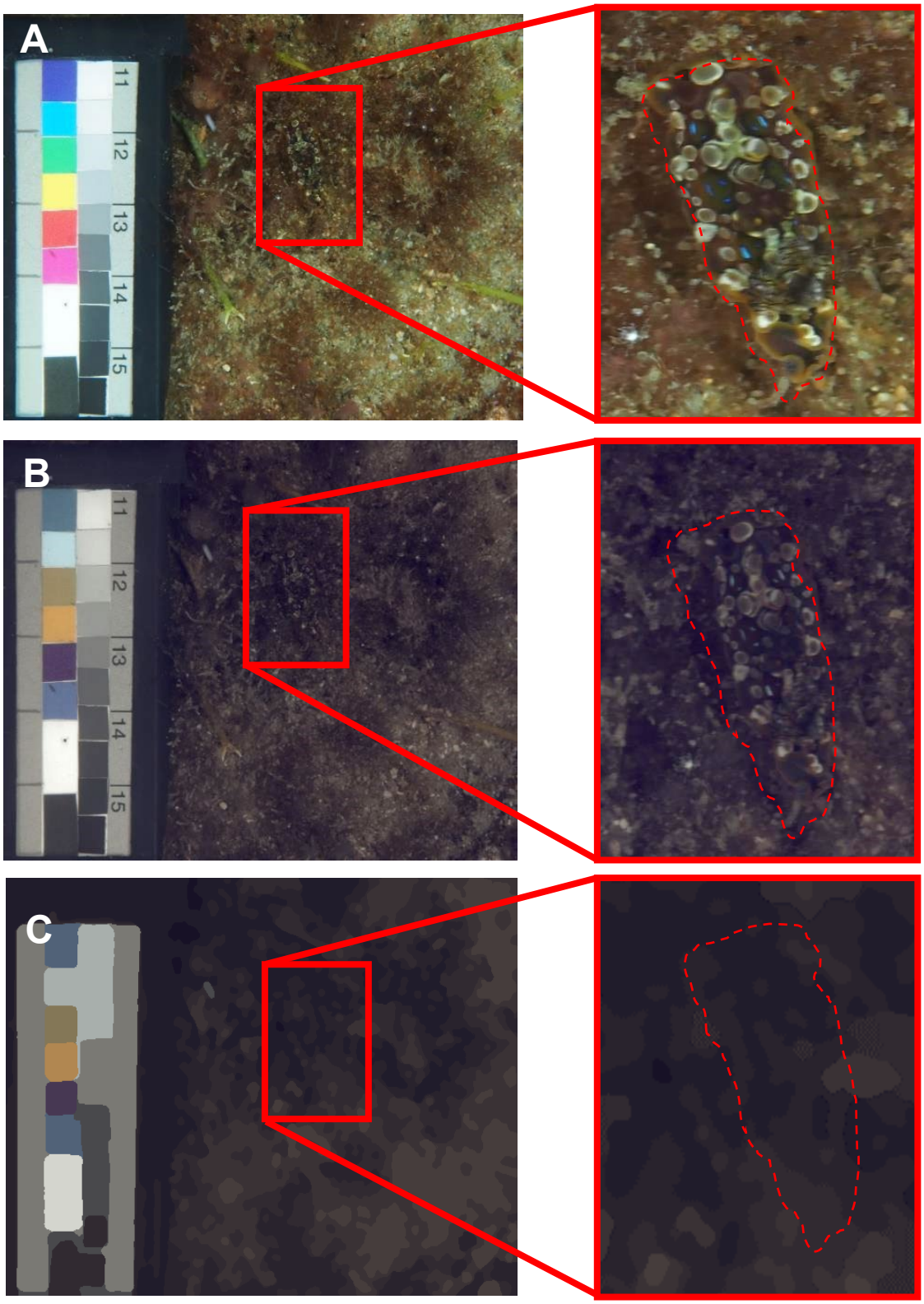

Figure S2.20: A) RAW image of a cryptic nudibranch (Dendrodoris krusensternii) against its natural background. The animal is highlighted with a dashed red line. B) The same image transformed into triggerfish vision (*R. aculeatus*) without visual acuity modelling. C) With RNL ranked filter and RNL clustering but no visual acuity modelling.

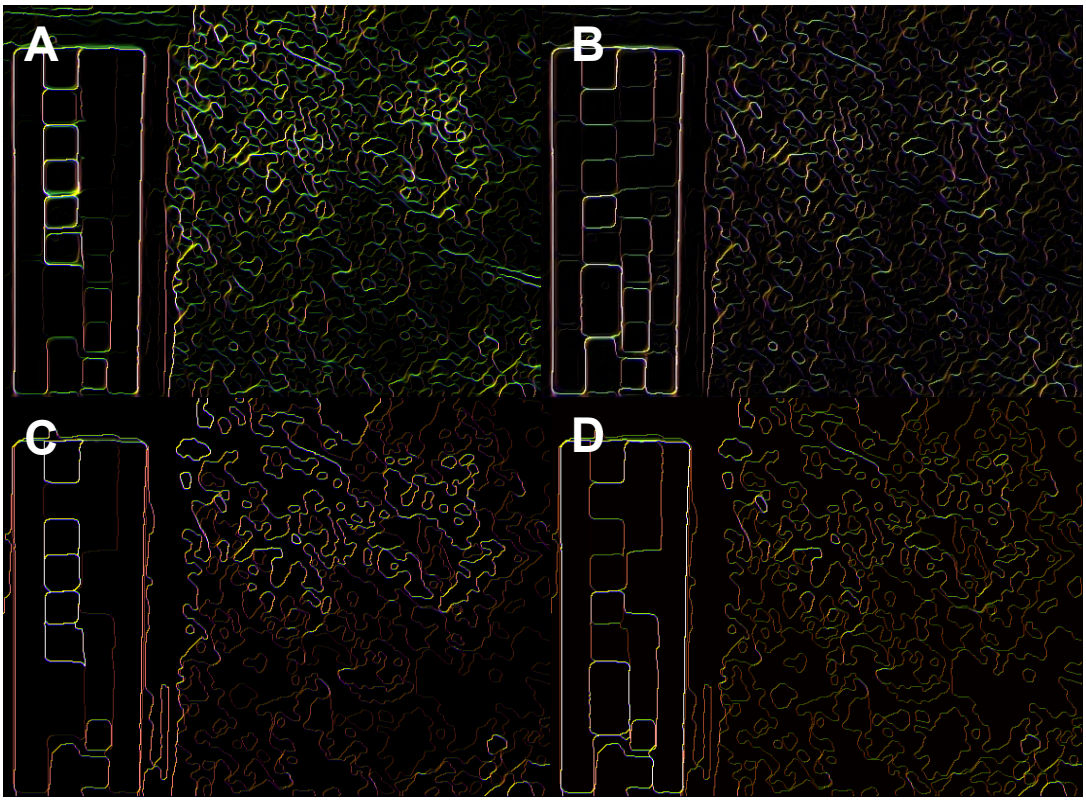

Figure S2.21: ΔS Local Edge Intensity images of Fig S2.17A. A & B: Unclustered C & D: RNL Clustered. A & C show chromatic edge intensities B & D achromatic edge intensities. Note how the clustering essentially just removes the low intensity edges. The animal is not visible in either one of the images. Intensity images can be quantified using the LEIA parameters.

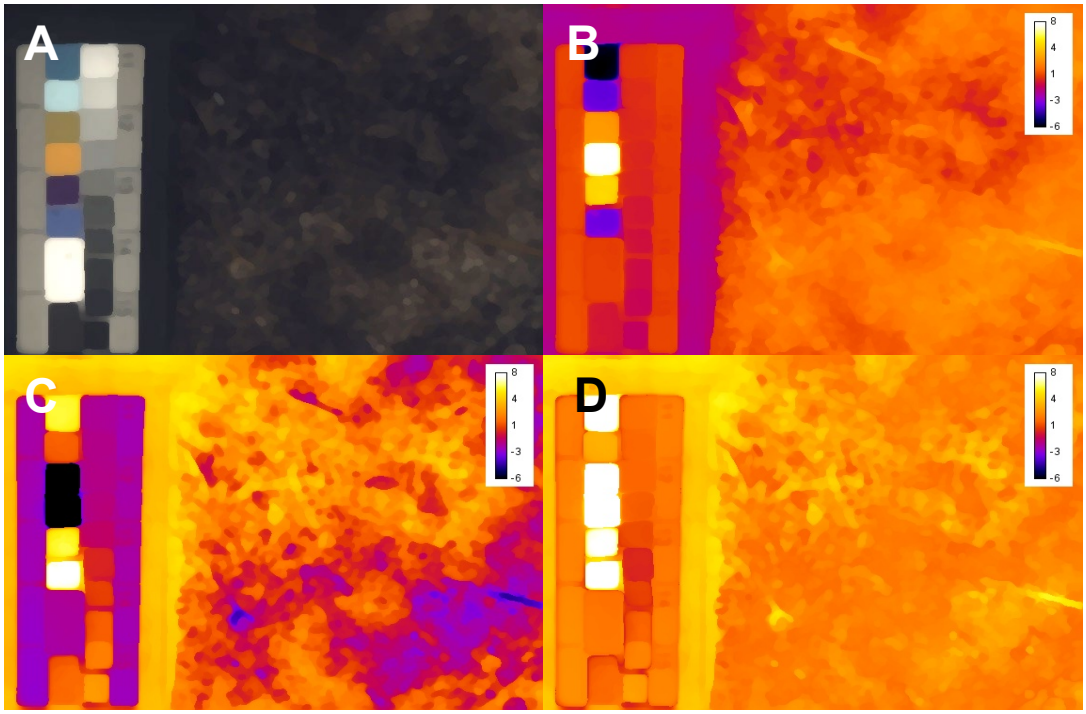

Figure S2.22. A: Unclustered image at 10cm viewing distance using triggerfish visual acuity and spectral sensitivity. B: X-axis chromaticity image. C: Y-axis chromaticity image. D: Saturation image. The user may want to apply pattern analysis and imageJ image analysis tools to quantify these images.

Deriving Animal + Background Parameters

To interpret the colouration of our two animals (separate as well as in contrast of their visual backgrounds) we need to analyse them separately as regions of interest (ROIs) in each picture.

Figure S2.23: The Region of Interest (ROI) selection for the animal vs. background comparison. Please see the online user guide for details on ROI selection. Note: The area of the background can also be standardised, e.g. using a fix animal to background area ratio if that is desirable.

The selection of the ROIs can be made in an RGB reconstructed colour image which is often easier than using the grey scale intensity image layers of a multispectral image. The ROI manager in ImageJ remembers the ROI selection so you can select the multispectral image and click on the ROI which will then show up. Thus, the ROI selection can be made at any of the two following stages:

1. Right after creating or opening a multispectral image
2. After translating the multispectral image into cone catches

The prerequisite is that the size of the image is the same between these changes, so the ROI remains the same. If you change the size of the image (i.e. after rescaling in the process of modelling visual acuity) and select the ROI it will not match anymore.

In this case we are analysing the animal separate from its background and thus (After modelling cone captures) we want to continue processing the ROIs separately from each other.

Because the ROIs are irregularly shaped, we can't use AcuityView 2.0 but instead must use the Gaussian filter to model spatial acuity of our triggerfish (see 'AcuityView 2.0 & Gaussian Convolution Filter' in this document). We choose a viewing distance of 10 cm and 30 cm for both nudibranchs. Note that any kind of acuity modelling quickly turns the cryptic pattern into a uniform brown (Fig. S2.24). The MRA (Minimum resolvable angle) should be set at 5 pixels/MRA or above to avoid losing information (See 'AcuityView 2.0 & Gaussian Convolution Filter'). Also note that we need to select a size standard prior to acuity modelling.

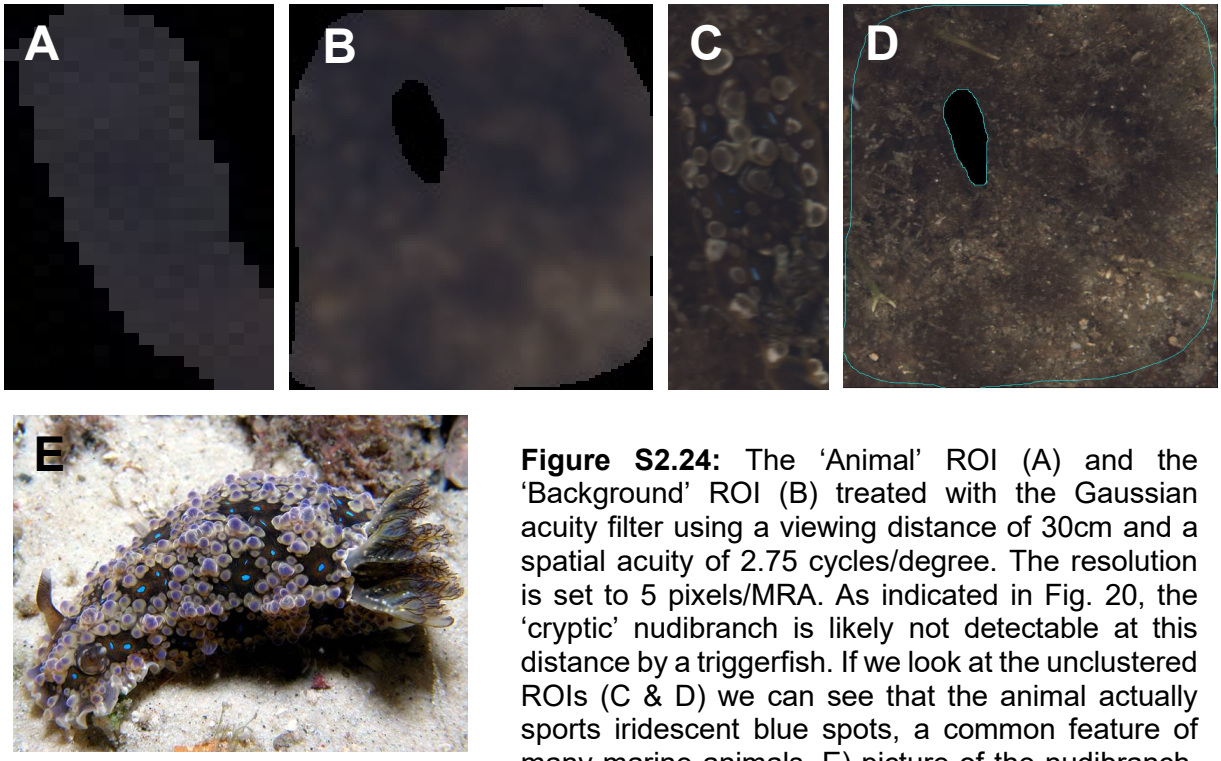

Figure S2.24: The 'Animal' ROI (A) and the 'Background' ROI (B) treated with the Gaussian acuity filter using a viewing distance of 30cm and a spatial acuity of 2.75 cycles/degree. The resolution is set to 5 pixels/MRA. As indicated in Fig. 20, the 'cryptic' nudibranch is likely not detectable at this distance by a triggerfish. If we look at the unclustered ROIs (C & D) we can see that the animal actually sports iridescent blue spots, a common feature of many marine animals. E) picture of the nudibranch, *Dendrodoris krusensternii* (by Dave Harasti) in close up on a more contrasting background.

The 'blurred' ROIs then need to be treated with the RNL ranked filter to remove most of the blur. For this we choose the following settings: 5 repeats with a radius of 5 pixels (the size of our MRA) and a falloff of 3. We set the noise ratios at 0.05 (mw), 0.05 (lw), 0.07 (sw) and 0.05 (dbl) (Fig. S2.23 A & C).

As Fig. S2.24 suggests, even at 10cm it is likely that our cryptic nudibranch does not bear any discriminable patterning when considering our triggerfish observer. The background most likely consists of a few brownish hues into which the cryptic nudibranch blends nicely. This notion of background matching is supported when looking at the similarity of the clustered nudibranch colour and its surrounding background. The nudibranch has a saturation contrast (Distance from the achromatic point in the log-transformed RNL colour space) of less than 0.1 ΔS, a chromatic contrast (distance between the animal and its background in the log- transformed RNL colour space) of 0.58 ΔS and a luminance Michelson contrast of 0.02%. We can also quantify the chromatic background matching of this assumedly cryptic nudibranch using a RNL colour map (Fig. S2.26). This shows us that our animal is an almost

perfect chromatic match to its background. The overlap measure provided by the colour map feature tells us that the animal ROI overlaps with 27.5% of the background ROI.

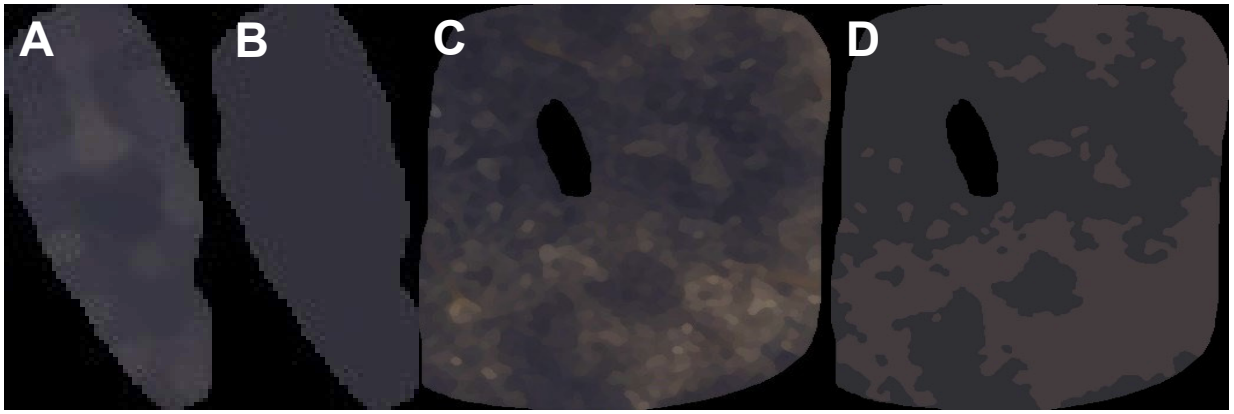

Figure S2.25: A) The RNL treated animal ROI from 10cm. B) The clustered animal ROI using a colour discrimination threshold of 3 ΔS and an achromatic discrimination threshold of 4 ΔS. Note that while patterning is visible in A the contrast is not sufficient to be picked up by the clustering, resulting in a single uniform cluster for the animal. C) The RNL treated background ROI from 10cm D) the clustered background using a colour discrimination threshold of 3 ΔS and an achromatic discrimination threshold of 4 ΔS. Note the difference to image S20c where no acuity modelling was applied.

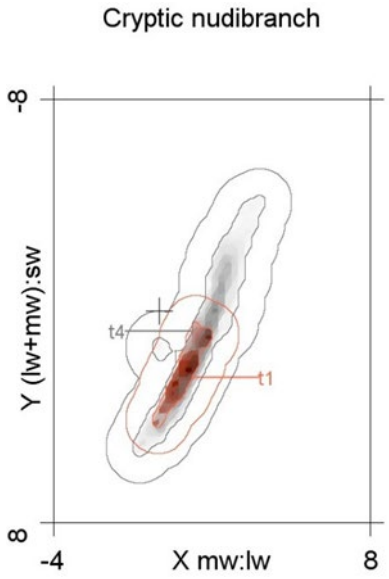

Figure S2.26: A colour map of our cryptic nudibranch (t1) and its visual background (t4). The darkness indicates the frequency of pixels in that area of the log transformed RNL colour space. The border line around each cloud corresponds to 1 ΔS. The cross indicates the location of the achromatic point. We can easily see that the animal is an almost perfect subsample of its visual background.

Based on this outcome for the cryptic nudibranch we can see that there is no information on pattern to analyse at very close distances. It would therefore lead to the conclusion that the selective pressure that lead to the evolution of the blue spots in *Dendrodoris krusensternii* is probably due to an animal with better spatial resolution than what we assume to be the case for our triggerfish (2.75 cycles/degree). It could also be that the blue spots contribute to the additive blurring that leads to the observed background matching. While we could go and analyse the ROIs using an even smaller viewing distance or no acuity modelling at all (i.e. assuming human-like spatial acuity), we do not do this here.

We can now look at our assumedly ‘aposematic’ nudibranch, *Phyllidia ocellata*. We do know (Cheney et al. unpublished data) that this species is highly distasteful to potential predators, but we now want to investigate if it also shows signs of being ‘conspicuous’ i.e. displaying vivid visual contrast that helps predators to remember and detect the animal.

First, we model spatial acuity with a 10cm viewing distance for each the animal and its visual background, using the same settings as in the previous example (Fig. S2.27).

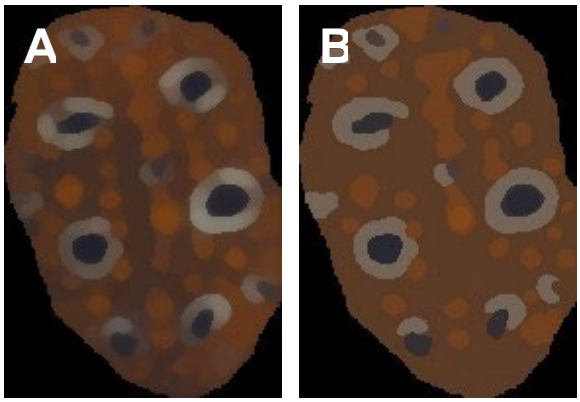

Figure S2.27: A) The RNL treated animal ROI from 10cm. B) The clustered animal ROI using a colour discrimination threshold of 3 ΔS and an achromatic discrimination threshold of 4 ΔS. C) The RNL treated background ROI from 10cm D) the clustered background using a colour discrimination threshold of 3 ΔS and an achromatic discrimination threshold of 4 ΔS. Note the similarity of the background to the cryptic nudibranch example.

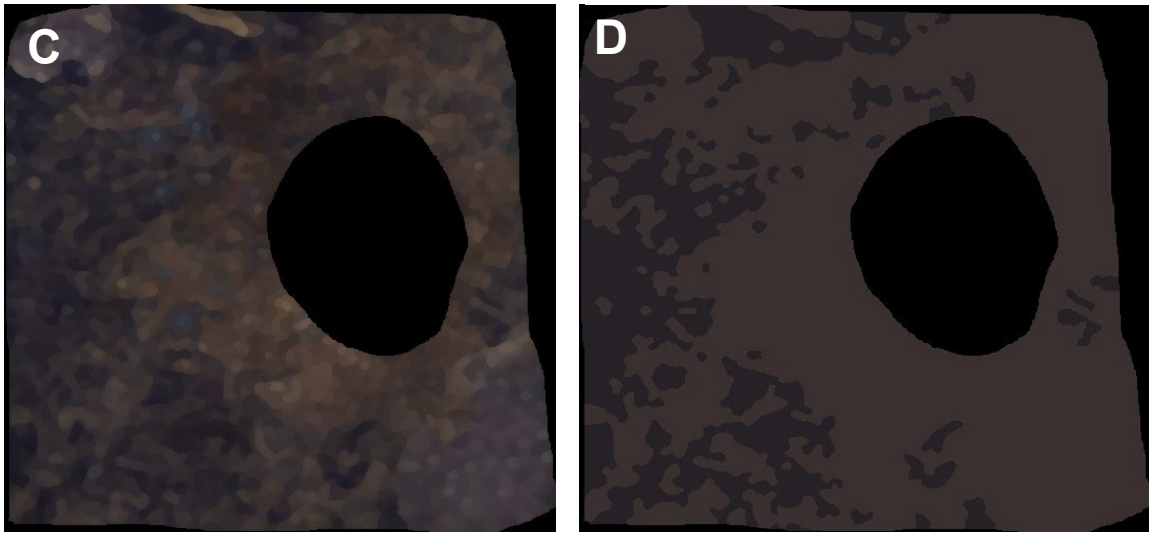

We can now use the clustered ROIs to run the pattern analyses on. This gives us all the pattern statistics of the adjacency analysis, the visual contrast analysis and the boundary strength analysis as well as descriptions of each colour pattern element in the ROIs. We can also use the RNL ranked filter treated images to estimate background matching using a colour map overlap analysis.

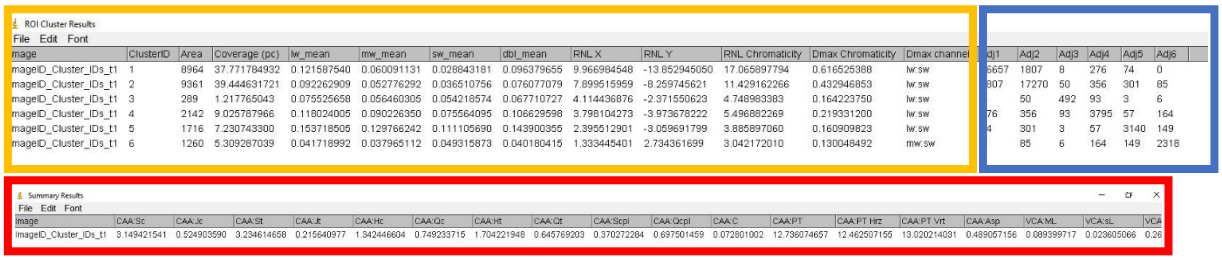

Figure S2.28: The output of the QCPA pattern analysis. The orange box contains information on each colour pattern element in the ROI. The blue box shows the adjacency analysis (horizontal and vertical output is possible which triples the parameter output). The red box shows all pattern parameters.

We will not dive any deeper into the analysis of the pattern parameters at this stage. However, we would like to point out that various pattern parameters will indicate animal-background contrast (Fig. S2.26) on top of several other measures indicating significant chromatic, achromatic and pattern contrast of our second animal against its background (e.g. Fig. S2.27). We will continue to elaborate worked examples and applications of specific tools in QCPA on the website (www.empiricalimaging.com) so please continue to check there on updates on worked examples, tutorial videos, user guides as well as to get in touch with the wider user community in the forum.

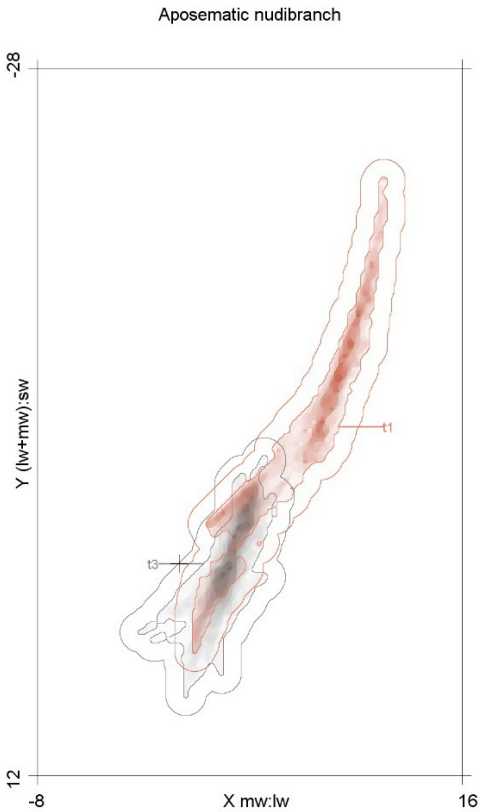

Figure S2.29: A colour map of our cryptic nudibranch (t1) and its visual background (t3). The darkness indicates the frequency of pixels in that area of the log-transformed RNL colour space. The border line around each cloud corresponds to 1 ΔS. The cross indicates the location of the achromatic point. In this case the animal shares a mere 8% overlap with its visual background.

Worked Example 2: Jersey Tiger Moth (*Euplagia quadripunctaria*)

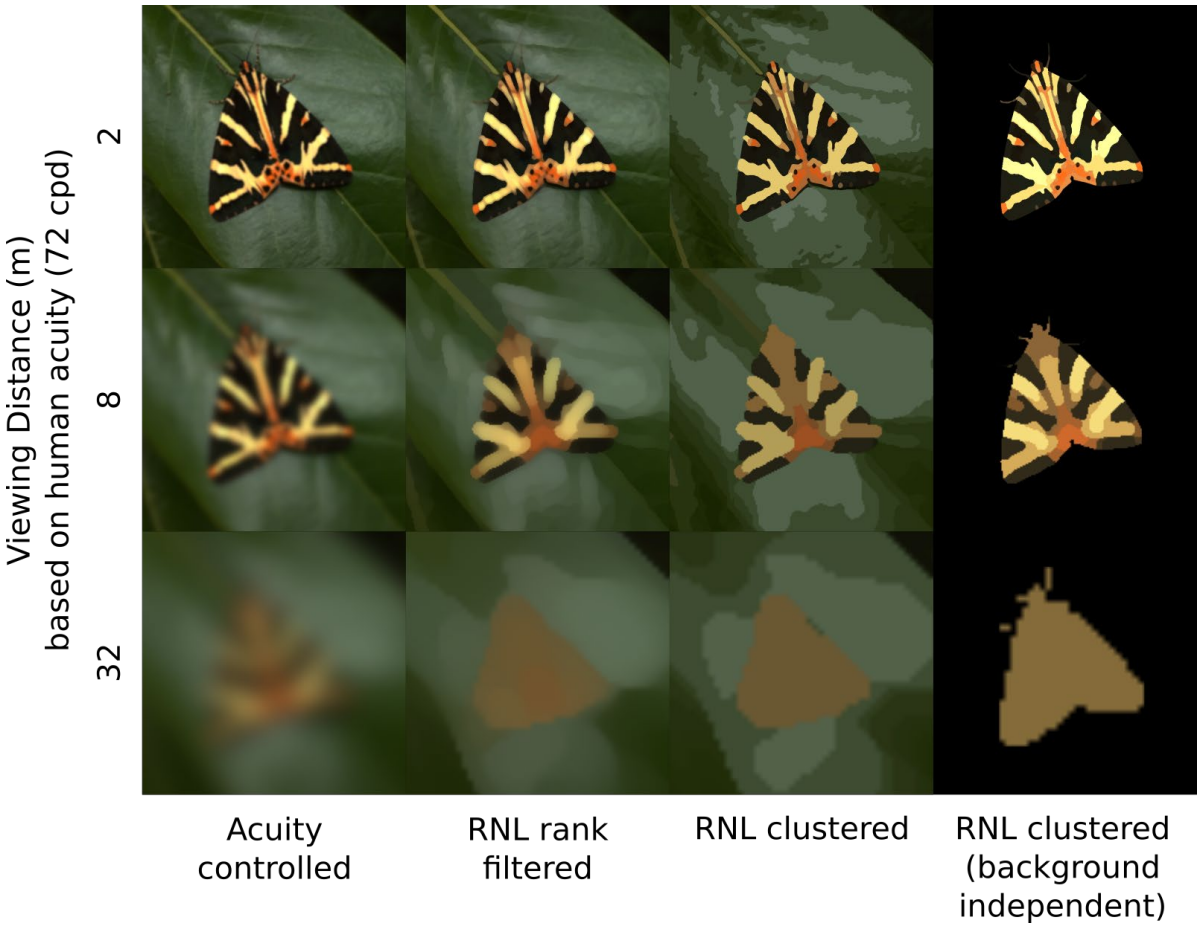

Figure S2.30: The aposematic warning colours of many species (such as this Jersey tiger moth *Euplagia quadripunctaria*) will blend together when viewed from a sufficient distance, and may camouflage the animal well against a neutral coloured background. This figure shows the QCPA processing steps at different simulated viewing distances. The QCPA framework can either measure whole images (left three columns), or 'regions of interest' measured independently of their backgrounds (right-hand column).

Worked Example 3: Oak Beauty Moth (*Biston strataria*)

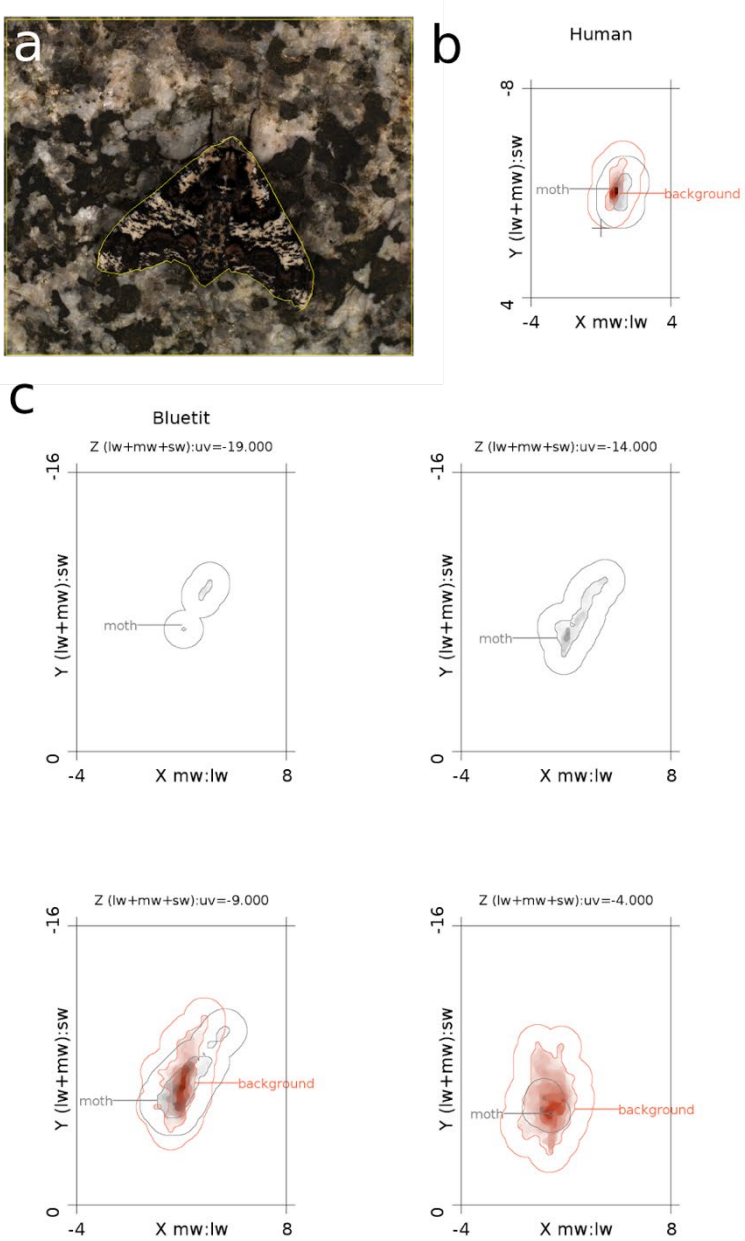

Figure S2.31`: 'Colour maps' are a novel colour visualisation and colour comparison tool introduced by the QCPA framework, capturing the entire range of colour gradients visible to a given receiver at a given distance in any part of a scene. These examples are produced from a multispectral photograph (visible and UV) of an oak beauty *Biston strataria* moth against a stone background (a) in human (trichromatic, b) and bluetit (tetrachromatic, c) colour-space. Colour intensity in the point clouds show the frequency of pixels at each point in the receptor noise limited colour space, while the boundary around each pixel cloud shows a ΔS radius of 1 'just noticeable difference', and the achromatic point (grey) is shown with a cross '+'. The moth is a good colour-match to its background in human-vision, with 28.3% colour overlap, and the moth colours sit within the 1 JND boundaries of the background. Bluetit vision is illustrated as a stack of maps through the UV-axis (in this instance at just four levels, c), which

show how the moth and background have substantially different colours in the UV dimension, with a colour overlap of just 1.4%

Appendix B – Supplementary Material: Chapter 3

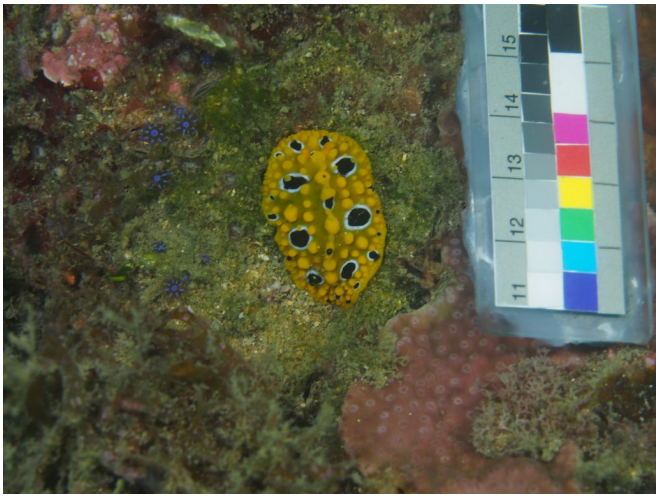

Figure S3.1: Picture of a nudibranch with the resin-cast colour standard. For detailed instructions and discussion see http://www.empiricalimaging.com/knowledge-base/make-your-own-colour-grey-standard/

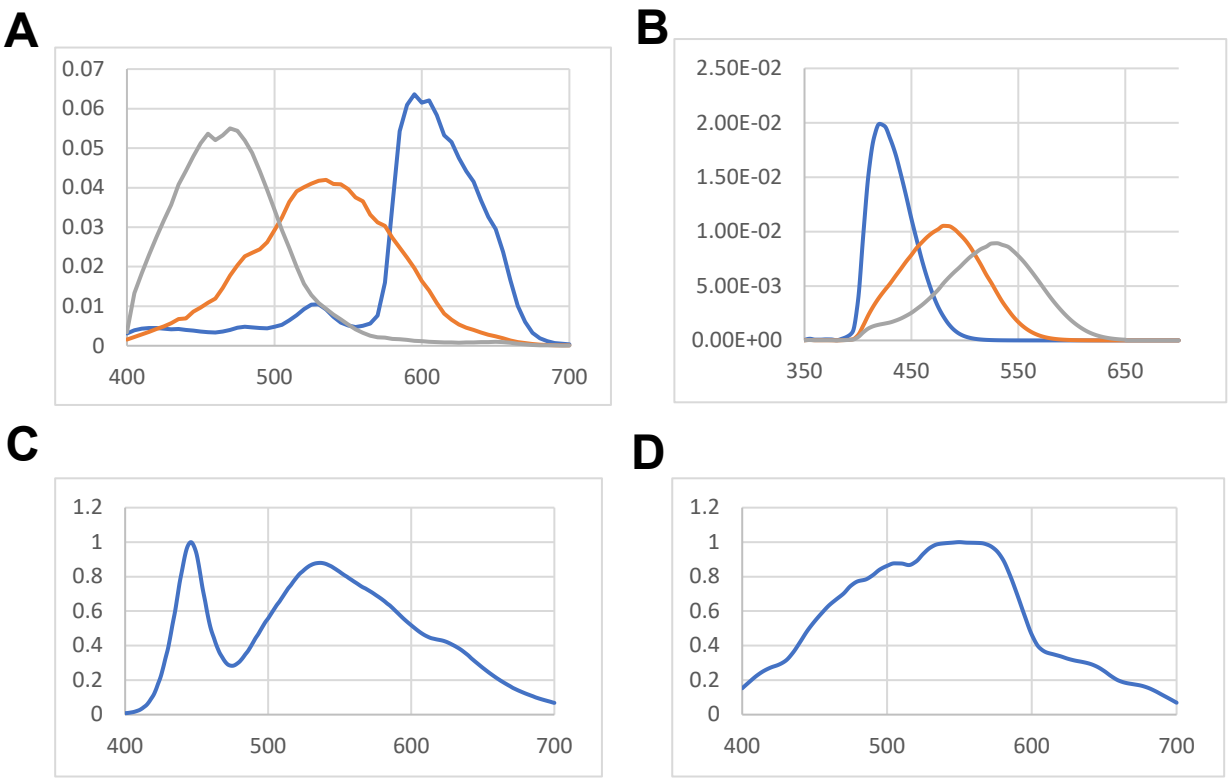

Figure S3.2: A: Spectral sensitivity of the camera used in this example (Olympus PEN-EPL5). The spectral sensitivity is available in the micaToolbox. B: Spectral sensitivity of the lagoon triggerfish (*R. aculeatus*) C: Light spectrum of the white LED video lights used for photography D: Light spectrum at 5m depth with a moderate amount of green algae in the water column.

Appendix C – Supplementary Material: Chapter 4

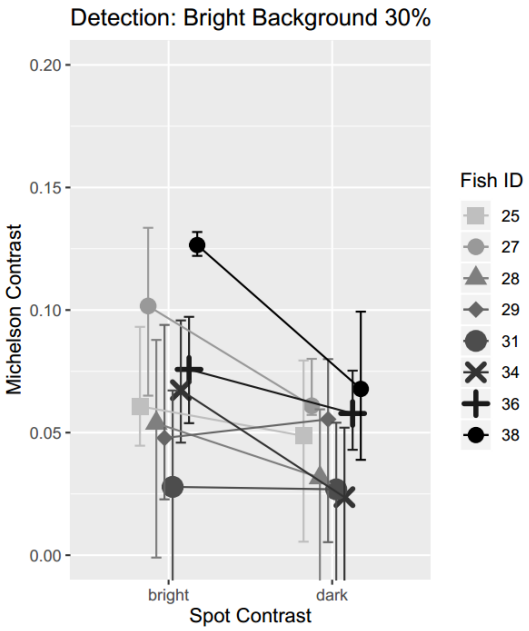

Figure S4.1: Individual detection thresholds for group 2 (bright background) at 30% correct choice.

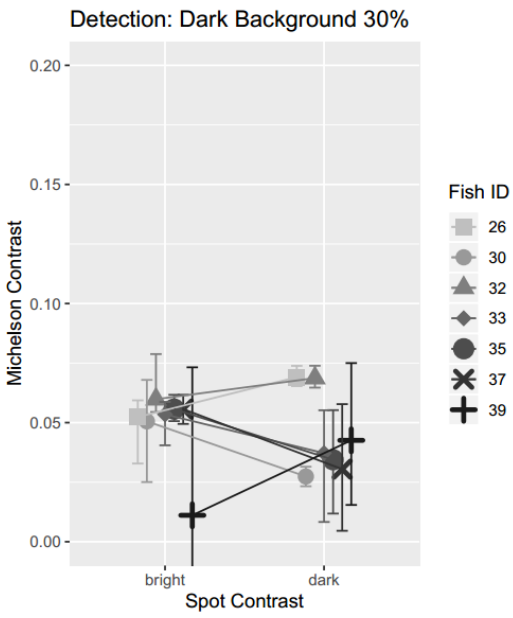

Figure S4.2: Individual detection thresholds for group 1 (dark background) at 30% correct choice.

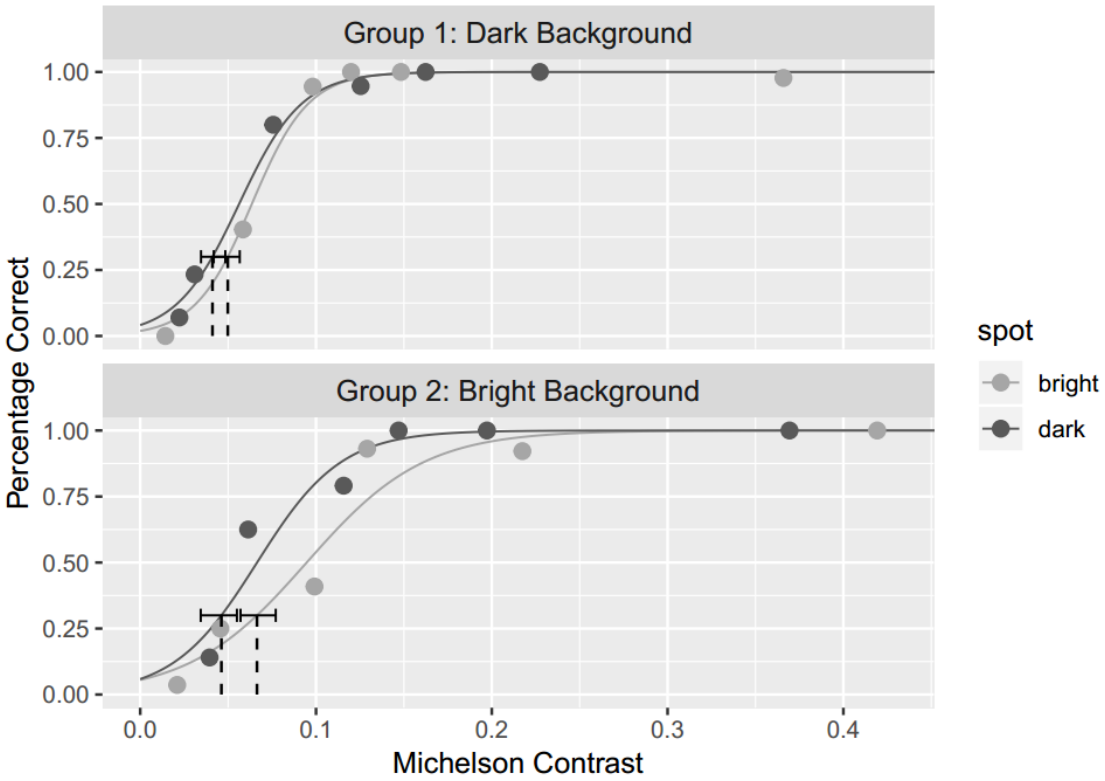

Figure S4.3: Detection thresholds at 30% correct choice.

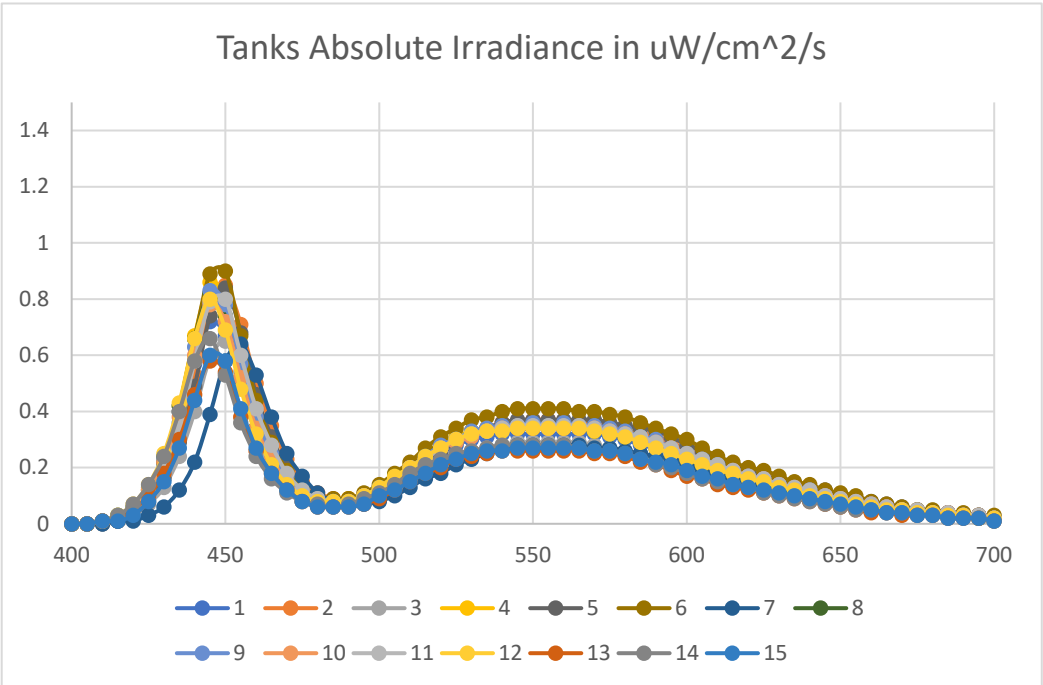

Figure S4.4: White LED light spectra in the aquaria

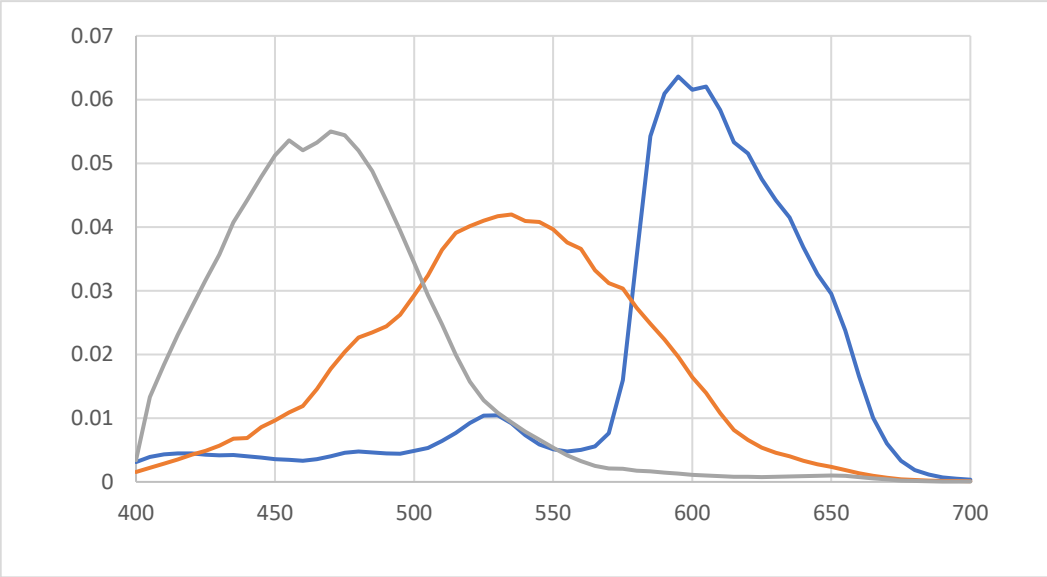

Figure S4.5: Camera spectral sensitivities, normalized for sum under curve = 1.

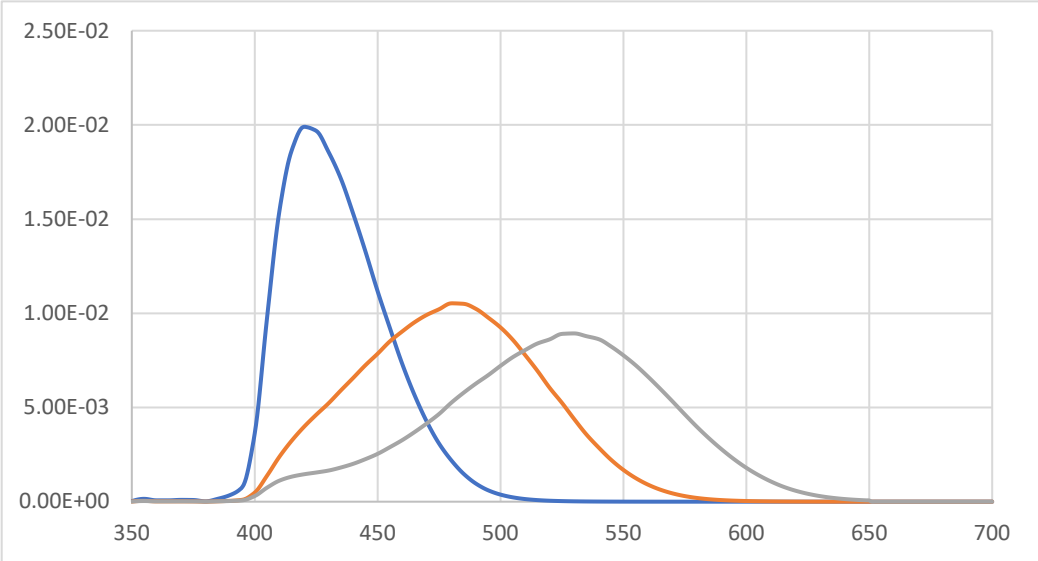

Figure S4.6: Triggerfish (Rhinecanthus aculeatus) spectral sensitivities, normalized for sum under curve = 1.

Appendix D – Co-authored Publications

These publications are provided as pre-accepted manuscripts due to legal requirements. Please use the DOI provided in the preliminary pages to source the published papers.

Conservation value of a subtropical reef in South East Queensland, Australia, highlighted by citizen science efforts

Monique G.G. Grol[A,B,C,M], Julie Vercelloni[A,D], Tania M. Kenyon[A,D,E], Elisa Bayraktarov[A,F], Cedric P. van den Berg[A,G,H], Daniel Harris[I,J], Jennifer A. Loder[A,C,K], Morana Mihaljević[A,J,L], Phebe I. Rowland[A], Chris M. Roelfsema[A,I,J]

[A] UniDive, The University of Queensland Underwater Club, 159 Sir William MacGregor Drive, St Lucia, QLD 4067, Australia

[B] CoralWatch, Queensland Brain Institute, The University of Queensland, St Lucia, QLD 4072, Australia

[C] Reef Citizen Science Alliance, Conservation Volunteers Australia, Ballarat, VIC 3350, Australia

[D] Australian Research Council Centre of Excellence for Coral Reef Studies, School of Biological Sciences, The University of Queensland, St Lucia, QLD 4072, Australia

[E] Marine Spatial Ecology Lab, School of Biological Sciences, The University of Queensland, St Lucia, QLD 4072, Australia

[F] Centre for Biodiversity and Conservation Science, The University of Queensland, St Lucia, QLD 4072, Australia

[G] Visual Ecology Lab, School of Biological Sciences, The University of Queensland, St Lucia, QLD 4072, Australia

[H] Sensory Neurophysiology Lab, Queensland Brain Institute, The University of Queensland, St Lucia, QLD 4072, Australia

[I] Remote Sensing Research Centre, School of Earth and Environmental Sciences, The University of Queensland, St Lucia, QLD 4072, Australia

[J] School of Earth and Environmental Sciences, The University of Queensland, St Lucia, QLD 4072, Australia

[K] Reef Check Australia, Brisbane, 1/377 Montague Rd, West End, QLD 4101, Australia

[L] Science Lab UZH, University of Zurich, 8057 Zurich, Switzerland

[M] Corresponding author. Email: mgggrol@hotmail.com

Abstract. Subtropical reefs are important habitats for many marine species and for tourism and recreation. Yet, subtropical reefs are understudied, and detailed habitat maps are seldom available. Citizen science can help fill this gap, while fostering community engagement and education. In this study, 44 trained volunteers conducted an ecological assessment of subtropical Flinders Reef using established Reef Check and CoralWatch protocols. In 2017, ten sites were monitored to provide comprehensive information on reef communities and to estimate potential local drivers of coral community structure. A detailed habitat map was produced by integrating underwater photos, depth measurements, wave exposure modelling and satellite imagery. Surveys showed that coral cover ranged from 14% to 67%. Site location and wave exposure explained 47% and 16% respectively of the variability in coral community composition. Butterflyfishes were the most abundant fish group with few invertebrates observed during the surveys. Reef impacts were three times lower than on other nearby

subtropical reefs. These findings can be used to provide local information to spatial management and Marine Park planning. To increase the conservation benefits and to maintain the health of Flinders Reef we recommend expanding the current protection zone from 500 to a 1000 m radius.

Additional keywords. benthic substrate mapping, coral composition, wave exposure, ecological assessment, CoralWatch, Reef Check Australia, Moreton Bay, subtropical reefs, citizen science.

Introduction

Subtropical reefs occur along the tropical-to-temperate transition zone and support unique assemblages of tropical, subtropical and temperate marine species (Harriott and Banks 2002; Harrison and Booth 2007; Davie *et al*. 2011; McPhee 2017). While subtropical reefs may have lower coral diversity than tropical reefs and do not rapidly form an accreting reef structure (McIlroy *et al*. 2019), the live coral cover forming subtropical reefs can be comparable to tropical reefs in some locations (Harrison *et al.* 1998; Wallace and Rosen 2006; Dalton and Roff 2013). Subtropical reefs offer important ecological habitat for migratory marine life such as humpback whales and recruiting coral reef fish (Booth *et al.* 2018; Noad *et al.* 2019). They also have social, cultural and economic value through activities such as fishing and tourism (Ross *et al.* 2019; Ruhanen *et al.* 2019).

Subtropical reefs are commonly promoted as potential refuges for the conservation of tropical reef species moving poleward due to climate change (Beger *et al.* 2011, 2014; Baird *et al.* 2012; Makino *et al.* 2014). Like their tropical counterparts, these subtropical reefs are subject to the effects of climate change, such as changes in

water temperature and chemistry (Beger *et al.* 2014; Sommer *et al.* 2014; Kim *et al*. 2019), as well as more localised anthropogenic stressors including pollution, eutrophication, overfishing, and physical habitat damage (Gibbes *et al.* 2014; McPhee 2017). In some instances, these issues may have even more profound and immediate effects on subtropical reefs due to the innate transitional nature of their environments (Beger *et al.* 2011). Research studies along the tropical-to-temperate transition in eastern Australia focus mainly on the ecological understanding of subtropical reefs at a regional or sub-regional spatial scale (Sommer *et al*. 2018; Kim *et al*. 2019). Detailed information of changes in community composition at finer spatial scales is often limited, which may hinder the development of management strategies for these unique ecosystems.

South East Queensland subtropical reefs, including reefs in Moreton Bay Marine Park, are recognised as ecological, diving and fishing hotspots (Smith *et al.* 2008; McPhee 2017). The many subtropical patch reefs in Moreton Bay feature high-latitude coral communities and are dominated by generalist, stress-tolerant species that are well adapted to marginal environmental conditions (Sommer *et al.* 2014). Like other subtropical reefs, their habitat structure at local scales is heavily influenced by wave energy and exposure (Dollar 1982; Jokiel *et al*. 2004; Wallace and Rosen 2006; Dalton and Roff 2013). Pressures from rapid urbanisation and population growth beyond the 2.3 million people (Australian Bureau of Statistics 2017) in South East Queensland have been highlighted for the semi-enclosed embayment area of Moreton Bay (Gibbes *et al*. 2014; Saunders *et al*. 2019) and are expected to increase in coming decades (Saunders *et al*. 2019). The collection of ecological monitoring and habitat mapping data in this region is therefore important to understand the condition and potential

impacts on subtropical reef habitats and associated wildlife (Smith *et al.* 2008; Done *et al.* 2017).

One of the most biodiverse and popular reefs in the region is Flinders Reef, which is located just outside the embayment of Moreton Bay. Previous studies on Flinders Reef have mostly focused on monitoring specific taxonomic groups such as fish (Johnson 2010), corals (Wells 1955; Harrison *et al.* 1998; Wallace *et al.* 2009; Dalton and Roff 2013; Sommer *et al.* 2017), sponges (Hooper and Kennedy 2002; Hooper and Ekins 2004) and molluscs (Devantier *et al.* 2010). Reef health impact surveys were restricted to a small portion of reef area and without consistency between sampling methodology (Beeden *et al.* 2014). Thus, despite these efforts, detailed information on benthic community composition at Flinders Reef and explicit habitat maps are limited. For instance, the current map of Flinders Reef is restricted to a simple outline of the exposed sandstone platform and includes ecological information at a reef scale. Citizen science programs are emerging as non-traditional sources of data contribution that engage the community in collecting, analysing and reporting on ecosystem health (Branchini *et al*. 2015a; Schlappy *et al*. 2017; Fritz *et al*. 2019). Citizen-generated data can complement traditional research and management programs with a higher frequency of surveys, covering a large spatial extent and accessing remote areas not commonly visited, with lower associated costs (Teleki 2012). Citizen science has been recently included into the international agenda for sustainable development goals of the United Nations (Fritz *et al*. 2019). Global citizen science coral reef programs including Reef Check (http://www.reefcheck.org) and CoralWatch (https://www.coralwatch.org) have been active in Moreton Bay since 2007 (Siebeck *et al.* 2006; Marshall *et al.* 2012; Loder *et al.* 2015). The data and information currently generated by Reef Check informs the annual report cards of Healthy Land and Water,

which assess the health of subtropical reefs in South East Queensland (https://hlw.org.au/report-card/).

In this study, citizen scientists monitored different sites at Flinders Reef, filling in gaps in data collection, providing relevant information for local management planning and producing a detailed reef habitat map. The objectives of this study, hereafter referred to as the Flinders Reef Ecological Assessment (FREA), were to: 1) develop a detailed benthic habitat map for Flinders Reef, 2) provide a detailed spatial characterisation of the community composition at a reef site scale, including benthic communities, reef impacts, abundance of fish and invertebrates and coral health status, and 3) estimate potential drivers of the coral community structure across the reef. Findings associated with our ecological assessment support ongoing science, management and conservation efforts, and highlight the efficacy of citizen science.

Materials and methods

Study location and site selection

Flinders Reef is located on a small sandstone platform (6.5 ha) three nautical miles north of Moreton Island in the northern part of Moreton Bay Marine Park, South East Queensland, Australia (26° 58.715' S, 153° 29.150' E) (Fig. 1). The location hosts a rich coral community with 125 documented species (Harrison *et al.* 1998; Harriott and Banks 2002; Wallace *et al.* 2009; Sommer *et al.* 2014). It is considered to be one of the most southern distribution ranges of many tropical coral and fish species including *Acropora* spp. and Labridae (Dalton and Roff 2013; McPhee 2017; Sommer *et al.* 2017). Since 2009, the reef has been a designated protected green zone under Marine Park management, which prohibits harvesting, fishing and anchoring within a 500 m radius from the centre of the reef platform (Fig. 1). The conservation park zone has a 2

km radius from the centre of Flinders Reef and a total of eight public moorings are available for activities allowed within this zone. As such, Flinders Reef is afforded some protection from human influences due to zoning status, and its distance from the mainland, which limits both visitation and land-based influences such as poor water quality (McPhee 2017). However, the reef remains subject to potential climate change influences and pressures from direct use.

To set up a representative monitoring and habitat mapping framework around Flinders Reef, ten survey sites were established at 5-10 m depth within the green zone area (Fig. 1). The ten sites were selected around the sandstone platform to capture representative areas with characteristic differences in exposure to wind speed and wave height, where prevailing wind and wave direction is east-south-east. Four of the ten sites are long-term Reef Check Australia monitoring sites: Alden's Cave, Coral Gardens, Turtle Cleaning Station and Plateland. Surveys were conducted in Austral spring (March) and autumn (September) in 2017 to capture potential seasonal changes in marine communities. One site, Arus Bale, was surveyed only in autumn due to adverse weather conditions.

Citizen science expertise and training

Approximately 100 members of the university dive club, The University of Queensland Underwater Club (UniDive), participated in the development of the FREA citizen science project and contributed over 10,000 volunteer hours. The participants were mostly students, staff or alumni within the university. UniDive has a long history of award-winning citizen science projects in South East Queensland (McMahon *et al.* 2002; Ford *et al.* 2003; Roelfsema *et al.* 2016, 2017). Ecological survey protocols were based on globally standardised Reef Check and CoralWatch survey methods. Prior to

field surveys, participants completed theoretical and practical training on ecological survey methods (Reef Check Australia and CoralWatch) and mapping survey methods, facilitated by experienced researchers. To take part in field activities, participants were required to hold a rescue diver certification (or equivalent) and successfully complete Reef Check Australia training by achieving a score of ≥85% on a theory test, ≥95% on an in-water species identification test and passing a practical in-water survey skills test.

Data collection

A total of 44 divers conducted a cumulative 500 survey dives over 23 daytrips, surveying and mapping Flinders Reef. Ongoing training and quality control were overseen by qualified trainers and researchers throughout the project's duration. Recorded data were compared for errors and inconsistencies via reviews of datasheets in the field and during data entry. If discrepancies were identified, recorded data were compared to survey photographs taken by the divers.

Baseline benthic habitat mapping

A preliminary benthic habitat map of Flinders Reef was created by applying an established protocol that involved delineating features visible in high spatial resolution satellite imagery using visual differences in colour and texture (Roelfsema *et al.* 2016, 2017). Habitat types were then further defined by overlaying the georeferenced field data onto satellite images for validation. The georeferenced field data included: 1) water depth measurements collected by boat echo sounder or diver, 2) maps of significant geological or ecological features identified through spatially-referenced visual census by divers, and 3) georeferenced benthic images collected by a diver towing a surface

GPS and photographing 1 m^2 benthic quadrats every 1 to 2 m along the survey area (Roelfsema *et al.* 2013).

Baseline ecological and reef impact surveys (Reef Check Australia)

Ecological and reef impact surveys using standardised Reef Check protocols (Hill and Wilkinson 2004; Hill 2005) were undertaken by conducting visual surveys of the benthos, reef health impacts, and selected invertebrate and fish indicator categories (see Supplementary Material Table 1). Reef Check surveys collect information on biological indicators that have a functional role on the reef. They serve individually as indicators of specific types of human impacts and collectively as a proxy for ecosystem health, based on the economic and ecological value, their sensitivity to human impacts and ease of identification (Hill and Loder 2013). The term 'category' is used to describe an individual species, family or group (see Supplementary Material Table 1). At each site, surveys were conducted along a transect which was comprised of four 20 m long segments used as replicates (hereafter referred to as surveyed segments). A 5 m gap was left between each replicate segment to avoid pseudo-replication. Benthic surveys documented living and non-living benthic categories using a point intercept sampling method to record the observed benthic category at 0.5 m intervals along each transect segment. The data were used to calculate a mean percent cover of each category per site. Along the same transect as benthic surveys, divers recorded indicator invertebrate abundance and signs of reef impacts in a 5 m wide belt transect (covering four 100 m^2 segments). To search the area, the divers swam 2.5 m perpendicular from the centre transect line and then switched back to cross the line and search the area on the other side, continually searching the survey area swimming in an S-shaped pattern. Visual census surveys for indicator fishes were undertaken on the same belt transect area to

record nominated fish categories. Divers conducting the fish surveys swam slowly along the transect line while searching within an imaginary 5 m wide and 5 m high tunnel. To ensure standardisation of data collection effort, the reef health impact, invertebrate and fish surveyors spent 7-10 minutes in each segment. Recognising the subtropical nature of Flinders Reef, existing Reef Check Australia protocols were modified by adding the indicator group 'corallimorphs' to the benthic surveys. Additional fish species were also incorporated into the fish surveys, including blue groper (*Achoerodus viridis),* spangled emperor *(Lethrinus nebulosus),* other emperors (Lethrinidae) and morwongs *(Cheilodactylus fuscus* and *C. vestitus*). For further analysis and visualisation purposes, indicator categories were consolidated into larger groups (see Supplementary Material Table 1).

Coral health surveys (CoralWatch)

Coral health was surveyed using CoralWatch protocols (Siebeck *et al.* 2006; Marshall *et al.* 2012). The CoralWatch coral health chart was used to compare the colour of living coral colonies to a pre-calibrated 6-point colour scale as a proxy for coral health, i.e. healthier corals are darker in colour. The coral health surveyor swam along the same 5 m wide belt transect and for five randomly selected coral colonies per segment, the growth form, the lightest colour score and darkest colour score were recorded, totalling 20 coral colonies assessed per site.

Wave exposure

Wave height at Flinders Reef was determined using a third-generation nearshore wave model Simulating WAves Nearshore (SWAN) version 41.31 (Booij *et al.* 1997). The SWAN model, and models such as XBeach (Roelvink *et al.* 2009), have been used

extensively in coastal and coral reef environments to propagate offshore deep-water wave heights to shallow water environments (Harris *et al.* 2018; Baldock *et al.* 2019). This provides wave exposure estimates for reef environments which have been used in previous ecological mapping and monitoring (e.g. Chollet and Mumby 2012). Wave inputs for the SWAN model were based on the 1976–2017 wave record from the Brisbane wave rider buoy operated by the Queensland Department of Environment and Science. The wave rider buoy is deployed in deep water, east of North Stradbroke Island and south-east of the field site. The average wave conditions during the 41-year period had a significant wave height *(H_s)* of 1.67 m, a wave period (*T*) of 9.43 s, and a south-east wave direction (Dir) of 120.7°. Bathymetry for the SWAN model was generated from the Australian bathymetry and topography 2009 data set (Ausbathy) produced by Geoscience Australia (Whiteway 2009). A nearest neighbour interpolation method was used to convert the 9 arc second Ausbathy grid to a 50 x 50 m bathymetric grid for Flinders Reef and surrounding region, including the north and east coast of Moreton Island. The default parameters in SWAN were selected for wave modelling. For more information refer to the SWAN website and user manual (http://swanmodel.sourceforge.net). Values of significant wave heights for each site were extracted based on the centre coordinates of each transect in a Universal Transverse Mercator (UTM) coordinate system.

Data and statistical analyses

Data manipulation

Differences between autumn and spring surveys were assessed using a Student's t-test based on the overall mean of measurements for the four survey types, i.e. benthos, reef impacts, invertebrates and fish. The assumptions of normality were met for these data.

As no significant differences were found, measurements were averaged between seasons (see Supplementary Material Table 2 and Figure 1). At each site, impact, invertebrate and fish surveys were calculated per 100 m^2 and benthic surveys were calculated as percent cover. Many of the reef impact categories are coral specific, hence areas with high coral cover may have a disproportionate number of impacts when compared to areas of low coral cover. To allow for direct comparison between sites of varying coral cover, the abundance of reef impacts was divided by the percent hard coral cover for that area.

Statistical analyses to estimate variability and drivers of coral community composition

A hierarchical clustering analysis was used to determine the spatial variability in the structure of coral communities among survey sites. Coral community structure was composed of seven hard coral and four soft coral categories (see Supplementary Material Table 1) and coverage was square root transformed to satisfy analysis assumptions. Clusters were estimated using a Bray-Curtis dissimilarity matrix using a complete linkage cluster aggregation method. Non-metric multidimensional scaling (nMDS) ordination was then used to visualise the structure of coral communities within sites based on the four segments surveyed per site.

The influence of site location and wave exposure on coral community composition was estimated using a permutational multivariate analysis of variance (PERMANOVA) based on Bray-Curtis dissimilarity distances with surveyed segments nested within sites and wave exposure formulated as a fixed effect. Analyses were performed using the R packages 'clustsig' (Whitaker and Christman 2014) and 'vegan' (Oksanen 2017) within R version 3.2.2 software (R Core Team 2016). Significance of

clusters and size effects in the PERMANOVA were tested using permutation approaches based on 999 permutations and a 5% error level.

Wave exposure expressed as low and high categories were correlated with coral community structure using the Pearson product moment correlation coefficient. Values of these coefficients and associated *P* values indicated the strength and direction of the correlation at a 5% error level. The two wave exposure categories were calculated using the median values of wave height across all sites.

Coral health chart analysis (CoralWatch)

CoralWatch coral heath scores were recorded for a total of 378 coral colonies. The average colour score at Flinders Reef and per site (± standard error (SE)) was calculated by pooling the two seasons (autumn and spring).

Results

Baseline benthic habitat mapping

The georeferenced habitat map created for Flinders Reef depicts substrate types, water depth and significant features (Fig. 2; Roelfsema *et al.* 2018). Prominent mapped features included vast branching hard coral beds at Coral Garden and large plate corals with diameters up to ~2 m at a depth of 10-15 m near Plate, and in the deeper water south of Alden Cave and Trevo. Encrusting and plate corals were observed mostly on the south-eastern side, with branching hard corals and soft corals on the western side. *Asparagopsis* sp. was the dominant macroalgae observed at Flinders Reef, while macroalgae in the genus *Laurencia* were more abundant in deeper waters (>15 m). Rock and rubble surfaces not covered by coral were covered by macroalgae or turf algae. Sandy areas were predominantly found in deeper waters (>15 m).

Ecological baseline

For the benthic surveys, rock was the most common benthic category, with an average cover across sites estimated to be 37.0% (± 3.38% SE) followed by hard coral (33.3 ± 5.12% SE) and soft coral (10.0 ± 2.10% SE). The sites with the highest and lowest hard coral cover were Coral Garden (66.9%) and Plate (14.1%), respectively (Fig. 3a).

Overall, the number of reef impacts detected was low with an average of 0.05 (± 0.01 SE) per 100 m^2 (Fig. 3b). The most common impacts observed were physical coral damage with an average of 0.12 (± 0.04 SE) occurrences per 100 m^2, followed by coral disease and unknown coral scars which both averaged 0.08 (± 0.02 and ± 0.01 SE, respectively) occurrences per 100 m^2. Turtle Cleaning and Arus Bale sites had the greatest prevalence of impacts, driven by coral physical damage and at Arus Bale also coral disease. Three reef impact categories were not observed: crown-of-thorns starfish (*Acanthaster planci*) scars and coral damage due to boat anchor or dynamite. The pooled results from the CoralWatch coral health chart colour indicator surveys showed an average colour score of 3.9 ± 0.07 SE. The highest average colour score was recorded at Trevo (4.4 ± 1.80 SE) and lowest average score at Arus Bale (2.7 ± 0.22 SE).

The average abundance of reported invertebrates was 6.65 (± 1.40 SE) individuals per 100 m^2 (Fig. 3c). The presence and abundance of indicator invertebrate categories varied between survey sites with the most diverse site being Plate, i.e. 5 out of 14 recorded taxa observed (Fig. 3c). Coral Garden had the highest number of invertebrates per 100 m^2 (2.14 ± 1.33 SE), primarily made up of anemones (9.50 per 100 m^2). Trevo and Sylvia Earle had the lowest abundance of invertebrates with an abundance of 0.29 (± 1.50 SE) invertebrates per 100 m^2. The most abundant invertebrate groups were sea urchins (especially *Diadema* spp.), gastropods (*Drupella*

spp.) and anemones with on average 2.35 (± 0.65 SE), 1.70 (± 1.02 SE) and 1.35 (± 0.91 SE) individuals per 100 m^2, respectively. The highest abundance of *Drupella* spp. was found at Donna (10.50 per 100 m^2).

Fish community composition was largely dominated by butterflyfishes which were recorded at each of the ten sites (Fig. 3d). A total of 524 butterflyfish individuals were counted during all surveys, representing 81.53% of the total counted fishes. On average, 6.12 (± 0.93 SE) butterflyfishes were recorded per 100 m^2 ranging from 2.62 at Donna to 12.10 at Turtle Cleaning. The second most dominant fish group was snapper with 40 individuals recorded (6.65% of total counted fishes) at seven sites and an average of 0.50 (± 0.16 SE) fish per 100 m^2, followed by morwong (0.39 ± 0.06 SE), sweetlip (0.20 ± 0.05 SE) and parrotfish (0.15 ± 0.05 SE) per 100 m^2.

Coral community analysis

Coral community composition at Coral Garden was distinct (89% dissimilarity, Cluster 1) from the remaining sites (Cluster 2, $P = 0.016$, Fig. 4a). The north-western sites (Turtle Cleaning and Plate) were different from the others (58% dissimilarity, Cluster 2); however, this clustering pattern was not significant. Cluster 1 was dominated by branching corals (Fig. 4b) representing 64.0% (± 13.45% SE) of the benthic cover at Coral Garden according to the ecological surveys. Cluster 2 comprised a mix of coral indicator groups. Coral community composition at the north-western sites, Turtle Cleaning and Plate, was characterised by plating and foliose hard corals. In comparison, sites on the eastern side of Flinders Reef, i.e. Alden Cave, North and Trevo, were characterised by encrusting hard coral (Fig. 4b).

Wave exposure and community composition

Sites located on the north-western side of Flinders Reef were the least exposed to waves. Significant wave height was 0.9 m for Turtle Cleaning and Plate, and 1.2 m at Coral Garden (Fig. 5a). Wave height for the seven remaining sites varied between 1.5 and 1.6 m (Fig. 5a). The median significant wave height across all sites was 1.54 m, separating the less exposed sites (located west to north of Flinders Reef) from the more exposed sites (east to south). There was a positive relationship between wave exposure and the proportion of encrusting corals (HCE, $P < 0.001$) and zoanthids (SCZ, $P = 0.008$), and a negative relationship between wave exposure and leathery soft coral (SCL, $P = 0.021$) (Fig 5b). Fragile hard corals (HCF, HCP and HCBR) and soft corals (SC) were associated with lower wave exposure, while more robust hard coral types (HCM, HC and HCE) were associated with higher wave exposure (Fig. 5c).

Site and wave exposure both had a significant effect on the coral community composition ($P < 0.001$) and explained 47% and 15.6% of the variability in hard corals, respectively (Table 1).

Discussion

The study provided a detailed ecological assessment of the community composition structure, a baseline benthic habitat map for Flinders Reef, and estimated the role of wave exposure in driving spatial heterogeneity in coral community structure. This information can be used to select long-term monitoring sites and shape management recommendations for future re-zoning plans.

Baseline benthic habitat mapping

Habitat maps form the basis and inventory of any decision-making process for Marine Park management, and this process will improve with increasing levels of spatial and

thematic map detail (Roelfsema *et al*. 2013). This study presents the first highly detailed habitat map, highlighting the importance of a citizen science approach providing this information. The habitat mapping approach can be accessed by marine citizen science projects to provide valuable maps, using basic mapping training, open source software, off-the-shelf low-cost compact underwater cameras, a handheld GPS and publicly available satellite imagery. As such, we hope this method will become more widely applied in coral reef surveys by providing detailed methodology protocols (this study; Roelfsema *et al*. 2017).

Baseline ecological assessment

This study highlights a remarkably high hard coral cover on a subtropical reef, with some sites having comparable coral cover to the Great Barrier Reef (De'ath *et al.* 2012). While physical coral damage, unknown coral scars and coral disease were recorded at all sites, overall impacts at Flinders Reef were three times lower than those observed for more accessible reef locations in Moreton Bay such as Point Lookout (Roelfsema *et al.* 2016). Coral health chart surveys indicated scores within the healthy range and suggested that corals were unaffected by coral bleaching at the time surveys were conducted. Previous studies before the establishment of the green zone reported anchor damage at Flinders Reef (Harrison *et al.* 1998). The lack of anchor damage in the present study suggests that the installation of moorings and establishment of a green zone (with no anchoring) may be effective in protecting the reef from damage. Yet, higher levels of coral damage were recorded at the most popular dive locations around Flinders Reef, which have the highest cover of branching coral. This could reflect damage by SCUBA divers but also the fragility of branching coral compared to other coral morphologies (Woodley *et al*. 1981). Further observational studies would be

required to understand potential drivers of this damage. The effectiveness of the green zone is also supported by the lack of fishing lines recorded during our impact surveys. However, there are anecdotal reports of fishing within the protected area, and close surveillance of poaching activities can be made difficult by the remoteness of the location.

The distribution and abundance of targeted invertebrates varied spatially, which is consistent with long-term Reef Check Australia findings (Loder *et al.* 2010; Mulloy *et al*. 2018). During the surveys, many closely related and functionally equivalent yet non target invertebrates were observed, including burrowing sea urchin (*Echinostrephus aciculatus*), blackfish (*Holothuria atra*), and black teatfish (*Holothuria whitmaei*). The abundance of corallivorous gastropods (*Drupella* spp.) was not related with the cover of hard coral nor with the recorded abundance of *Drupella* scars, however, further data collection is needed to confirm this trend. Corallivorous gastropods formed isolated aggregations in a few surveyed sites (e.g. Donna and Turtle Cleaning), but the overall distribution of gastropods (*Drupella* spp.) was low; as observed in other coastal waters (Morton and Blackmore 2009). The high abundance of anemones at Coral Garden may be facilitated by the low wave exposure at this site relative to the other sites. A previous survey of subtropical anemones found that abundance was significantly higher on leeward reef sites compared to those that were more exposed (Richardson *et al.* 1997).

Butterflyfishes were observed at all survey sites and were most abundant at Turtle Cleaning. High butterflyfish abundance has been observed in other locations like Flinders Reef (Loder *et al.* 2010; Mulloy *et al.* 2018). Many butterflyfishes are corallivores that mainly target hard coral, while some species prefer soft coral polyps as a food source (Cole *et al.* 2008). They have distinct prey preferences that can be

specific to one coral species, genus or growth form (Cole *et al.* 2008), which can limit their abundance and distribution. Fish community composition and abundance is often influenced by live coral cover and structural complexity (Jennings *et al.* 1996; Grol *et al.* 2011), which may explain the high fish abundance observed at Coral Garden. However, aside from butterflyfishes, fish abundances were comparable to the low abundances recorded at other subtropical reefs in South East Queensland (Mulloy *et al.* 2018). While fish surveys were limited to a confined survey area near the sandstone platform, many of the surveyed fish groups may prefer deeper areas away from currents, surge and exposure. Additionally, parrotfish and grouper abundance may have been underestimated due to the inclusion of only larger sized individuals (surveys only included parrotfish >20 cm and grouper >30 cm); smaller parrotfishes were observed during the surveys, but not included in the data collection (*personal observation, M Grol*). Smaller juvenile fishes are known to use shallower reef areas as nurseries and have smaller home ranges compared to adult fish (Dahlgren *et al.* 2006; Huijbers *et al.* 2008).

Wave exposure and coral community composition

There was a clear zonation in coral community composition, notably influenced by site location and wave exposure. Soft corals and more fragile hard coral morphologies such as branching corals were associated with the north-western reef sites, characterised by lower wave exposure. More robust hard coral morphologies were found at the exposed eastern and south-eastern sites. Branching hard corals are more susceptible to damage from waves and storm events (Woodley *et al.* 1981), which may explain the dominance of fragile branching coral on the sheltered side of Flinders Reef at sites like Coral Garden. The observed coral cover and zonation patterns align with previous studies at

Flinders Reef (Dalton and Roff 2013; Harrison *et al.* 1998, respectively), as well as broader studies on the influence of wave exposure on high-latitude coral assemblages (Bradbury and Young 1981; Dollar 1982). In addition to wave exposure, coral community composition may be influenced by the intensity and regularity of disturbances including recurring bleaching events (Spalding and Brown 2015; Hughes *et al.* 2018; Kim *et al.* 2019) or storms (Cheal *et al.* 2017), patterns of coral recruit settlement (Done 1982) and the depth at which the coral community is located (Roberts *et al.* 2015). Depth in this study was considered equal as transects fell within the same depth range.

Recommendations for monitoring

The habitat mapping and ecological survey results show that Sylvia Earle has distinctly different habitat characteristics compared to the other sites surveyed at Flinders Reef. Sylvia Earle is located on the western more sheltered side of Flinders Reef but is still exposed to the pre-dominant east-south-eastern wind and wave direction. This site is less rugose, and has a steep slope compared to all other sites. It may be beneficial to review long-term monitoring sites with Reef Check Australia to consider the feasibility of expanding representational monitoring locations, e.g. include Sylvia Earle in future monitoring. Furthermore, the indicator species included in the Reef Check Australia protocol were selected for broad geographic coverage with a focus on tropical species (Hodgson 2000). Including additional survey categories for benthos, fish and invertebrates relevant to subtropical regions in future surveys, as well as smaller size classes of parrotfish and groupers, may improve ecosystem health monitoring of subtropical reefs. The continued inclusion of tropical species in these surveys will be increasingly important to detect 'tropicalization' of subtropical marine environments,

i.e. the movement of tropical species poleward (Burrows *et al.* 2011; Baird *et al.* 2012; Poloczanska *et al.* 2013; Beger *et al.* 2014; Sommer *et al.* 2014).

Recommendations for management

The current Flinders Reef green zone includes a 500 m radius circle from the centre of the Flinders Reef sandstone platform. The ecological assessment and habitat mapping provide a detailed description of the benthic composition of Flinders Reef and highlight deeper reef habitats that are excluded from the green zone. This may prompt consideration for expansion of the green zone to a circular area of a 1000 m radius. Such an expansion would result in: inclusion of all areas mapped with coral communities to a depth of 25 m; a two-fold increase in protected area of benthic categories that include corals; and a three-fold increase in protected area that include rocky substrate (Figs 1 and 2, orange polygon), which is required for coral settlement and post-settlement survival (Yadav *et al.* 2016). Furthermore, green zones have been shown to enhance recreational fishing opportunities outside of the protected area through exports of increased fish biomass and abundance (Emslie *et al.* 2015), benefiting both fishermen and the ecosystem.

The role of citizen science and relevance for subtropical reefs

This study showcases the value of citizen science as an approach that can complement traditional scientific and management approaches and engage local community members to learn about and take active steps to care for local environments (Fritz *et al*. 2019). In addition to generating data, citizen science programs improve community knowledge about ecosystem functions and threats and subsequently enhance public stewardship of those ecosystems (Marshall *et al.* 2012; Teleki 2012; Branchini *et al.*

2015b). The FREA citizen science project brought together more than 100 local divers and created many opportunities for them to learn about the ecology of subtropical reefs. Moreover, the project enhanced broader community support and understanding of subtropical reefs through a range of communication tools including a technical report, coffee table photo book, posters, television segments and community events. The study offered a platform for constructive discussions and applications around the monitoring, management and stewardship of Flinders Reef into the future. The FREA project also characterised the fine-scale structure of coral communities on subtropical reefs, to better understand their dynamics and inform best-practice management.

Acknowledgements

We would like to acknowledge the 44 core survey divers and many additional UniDive volunteers who spent more than 10,000 hours on the FREA project. Financial support was given by the Queensland Parks and Wildlife Services, Honourable Dr Steven Miles the former Minister for Environment and the Great Barrier Reef at the time of the research, Solar School, Healthy Land and Water, and those who supported the ING Dreamstarter crowd funder. In-kind support provided by Point Lookout Scuba Dive Charters (Ken Holzheimer); The University of Queensland Boating and Diving; Moreton Island Adventures; Tangatours; Queensland Parks and Wildlife Service; Geoimage; Dr Ian Tibbets, The University of Queensland; Aquatic Centre, The University of Queensland; Reef Check Australia and CoralWatch. At last, we thank our independent reviewers JAK and MGE.

Conflicts of interest

The authors declare no conflicts of interest.

References

Australian Bureau of Statistics (2017). 'Census 2016'. Available at http://www.abs.gov.au/websitedbs/D3310114.nsf/Home/census [accessed 22 February 2019].

Baird, A., Sommer, B., and Madin, J. (2012). Pole-ward range expansion of *Acropora* spp. along the east coast of Australia. *Journal of the International Society for Reef Studies* **31**, 1063-1063.

Baldock, T. E., Shabani, B., and Callaghan, D. P. (2019). Open access Bayesian Belief Networks for estimating the hydrodynamics and shoreline response behind fringing reefs subject to climate changes and reef degradation. *Environmental Modelling & Software* **119**, 327-340.

Beeden, R., Turner, M., Dryden, J., Merida, F., Goudkamp, K., Malone, C., Marshall, P., Birtles, A., and Maynard, J. (2014). Rapid survey protocol that provides dynamic information on reef condition to managers of the Great Barrier Reef. *An International Journal Devoted to Progress in the Use of Monitoring Data in Assessing Environmental Risks to Man and the Environment* **186**, 8527-8540.

Beger, M., Babcock, R., Booth, D. J., Bucher, D., Condie, S. A., Creese, B., Cvitanovic, C., Dalton, S., Harrison, P., Hoey, A., Jordan, A., Loder, J., Malcolm, H., Purcell, S., Roelfsema, C., Sachs, P., Smith, S., Sommer, B., Stuartsmith, R., Thomson, D., Wallace, C., Zann, M., and Pandolfi, J. (2011). Research challenges to improve the management and conservation of subtropical reefs to tackle climate change threats.

(Findings of a workshop conducted in Coffs Harbour, Australia on 13 September 2010). *Ecological Management & Restoration* **12**, e7-e10.

Beger, M., Sommer, B., Harrison, P. L., Smith, S. D. A., and Pandolfi, J. M. (2014). Conserving potential coral reef refuges at high latitudes. *Diversity and Distributions* **20**, 245-257.

Booij, N., Holthuijsen, L. H., and Ris, R. C. (2001). The "SWAN" wave model for shallow water. *Coastal Engineering Proceedings*.

Booth, D. J., Beretta, G. A., Brown, L., and Figueira W. F. (2018). Predicting success of range-expanding coral reef fish in temperate habitats using temperature-abundance relationships. *Frontiers in Marine Science* **5**, 31.

Bradbury, R. H., and Young, P. C. (1981). The effects of a major forcing function, wave energy, on a coral reef ecosystem. *Marine Ecology Progress Series* **5**, 229-241.

Branchini, S., Meschini, M., Covi, C., Piccinetti, C., Zaccanti, F., and Goffredo, S. (2015b). Participating in a citizen science monitoring program: Implications for environmental education. *PLoS One* **10**, e0131812.

Branchini, S., Pensa, F., Neri, P., Tonucci, B., Mattielli, L., Collavo, A., Sillingardi, M., Piccinetti, C., Zaccanti, F., and Goffredo, S. (2015a). Using a citizen science program to monitor coral reef biodiversity through space and time. *Biodiversity and Conservation* **24**, 319-336.

Burrows, M. T., Schoeman, D. S., Buckley, L. B., Moore, P., Poloczanska, E. S., Brander, K. M., Brown, C., Bruno, J. F., Duarte, C. M., Halpern, B. S., Holding, J., Kappel, C. V., Kiessling, W., O'Connor, M. I., Pandolfi, J. M., Parmesan, C., Schwing,

F. B., Sydeman, W. J., and Richardson, A. J. (2011). The pace of shifting climate in marine and terrestrial ecosystems. *Science* **334**, 652-655.

Cheal, A. J., MacNeil, M. A., Emslie, M. J., and Sweatman, H. (2017). The threat to coral reefs from more intense cyclones under climate change. *Global Change Biology* **23**, 1511-1524.

Chollett, I., and Mumby, P. (2012). Predicting the distribution of Montastraea reefs using wave exposure. *Coral Reefs* **31**, 493-503.

Cole, A. J, Pratchett, M. S., and Jones, G. P. (2008). Diversity and functional importance of coral feeding fishes on tropical coral reefs. *Fish and Fisheries* **9**, 286-307.

Dahlgren, C., Kellison, G., Adams, A., Gillanders, B., Kendall, M., Layman, C., Ley, J., Nagelkerken, I., and Serafy, J. (2006). Marine nurseries and effective juvenile habitats: concepts and applications. *Marine Ecology Progress Series* **312**, 291-295.

Dalton, S. J., and Roff, G. (2013). Spatial and temporal patterns of eastern Australia subtropical coral communities. *PLoS ONE* **8**, e75873.

Davie, P., Cranitch, G., Wright, J., and Cowell, B. (2011). 'Wild Guide to Moreton Bay and adjacent coasts. Vol. 1' 2nd Edn. (The Queensland Museum: South Brisbane.).

De'ath, G., Fabricius, K. E., Sweatman, H., and Puotinen, M. (2012). The 27–year decline of coral cover on the Great Barrier Reef and its causes. *Proceedings of the National Academy of Sciences* **109**, 17995.

DeVantier, L., Williamson, D., and Willan, R. (2010). Nearshore marine biodiversity of the Sunshine Coast, South-East Queensland: Inventory of molluscs, corals and fishes July 2010. Australia. 10.13140/RG.2.1.4709.3923.

Dollar, S. (1982). Wave stress and coral community structure in Hawaii. *Journal of the International Society for Reef Studies* **1**, 71-81.

Done, T. (1982). Patterns in the distribution of coral communities across the central Great Barrier Reef. *Journal of the International Society for Reef Studies* **1**, 95-107.

Done, T., Roelfsema, C., Harvey, A., Schuller, L., Hill, J., Schläppy, M-L., Lea, A., Bauer-Civiello, A., and Loder, J. (2017). Reliability and utility of citizen science reef monitoring data collected by Reef Check Australia, 2002–2015. *Marine Pollution Bulletin* **117**, 148-155.

Emslie, M. J., Logan, M., Williamson, D. H., Ayling, A. M., Macneil, A. M., Ceccarelli, D., Cheal, A. J., Evans, R. D., Johns, K. A., Jonker, M. J., Miller, I. R., Osborne, K., Russ, G. R., and Sweatman, H. P. A. (2015). Expectations and outcomes of reserve network performance following re-zoning of the Great Barrier Reef Marine Park. *Current Biology* **25**, 983-992.

Ford, S., Langridge, M., Roelfsema, C., Bansemer, C., Pierce, S., Cabrera, K. G., Fellegrada, I., McMahon, K., Keller, M., Joyce, K., Aurish, N., and Prebble, C. (2003). Surveying habitats critical to the survival of grey nurse sharks in south-east Queensland. Unidive, Brisbane, Australia.

Fritz, S., See, L., Carlson, T., Haklay, M., Oliver, J. L., Fraisl, D., Mondardini, R., Brocklehurst, M., Shanley, L. A., Schade, S., Wehn, U., Abrate, T., Anstee, J., Arnold,

S., Billot, M., Campbell, J., Espey, J., Gold, M., Hager, G., He, S., Hepburn, L., Hsu, A., Long, D., Masó, J., McCallum, I., Muniafu, M., Moorthy, I., Obersteiner, M., Parker, A. J., Weisspflug, M., and West, S. (2019). Citizen science and the United Nations sustainable development goals. *Nature Sustainability* **2**, 922-930.

Gibbes, B., Grinham, A., Neil, D., Olds, A., Maxwell, P., Connolly, R., Weber, T., Udy, N., and Udy, J. (2014). Moreton Bay and its estuaries: A sub-tropical system under pressure from rapid population growth. In 'Estuaries of Australia in 2050 and beyond'. (Ed. E. Wolanski.) pp. 203-222. (Springer, Dordrecht, Netherlands.)

Grol, M. G. G., Nagelkerken, I., Bosch, N., and Meesters, E. H. (2011). Preference of early juveniles of a coral reef fish for distinct lagoonal microhabitats is not related to common measures of structural complexity. *Marine Ecology Progress Series* **432**, 221-233.

Harriott, V., and Banks, S. (2002). Latitudinal variation in coral communities in eastern Australia: A qualitative biophysical model of factors regulating coral reefs. *Journal of the International Society for Reef Studies* **21**, 83-94.

Harris, D. L., Rovere, A., Casella, E., Power, H., Canavesio, R., Collin, A., Pomeroy, A., Webster, J. M., and Parravicini, V. (2018). Coral reef structural complexity provides important coastal protection from waves under rising sea levels. *Science Advances* **4**.

Harrison, P. L., and Booth, D. J. (2007). Coral reefs: Naturally dynamic and increasingly disturbed ecosystems. In ‘Marine Ecology’. (Eds S. D. Connell and B. M. Gillanders.) pp. 316-377. (Oxford University Press Melbourne.)

Harrison, P. L., Harriott, V. J., Banks, S. A., and Holmes, N. J. (1998). The coral communities of Flinders Reef and Myora Reef in the Moreton Bay Marine Park, Queensland, Australia. In 'Moreton Bay and Catchment'. (Eds L. R. Tibbetts, N. J. Hall and W.C. Dennison.) pp. 525-536. (Moreton Bay and catchment, School of Marine Science, The University of Queensland, Brisbane, Australia.)

Hill, J. (2005). Reef Check Australia training manual. Reef Check Foundation Ltd, Townsville, Australia.

Hill, J., and Loder, J. (2013). Reef Check Australia Survey Methods. Reef Check Foundation Ltd, Townsville, Australia.

Hill, J., and Wilkinson, C. (2004). Methods for ecological monitoring of coral reefs. Australian Institute of Marine Science, Townsville, Australia.

Hodgson, G. (2000). Coral reef monitoring and management using Reef Check. *Integrated Coastal Zone Management* **1**, 169-179.

Hooper, J. N. A., and Ekins, M. (2004). Collation and validation of museum collection databases related to the distribution of marine sponges in northern Australia. Technical Reports of the Queensland Museum, Number 002, Australia.

Hooper, J. N. A., and Kennedy, J. A. (2002). Small-scale patterns of sponge biodiversity (Porifera) from the Sunshine Coast reefs, eastern Australia. *Invertebrate Systematics* **16**, 637-653.

Hughes, T. P., Anderson, A. D., Connolly, S. R., Heron, S. F., Kerry, J. T., Lough, J. M., Baird, A. H., Baum, J. K., Berumen, M. L., Bridge, T. C., Claar, D. C., Eakin, C. M., Gilmour, J. P., Graham, N. A. J., Harrison, H., Hobbs, J-P. A., Hoey, A. S.,

Hoogenboom, M., Lowe, R. J., McCulloch, M. T., Pandolfi, J. M., Pratchett, M., Schoepf, V., Torda, G., and Wilson, S. K. (2018). Spatial and temporal patterns of mass bleaching of corals in the Anthropocene. *Science* **359**, 80-83.

Huijbers, C. C. M., Grol, M. G. G., and Nagelkerken, I. (2008). Shallow patch reefs as alternative habitats for early juvenile of some mangrove/seagrass-associated fish species in Bermuda. *Revista de Biologia Tropical* **56**, 161-169.

Jennings, S., Boullé, D., and Polunin, N. (1996). Habitat correlates of the distribution and biomass of Seychelles' reef fishes. *Environmental Biology of Fishes* **46**, 15-25.

Johnson, J. W. (2010) Fishes of the Moreton Bay Marine Park and adjacent continental shelf waters, Queensland, Australia. *Memoirs of the Queensland Museum* **54**, 299-353.

Jokiel, P. L., Brown, E. K., Friedlander, A., Rodgers, S. K. U., and Smith, W. R. (2004). Hawaii coral reef assessment and monitoring program: Spatial patterns and temporal dynamics in reef coral communities. *Pacific Science* **58**, 159-174.

Kim, S. W., Sampayo, E. M., Sommer, B., Sims, C. A., Gomez-Cabrera, M. D. C., Dalton, S. J., Beger, M., Malcolm, H. A., Ferrari, R., Fraser, N., Figueira, W. F., Smith, S. D. A., Heron, S. F., Baird, A. H., Byrne, M., Eakin, C. M., Edgar, R., Hughes, T. P., Kyriacou, N., Liu, G., Matis, P. A., Skirving, W. J., and Pandolfi, J. M. (2019). Refugia under threat: Mass bleaching of coral assemblages in high-latitude eastern Australia. *Global Change Biology* **25,** 3918-3931.

Loder, J., Bauer, A., Byrne, C., Lea, A., and Salmond, J. (2010). Reef Check Australia, South East Queensland, survey season summary report. Reef Check Foundation Ltd, Townsville, Australia.

Loder, J., Done, T., Lea, A., Bauer, A., Salmond, J., Hill, J., Galway, L., Kovacs, E., Roberts, J., Walker, M., Mooney, S., Pribyl, A., and Schläppy, M. L. (2015). Citizens & reef science: A celebration of Reef Check Australia's volunteer reef monitoring, education and conservation programs 2001-2014. Reef Check Foundation Ltd, Townsville, Australia.

Makino, A., Yamano, H., Beger, M., Klein, C. J., Yara, Y., and Possingham, H. P. (2014). Spatio-temporal marine conservation planning to support high-latitude coral range expansion under climate change. *Diversity and Distributions* **20**, 859-871.

Marshall, N. J., Kleine, D. A., and Dean, A. J. (2012). CoralWatch: education, monitoring, and sustainability through citizen science. *Frontiers in Ecology and the Environment* **10,** 332-334.

McIlroy, S. E., Thompson, P. D., Yuan, F. L., Bonebrake, T. C., and Baker, D. M. (2019) Subtropical thermal variation supports persistence of corals but limits productivity of coral reefs. *Proceedings of the Royal Society B: Biological Sciences* **286**, 20190882.

McMahon, K., Bansemer, C., Fellegara, I., Keller, M., Kerswell, A., Kwik, J., Longstaff, B., Roelfsema, C. M., Thomas, J., and Stead, J. (2002). A baseline assessment of the flora and fauna of North Stradbroke Island dive sites, Queensland. Unidive, Brisbane, Australia.

McPhee, D. P. (2017). 'Environmental history and ecology of Moreton Bay'. (CSIRO Publishing, Clayton South, Victoria, Australia.)

Morton, B., and Blackmore, G. (2009). Seasonal variations in the density of and corallivory by *Drupella rugosa* and *Cronia margariticola* (Caenogastropoda: Muricidae) from the coastal waters of Hong Kong: 'plagues' or 'aggregations'? *Journal of the Marine Biological Association of the United Kingdom* **89**, 147-159.

Mulloy, R., Salmond, J., Passenger, J., and Loder, J. (2018). Reef Check Australia 2017-18 South East Queensland season summary report. Reef Check Foundation Ltd, Brisbane, Australia.

Noad, M. J., Kniest, E., and Dunlop R. A. (2019). Boom to bust? Implications for the continued rapid growth of the eastern Australian humpback whale population despite recovery. *Population Ecology* **61**, 198-209.

Oksanen, J., Guillaume Blanchet, F., Friendly, M., Kindt, R., Legendre, P., McGlinn, D., Minchin, P. R., O'Hara, R. B., Simpson, G. L., Stevens, M. H. H., Szoecs, E., and Wagner, H. (2017). Community ecology package. In 'R Package version 2.4-2'. vegan.

Poloczanska, E. S., Brown, C. J., Sydeman, W. J., Kiessling, W., Schoeman, D. S., Moore, P. J., Brander, K., Bruno, J. F., Buckley, L. B., Burrows, M. T., Duarte, C. M., Halpern, B. S., Holding, J., Kappel, C. V., O'Connor, M. I., Pandolfi, J. M., Parmesan, C., Schwing, F., Thompson, S. A., and Richardson, A. J. (2013). Global imprint of climate change on marine life. *Nature Climate Change* **3**, 919.

R Core Team (2016). R: a language and environment for statistical computing. In 'R Foundation for Statistical Computing'. R Core Team: Vienna, Austria.

Richardson, D. L., Harriott, V. J., and Harrison, P. L. (1997). Distribution and abundance of giant sea anemones (Actiniaria) in subtropical eastern Australian waters. *Marine and Freshwater Research* **48**, 59-66.

Roberts, T., Moloney, J., Sweatman, H., and Bridge, T. (2015). Benthic community composition on submerged reefs in the central Great Barrier Reef. *Journal of the International Society for Reef Studies* **34**, 569-580.

Roelfsema, C. M., Andersen, R., Arlow, P., Barrenger, T., Bray, P., Grol, M. G. G., Kunze, J., O'Hagen, A., Pheasant, M., Pollard, L., Stenhouse, M., and Stetner, D. (2018). 2017 Habitat maps derived from Flinders Reef Ecological Assessment (FREA) surveys, Queensland, Australia in ArcGIS (shapefile) format. Available at PANGAEA, https://doi.org/10.1594/PANGAEA.890756.

Roelfsema, C., Bayraktarov, E., Van den Berg, C., Breeze, S., Grol, M., Kenyon, T., de Kleermaeker, S., Loder, J., Mihaljević, M., Passenger, J., Rowland, P., Vercelloni, J., and Wingerd, J. (2017). Ecological assessment of the flora and fauna of Flinders Reef. Unidive, Brisbane, Australia.

Roelfsema, C., Phinn, S., Jupiter, S., Comley, J., and Albert, S. (2013). Mapping coral reefs at reef to reef-system scales, 10s–1000s km^2, using object-based image analysis. *International Journal of Remote Sensing* **34**, 6367-6388.

Roelfsema, C., Thurstan, R., Beger, M., Dudgeon, C., Loder, J., Kovacs, E., Gallo, M., Flower, J., Cabrera, K. G., Ortiz, J., Lea, A., and Kleine, D. (2016). A citizen science approach: A detailed ecological assessment of subtropical reefs at Point Lookout, Australia. *PLoS ONE* **11**, e0163407.

Roelvink, D., Reniers, A., van Dongeren, A., van Thiel de Vries, J., McCall, R., and Lescinski, J. (2009). Modelling storm impacts on beaches, dunes and barrier islands. *Coastal Engineering* **56**, 1133-1152.

Ross, H., Jones, N., Witt, K., Pinner, B., Shaw, S., Rissik, D., and Udy, J. (2019). Values towards Moreton Bay and catchments. In 'Moreton Bay Quandamooka & Catchment: Past, present, and future.' (Eds I. R. Tibbetts, P. C. Rothlisberg, D. T. Neil, T. A. Homburg, D. T. Brewer and A. H. Arthington.) The Moreton Bay Foundation. Brisbane, Australia. Available at https://moretonbayfoundation.org/.

Ruhanen, L., Orams, M., and Whitford, M. (2019). Tourism in the Moreton Bay Region. In 'Moreton Bay Quandamooka & Catchment: Past, present, and future.' (Eds I. R. Tibbetts, P. C. Rothlisberg, D. T. Neil, T. A. Homburg, D. T. Brewer and A. H. Arthington.) The Moreton Bay Foundation. Brisbane, Australia. Available at https://moretonbayfoundation.org/

Saunders, M., Runting, R., Charles-Edwards, E., Syktus, J., and Leon, J. (2019). Projected changes to population, climate, sea-level and ecosystems. In Moreton Bay Quandamooka & Catchment: Past, present, and future.' (Eds I. R. Tibbetts, P. C. Rothlisberg, D. T. Neil, T. A. Homburg, D. T. Brewer and A. H. Arthington.) The Moreton Bay Foundation. Brisbane, Australia. Available at https://moretonbayfoundation.org/

Schläppy, M-L., Loder, J., Salmond, J., Lea, A., Dean, A. J., and Roelfsema, C. M. (2017). Making waves: Marine citizen science for impact. *Frontiers in Marine Science* **4**, 146.

Siebeck, U., Marshall, N., Klüter, A., and Hoegh-Guldberg, O. (2006). Monitoring coral bleaching using a colour reference card. *Journal of the International Society for Reef Studies* **25**, 453-460.

Smith, S. D. A, Rule, M. J., Harrison, M., and Dalton, S. J. (2008). Monitoring the sea change: preliminary assessment of the conservation value of nearshore reefs, and existing impacts, in a high-growth, coastal region of subtropical eastern Australia. *Marine Pollution Bulletin* **56**, 525-534.

Sommer, B., Beger, M., Harrison, P. L., Babcock, R. C., and Pandolfi, J. M. (2018). Differential response to abiotic stress controls species distributions at biogeographic transition zones. *Ecography* **41**, 478-490.

Sommer, B., Harrison, P. L., Beger, M., and Pandolfi, J. M. (2014). Trait mediated environmental filtering drives assembly at biogeographic transition zones. *Ecology* **95**, 1000-1009.

Sommer, B., Sampayo, E. M., Beger, M., Harrison, P. L., Babcock, R. C., and Pandolfi, J. M. (2017). Local and regional controls of phylogenetic structure at the high-latitude range limits of corals. *Proceedings of the Royal Society Biological Sciences Series B* **284**, 20170915.

Spalding, M. D., and Brown, B. E. (2015). Warm-water coral reefs and climate change. *Science* **350**, 769-771.

Teleki, K. A. (2012). Power of the people? *Aquatic Conservation: Marine and Freshwater Ecosystems* **22**, 1-6.

Wallace, C. C., and Rosen, B. R. (2006). Diverse staghorn corals (Acropora) in high-latitude Eocene assemblages: Implications for the evolution of modern diversity patterns of reef corals. *Proceedings of the Royal Society B: Biological Sciences* **273**, 975-982.

Wallace, C. C., Fellegara, I., Muir, P. R., and Harrison, P. L. (2009). The scleractinian corals of Moreton Bay, eastern Australia: High latitude, marginal assemblages with increasing species richness. *Memoirs of the Queensland Museum* **54**, 1-118.

Wells, J. W. (1955). 'Recent and subfossil corals of Moreton Bay, Queensland.' (University of Queensland Press: Queensland, Australia).

Whitaker, D., and Christman, M. (2014). Clustsig: Significant cluster analysis. In 'R Package version 1.1'. vegan.

Whiteway, T. G. (2009). Australian bathymetry and topography grid, June 2009. Geoscience Australia Record 2009/21, Australia.

Woodley, J. D., Chornesky, E. A., Clifford, P. A., Jackson, J. B. C., Kaufman, L. S., Knowlton, N., Lang, J. C., Pearson, M. P., Porter, J. W., Rooney, M. C., Rylaarsdam, K. W., Tunnicliffe, V. J., Wahle, C. M., Wulff, J. L, Curtis, A. S. G., Dallmeyer, M. D., Jupp, B. P., Koehl, M. A. R., Niegel, J., and Sides, E. M. (1981). Hurricane Allen's impact on Jamaican coral reefs. *Science* **214**, 749-755.

Yadav, S., Rathod, P., Alcoverro, T., and Arthur, R. (2016). "Choice" and destiny: The substrate composition and mechanical stability of settlement structures can mediate coral recruit fate in post-bleached reefs. *Journal of the International Society for Reef Studies* **35**, 211-222.

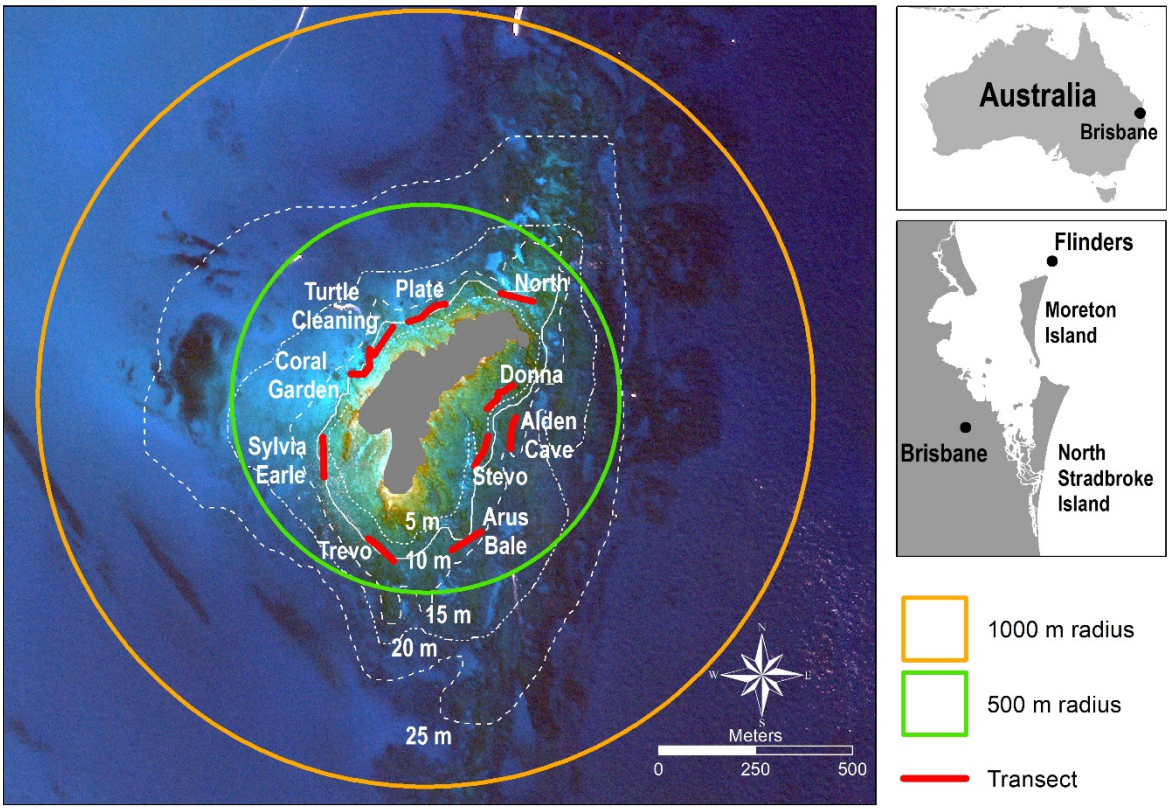

Fig. 1. Satellite image of Flinders Reef with the approximate transect location and direction indicated in red lines (site names in white). The Marine National Park "green" zone (500 m radius) where no fishing or anchoring is allowed is designated by the green line. Orange line (1000 m radius) represents the suggested extension of the green zone (see Discussion). The four Reef Check Australia long-term monitoring sites are Turtle Cleaning, Coral Garden, Plate and Alden Cave, respectively. Turtle Cleaning Station, Coral Gardens, Alden's Cave and Plateland in Reef Check Australia reporting. The grey area indicates the predominantly exposed area of Flinders Reef, and the inset maps on the right show the location of Flinders Reef in Moreton Bay and in Australia. The prevailing wind direction for Flinders Reef is east-south-east. Source image: WorldView 2 image Digital Globe (2017), 2m x 2m pixels.

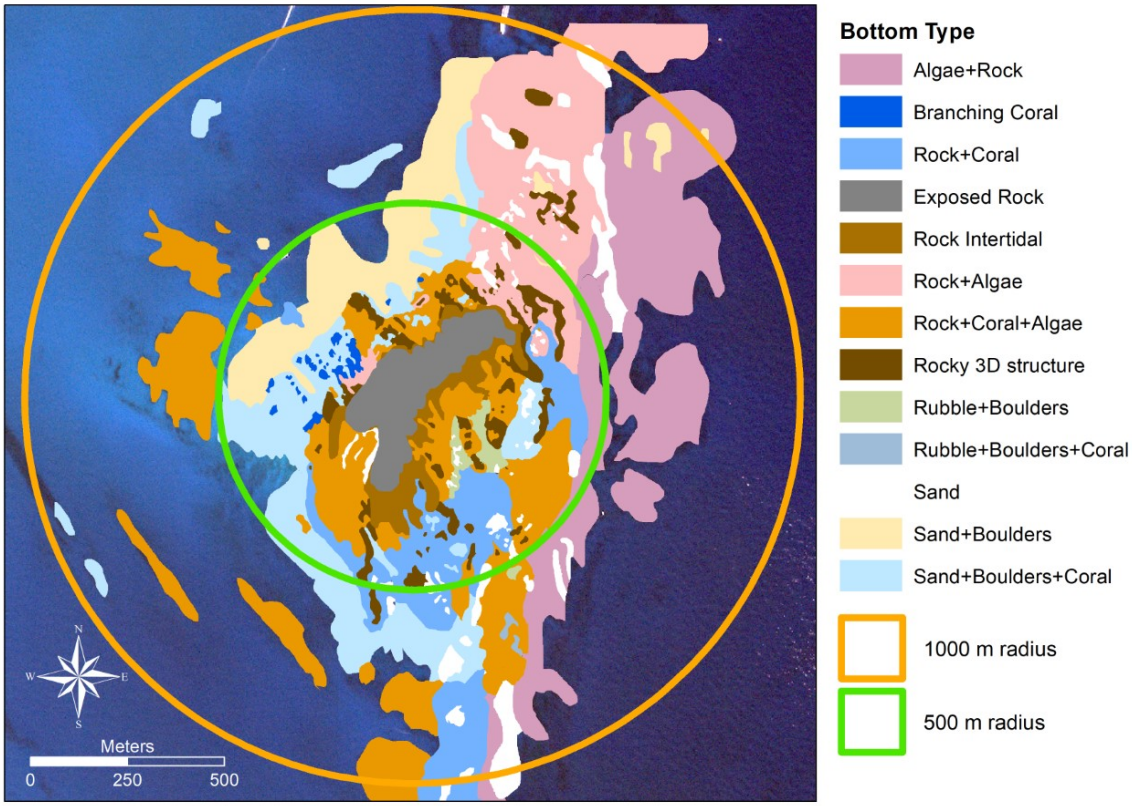

Fig. 2. Detailed habitat map of prominent substrate types for Flinders Reef, South East Queensland, Australia. Marine National Park green zone (500 m radius, green line), where neither fishing nor anchoring is allowed, could be extended with an additional 500 m buffer zone (1000 m radius, orange line) where no anchoring nor fishing would be allowed. This would result in a two-fold increase in protected surface area for benthic categories that compromise corals; and a three-fold increase of protected area that include rocky substrate. The mapped areas were overlayed on satellite imagery, except for the predominantly sandy areas.

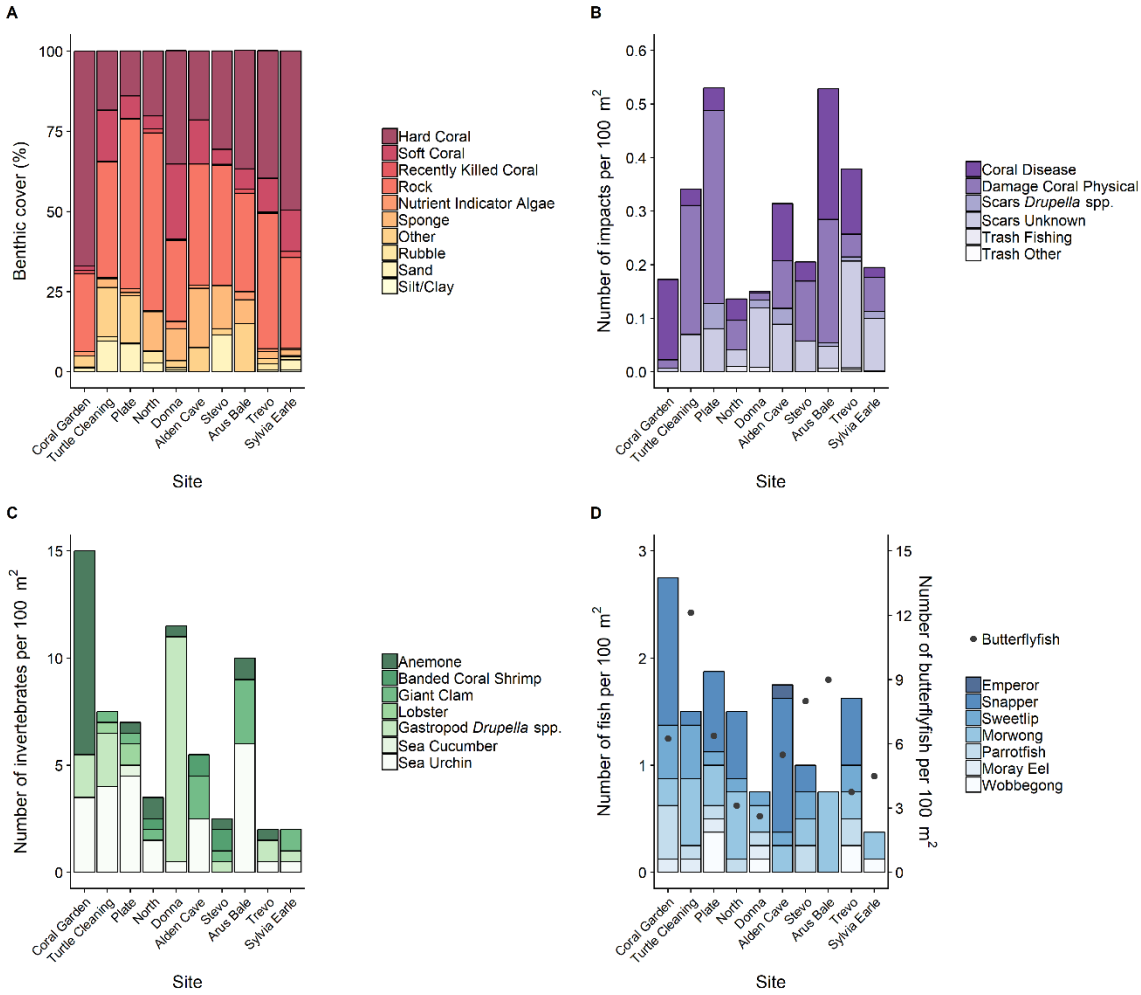

Fig. 3. Overview of the major ecological groups recorded during the surveys per site. (*a*) Benthic groups expressed as percent cover per site. (*b*) Average number of impacts per site per 100 m^2, normalized for hard coral cover. (*c*) Average number of invertebrates found per site per 100 m^2 and (*d*) average number of fish per site per 100 m^2 with the average number of butterflyfish per 100 m^2 displayed on the secondary y-axis (dots). Groups were based on surveyed ecological categories and absent categories/groups were omitted from the panels.

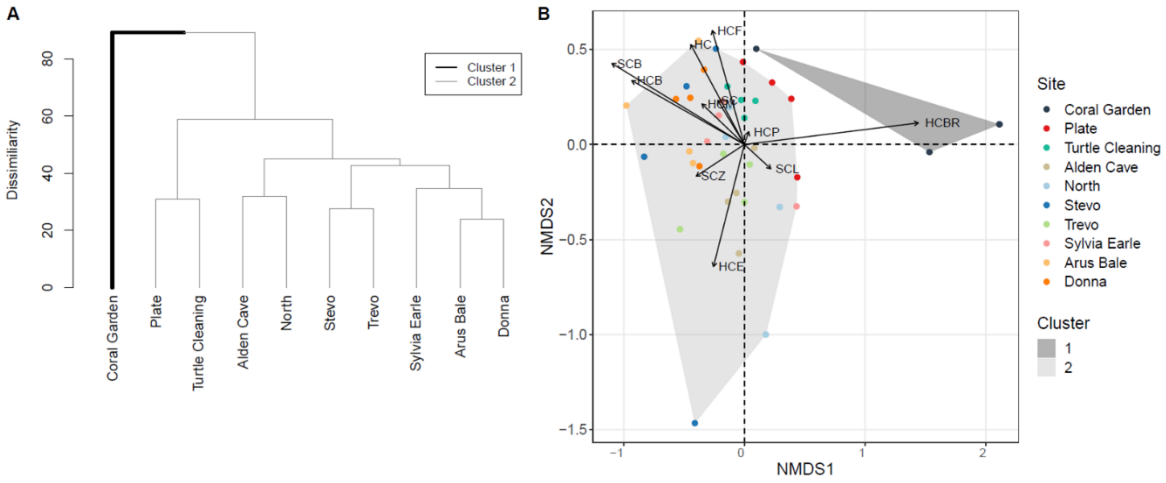

Fig. 4. Spatial dissimilarities in the structure of coral communities. (*a*) Dendrogram depicting the hierarchical clustering of the surveyed sites based on coral community composition. (*b*) Non-metric multidimensional scaling (nMDS) plot (stress = 1.74%), illustrating differences in the structure of coral communities within surveyed sites. Arrows indicate the coral community groups driving the nMDS. Cluster 1 and 2 identified in the dendrogram (Panel A) are represented by grey polygons in Panel B. Benthic categories: HC = Hard Coral, HCP = Hard Coral Plate, HCBR = Hard Coral Branching, HCF = Hard Coral Foliose, HCM = Hard Coral Massive, HCB = Hard Coral Bleached, HCE = Hard Coral Encrusting, SC = Soft Coral, SCL = Soft Coral Leathery, SCB = Soft Coral Bleached, and SCZ = Soft Coral Zooanthid.

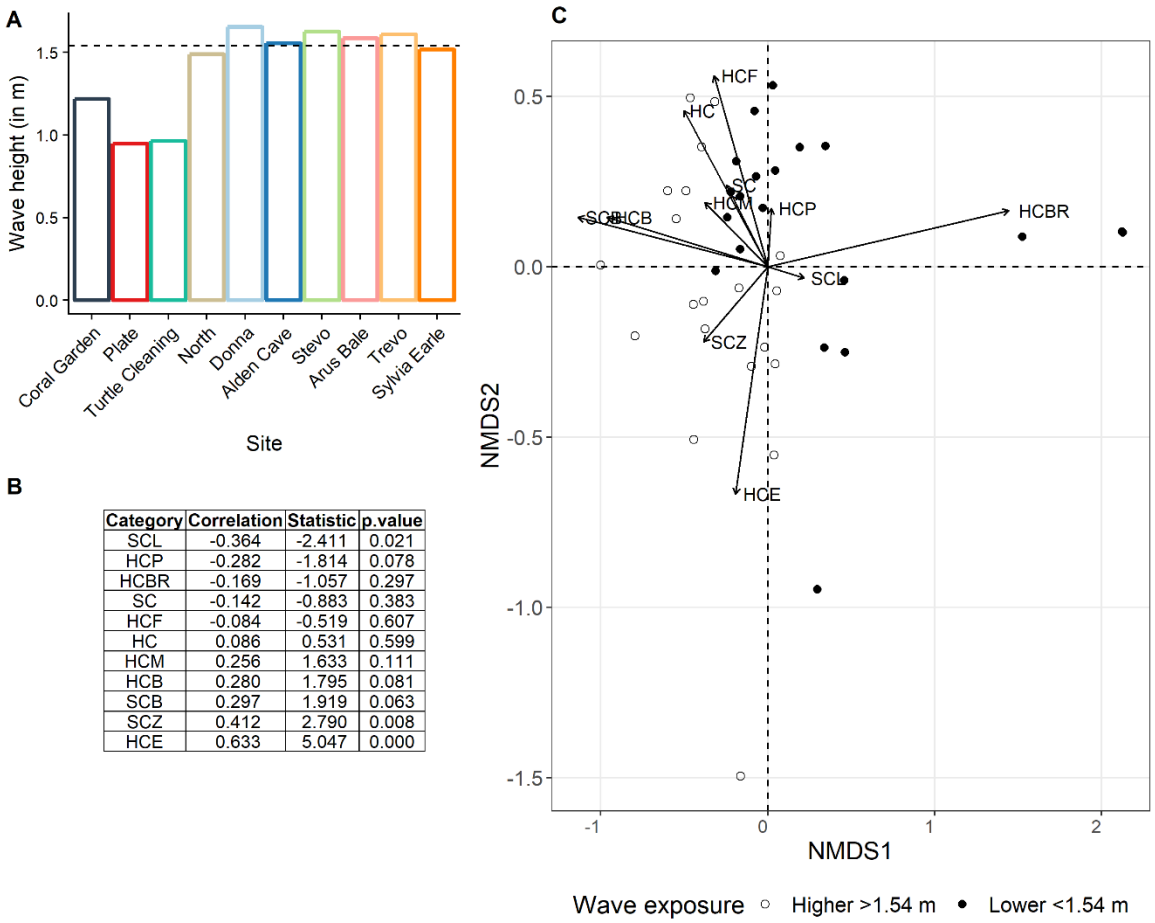

B

Category	Correlation	Statistic	p.value
SCL	-0.364	-2.411	0.021
HCP	-0.282	-1.814	0.078
HCBR	-0.169	-1.057	0.297
SC	-0.142	-0.883	0.383
HCF	-0.084	-0.519	0.607
HC	0.086	0.531	0.599
HCM	0.256	1.633	0.111
HCB	0.280	1.795	0.081
SCB	0.297	1.919	0.063
SCZ	0.412	2.790	0.008
HCE	0.633	5.047	0.000

Fig. 5. Drivers of the structure of coral communities at Flinders Reef. (*a*) Modelled values of wave height extracted from the SWAN model (Whiteway 2009) at each surveyed site. The dotted line shows the median value of 1.54 m, used to separate sites with lower and higher levels of wave exposure. (*b*) Pearson correlation values and associated statistics between coral categories and wave height ranked from most negative correlations to the most positive. (*c*) nMDS scaling plot with surveyed segments coloured by wave exposure level (open circles = high exposure >1.54 m; filled circles = low exposure <1.54 m). Benthic categories: HC = Hard Coral, HCP = Hard Coral Plate, HCBR = Hard Coral Branching, HCF = Hard Coral Foliose, HCM = Hard Coral Massive, HCB = Hard Coral Bleached, HCE = Hard Coral Encrusting, SC = Soft Coral, SCL = Soft Coral Leathery, SCB = Soft Coral Bleached, and SCZ = Soft Coral Zooanthid.

Table 1. The effect of site and wave height on coral community composition. Summary PERMANOVA output including coral community composition as response variable, and wave height and site as fixed effect explanatory variables.

	Df	SS	MS	F	R^2	*P* value
Wave height	1	0.9774	0.97743	12.5046	0.15594	<0.001
Site	8	2.9458	0.36822	4.7108	0.46996	<0.001
Residuals	30	2.345	0.07817		0.37411	
Total	39	6.2682			1	

Intertidal gobies acclimate rate of luminance change for background matching with shifts in seasonal temperature

Carmen RB da Silva[1,2*], Cedric P van den Berg[1], Nicholas D Condon[3], Cynthia Riginos[1], Robbie S Wilson[1], Karen L Cheney[1,4]

[1] *School of Biological Sciences, The University of Queensland, St Lucia 4072, Australia*

[2] *School of Biological Sciences, Monash University, Clayton 3800, Australia*

[3] *Institute for Molecular Biosciences, The University of Queensland, St Lucia 4072, Australia*

[4] *Queensland Brain Institute, The University of Queensland, St Lucia, 4072, Australia*

* *Corresponding author*

Abstract

1. Rate of colour change and background matching capacity are important functional traits for avoiding predation and hiding from prey. Acute changes in environmental temperature are known to impact the rate at which animals change colour, and therefore may affect their survival.
2. Many ectotherms have the ability to acclimate performance traits such as locomotion, metabolic rate and growth rate with changes in seasonal temperature. However, it is unclear how other functional traits that are directly linked to behaviour and survival respond to long-term changes in temperature (within an individual's lifetime).
3. We assessed whether the rate of colour change is altered by long-term changes in temperature (seasonal variation) and if rate of colour change can acclimate to seasonal thermal conditions. We used an intertidal rock-pool goby, *Bathygobius cocosensis,* to test this and exposed individuals to representative seasonal mean temperatures (16 °C or 31 °C, herein referred to cold and warm-exposed fish, respectively) for nine weeks and then tested their rate of luminance change when placed on white and black backgrounds at acute test temperatures 16 °C and 31 °C. We modelled rate of luminance change using the visual sensitives of a coral trout (*Plectropmus leopardus*) to determine how well gobies matched their backgrounds in terms of luminance contrast to a potential predator.
4. After exposure to long-term seasonal conditions, the warm-exposed fish had faster rates of luminance change and matched their background more closely when tested at 31 °C than at 16 °C. Similarly, the cold-exposed fish had faster rates of luminance change and matched their backgrounds more closely at 16 °C than at 31 °C. This demonstrates that rate of luminance change can be adjusted to compensate for long-term changes in seasonal temperature.

5. This is the first study to show that animals can acclimate rate of colour change for background matching to seasonal thermal conditions. We also show that rapid changes in acute temperature reduce background matching capabilities. Stochastic changes in climate are likely to affect the frequency of predator-prey interactions which may have substantial knock-on effects throughout ecosystems.

Keywords: Acclimation, Plasticity, Colour change, Luminance change, Intertidal, Camouflage, Background matching, Thermal performance

Introduction

Fluctuations in environmental temperature impact the physiology, function and fitness of animals (Deutsch *et al.* 2008; Tewksbury, Huey & Deutsch 2008; Hoffmann & Sgro 2011; Seebacher, White & Franklin 2015). Animals can respond to variation in temperature within their lifetime via behavioural thermoregulation (e.g. migrating, hiding in a cooler location or panting) or by acclimating to the changed thermal conditions (Wilson & Franklin 2002; Angilletta 2009; Beaman, White & Seebacher 2016). Acclimation, also known as reversible plasticity, occurs when an individual changes its underlying physiology to maintain performance and function in changed environmental conditions (Wilson & Franklin 2002; Beaman, White & Seebacher 2016). Acclimation to changed thermal conditions is likely to help buffer animals to increasing temperatures associated with climate change. It is important to explore how functional traits respond to changes in temperature and how these responses affect animal ecology and evolution.

We know that many ectotherms can modify their physiological function in response to long-term changes in their thermal environment within their lifetime, including traits like metabolic rate, growth and locomotor performance, which allows maintenance of performance with changed thermal conditions (Angilletta 2009). For example, *Gambusia holbrooki* (mosquito fish) have the capacity to acclimate their muscle structure, swimming speeds, and mating success to seasonal thermal change (Hammill, Wilson & Johnston 2004; Wilson, Condon & Johnston 2007). Although many studies have assessed thermal performance of locomotion and metabolism, we are yet to understand how long-term changes in temperature will affect behaviours such as physiologically-based anti-predator defences. For example, many animals use colour change to match the background against which they are viewed to prevent detection from predators or prey, or use aposematic colouration (e.g. flashing rings of a blue ringed

107 octopus when disturbed) to warn off predators (Sköld, Aspengren & Wallin 2013; Cheney,
108 Cortesi & Nilsson Sköld 2017; Ruxton *et al.* 2018). The rate at which animals change colour
109 can directly impact survival, as slow colour change may significantly increase the chance of
110 cryptic prey being detected by predators (Stevens 2016; Duarte, Flores & Stevens 2017;
111 Stevens *et al.* 2017).
112
113 The rate at which animals change their body colouration is dependent on the mechanism used
114 for colour change. Morphological colour change occurs over days or weeks during which the
115 composition and number of chromatophores (skin pigment cells) is altered (long-term colour
116 change response) (Auerswald *et al.* 2008; Duarte, Flores & Stevens 2017). Physiological colour
117 change occurs at a rapid rate (seconds/minutes) as pigment granules within chromatophores
118 disperse or aggregate using neuromuscular movement (short-term colour change response), or
119 more slowly via changes in hormone concentrations, such as melatonin (Sköld, Aspengren &
120 Wallin 2013; Caro, Sherratt & Stevens 2016; Stevens 2016; Duarte, Flores & Stevens 2017).
121 Rapid changes in colour (hue and saturation), luminance (perceived brightness) or pattern can
122 allow animals to match fine scale environmental heterogeneity, permitting animals to move
123 more freely without suffering a mismatch with visual backgrounds (Duarte, Flores & Stevens
124 2017). Rates of physiological colour change in amphibians and fish are dependent on
125 temperature, and thus an animal's ability to match their background may be hindered by acute
126 fluctuations in environmental temperature (Cole 1939; King, Hauff & Phillips 1994; Camargo,
127 Visconti & Castrucci 1999; Lin, Lin & Huang 2009). It is unclear how responses to longer-
128 term temperature change might modulate the effects of acute temperature variation on the rate
129 of colour change. For example, the depressive effects of cold temperature on the rate of colour
130 change might be compensated for by phenotypic responses to longer-term exposure to cold
131 temperatures (i.e. acclimation).

132

133 We tested if rate of luminance change can acclimate to long-term seasonal change in an
134 intertidal rock-pool fish, *Bathygobius cocosensis*. Animals that live within the rocky-intertidal
135 zone are ideal to assess how temperature alters short- and long-term thermal performance as
136 they are exposed to diurnal tidal thermal fluctuations as well as seasonal thermal variation
137 (Helmuth & Hofmann 2001; Somero 2002). *Bathygobius cocosensis* has the capacity to
138 acclimate physiological characteristics such as burst swimming speed, maximum metabolic
139 rate, and metabolic scope, to seasonal thermal conditions (da Silva, Riginos & Wilson 2019),
140 and they have been observed to change their luminance in the field (light against sand, dark
141 against rocks) (personal observations). Other goby species are also known to alter their
142 appearance (short-term physiological colour change) in terms of colour, luminance and pattern,
143 to match their visual backgrounds and remain cryptic from predators within rock-pools
144 (Stevens, Lown & Denton 2014; Smithers, Wilson & Stevens 2017; Smithers *et al.* 2018).
145 Rock-pools are comprised of many different background types (e.g. rock, sand or algae), where
146 animals must change colour rapidly if they are to move and remain camouflaged in their
147 environment (Stevens, Lown & Denton 2014; Stevens 2016; Smithers, Wilson & Stevens
148 2017). Matching body luminance to surrounding background luminance for camouflage is
149 particularly important because motion, texture and shape of objects is largely conveyed by an
150 animal's ability to perceive luminance contrast (Cronin *et al.* 2014; Ruxton *et al.* 2018). In
151 addition, *B. cocosensis* more readily change luminance rather than hue so we focused on rate
152 of luminance change rather than rate of hue/colour change. No previous studies that we are
153 aware of have investigated if rate of luminance change for background matching (i.e. when an
154 animal's appearance generally matches the colour, lightness and pattern of its background
155 (Stevens & Merilatita 2009)) can acclimate with seasonal temperature change.
156

157 To assess whether *B. cocosensis* has the capacity to acclimate rate of luminance change to
158 seasonal thermal conditions, we exposed half of the study population to warm conditions (31
159 °C) and the other half to cold (16 °C) conditions for nine weeks. These temperature treatments
160 were based on seasonal temperatures *B. cocosensis* are exposed to in nature and can acclimate
161 other physiological traits to (da Silva, Riginos & Wilson 2019). We then assessed rate of
162 luminance change with each fish being tested against both white and black backgrounds at 16
163 °C and 31 °C acute test temperatures. To investigate how well *B. cocosensis* matched their
164 background we modelled how luminance changes might be perceived by a potential predatory
165 fish using photoreceptor sensitivities of the coral trout (*Plectropmus leopardus*). We
166 hypothesised that long-term exposure to different seasonal temperatures would enable *B.*
167 *cocosensis* to acclimate rate of luminance change to different seasonal temperatures, when
168 matching both darker and lighter background habitats colours. Therefore, we expect the warm-
169 exposed fish to have faster rates of luminance change (to match their background colour) at 31
170 °C than 16 °C when placed against a black or white background, and the cold-exposed fish to
171 have faster rates of luminance change at 16 °C than 31 °C against both background colours. If
172 animals can acclimate rate of luminance change (for background matching) with thermal
173 change it may mediate the frequency of predator-prey interactions. For example, prey may be
174 able to remain cryptic from predators in warmer thermal environments which will reduce
175 pressure on prey species populations, or predators may be able to remain cryptic from prey
176 which will maintain their energetic requirements. If animals can't acclimate rate of luminance
177 change with changes in temperature, climate change may indirectly change rates of predator-
178 prey interactions if prey and/or predators become less cryptic.
179

Methods

Bathygobius cocosensis (n = 80) were collected from the rocky inter-tidal zone at Point Cartwright, SE Queensland, Australia (26.6804°S, 153.1390°E) in November 2016. All fish were collected using a battery-operated bilge-pump and hand nets. Fish (22 – 47 mm standard length – tip of nose to last vertebrae) were transported to The University of Queensland by vehicle in oxygen-saturated bags within an insulated container. Fish were anesthetized (0.3 x 10^{-3} mg L^{-1} of Aqui-S®) (Malard, McGuigan & Riginos 2016) and tagged dorsally between their head and first dorsal fin, with unique Visible Implant Elastomer (VIE) florescent subdermal tags (Northwest Marine Technologies®, Inc.) for individual recognition. VIE tags do not affect growth rates or survival in fish (FitzGerald, Sheehan & Kocik 2004). Fish were split into two treatments: warm fish (n = 40) were randomly allocated to 6 tanks (~ 7 fish per tank) set at 31 °C and cold fish (n = 40) were randomly allocated to 6 tanks (~ 7 fish per tank) set at 16 °C. Fish were housed in 60L glass tanks with shells provided for shelter. Fish were exposed to a 12:12hr 6am – 6pm light dark cycle in a controlled temperature room at The University of Queensland. Fish were held for nine weeks in treatment conditions before the start of luminance change testing, as it usually takes several weeks to acclimate to changed thermal conditions (Seebacher *et al.* 2005).

Before testing, fish were brought to test temperature at a rate of 5 °C per hour, as deemed an appropriate rate for intertidal fish (Schulte, Healy & Fangue 2011). Rate of change in dorsal body luminance was measured in a full factorial design where individuals from warm and cold-exposed treatment groups were tested against both white and black backgrounds at 16 °C and 31 °C. This resulted in four test groups: white background at 16 °C; white background at 31 °C; black background at 16 °C; black background at 31 °C. Fish from each treatment group were randomly assigned to test conditions (by temperature and colour) so order of test

temperature or colour would not affect results (a fully crossed experimental design). Fish were tested in a controlled temperature room (16 °C or 31 °C) at The University of Queensland under LED lights (Arlec 9 Watt Slim Bar Lights) to ensure environmental lighting conditions were consistent across trials.

Experimental preparation

For testing, containers were created by spray-painting matt black or white (MMP industrial Pty Ltd, Mulgrave, NSW, AUS) onto PVC plastic sheets to line the inside of 8cm x 15cm x 4cm plastic testing containers. Once dry, the luminance of the paint colour was obtained by taking a photograph of the painted containers with a calibrated Samsung NX1000 with Nikkor EL 80mm lens camera. We used the Multispectral Image Analysis and Calibration (MICA) Toolbox plugin (Troscianko & Stevens 2015) in the program ImageJ (https://imagej.nih.gov/ij/) to normalise and linearise the photograph. Reflectance of the black and white backgrounds was measured as the sum of the red, green and blue channel of a given background relative to a hypothetical 100% white standard. We used a spectrophotometer (USB2000 Ocean Optics©, Largo, FL USA) (https://oceanoptics.com/) with a 180° cosine corrector, 400µm bifurcated optical fiber cable and a PX-2 light source to determine the luminance of the grey standard (black and white Kodak colour squares), which were used to normalise and linearise each photograph, and to determine the illuminant light spectrum provided by our artificial light source (Arclec 9 Watt Slim Bar Lights). For holding fish before they were tested, intermediate grey backgrounds were produced by printing a grey 50% luminance background onto Kodak printing paper using an HP laser jet printer (HP LaserJet Pro 400 colour M451dn) for the fish to be held in prior to testing. The intermediate background was then laminated with matt sheets to reduce reflection and to ensure they were waterproof.

Experimental protocol

Fish were first placed into the intermediate grey background for 10 minutes to ensure that all fish were exposed to the same conditions before testing. The fish were photographed at the end of the 10 minutes using the calibrated Samsung NX1000 with Nikkor EL 80mm lens camera, with a fixed aperture, manual white balance settings, and with a grey standard (Kodak colour squares) for image calibration within the photo frame. Photographs were taken in RAW format. Fish were swiftly (< 5 seconds) transferred with a small dip net into either the white or the black background container at either 16 °C or 31 °C and photographed immediately and once every 15 seconds for 10 minutes with the colour standard for image calibration within each photo. Each fish was tested separately to avoid stimulating a behavioural change in luminance. On the last day of testing, mass (g) and standard length (mm) of each fish was measured.

Image Analysis

We quantified dorsal body luminance of gobies through the eye of a potential predatory coral trout (*Plectropmus leopardus*). To do this, we used the MICA Toolbox plugin (Troscianko & Stevens 2015) in the program ImageJ (https://imagej.nih.gov/ij/). Images were calibrated and turned into 16-bit multispectral images using a grey standard with 73.3% and 5.1% reflectance (Figures 1 & 2). Colour vision modelling using calibrated digital photography relies on detailed knowledge about the spectral sensitivities of both the potential animal viewer, the camera settings and the illumination within the image. Coral trout have single cones that contain a short wavelength sensitive pigment (λ_{max} = 455nm); and double cones that exhibit broad absorbance spectra ranging from 507 to 532 nm (mean λ_{max} = 522 nm) (Cortesi *et al.* 2016). In fish, luminance is likely to be processed by double cones, as it is in birds and reptiles (Lythgoe, 1979); therefore, we used the mean λ_{max} of double cone members (522 nm) to model luminance perception. Although coral trout are unlikely to be the main predator of *B. cocosensis* along

255 Australia's East coast, their visual capacity is likely to be similar to many other predatory
256 teleosts (Losey *et al.* 2003).
257
258 Within the MICA toolbox we modelled double cone photoreceptor stimulation (f_{dbl}) as a proxy
259 for luminance. The visual (cone mapping) model included information on the type of camera
260 (Samsung NX1000), lens (80mm Nikkor EL), the artificial lighting used to take the
261 photographs (Arlec 9 Watt Slim Bar Lights), the coral trout visual sensitives (Cortesi *et al.*
262 2016), and the model illuminant (400-700nm daylight) (gobies are found in very shallow water
263 so we modelled them being in a clear-sky daylight spectrum) (cone catch model in
264 supplementary material). Examples (reconstructed RGB images) of cone catch images of
265 gobies against black and white backgrounds through coral trout in comparison to human colour
266 vision are shown in Figures 1 and 2.
267
268 Using the visual models for each photograph, we assessed the luminance of each goby at each
269 time point as the median coral trout double cone stimulation across our region of interest (ROI).
270 An ROI was drawn around the inside edge of each goby (a triangle from their pectoral fins
271 down their body and tail to avoid the elastomer tag) and calculated the median luminance. As
272 thousands of photos were generated for this experiment ($n > 5000$), we used an ImageJ based
273 script to partially automate this process for each photograph (ImageJ script in supplementary
274 data).
275
276 We calculated the achromatic perceptual distance (ΔS) (how closely the goby matches its
277 background through the eye of a coral trout in terms of perceived brightness), between each
278 goby and its visual background using the receptor noise limited model (Vorobyev & Osorio
279 1998). The receptor noise limited model assumes the inherent noise in photoreceptors

ultimately limits contrast perception. Animal-background contrast was measured at each time point and against white and black backgrounds to assess the achromatic contrast between the goby and its background throughout the duration of testing. Achromatic perceptual distance (ΔS) was calculated according to equation 4 & 7 from Siddiqi *et al.* (2004) (eq. 1 & 2)

$$\Delta f_{dbl} = \ln(l_1) - \ln(l_2) \qquad \text{(equation 1)}$$

$$\Delta S = |\Delta f_{dbl}/\omega_{dbl}| \qquad \text{(equation 2)}$$

where, l_1 is the % double cone stimulation (f_{dbl}) of the background (white or black background), l_2 is the % double cone stimulation (f_{dbl}) of the goby polygon (ROI), and ω_{dbl} is the weber fraction of the double cone receptor channel as per Cortesi *et al.* 2006. Achromatic perceptual distance was measured at the start and end of each trial to measure how well matched a fish was to its background. The change in achromatic perceptual distance between those two times was calculated to determine if fish achieved a greater match during the trial. Threshold values that determine if a change in perceived achromatic distance are distinguishable (i.e. whether goby can be distinguished from its background by the coral trout) have been suggested to be above 1ΔS (Siddiqi *et al.* 2004), however, we used a conservative threshold assumption of 3ΔS as suggested by Abernathy *et al.* (2017). Therefore, the greater the achromatic perceptual distance, the more contrasting the goby is against its background, increasing the likelihood of detection by a coral trout. The lower the achromatic perceptual distance, the harder the goby is to detect against its background to the coral trout.

Statistical analysis

Rate of Luminance Change

We assessed rate of luminance change over the first four minutes of testing (rather than the full ten minutes test period) as the slopes were generally steepest and most linear over this time

305 (Supplementary Figure 1). Using the first four minutes of luminance change allowed us to
306 identify how an animal's short-term background matching response might be affected by a
307 change in water temperature (i.e. if an animal takes many minutes to change luminance they
308 are more likely to be noticed than an individual that can match their background within a few
309 seconds or minutes). When comparing rates of luminance change positive slopes indicate a
310 brightening in fish skin pigment and negative slopes indicate darkening.
311
312 To assess whether long-term exposure to warm or cold thermal conditions altered the rate at
313 which gobies changed their luminance at different test temperatures, we ran linear mixed effect
314 models using the package nlme (Pinheiro *et al.* 2018) for each background colour (black or
315 white) in the statistical program R version 1.1453 (R Core Team 2018). Long-term exposure
316 (warm or cold) was set as a categorical variable and test temperature (16 °C or 31 °C) was set
317 as a continuous variable. Fish mass, standard length and test time were included as covariates,
318 and fish identification number was nested within tank number and was set as a random variable.
319 Fish length was eventually removed from the final model because it was correlated with fish
320 mass. An interaction between acute test temperature and long-term thermal exposure was
321 included in the full model. Model reduction was used to test if the interaction between acute
322 test temperature and long-term thermal exposure had a significant effect on rate of luminance
323 change to assess if *B. cocosensis* could acclimate rate of luminance change to long-term thermal
324 exposure. Models were compared with one another using a likelihood ratio test using the lmtest
325 library in R (Zeileis & Hothorn 2002). As we hypothesised that *B. cocosensis* would acclimate
326 rate of luminance change to seasonal thermal conditions, we expected that there would be a
327 significant interaction between long-term exposure temperature (warm or cold) and test
328 temperature on rate of luminance change when the fish are tested against both black and white
329 backgrounds. We also predicted the sign of the estimate of the interaction term to determine

330 the directionality of the effect of long-term thermal exposure and acute test temperature on rate
331 of luminance change against black and white backgrounds. Against a black background we
332 would expect the estimate of the interaction term to be negative, as the cold-exposed fish are
333 likely to turn darker faster (lower luminance value) at 16 °C than 31 °C (positive slope) and the
334 warm-exposed fish to turn darker faster at 31 °C than 16 °C (negative slope). Therefore, the
335 difference between the cold- and warm-exposed fish rates of luminance change across test
336 temperature is likely to produce a negative estimate for the interaction term between test
337 temperature and long-term thermal exposure group (cold-exposed group is always used as the
338 reference group) (Faraway 2016). In contrast, we expect the estimate for the interaction term
339 between long-term thermal exposure and acute test temperature to be positive when fish are
340 tested against a white background. In this case, we expect the cold-exposed fish to turn lighter
341 faster at 16 °C than 31 °C (negative slope), and the warm-exposed fish to turn lighter faster at
342 31 °C than 16 °C (positive slope). Therefore, the difference in slope (interaction term estimate)
343 between the cold-exposed and warm-exposed fish is likely to be positive.
344
345 *Long-term effect of temperature on luminance*
346 We assessed if long-term thermal exposure affected the starting luminance of *B. cocosensis*
347 against the white, black and intermediate grey backgrounds. We used separate linear models
348 (black, white and intermediate grey background) to compare the starting luminance (first
349 photograph taken during the 10 minute trial) of warm- and cold-exposed fish. Linear models
350 included long-term exposure group as categorical variable and fish mass as a continuous
351 variable. Like the statistical methods outlined above, we used model reduction and comparison
352 using likelihood ratio tests to examine if long-term exposure group had an effect on starting
353 luminance.
354

355 *Coral trout visual perception*

356 We assessed if the gobies became more or less distinguishable from their backgrounds to the
357 coral trout throughout the duration of the testing period by assessing their total change in
358 achromatic perceptual distance (10 minutes). We calculated mean achromatic perceptual
359 distance at the start (0 seconds) and end (10 minutes) of the testing period and calculated the
360 total change in achromatic perceptual distance to determine the degree of ecologically
361 significant luminance change the gobies underwent for each test temperature and background.
362 We used the full 10-minute test period, rather than the first four minutes to capture how well
363 the gobies could eventually match their background (slower background matching response).
364 We used the same model structure as "*rate of luminance change*" above to assess how long-
365 term thermal exposure and test temperature affected total change in achromatic perceptual
366 distance over time. Greater positive changes in achromatic perceptual distance over time
367 indicate that the gobies became less distinguishable against their background, negative values
368 indicate that the goby became more distinguishable against its background. Again, we expect
369 there to be a significant interaction between long-term thermal exposure group and test
370 temperature on total change in achromatic perceptual distance indicating that *B. cocosensis* can
371 acclimate total change in achromatic perceptual distance with long-term thermal exposure. We
372 expect the warm-exposed fish to have greater total changes in achromatic perceptual distance
373 at 31 °C than 16 °C against black and white backgrounds (positive slope), and the cold-exposed
374 fish to have greater changes in achromatic perceptual distance at 16 °C than at 31 °C (negative
375 slope). Therefore, we expect the estimate of the interaction term to be positive for both the
376 black and the white background total change in achromatic perceptual distance models. All
377 figures were produced using ggplot2 (Wickham 2016).
378

Results

Rate of luminance change

Black background

Long-term thermal exposure (warm or cold) impacted the rate of luminance change in *B. cocosensis* at 16 °C and 31 °C against a black background (Figure 3a). The interaction between long-term thermal exposure and acute test temperature had a significant effect on rate of luminance change when the fish were tested against a black background (LRT: $\chi^2_{(1)}$= 12.671, P = 0.0003) (Figure 3a). We found that the sign of the estimate for the interaction between long-term thermal exposure and acute test temperature was negative (estimate = -0.0006 ± 0.001) (cold-exposed group used as the reference group). This suggests that the warm-exposed fish have a more negative slope than the cold-exposed fish across acute test temperature, indicating that the warm-exposed fish turn darker faster than the cold-exposed fish at warm test temperatures and the cold-exposed fish turn darker faster than the warm-exposed fish at cold test temperatures (Figure 3a). This finding supports our hypothesis that rate of luminance change can acclimate to seasonal thermal conditions in an intertidal fish. Fish mass did not affect rate of luminance change against a black background (LRT: $\chi^2_{(1)}$= 0.954, P = 0.329).

White background

Long-term thermal exposure (warm or cold) also impacted the rate of luminance change in *B. cocosensis* at 16 °C and 31 °C against a white background. The interaction between long-term thermal exposure and acute test temperature also had a significant effect on rate of luminance change when the fish were tested against a white background (LRT: $\chi^2_{(1)}$= 9.976, P = 0.0016) (Figure 3b). We found that the sign of the estimate for the interaction between long-term exposure temperature and acute test temperature was positive (estimate = 0.0018 ± 0.0003).

403 This suggests that the warm-exposed fish have a more positive slope than the cold-exposed
404 fish across test temperature, indicating that the warm-exposed fish turn lighter faster than the
405 cold-exposed fish at warm test temperatures and the cold-exposed fish turn lighter faster than
406 the warm-exposed fish at cold test temperatures (Figure 3b). Therefore, the difference between
407 the cold-exposed fish slope (rate of luminance change across test temperature) and warm-
408 exposed fish slope (estimate coefficient) is positive, supporting our hypothesis (Figure 3b).
409 Fish mass did not affect rate of luminance change against a white background (LRT: $\chi^2_{(1)}$=
410 0.212, P = 0.645).
411
412 On average gobies were able to turn darker faster than lighter (Supplementary Table 1). In
413 addition, gobies were able to change luminance (to better match their backgrounds) faster at
414 31 °C than 16 °C on average (Supplementary Table 1).
415
416 **Long-term effect of temperature on luminance**
417 As the fish are partially translucent, their luminance was affected by the background colour
418 (white or black) that they were tested on. When placed on the white background, at the start of
419 the 10 minute test period, the fish were 32.3% f_{dbl} on average, and when placed against a black
420 background, fish were 9.9% f_{dbl} on average (where higher f_{dbl} percentages are 'lighter'). To
421 assess if long-term warm or cold exposure influenced starting luminance, we ran a linear model
422 and found that exposure group (warm or cold) altered starting luminance when placed against
423 a white background (LRT: $\chi^2_{(1)}$= 11.018, P = 0.0009), and had a small, but significant effect
424 on starting against the black background (LRT: $\chi^2_{(1)}$ = 4.13, P = 0.042). We quantified the
425 luminance of each fish at the end of the 10 minute intermediate grey background standardising
426 period prior to testing, here we found that the cold-exposed fish had slightly higher luminance
427 values on average (LRT: $\chi^2_{(1)}$ = 4.79, P = 0.03) (Supplementary Figure 2).

Coral trout visual perception

Black background

Long-term exposure to warm or cold conditions altered the total change in achromatic perceptual distance (change in degree of background matching over time) against the black background (ΔS at 0 mins – ΔS time at 10 mins) (Figure 4a). The interaction between long-term thermal exposure and test temperature effected how well the gobies were able to match the luminance of their background (LRT: $\chi^2_{(1)}$=13.24, P = 0.0003) (Figure 4a). We found that the sign of the interaction term estimate was positive (estimate = 0.55 ± 0.19). This shows that the warm-exposed gobies became more similar to their background when tested at 31 °C than 16 °C (positive slope), and the cold-exposed fish became more similar to the black background at 16 °C than 31 °C (negative slope), indicating a seasonal thermal acclimation response to warm or cold conditions (Figure 4a). Therefore, total achromatic perceptual distance (background matching) can acclimate to seasonal thermal conditions in *B. cocosensis*, as predicted. All experimental groups, except the warm-exposed fish at 16 °C, showed an ecologically significant total change in luminance across the test period through the eye of a coral trout when tested against a black background (ΔS > 3) (Supplementary Table 2). These results indicate that *B. cocosensis* are undergoing ecologically significant dark background matching in terms of decreasing luminance, which would likely make them less obvious to a coral trout. Their end change in achromatic perceptual distance values, however, remain greater than 3 ΔS, meaning that they are still distinguishable from their background to a coral trout. An example of *B. cocosensis* turning darker over time is shown in Figure 1.

White background

When tested against the white background the interaction between long-term thermal exposure group and test temperature also affected how well the gobies matched their background

453 luminance (LRT: $\chi^2_{(1)} = 4.69, P = 0.030$) (Figure 4b). As predicted, we found a positive estimate
454 coefficient (estimate = 0.26 ± 0.17) for the interaction term. The warm-exposed gobies matched
455 their backgrounds more closely at 31 °C than at 16 °C (positive slope) and the cold-exposed
456 gobies matched their backgrounds more closely at 16 °C than at 31 °C (negative slope). All
457 total changes in luminance over time were lower than 3 ΔS (Supplementary Table 3), and
458 therefore, the gobies are likely to look the same to a predatory coral trout at the start and end
459 of testing. As the final achromatic contrasts (between the goby and its background) were all
460 over 3ΔS, the gobies were also always distinguishable against their white background. An
461 example of a goby not becoming indistinguishable to its white background over time is shown
462 in Figure 2.
463

464 **Discussion**

465 Intertidal gobies have the ability to change their luminance to match light or dark backgrounds
466 in their environment. For the first time, we provide an example of an animal acclimating rate
467 of luminance change for background matching with seasonal thermal conditions. This is an
468 example of physiology and thermal performance mediating predator avoidance behaviour in
469 an animal that resides in a variable thermal environment.
470

471 We found evidence of gobies acclimating both rate of luminance change and how well they
472 matched their background to seasonal thermal conditions (long-term thermal exposure groups).
473 Specifically, gobies that were exposed to warm thermal conditions had faster rates of
474 luminance change and matched their backgrounds more closely at 31 °C than at 16 °C against
475 black and white backgrounds (Figure 3 & 4). We found the same pattern, but in reverse, for
476 the cold-exposed fish (Figures 3 & 4). Overall, these findings support the hypothesis that *B.*

477 *cocosensis* have the capacity to acclimate rate of luminance change to seasonal temperatures,
478 which was predicted based on their ability to acclimate other ecologically important traits such
479 as burst swimming speed and maximum metabolic rate (da Silva, Riginos & Wilson 2019).
480
481 The capacity *B. cocosensis* have to acclimate rate of luminance change to seasonal
482 temperatures is likely to be an adaptive response to remain inconspicuous against different
483 backgrounds in heterogeneous rock-pools. Changes in seasonal thermal means in south-east
484 Queensland are predictable (da Silva, Riginos & Wilson 2019), and these predictable shifts in
485 seasonal temperature are likely to enable thermal acclimation of background matching to be
486 beneficial for survival in this context (DeWitt 1998; Gabriel 2005). Short-term thermal
487 fluctuations in rock-pool temperature, however, are likely to reduce background matching
488 capacities, as the gobies had reduced background matching ability in test temperatures they
489 were not acclimated to.
490
491 Interestingly, we found some potentially maladaptive pigment darkening responses when fish
492 were placed into test temperatures that they were not acclimated to (against the white
493 background) (Figure 3). The observed darkening responses (when an increase in luminance
494 rather than decrease would improve background matching) is likely to be a physiological stress
495 response. This may be explained by malfunctioning of chromatophore physiology at non-
496 optimal temperatures. Aggregation of chromatophores (associated with an increase in
497 luminance) through neuromuscular activity (rapid physiological colour change mechanism)
498 requires ATP (Sköld *et al.* 2016) and is hypothesized to be more energetically taxing than
499 dispersing them, as the contraction/aggregation of muscles requires more energy than
500 relaxing/dispersing them (Curtin & Woledge 1974; Barclay 1994). This suggests that
501 chromatophores may be unable to aggregate their pigments optimally in temperatures that they

502 have not thermally acclimated to, and as a result, lose control and disperse their pigments
503 resulting in a darker phenotype. A darkening response could potentially also be explained as a
504 stress response to being handled, however, the cold-exposed fish were able to increase their
505 luminance when placed against a white background at 16 °C despite being handled in the same
506 way as the warm-exposed fish that became darker when placed against a white background at
507 16 °C.
508
509 We also found that *B. cocosensis* turn darker at a faster rate on average than brighter. These
510 results are consistent with other studies on another goby species, *Gobius paganellus*, and a
511 species of bullfrog, *Rana catesbeina*, which also turned darker faster than lighter when placed
512 against different background colours (Camargo, Visconti & Castrucci 1999; Smithers *et al.*
513 2018). Rock-pool fish are likely to escape to rocky-crevices when threatened by predators
514 (White and Brown 2015), and rapid darkening could be an adaptive response enabling rock-
515 pool fish to become indistinguishable from rocky-hiding spots. Conversely, a study on
516 *Fundulus* (killifish), a temperate intertidal fish, had a higher capacity to turn lighter at a faster
517 rate than darker (Cole 1939). Perhaps killifish have evolved the capacity to turn light quickly
518 in white sandy areas, to be less conspicuous to predators and prey while basking in the sun and
519 hunting for small invertebrates. *Bathygobius cocosensis* have been observed to match sandy
520 and pebbly rock-pool habitats well during field surveys, however, *B. cocosensis* are rarely
521 exposed to very bright white backgrounds in their natural habitat. Sandy coloured habitats are
522 more common "light" habitats in the wild. *Bathygobius cocosensis* were sometimes observed
523 to take on a banded phenotype in this study, which might help them camouflage in sandy or
524 pebbly environments (Figure 5). The darkened band may also explain the average slight
525 darkening response that some of the warm-exposed gobies show when placed against white
526 backgrounds in 31°C. A light sand coloured or mottled patterned background could be used

527 instead of a white background to better simulate a natural "light" luminance change response
528 in *B. cocosensis* in future experiments as they better match visual backgrounds in the wild.
529 This is similarly discussed by Smithers, Wilson and Stevens (2017) where they show that
530 *Gobius paganellus* could change colour and pattern with visual background but had difficulty
531 matching the full luminance of their artificial background.
532
533 Long-term exposure to seasonal conditions was also found to affect baseline goby luminance.
534 Cold-exposed fish were found to have higher luminance values at the end of the grey
535 standardization period and start of testing when placed on both white and black backgrounds.
536 The increased average luminance found in the cold-exposed gobies may be driven by increased
537 concentration of melatonin. The effect melatonin has on melanophore aggregation or
538 dispersion has previously been shown to be seasonally dependent in a tropical reef fish *Rasbora*
539 *daniconius* (Ovais *et al.* 2015). During summer months, increased concentrations of melatonin
540 have an inverse aggregation response, whereas higher concentrations of melatonin correlates
541 with lower melanophore aggregation and phenotype darkening. During winter months,
542 however, increases in melatonin concentrations are positively correlated with melanophore
543 aggregation, and therefore, phenotype brightening (Ovais *et al.* 2015). The average higher
544 luminance values observed in the cold-exposed fish may be explained by melatonin induced
545 melanophore aggregation in cold temperatures, simulating winter. The effect melatonin has on
546 the aggregation or dispersal of melanosomes however, is highly species dependent (Nishi &
547 Fujii 1992; Ovais *et al.* 2015).
548
549 Climate change has indirect effects on species interactions such as increased predator attack
550 rates, increased parasite loads, competition and symbioses (Gunderson, Tsukimura & Stillman
551 2017). The capacity *B. cocosensis* has to acclimate rate of luminance change (for background

552 matching) to seasonal thermal conditions may act as a buffer to increased predator attack rates
553 as they may be able to remain cryptic and therefore maintain predator-prey interaction rates
554 with global warming. If predator species can also acclimate rate of luminance change for
555 background matching, predator attack rates may continue to increase with further climate
556 change. It is difficult to predict how climate change will continue to affect the frequency of
557 predator-prey interactions; however, this study provides a stepping-stone to understanding a
558 mechanistic basis for how climate change may alter behaviourally mediated species
559 interactions.
560
561 This is the first study to show that long-term exposure to different thermal conditions can affect
562 rate of background matching, and that it is possible for animals to acclimate rate of luminance
563 change and background matching capacity to seasonal conditions. Rate of luminance change
564 for camouflage is an important ecological trait that affects survival and fitness (Troscianko *et*
565 *al.* 2016), and it should be taken into account when modelling species responses to climate
566 change, along with other important traits such as metabolism and locomotion. In conclusion,
567 we propose that gaining a more comprehensive understanding on how temperature change
568 affects behavioural traits is likely to shine light on how climate change will influence predator-
569 prey dynamics. Lastly, further research on the potential for behavioural trait plasticity to evolve
570 with changing climates will improve our current predictions on how species and populations
571 will respond to further climate warming.
572
573 **Acknowledgements**
574 We thank Natalie Freeman, Andrew Hunter and Julian Beaman for their help. Thank you to
575 the Journal of Animal Ecology associate editor and reviewers for providing helpful feedback.

Animal ethics was approved by The University of Queensland Animal Ethics Unit (QS2015/MAN340).

Authors' contributions

da Silva, van den Berg, Riginos, Wilson and Cheney conceptualised the study. da Silva conducted the experiments with assistance from van den Berg. Condon wrote the ImageJ code. da Silva, van den Berg, Wilson, Riginos and Cheney contributed to the writing of the manuscript. All authors gave final approval.

Data Accessibility Statement

Data will be made available on Dryad.

References

Angilletta, M.J. (2009) Thermal adaptation: a theoretical and empirical synthesis. *Thermal Adaptation: A Theoretical and Empirical Synthesis*, 1-290.

Auerswald, L., Freier, U., Lopata, A. & Meyer, B. (2008) Physiological and morphological colour change in Antarctic krill, *Euphausia superba*: a field study in the Lazarev Sea. *Journal of Experimental Biology,* **211,** 3850-3858.

Barclay, C. (1994) Efficiency of fast-and slow-twitch muscles of the mouse performing cyclic contractions. *Journal of Experimental Biology,* **193,** 65-78.

Beaman, J.E., White, C.R. & Seebacher, F. (2016) Evolution of plasticity: mechanistic link between development and reversible acclimation. *Trends in Ecology & Evolution,* **31,** 237-249.

Camargo, C.R., Visconti, M. & Castrucci, A. (1999) Physiological color change in the bullfrog, *Rana catesbeiana*. *Journal of Experimental Zoology,* **283,** 160-169.

Caro, T., Sherratt, T.N. & Stevens, M. (2016) The ecology of multiple colour defences. *Evolutionary ecology,* **30,** 797-809.

Cheney, K.L., Cortesi, F. & Nilsson Sköld, H. (2017) Regulation, constraints and benefits of colour plasticity in a mimicry system. *Biological Journal of the Linnean Society,* **122,** 385-393.

Cole, W.H. (1939) The effect of temperature on the color change of *Fundulus* in response to black and to white backgrounds in fresh and in sea water. *Journal of Experimental Zoology,* **80,** 167-172.

Cortesi, F., Musilová, Z., Stieb, S.M., Hart, N.S., Siebeck, U.E., Cheney, K.L., Salzburger, W. & Marshall, N.J. (2016) From crypsis to mimicry: changes in colour and the configuration of the visual system during ontogenetic habitat transitions in a coral reef fish. *Journal of Experimental Biology,* **219,** 2545-2558.

613 Cronin, T.W., Johnsen, S., Marshall, N.J. & Warrant, E.J. (2014) *Visual ecology*. Princeton
614 University Press.
615 Curtin, N.A. & Woledge, R.C. (1974) Energetics of relaxation in frog muscle. *The Journal of*
616 *physiology,* **238,** 437-446.
617 da Silva, C.R.B., Riginos, C. & Wilson, R.S. (2019) An intertidal fish shows thermal
618 acclimation despite living in a rapidly fluctuating environment. *Journal of*
619 *Comparative Physiology B*, 1-14.
620 Deutsch, C.A., Tewksbury, J.J., Huey, R.B., Sheldon, K.S., Ghalambor, C.K., Haak, D.C. &
621 Martin, P.R. (2008) Impacts of climate warming on terrestrial ectotherms across
622 latitude. *Proceedings of the National Academy of Sciences,* **105,** 6668-6672.
623 Duarte, R.C., Flores, A.A. & Stevens, M. (2017) Camouflage through colour change:
624 mechanisms, adaptive value and ecological significance. *Philosophical Transactions*
625 *of the Royal Society B: Biological Sciences,* **372,** 20160342.
626 DeWitt, T.J. (1998) Costs and limits of phenotypic plasiticty: tests with predator-induced
627 morphology and life history in a freshwater snail. *Journal of Experimental Biology.*
628 **11,** 465-480.
629 Faraway, J. (2016) *Extending the linear model with R: generalized linear, mixed effects and*
630 *nonparametric regression models*. Chapman and Hall/CRC.
631 FitzGerald, J.L., Sheehan, T.F. & Kocik, J.F. (2004) Visibility of visual implant elastomer
632 tags in Atlantic salmon reared for two years in marine net-pens. *North American*
633 *Journal of Fisheries Management,* **24,** 222-227.
634 Gabriel, W. (2005) How stress selects for reversible phenotypic plasticity. *Journal of*
635 *Evolutionary Biology*. **18,** 873-883.
636 Gunderson, A.R., Tsukimura, B., Stillman, J.H. (2017) Indirect effects of global change:
637 from physiological and behavioural mechanisms to ecological consequences.
638 Integrative and Comparative Biology, 57, 48-54
639 Hammill, E., Wilson, R.S. & Johnston, I.A. (2004) Sustained swimming performance and
640 muscle structure are altered by thermal acclimation in male mosquitofish. *Journal of*
641 *thermal Biology,* **29,** 251-257.
642 Helmuth, B.S. & Hofmann, G.E. (2001) Microhabitats, thermal heterogeneity, and patterns of
643 physiological stress in the rocky intertidal zone. *The Biological Bulletin,* **201,** 374-
644 384.
645 Hoffmann, A.A. & Sgro, C.M. (2011) Climate change and evolutionary adaptation. *Nature,*
646 **470,** 479.
647 King, R.B., Hauff, S. & Phillips, J.B. (1994) Physiological color change in the green treefrog:
648 responses to background brightness and temperature. *Copeia*, 422-432.
649 Lin, Q., Lin, J. & Huang, L. (2009) Effects of substrate color, light intensity and temperature
650 on survival and skin color change of juvenile seahorses, *Hippocampus erectus* Perry,
651 1810. *Aquaculture,* **298,** 157-161.
652 Losey, G., McFarland, W., Loew, E., Zamzow, J., Nelson, P. & Marshall, N. (2003) Visual
653 biology of Hawaiian coral reef fishes. I. Ocular transmission and visual pigments.
654 *Copeia,* **2003,** 433-454.
655 Lythgoe, J. N. (1979). *The ecology of vision*. Oxford: Clarendon Press.
656 Malard, L.A., McGuigan, K. & Riginos, C. (2016) Site fidelity, size, and morphology may differ by
657 tidal position for an intertidal fish, *Bathygobius cocosensis* (Perciformes-Gobiidae), in
658 Eastern Australia. *PeerJ,* **4,** e2263.
659 Nishi, H. & Fujii, R. (1992) Novel receptors for melatonin that mediate pigment dispersion
660 are present in some melanophores of the pencil fish (*Nannostomus*). *Comparative*
661 *Biochemistry and Physiology Part C: Comparative Pharmacology,* **103,** 263-268.

662 Ovais, M., Srivastava, S.K., Sumoona, S. & Mubashshir, M. (2015) Evidence for the
663 presence of novel β-melatonin receptors along with classical α-melatonin receptors in
664 the fish *Rasbora daniconius* (Ham.). *Journal of Receptors and Signal Transduction,*
665 **35,** 238-248.
666 Pinheiro, J., Bates, D., DebRoy, S., Sarkar, D. & Team, R.C. (2018) nlme: linear and
667 nonlinear mixed effects models. R package version 3.1-137. *R Found. Stat. Comput.*
668 *https://CRAN. R-project.*
669 R Core Team (2018) R Foundation for Statistical Computing; Vienna, Austria: 2014. *R: A*
670 *language and environment for statistical computing*, 2013.
671 Ruxton, G.D., Allen, W.L., Sherratt, T.N. & Speed, M.P. (2018) *Avoiding attack: the*
672 *evolutionary ecology of crypsis, aposematism, and mimicry*. Oxford University Press.
673 Schulte, P.M., Healy, T.M. & Fangue, N.A. (2011) Thermal performance curves, phenotypic
674 plasticity, and the time scales of temperature exposure. *Integrative and comparative*
675 *biology,* **51,** 691-702.
676 Seebacher, F., Davison, W., Lowe, C.J. & Franklin, C.E. (2005) A falsification of the thermal
677 specialization paradigm: compensation for elevated temperatures in Antarctic fishes.
678 *Biology letters,* **1,** 151-154.
679 Seebacher, F., White, C.R. & Franklin, C.E. (2015) Physiological plasticity increases
680 resilience of ectothermic animals to climate change. *Nature Climate Change,* **5,** 61.
681 Siddiqi, A., Cronin, T.W., Loew, E.R., Vorobyev, M. & Summers, K. (2004) Interspecific
682 and intraspecific views of color signals in the strawberry poison frog *Dendrobates*
683 *pumilio*. *Journal of Experimental Biology,* **207,** 2471-2485.
684 Sköld, H.N., Aspengren, S., Cheney, K.L. & Wallin, M. (2016) Fish chromatophores—from
685 molecular motors to animal behavior. *International Review of Cell and Molecular*
686 *Biology*, pp. 171-219. Elsevier.
687 Sköld, H.N., Aspengren, S. & Wallin, M. (2013) Rapid color change in fish and amphibians–
688 function, regulation, and emerging applications. *Pigment cell & melanoma research,*
689 **26,** 29-38.
690 Smithers, S.P., Rooney, R., Wilson, A. & Stevens, M. (2018) Rock pool fish use a
691 combination of colour change and substrate choice to improve camouflage. *Animal*
692 *behaviour,* **144,** 53-65.
693 Smithers, S.P., Wilson, A. & Stevens, M. (2017) Rock pool gobies change their body pattern
694 in response to background features. *Biological Journal of the Linnean Society,* **121,**
695 109-121.
696 Somero, G.N. (2002) Thermal physiology and vertical zonation of intertidal animals: optima,
697 limits, and costs of living. *Integrative and comparative biology,* **42,** 780-789.
698 Stevens, M. (2016) Color change, phenotypic plasticity, and camouflage. *Frontiers in*
699 *Ecology and Evolution,* **4,** 51.
700 Stevens, M., Broderick, A.C., Godley, B.J., Lown, A.E., Troscianko, J., Weber, N. & Weber,
701 S.B. (2015) Phenotype–environment matching in sand fleas. *Biology letters,* **11,**
702 20150494.
703 Stevens, M., Merilaita, S. (2009) Animal camouflage: current issues and new perspectives.
704 *Philos Trans R Soc Lond B Biol Sci*, **364**: 423-427.
705 Stevens, M., Lown, A.E. & Denton, A.M. (2014) Rockpool gobies change colour for
706 camouflage. *PLoS One,* **9,** e110325.
707 Stevens, M., Troscianko, J., Wilson-Aggarwal J.K., Spottiswoode, C.N. (2017)
708 Improvement of individual camouflage through background choice in ground-
709 nesting birds. *Nature Ecology and Evolution*, **1,** 1325-1333.

710 Stuart-Fox, D.M., Moussalli, A., Marshall, N.J. & Owens, I.P. (2003) Conspicuous males
711 suffer higher predation risk: visual modelling and experimental evidence from lizards.
712 *Animal behaviour,* **66,** 541-550.
713 Tewksbury, J.J., Huey, R.B. & Deutsch, C.A. (2008) Putting the heat on tropical animals.
714 *Science,* **320,** 1296-1297.
715 Troscianko, J. & Stevens, M. (2015) Image calibration and analysis toolbox–a free software
716 suite for objectively measuring reflectance, colour and pattern. *Methods in Ecology*
717 *and Evolution,* **6,** 1320-1331.
718 Troscianko, J., Wilson-Aggarwal, J., Stevens, M., Spottiswoode, C.E. (2016) Camouflate
719 predicts survival in ground-nesting birds. *Scientific Reports*, **6**, 19966.
720 Vorobyev, M. & Osorio, D. (1998) Receptor noise as a determinant of colour thresholds.
721 *Proceedings of the Royal Society of London. Series B: Biological Sciences,* **265,** 351-
722 358.
723 Wickham, H. (2016) ggplot2: Elelant graphics for data analysis. Springer-Verlag New York.
724 ISBN: 978-3-319-24277-4.
725 Wilson, R.S., Condon, C.H. & Johnston, I.A. (2007) Consequences of thermal acclimation
726 for the mating behaviour and swimming performance of female mosquito fish.
727 *Philosophical Transactions of the Royal Society B: Biological Sciences,* **362,** 2131-
728 2139.
729 Wilson, R.S. & Franklin, C.E. (2002) Testing the beneficial acclimation hypothesis. *Trends*
730 *in Ecology & Evolution,* **17,** 66-70.

731 White, G.E. & Brown, C. (2015) Microhabitat use affects goby (Gobiidae) cue choice in
732 spatial learning task. *Journal of Fish Biology*, **86**, 1305 - 1318

733 Zeileis, A., Hothorn, T. (2002) Diagnostic checking in regression relationships. R News, 2, 1-
734 10

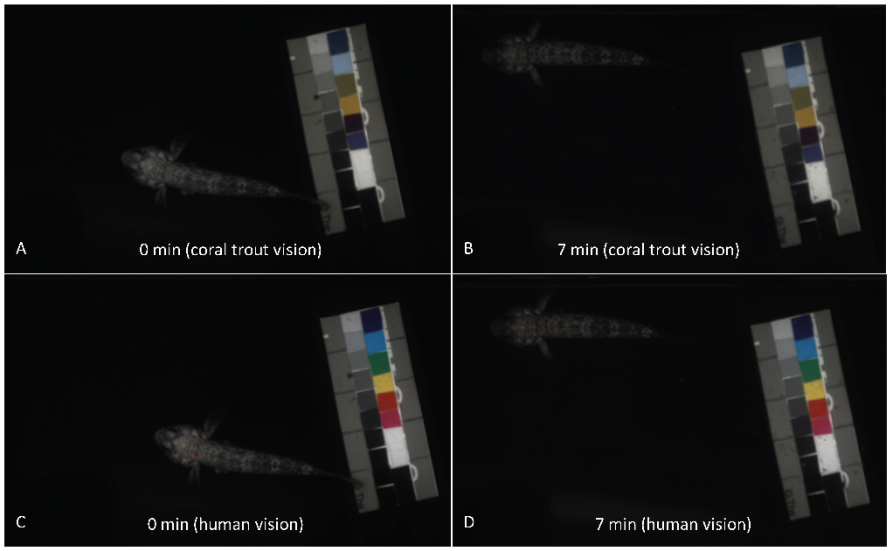

Figure 1. Modelled images (reconstructed RGB images) of a warm exposed goby tested at 31 °C against a black background. A: As seen through the eye of a coral trout at the start of testing (time = 0 seconds). B: Through the eye of a coral trout after 7 minutes. C: Through the eye of a human at the start of testing (time = 0 seconds). D: Through the eye of a human after 7 minutes of testing.

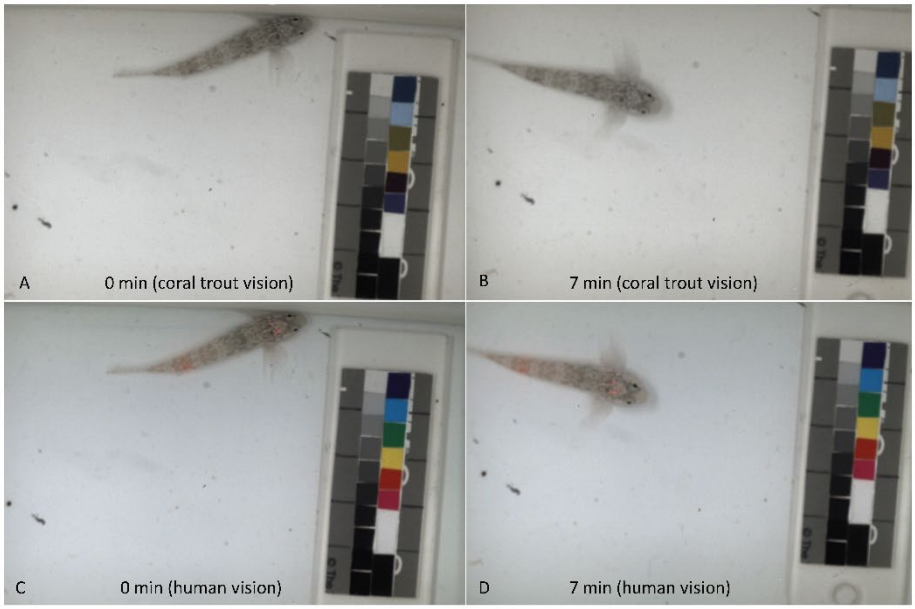

Figure 2. Modelled images (reconstructed RGB images) of a cold exposed goby tested at 16 °C against a white background. A: As seen through the eye of a coral trout at the start of testing (time = 0 seconds). B: Through the eye of a coral trout after 7 minutes. C: Through the eye of a human at the start of testing (time = 0 seconds). D: Through the eye of a human after 7 minutes of testing. The dorsal pink elastomer identification tags can be observed in the human vision photographs.

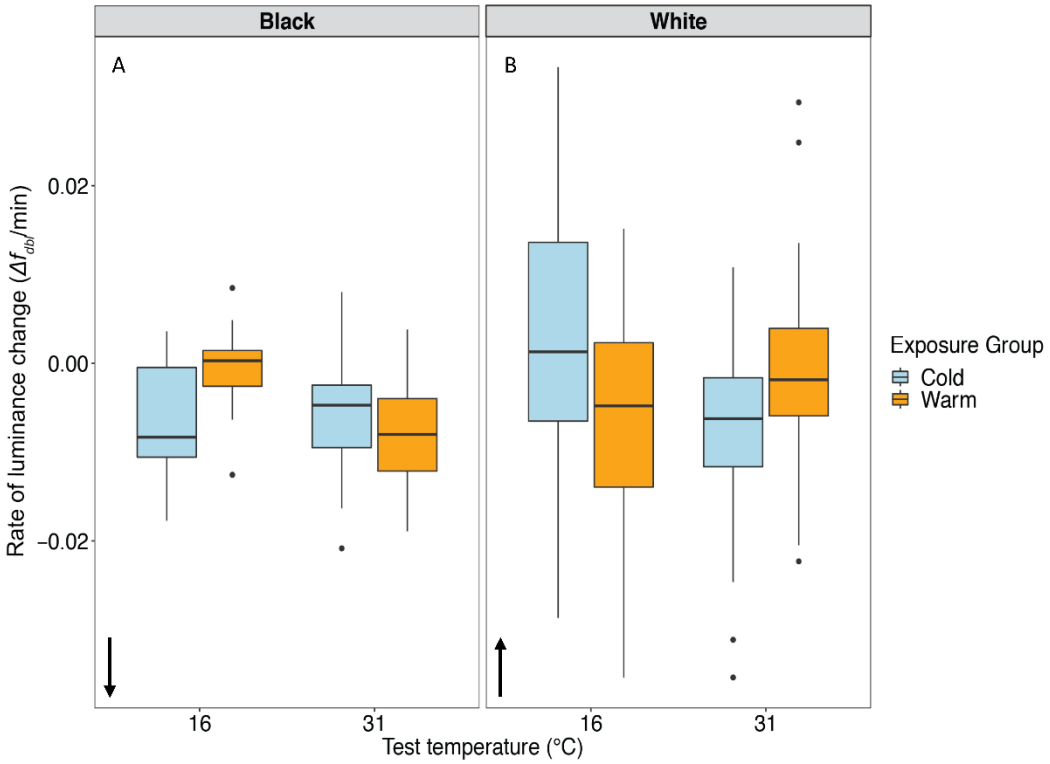

Figure 3. Rate of luminance change (over the first four minutes of testing) for warm and cold exposed fish at acute test temperatures against a black (left panel) and white (right panel) background. Negative rates of luminance change indicate a darkening in fish luminance and positive values indicate a brightening in fish luminance. Arrows indicate the correct direction of luminance change for background matching.

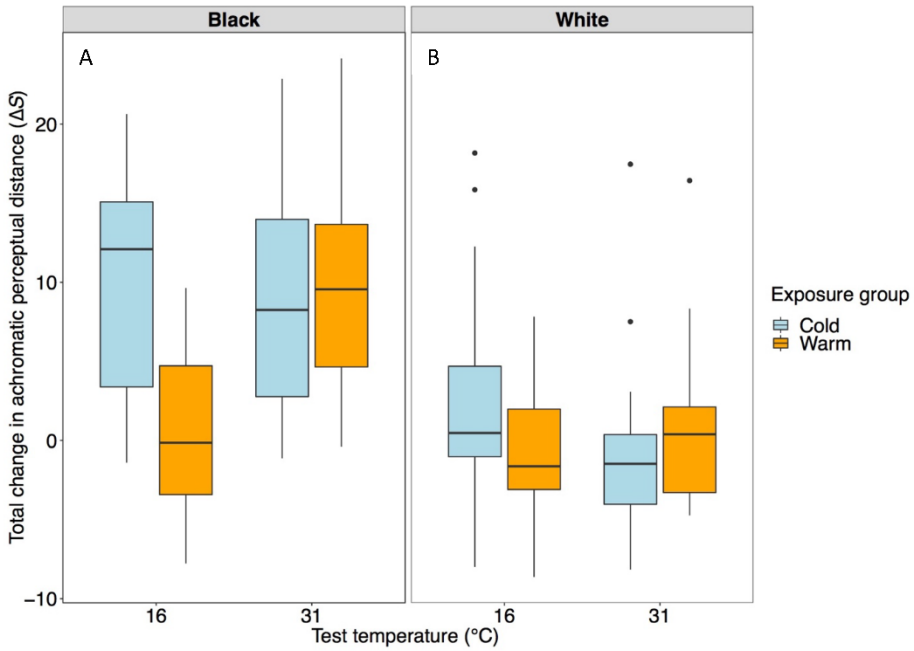

Figure 4. Total change in achromatic perceptual distance between the dorsal body of the goby and its background from the start to end of testing at each test temperature. Greater changes in achromatic perceptual distance indicate that the goby becomes more similar to its background luminance during the testing period. Negative changes in achromatic perceptual distance indicates that the goby has become more distinguishable from its background luminance.

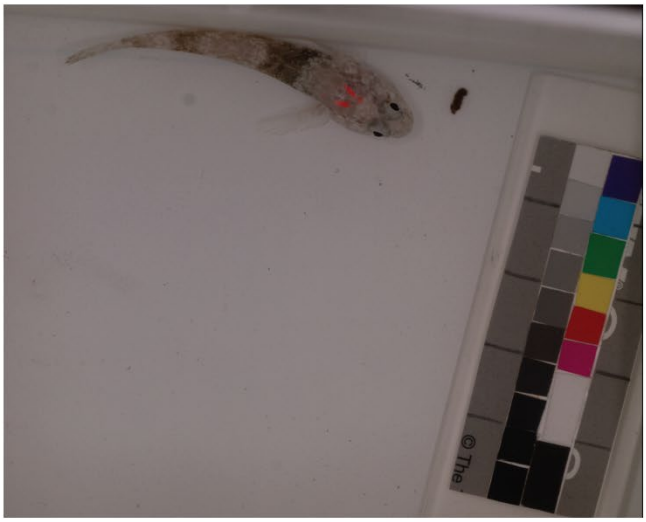

Figure 5. Example of a goby taking on a banded pattern. This image was taken of a warm exposed goby at 31°C.

Table 1. Linear mixed effect model summary of the effect of mass and the interaction between long-term temperature exposure and test temperature on the rate of luminance change in *Bathygobius cocosensis* against a black and white background.

Black background			
Coefficient	**Estimate ± SE**	***df***	***t*-value**
Intercept	-0.009 ± 0.003	47	-2.9
Mass	0.001 ± 0.001	29	0.95
Long-term thermal exposure (warm) * test temperature	-0.0006 ± 0.001	29	-3.75
White background			
Coefficient	**Estimate ± SE**	***df***	***t*-value**
Intercept	0.017 ± 0.006	48	2.45
Mass	-0.0012 ± 0.002	30	-0.45
Long-term thermal exposure (warm) * test temperature	0.0018 ± 0.0003	30	3.20

Table 2. Linear mixed effect model summary of the effect of mass and the interaction between long-term thermal exposure and test temperature on total change in achromatic perceptual distance (ΔS) when *Bathygobius cocosensis* is placed against a black background and white background.

Black background			
Coefficients	**Estimate ± SE**	***df***	***t-value***
Intercept	11.0 ± 3.6	41	3.04
Mass	-1.4 ± 1.4	28	-0.97
Long-term thermal exposure (warm) * test temperature	0.55 ± 0.19	28	2.80
White Background			
Coefficients	**Estimate ± SE**	***df***	***t-value***
Intercept	4.7 ± 3.31	42	1.48
Mass	1.33 ± 1.16	31	1.14
Long-term thermal exposure (warm) * test temperature	0.26 ± 0.17	31	1.5

Supplementary material

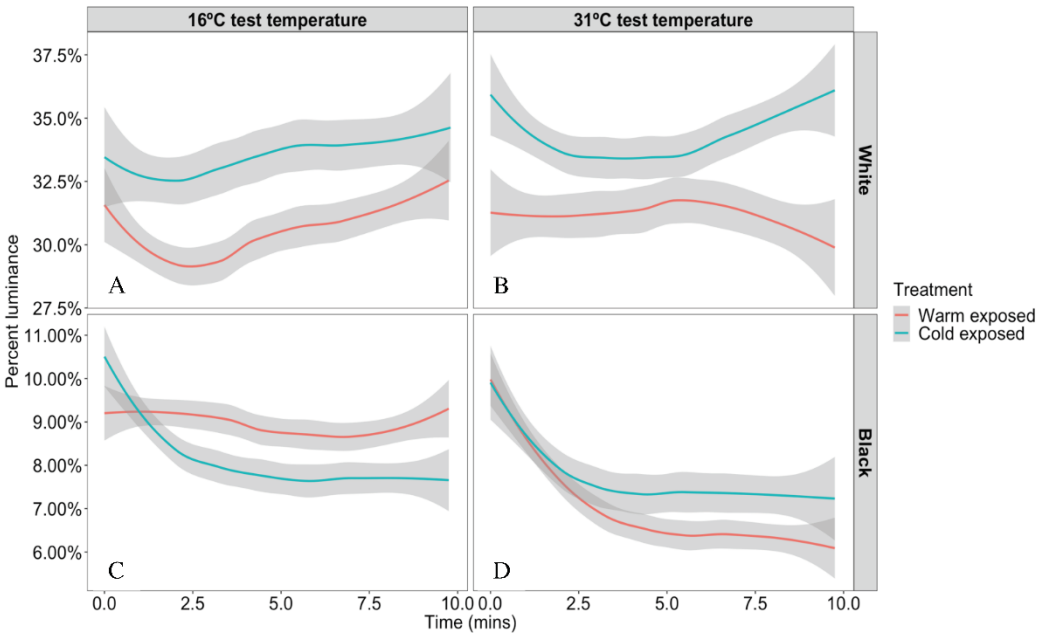

Supplementary Figure 1. Mean change in luminance (f_{dbl}) (with standard error in grey) over 10 minutes for the long-term warm (31°C) and cold exposed fish (16°C). A) against a white background at 16°C; B) against a white background at 31°C; C) against a black background at 16°C; D) against a black background at 31°C. Increases in luminance indicate a lightening response and decreases in luminance indicates a darkening response.

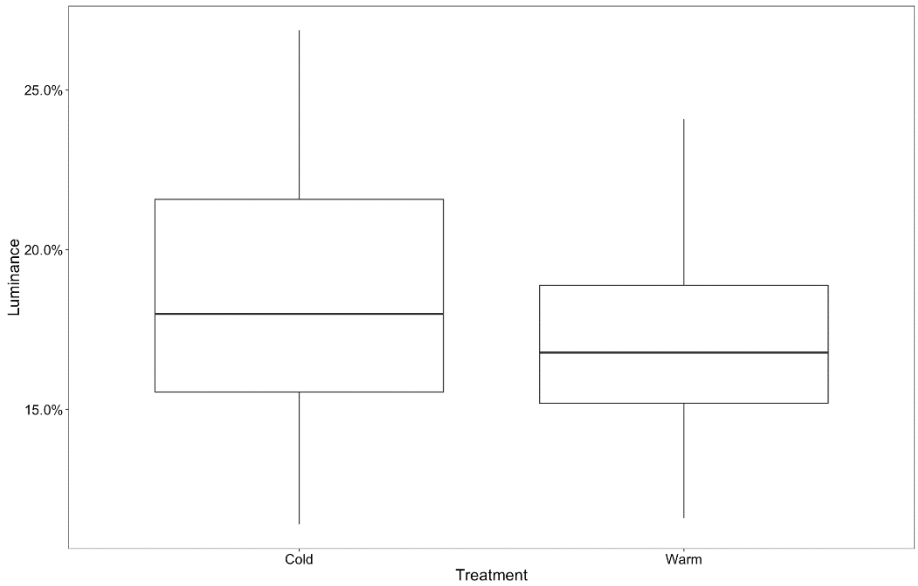

Supplementary Figure 2. Warm and cold exposed fish luminance (f_{dbl}) after exposure to a grey background for 10 minutes.

Supplementary table 1. Mean rates of *Bathygobius cocosensis* luminance change (Δf_{dbl}/min) for each exposure group in each test treatment during the first four minutes of testing. *indicates correct colour change direction for background matching.

Test temperature	Colour	Warm exposed average rate of luminance change (Δf_{dbl}/min) ± SE	Cold exposed average rate of luminance change (Δf_{dbl} /min) ± SE
16°C	Black	-0.0004* ± 0.001	-0.0068* ± 0.002
31°C	Black	-0.0084* ± 0.001	-0.0056* ± 0.002
16°C	White	-0.0066 ± 0.003	0.0035* ± 0.003
31°C	White	-0.0033 ± 0.002	-0.0081 ± 0.003

Supplementary table 2: Mean achromatic perceptual difference (ΔS, difference between goby luminance and background luminance) at the start, end, and total change in achromatic perceptual distance over test time against a black background (top panel) and white background (bottom panel) over testing through the eye of a coral trout. ΔS above 3 indicate that a noticeable change in goby appearance would have occurred to the coral trout (indicated by *).

Black background			
Treatment	**Start μ ΔS ± SE**	**End μ ΔS ± SE**	**Total ΔS**
Warm exposed 31°C test temperature	31.7 ± 1.26	22.05 ± 1.32	**9.65***
Cold exposed 31°C test temperature	32.79 ± 1.87	24.01 ± 1.63	**8.78***
Warm exposed 16°C test temperature	31.03 ± 1.31	30.29 ± 1.41	**0.74**
Cold exposed 16°C test temperature	35.78 ± 1.12	25.57 ± 1.59	**10.21***
White background			
Treatment	**Start μ ΔS ± SE**	**End μ ΔS ± SE**	**Total ΔS**
Warm exposed 31°C test temperature	17.34 ± 1.09	16.89 ± 0.91	**0.45**
Cold exposed 31°C test temperature	14.04 ± 1.00	15.08 ± 1.03	**-1.04**
Warm exposed 16°C test temperature	16.44 ± 1.10	17.93 ± 1.03	**-1.49**
Cold exposed 16°C test temperature	16.99 ± 1.40	14.42 ± 0.67	**2.57**

Pattern edges improve predator learning of aposematic signals

Naomi F. Green[1], Holly H. Urquhart[1], Cedric P. van den Berg[1], N. Justin Marshall[2], Karen L. Cheney[1,2]

Author affiliations

[1]School of Biological Sciences, The University of Queensland, Brisbane, Queensland, 4072, Australia

[2]Queensland Brain Institute, The University of Queensland, Brisbane, Queensland, 4072, Australia

Communicating author: naomi.green@uq.net.au

Running title: *Pattern edges improve predator learning*

Lay Summary

Many animals use body patterns, such as stripes and spots, to prevent them from being detected by predators or prey, or to highlight that they are toxic and should be avoided. Using behavioral experiments with fish, our study finds that color patterns that contain a larger amount of pattern edge enables predators to learn to avoid warning signals more quickly.

Abstract

Edges are salient visual cues created by abrupt changes in luminance and color, and are crucial in perceptual tasks such as motion detection and object recognition. Disruptively colored animals exploit edge detection mechanisms to obscure their body

outline and/or to conceal themselves against their background. Conversely, aposematic species may use contrasting patterns with well-defined edges to create highly salient, memorable warning signals. In this study, we investigated how the amount of internal pattern edge, colored area, pattern type or shape repetition of warning signals influenced avoidance learning in the triggerfish, *Rhinecanthus aculeatus.* Using six different warning signals, we found that fish learnt to avoid aposematic signals faster when they featured more internal pattern edge. We found little evidence that the amount of colored area or pattern type affected learning rates. An optimal amount of pattern edge within a warning signal may therefore improve how warning signals are learnt. These findings offer important insights into the evolution of prey warning signal evolution and predator psychology.

Keywords: color patterns, learning, body outlining, warning signals, aposematism, coral reef fish.

INTRODUCTION

When viewing a scene, edges are perceived as abrupt changes in luminance and color, and provide key information about object boundaries and the structure of the environment. In conjunction with additional cues such as color, symmetry and shape, edges underpin crucial perceptual tasks such as navigation (Lau et al. 2006; Harris et al. 2007), object recognition (Webster et al. 2013), figure-ground organization (Driver and Bayliss 1996) and depth perception (Palmer and Ghose 2008). Indeed, vertebrate visual systems are optimally configured for edge detection via retinal lateral inhibition, in which stimulated neurons inhibit the excitation of neighboring photoreceptors,

increasing the contrast and sharpness of the visual response (Enroth-Cugell and Pinto 1972).

Many animals, such as the leopard (*Panthera pardus*) (Allen et al. 2011), the peach blossom moth (*Thyatira batis*) (Schaefer and Stobbe 2006), and the spotted grass frog (*Limnodynastes tasmaniensis*) (Osorio and Srinivasan 1991) display highly contrasting body patterns to inhibit detection of their body outline by predators or prey against complex visual scenery (Thayer 1909; Cott 1940; Cuthill et al. 2005; Endler 2006; Stevens et al. 2006). Disruptively colored animals may also exhibit non-marginal, contrasting patterns that disguise telltale body parts such as eyes or limbs (Thayer 1909; Cott 1940; Cuthill and Székely 2009). Illusory contours may also be used to segment the body surface and prevent them being recognised as a singular, cohesive figure (Stevens et al. 2009).

Conversely, contrasting patterns with well-defined edges may be used as warning signals by aposematic prey (Poulton 1890). Chromatically or achromatically contrasting edges within a pattern may increase the detectability of prey against the background (Troscianko et al 2017), improve recognition of aposematic prey (Guilford 1986) and enhance predator learning (Osorio et al 1999). Pattern edges may be provided by spots, stripes or circles within the warning signal, or run parralel to the prey contour to enhance the body outline (Cott 1940; Hailman 1977). It is also proposed that many animals display eye-catching borders to accentuate their body profile and emphasize their characteristic shape (Cott 1940; Hailman 1977). Outlining is expected to be particularly important in flat animals such as butterflies (e.g. *Papilio ulysses*), and marine invertebrates such as flatworms (e.g. *Pseudobiceros gloriosus*), and nudibranch mollusks (e.g. *Chromodoris elisabethina)*. Such animals lack the conspicuousness of a

bulky form, and have a single prominent contour that appears similar from most vantage points (Hailman 1977).

Previous research investigating the role of pattern in warning signals has produced conflicting results. Black internal patterns have been shown to reduce avian attacks toward both spotted ladybirds (Dolenská et al. 2009), and striped, caterpillar-like models (Barnett et al. 2016), compared with unpatterned prey. Similarly, avoidance of striped prey against complex backgrounds was learned faster by blue tits compared to unstriped stimuli, and irregularly striped and regularly striped prey, with a similar amount of edge were learnt at an equal rate (Aronsson and Gamberale-Stille, 2013). This may indicate that the amount of pattern edge may influence predator learning, rather than pattern type, regularity or symmetry. In other studies, internal patterns were not shown to reduce predation on painted mealworms (Aronsson and Gamberale-Stille 2009) or model frogs (Hegna et al. 2012); however, in these studies the signals were either small, inconspicuous spots without sharp, defined edges (Hegna et al. 2012), or were simple patterns, featuring short, horizontal stripes which provided limited pattern edges (Aronsson and Gamberale-Stille 2009).

The majority of previous studies investigating the role of patterns in warning signals have focused on how patterns are detectable from the background, and how this influences predator learning. Fewer empirical studies have investigated how the pattern design may impact predator learning without considering detectability (Guilford and Dawkins 1991; but see Wüster et al. 2004). Therefore, in this study, we investigated how the design of patterns improves the rate at which predators learn to avoid aposematic signals. We investigated whether pattern design influenced predator learning by conducting behavioral experiments in aquaria with triggerfish, *Rhinecanthus aculeatus*. We examined the learning speed when six groups of fish were

presented with different aposematic stimuli that varied in the amount of internal pattern edge, colored area, pattern type (spots, stripes, concentric circles or outlines) and shape repetition. Our results provide insights to the role of contrasting patterns in warning signals.

2. METHODS

a) Study species

We used the triggerfish *R. aculeatus* as our study species as they co-occur with a variety of aposematic species throughout their range, such as nudibranchs and cephalopods (e.g. Hapalochlaena sp.), but we are unaware of any aposematic species at our study site that display similar color patterns to the ones used in our experiment. This species is a benthic generalist feeder known to feed on mollusks, algae, worms, crustaceans and other fish (Randall 1981) and therefore conducts daily visually mediated foraging behavour. In addition, they are easy to keep in aquaria, and are highly trainable, as per (Pignatelli et al. 2010; Cheney et al 2013). Their trichromatic visual system has been investigated in detail: they have single and double cones, arranged in a regular mosaic (Champ et al. 2014). The single cones house the short-wavelength pigment (λ_{max} = 420 nm) and the two members of the double cone house the medium and long-wavelength pigments (λ_{max} = 480 nm and 528 nm) (Pignatelli et al. 2010; Cheney et al 2013). This species has relatively low visual acuity, at approximately 1.75 cycles per degree, according to behavioral data (Champ et al. 2014); however, they can readily discriminate patterns similar in size to those in the current study (Champ et al. 2014; Newport et al. 2017).

In total, we used 58 wild caught individuals, which ranged in size from 4 to 15

cm standard length (SL). Fish were collected on snorkel using hand-nets from shallow (depth 1-3 m), sandy and rocky areas off Lizard Island, Great Barrier Reef, Australia (14º40'S, 145º 28'E). Fish were kept in individual tanks that ranged from 50 to 100 L (W: 30-50 cm; L: 40-100 cm; H: 30-40 cm) depending on their body size, and allowed to acclimatize for at least one week before the experiment commenced.

Experiments were conducted at Lizard Island Research Station during February-March 2017 and all fish were returned to their collection sites after testing. Tanks were illuminated by natural sunlight and experiments were conducted between 6am and 6pm. Fish were collected under a Queensland General Fisheries Permit (#161624) and a Great Barrier Reef Marine Parks Authority Permit (#G12/35688). This research was conducted in accordance with approval granted by the University of Queensland's Animal Ethics Committee (SBS/111/14/ARC).

b) Behavioral experiments

To examine the rate at which fish learnt avoidance of different color patterns, we used a paired choice test, in which fish were trained to peck on visual stimuli in order to receive a food reward. During testing, fish were presented simultaneously with a pair of circular (diameter 2.5 cm), laminated stimuli, consisting of one white, non-aposematic stimulus (S+) and one colored, aposematic stimulus (S-) ie. differential appetitive-aversive conditioning experiment. The non-aposematic stimulus remained the same for all fish to ensure that this stimulus did not influence learning. The aposematic stimuli varied in the amount of internal pattern edge, colored area, pattern type or shape repetition (Table 1). Aposematic stimuli were not designed to resemble the warning signal of a particular species, but instead to test learning of common patterns and colors seen in many warning signals. We also used yellow because this

color allows us to relate our finding to previous research on this topic (Winters et al. 2017).

Stimuli were printed using a HP Officejet H470 inkjet printer on Epson photo quality paper and laminated. They were then attached to a white, vertical feeding board (20 x 30cm) with hook and loop Velcro stickers, and positioned 10 cm apart and 15 cm from the bottom of the board. To prevent fish from seeing the stimuli before the experiment began, an opaque partition was placed across the center of the tank while the feeding board was positioned at the far end. Once the partition was removed, fish were allowed to swim into the testing arena and peck one of the stimuli.

If fish pecked the white, non-aposematic stimulus (S+), they were rewarded with a small piece (0.5cm x 0.5cm) of palatable food, but if they pecked the colored, aposematic stimulus (S-), they received a small piece of unpalatable food. Palatable food was prepared by combining 6 g frozen squid mantle, 3 g gelatin and 10 ml of water; while unpalatable food consisted of 6 g sodium alginate and 10 ml water. Food was presented using forceps from above to ensure that fish did not use olfactory cues during experiments. Both food types had a semi-solid consistency and were similar in color and texture. Unpalatable food was immediately spat out by the fish (> 95% of trials), while palatable food was readily consumed (> 95% of trials).

Four trials were conducted with each fish per session, and fish completed one or two sessions per day. Fish completed between 7 and 30 sessions in total (28-120 trials). To ensure that fish demonstrated learnt avoidance of the aposematic stimulus and sustained this for several days, we required them to select the non-aposematic stimulus in >80% of the trials over 3 days (7 sessions). Therefore, fish were required to select the non-aposematic stimulus on 23 out of 28 trials (82% correct). During testing,

the position of the colored, aposematic stimuli (left or right) was pseudo-randomized so that it did not remain the same for more than 2 successive trials.

Prior to testing, fish were trained to peck at the feeding board by placing small amounts of chopped squid directly below two very small, black crosses (0.5 cm x 0.5 cm, 15 cm apart) displayed on the feeding board. Crosses were required to provide a target for the fish while learning to peck the feeding board for food; however, the crosses differed significantly in size, color and pattern from all experimental stimuli, to prevent this impacting learning during the experiment. Once fish learnt to peck at the crosses, squid was removed from the feeding board, and instead, fish were fed immediately after they had pecked either cross, with squid held with forceps from above. Fish took between 1 to 3 weeks to be trained to this behavior and were required to demonstrate this behavior confidently, by immediately approaching the board and pecking on either cross for 5 sessions before testing commenced. During testing, the crosses were then replaced with the white, non-aposematic (S+) and colored, aposematic (S-) stimuli, and experimental trials commenced.

Stimuli were designed to disentangle whether differences in learning rates were due to the amount of pattern edge, the amount of colored area, shape repetition, or pattern type. Here we use the term ‘pattern’ to refer to any colored element within a signal (not necessarily repetitive). We use the term ‘pattern edge’ to refer to edges created by the yellow colored areas in the signal, which were internal patterns in stimuli A-E, but included the internal and external edge in stimulus F (single circle). Stimuli were designed in Adobe Illustrator, and pattern edge and colored area were determined using simple geometric equations.

Eight fish could not be trained to a satisfactory level and therefore did not

progress to the testing phase. The remaining fish (n = 50) were randomly allocated to 6 groups, which were each trained to avoid a different aposematic stimulus (S-, see Table 1). There was no significant difference in fish size between groups (one-way ANOVA: F= 0.59, d.f.= 5, p=0.70).

Learning rates for each group were compared with another group that had a similar pattern type, but differed in the amount of internal pattern edge, colored area, and/or shape repetition (Table 1). 'Spots' consisted of Group A (n = 9; nine yellow spots) and Group B (n = 7; single yellow spot) both of which featured internal spots; however, Group A, had more internal pattern edge and more shape repetition than Group B, but a similar amount of colored area (Table 1). 'Stripes' consisted of Group C (n = 8; four vertical stripes) and Group D (n = 10; single yellow vertical stripe) which both featured vertical stripes; however, Group C had more pattern edge, more shape repetition and more colored area than Group D. Finally, 'Circles', comprised Group E (n = 7; four open circles) and F (n = 9; single circle that outlines the stimulus) which both featured open circles; however, Group E, had more shape repetition than Group F but a similar amount of pattern edge and colored area. Data from Group F has been presented previously (Winters et al. 2017).

We predicted three possible scenarios: first, if an increased amount of pattern edge improved predator learning, we would expect a difference in the learning rate for 'Spots' (Group A would learn more quickly than B) and 'Stripes' (Group C would learn more quickly than D), but not for 'Circles' (Group E would learn at the same rate as Group F) (Table 1). Second, if an increased amount of colored area improved learning, we would expect Group B to learn more quickly than Group D and also predict a difference in learning rate in 'Stripes' (Group C would learn more quickly than D), but not between paired groups for 'Spots' or 'Circles'. Third, if differences were due to

increased repetition of shape alone, we anticipated that there would be a difference for all patterns ('Spots': Group A would be learnt more quickly than B; 'Stripes': Group C learnt more quickly than D; and 'Circles': Group E learnt more quickly than F).

We then compared results from groups A, C, E and F to determine whether pattern type affected predator learning of aposematic stimuli. Stimuli from these groups featured a similar amount of pattern edge and colored area, but differed in pattern type (spots, stripes, circles) (Table 1). The amount of pattern edge and colored area varied slightly between these stimuli due to differences in geometry; however, the stimuli we used were designed to ensure that both of these features were as similar as possible.

c) Statistical analyses

We analyzed the data using a cox proportional hazards survival analysis and the function coxph, in the survival package (Therneau 2015) in R v.3.1.3 (R Core Team 2015). In our data, the 'survival time' was the number of sessions taken to reach the learning criteria. The general form of the model is:

$$h(t)=h_0(t)\times exp(b_1x_1+b_2x_2+...+b_px_p)$$

where, t is the survival time, $h(t)$ is the observed hazard rate (the chance of the event occurring), $h_0(t)$ is the baseline hazard, determined by the covariates ($x_1, x_2...x_p$) and the coefficients ($b_1, b_2...b_p$) denote the effect size of the covariates.

Survival analyses were used because, unlike Generalized Linear Mixed Models, they allow the time to an event to be analyzed even if the event never occurred or the dataset is incomplete (right censored data) (Fox and Weisberg 2011). This meant that

data for fish that never reached the learning criteria, or which completed a different number of trials could be included.

We used the Cox proportional hazard model as this allows additional covariates to be included in the model (Fox and Weisberg 2011), allowing us to account for fish size as an indicator of age and prior experience. However, size (Total Length, mm) was not statistically significant in any of our analyses ($p > 0.09$). Our data met the assumption of proportional hazards, which we tested using the function cox.zph in R, ($p > 0.05$ for all treatments)

3. RESULTS

We found that fish learnt avoidance of the aposematic color pattern significantly faster when the stimulus featured a greater amount of internal pattern edge. Pairwise comparisons indicated that for 'Spots', Group A learnt avoidance faster than Group B (Hazard Ratio (β)= 0.07, $Z = -2.38$, 95% Confidence Interval (CI): 0.01-0.62, $p = 0.02$; Figure 1a) and for 'Stripes', Group C learnt avoidance faster than Group D ($\beta = 0.15$, $Z = -2.48$, CI = 0.03-0.67, $p = 0.01$; Fig 1b). For 'Circles', there was no significant difference between groups E and F ($\beta = 0.72$, $Z = -0.59$, CI = 0.24-2.16, $p = 0.55$; Fig 1c).

To ensure that these results were attributable to the amount of edge, not the amount of coloured area, we also compared the learning rate of Group B and Group D, which differed in coloured area but had the same amount of edge and found no significant difference ($\beta = 2.79$, $Z = 1.07$, CI = 0.42-18.37, $p = 0.29$). Learning rates may have been confounded if some patterns were more easily discriminated from the white, non-aposematic stimuli, which may have occurred with an increase amount of yellow; however, this was not the case.

When the amount of edge was similar, but the pattern type differed, there was no significant difference in learning rates between spots, stripes, outlines or circles (Groups A, C, E and F respectively) ($\beta = 0.69$, $Z = -0.69$, CI = 0.24 – 1.90, $p = 0.45$; Fig 1d).

4. DISCUSSION

The fish in our study learnt to avoid colored stimuli more quickly when there was a greater amount of internal pattern edge. We did not find evidence that the number of repetitive elements, amount of colored area, nor pattern type (spots, stripes or circles), affected predator learning. Our results support the hypothesis that although color may be the best learnt component of a visual signal (Aronsson and Gamberale-Stille 2008), patterns, and more specifically internal pattern edges, are key tactical components (Osorio et al. 1999) used to improve predator learning.

Edges may enhance predator learning of aposematic signals as highly contrasting transitions evoke a stronger response in the retina compared to gradual changes in luminance and color (Bruce et al. 1996). As the eyes scan an image, the amount of edge transitions will determine the amount of stimulation across the retina and increase the overall salience of a signal (Endler 2012). Aposematic patterns use edges that are highly contrasting and combine abrupt, simultaneous changes in both luminance and color, which distinguish them from the many false edges produced by variations in texture and illumination in natural scenes (Troscianko et al. 2009). Although we found that the amount of edge within a pattern improved predator learning, an optimal level may be set by the visual acuity of the predator and the complexity of the background. Beyond this limit, highly complex patterns with a

profuse amount of pattern edges may appear blurred and inconspicuous, due to the decreased spatial frequency. Indeed, highly complex body patterns, such as reticulated patterns that feature a high amount of internal pattern edge, may become harder to learn as edges become less detectable.

We found no difference in learning rates for different pattern types when we controlled for the amount of edge within the stimuli, however the pattern displayed in a warning signal may be determined by a range of other factors. Pattern type will be important to detection in natural environments, where conspicuousness may be enhanced through pattern edges that contrast with the orientation (Webster et al. 2009) or spatial frequency of common lines within their habitat (Godfrey et al. 1987; Phillips et al. 2017). While spots and stripes may evolve because they are developmentally simple to produce (Turing 1952), or because spots are well suited to stimulate the circular receptive fields of vertebrate retinal ganglion cells (Lythgoe 1979; Stevens 2005), while stripes may provide camouflage from a distance (Barnett et a. 2016). Concentric rings such as eye spots, are abundant in animal signals and may function to confuse or startle predators, by mimicking the pupil and iris of vertebrate eyes (for example, Blest 1957; De Bona et al. 2015). However, we propose that in some cases concentric rings may evolve to increase the amount of salient edges within a pattern. Indeed, this is consistent with recent research suggesting that some eyespots deter predators through increased conspicuousness, not through eye mimicry (Stevens 2009).

Shape is an important component of predator search images (Troscianko et al 2009) and so patterns which accentuate this, such as body outlining, are expected to aid predator detection and recognition (Cott 1940; Hailman 1977). We did not find evidence to support this hypothesis in our study, with stimuli featuring a yellow outline (Group F), learnt at the same rate as signals featuring spots and stripes (Figure 1d).

However, body outlining may be more important to increase prey conspicuousness in natural scenes, as opposed to learning speed. In a previous study (Winters et al. 2017), it was demonstrated that triggerfish only learnt avoidance of one element of a multicomponent warning signal, rather than the entire signal. Fish learnt to avoid the yellow outline of a multicomponent warning signal, but not internal red spots. However, it was previously unclear whether this was because the yellow outline highlighted the shape of the stimulus, or whether it was a shape or edge effect. The present study untangles these different hypotheses and suggests that the yellow rim was likely learnt preferentially because it provided more internal pattern edges.

The amount of edge within a pattern and pattern repetition are tightly correlated. In our study, fish learnt to avoid a single circle (Group F) more quickly than a single spot (Group B), which differed only in the amount of pattern edge and not in shape repetition (Figure 1c), suggesting that the amount of pattern edge is more important than regularity or repetition alone. Indeed, in a previous study, birds learnt to avoid prey featuring the same amount of edge at a similar rate, regardless of whether stimuli were regularly or irregularly striped (Aronsson and Gamberale-Stille 2013). However, in our study, the combined effect of increased edge contrasts, repetition and enhanced symmetry may have improved learning.

Although large signal size increases conspicuousness and effectiveness of warning signals (Remmel and Tammarub 2011), many defended prey such as bees, wasps, lady beetles and nudibranch molluscs are constrained by a small size and limited body surface. In terms of geometry, the ratio of edge to colored area is higher for stripes (rectangles) compared with spots (circles); indeed, in our study, we required nine spots to equal the edge of four stripes (Table 1). Stripes therefore offer the advantage of more conspicuous edge transitions when the size of a warning signal is constrained, or when

color is provided by a rare or costly pigment. However, the evolution of pattern geometry is complex, and influenced by additional factors such as body shape. For example, nudibranch mollusks have elongated, elliptical bodies, and so longitudinal stripes emphasize their primary body axis. In comparison, small, circular animals such as ladybirds may evolve spots because they provide patterns that replicate their body shape and provide curved edges which run parallel to their circular body outline to enhance conspicuousness (Troscianko et al. 2017).

We used wild caught fish and therefore unfortnuately cannot account for their prior experience of colored stimuli, which may have influenced our results. However, we are unaware of aposematic species at the collection site of our fish with color patterns similar to those used in our experiment. Ideally, it would have been ideal to use wild caught reef fish raised from light-trapped larvae; however, large fish such as triggerfish are rarely caught using such methods (KLC, pers. obs.). Our sample sizes were relatively small (n = 7-10 per group, total = 58 fish), which was the maximum number that could be housed and trained in separate aquaria simultaneously. However, for pairs where a non significant result was expected, the results were very similar between groups (between 'Circles': Group E and F, $p = 0.554$) and for Groups A, C, E and F, $p = 0.36$), and so we were unlikely to get a significant result with a larger sample size.

In conclusion, we have provided evidence that warning signals that display increased internal pattern edges, provided by spots, stripes or circles, improve predator avoidance learning. Our research provides new insights into the value and function of patterns in warning signals, and has important implications for signal evolution and pattern geometry. Understanding how signal receivers respond to different components of visual signals will help us to reveal how complex color signals evolve and are

maintained.

References

Allen WL, Cuthill IC, Scott-Samuel NE & Baddeley R. 2011. Why the leopard got its spots: relating pattern development to ecology in felids. *Proc. Royal Soc. B.* **278**, 1373-380. (doi:10.1098/rspb.2010.1734).

Aronsson M, Gamberale-Stille G. 2008. Domestic chicks primarily attend to colour, not pattern, when learning an aposematic coloration. *Anim. Behav.* **75**, 417-423. (doi:10.1016/j.anbehav.2007.05.006).

Aronsson M, Gamberale-Stille G. 2009. Importance of internal pattern contrast and contrast against the background in aposematic signals. *Behav. Ecol*. **20**, 1356-1362. (doi:10.1093/beheco/arp141).

Aronsson M, Gamberale-Stille G. 2013. Evidence of signaling benefits to contrasting internal color boundaries in warning coloration. *Behav. Ecol*. 24, 349-354. (doi:10.1093/beheco/ars170).

Barnett JB, Scott-Samuel NE, Cuthill IC. 2016. Aposematism: balancing salience and camouflage. *Biol. Lett.* **12**. (doi:10.1098/rsbl.2016.0335).

Blest A. 1957. The function of eyespot patterns in the Lepidoptera. *Behaviour.* **11**, 209-256.

Bruce V, Green PR, Georgeson MA. 1996. *Visual Perception: Physiology, Psychology and Ecology*. East Sussex, UK, Psychology Press.Champ CM, Wallis G, Vorobyev M, Siebeck UE, Marshall NJ. 2014. Visual acuity in a species of coral reef fish: *Rhinecanthus aculeatus*. *Brain Behav. Evol.* **83**, 31-42. (doi:10.1159/000356977).

Cheney KL, Newport C, McClure EC, Marshall NJ. 2013. Colour vision and response bias in a coral reef fish. *J. Exp. Biol.* **216**, 2967-2973. (doi: 10.1242/jeb.087932).

Cott HB. 1940. *Adaptive Coloration in Animals*. United Kingdom, Methuen, Oxford University Press.

Cuthill IC, Stevens M, Sheppard J, Maddocks T, Parraga CA, Troscianko TS. 2005. Disruptive coloration and background pattern matching. *Nature.* **434**, 72-74.

Cuthill IC, Székely A. 2009. Coincident disruptive coloration. *Philos. Trans. Royal Soc. B,* **364**, 489-496. (doi:10.1098/rstb.2008.0266).

De Bona S, Valkonen JK, López-Sepulcre A, Mappes J. 2015. Predator mimicry, not conspicuousness, explains the efficacy of butterfly eyespots. *Proc. Royal Soc. B.* **282**. (doi:10.1098/rspb.2015.0202).

Dolenská M, Nedvěd O, Veselý P, Tesařová M, Fuchs R. 2009. What constitutes optical warning signals of ladybirds (Coleoptera: Coccinellidae) towards bird predators: colour, pattern or general look? *Biol. J. Linn. Soc.* **98**, 234-242. (doi:10.1111/j.1095-8312.2009.01277.x).

Driver J, Baylis GC. 1996. Edge-assignment and figure–ground segmentation in short-term visual matching. *Cogn. Psychol.* **31**, 248-306. (doi:https://doi.org/10.1006/cogp.1996.0018).

Endler JA. 2006. Disruptive and cryptic coloration. *Proc. Royal Soc. B.* **273**, 2425-2426. (doi:10.1098/rspb.2006.3650).

Endler JA. 2012. A framework for analysing colour pattern geometry: adjacent colours. *Biol. J. Linn. Soc.* **107**, 233-253. (doi:10.1111/j.1095-8312.2012.01937.x).

Enroth-Cugell C, Pinto LH. 1972. Properties of the surround response mechanism of cat retinal ganglion cells and centre-surround interaction. *J. Physiol.* **220**, 403-439.

Fox J, Weisberg S. 2011. *An R Companion to Applied Regression,* 2nd Ed. Thousand Oaks, CA.

Godfrey D, Lythgoe JN, Rumball DA. 1987. Zebra stripes and tiger stripes: the spatial frequency distribution of the pattern compared to that of the background is significant in display and crypsis. *Biol. J. Linn. Soc.* **32**, 427-433. (doi:10.1111/j.1095-8312.1987.tb00442.x).

Guilford T. 1986. How do warning colours work? Conspicuousness may reduce recognition errors in experienced predators. *Anim. Behav.* **34,** 286–288.

Guilford T, Dawkins, MS 1991. Receiver psychology and the evolution of animal signals. *Anim Behav* **42**, 1-14. (doi:10.1016/S0003-3472(05)

Hailman JP. 1977. *Optical Signals: Animal Communication and Light*. London, UK, Indiana University Press.

Harris RA, Graham P, Collett, TS. 2007. Visual cues for the retrieval of landmark memories by navigating wood ants. *Curr. Biol.* **17**, 93-102. (doi:10.1016/j.cub.2006.10.068).

Hegna RH, Saporito RA, Gerow KG, Donnelly MA. 2012. Contrasting colors of an aposematic poison frog do not affect predation. *Ann. Zool. Fennici*. **48**, 29-38. (doi:10.5735/086.048.0103).

Lau KK, Roberts S, Biro D, Freeman R, Meade J, Guilford T. 2006. An edge-detection approach to investigating pigeon navigation. *J. Theor. Biol*. **239**. 71-78. (doi:10.1016/j.jtbi.2005.07.013).

Lythgoe JN. 1979. *The Ecology of Vision*. Oxford, New York, Clarendon Press.

Newport C, Green NF, McClure EC, Osorio DC, Vorobyev M, Marshall NJ, Cheney KL. 2017. Fish use colour to learn compound visual signals. *Anim. Behav.* **125**, 93-100. (doi:10.1016/j.anbehav.2017.01.003).

Osorio D. Jones CD, Vorobyev M. 1999. Accurate memory for colour but not pattern contrast in chicks. *Curr. Biol.* **9**, 199-202. (doi:10.1016/S0960-9822(99)80089-X).

Osorio D, Srinivasan MV. 1991. Camouflage by edge enhancement in animal coloration patterns and its implications for visual mechanisms. *Proc. Royal Soc. B.*.**244**. (doi:10.1098/rspb.1991.0054).

Palmer SE, Ghose T. 2008. Extremal edges: a powerful cue to depth perception and figure-ground organization. *Psychol. Sci.* **19**, 77-84. (doi:10.1111/j.1467-9280.2008.02049.x).

Phillips GAC, How MJ, Lange JE, Marshall NJ, Cheney KL. 2017. Disruptive colouration in reef fish: does matching the background reduce predation risk? *J. Exp. Biol.* **220**, 1962-1974. (doi:10.1242/jeb.151480).

Pignatelli V, Champ C, Marshall J, Vorobyev M. 2010. Double cones are used for colour discrimination in the reef fish, *Rhinecanthus aculeatus*. *Biol. Lett.* **6**, 537-539. (doi:10.1098/rsbl.2009.1010).

Poulton EB. 1890. *The Colors of Animals: their Meaning and Use, Especially Considered in the Case of Insects*. New York, Appleton.

Randall JE. 1981. *Underwater Guide to Hawaiian Reef Fishes*. Newtown Square, Pennsylvania, Harrowood Books.

R Core Team. 2015. *R: a language and environment for statistical computing*. Vienna, Austria: R Foundation for Statistical Computing. See http://www.R-project.org.

Remmel T, Tammarub T. 2011. Evidence for the higher importance of signal size over body size in aposematic signaling in insects. *J. Insect Sci.* **11**, 4. (doi:10.1673/031.011.0104).

Schaefer HM, Stobbe N. 2006. Disruptive coloration provides camouflage independent of background matching. *Proc. Royal Soc. B.* **273**, 2427-2432. (doi: 10.1098/rspb.2006.3615).

Singh R, Mukhopadhyay K. 2011. Survival analysis in clinical trials: Basics and must know areas. Perspect Clin Res. **2**, 145-148. (doi:10.4103/2229-3485.86872).

Stevens M. 2005. The role of eyespots as anti-predator mechanisms, principally demonstrated in the Lepidoptera. *Biol. Rev.* **80**, 573-588. (doi:10.1017/S1464793105006810).

Stevens M, Cantor A, Graham J. 2009. The function of animal 'eyespots': Conspicuousness but not eye mimicry is key. *Curr. Zoo.* **55**.

Stevens M, Cuthill IC, Windsor AMM, Walker HJ. 2006. Disruptive contrast in animal camouflage. *Proc. Royal Soc. B.* **273**. (doi:10.1098/rspb.2006.3614).

Stevens M, Winney IS, Cantor A, Graham J. 2009. Outline and surface disruption in animal camouflage *Proc. Royal Soc. B.* **276**, 781-786. (doi:10.1098/rspb.2008.1450).

Thayer GH. 1909. *Concealing Colouration in the Animal Kingdom: An Exposition of the Laws of Disguise through Colour and Pattern; Being a Summary of Abbott H. Thayer's Discoveries.* New York, Macmillan.

Therneau TM. 2015. A Package for Survival Analysis in S. 2.38 ed. http://CRAN.R-project.org/package=survival.

Troscianko T, Benton CP, Lovell GP, Tolhurst DJ, Pizlo Z. 2009. Camouflage and visual perception. *Philos. Trans. Royal Soc. B,* **364**. (doi:10.1098/rstb.2008.0218).

Troscianko J, Skelhorn J, Stevens M. 2017. Quantifying camouflage: how to predict detectability from appearance. *BMC Evol. Biol.* **17**. (doi:10.1186/s12862-016-0854-2).

Turing AM. 1952 The chemical basis of morphogenesis. *Philos. Trans. Royal Soc*. B. **237,** 37-72**. (**doi 10.1098/rstb.1952.0012).

Webster RJ, Callahan A, Godin J-GJ, Sherratt TN. 2009. Behaviourally mediated crypsis in two nocturnal moths with contrasting appearance. *Philos. Trans. Royal Soc. B,* **364**, 503-510. (doi:10.1098/rstb.2008.0215).

Webster RJ, Hassall C, Herdman CM, Godin JGJ, Sherratt TN. 2013. Disruptive camouflage impairs object recognition. *Biol. Lett.* **9**. (doi:10.1098/rsbl.20130501).

Winters AE, Green NF, Wilson NG, How MJ, Garson MJ, Marshall NJ, Cheney KL. 2017. Stabilizing selection on individual pattern elements of aposematic signals. *Proc. Royal Soc. B.* **284**. (doi:10.1098/rspb.2017.0926).

Wüster W, Allum CSE, Bjargardóttir IB, Bailey KL, Dawson KJ, Guenioui J, Lewis J, McGurk J, Moore AG, Niskanen M, et al. 2004. Do aposematism and Batesian mimicry require bright colours? A test, using European viper markings. *Proc. Royal Soc. B.* **271**, 2495. (doi: 10.1098/rspb.2004.2894)

Table 1: Aposematic (S-) signals used indicating group name, amount of pattern edge (mm) and colored area (mm^2) that each stimulus contained. Grey shading indicate the groups that were compared to determine whether pattern type (rather than the amount of edge) influenced learning rate (Fig. 1d). Grey outlines around stimuli in the table, only show edges of stimuli area, rather than the presence of a colored edge.

	Spots		Stripes		Circles	
S-						
Group	A	B	C	D	E	F
Edge (mm)	170	50	178	45	176	176
Colored Area (mm^2)	254	202	198	50	176	176

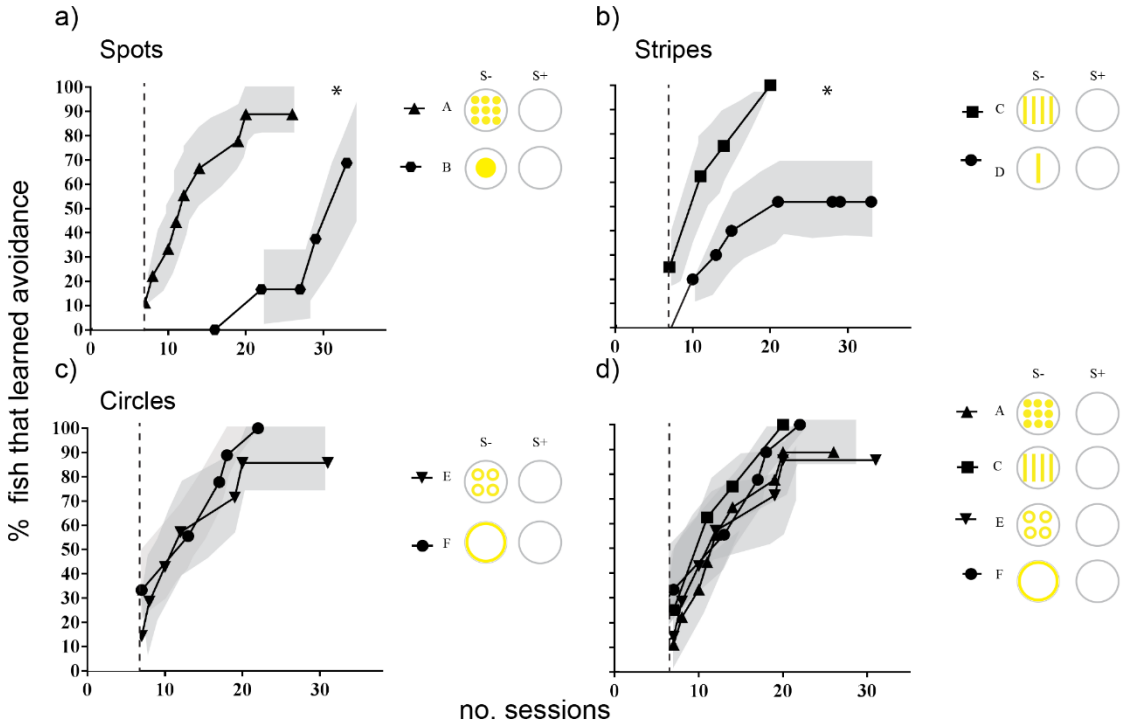

Figure 1. The % of fish that learned avoidance of an aposematic stimulus (S-) over a plain white non-aposematic stimulus (S+) after a given number of sessions: a) 'Spots'; b) 'Stripes'; c) 'Circles'; d) comparison of different patterns with equal amount of edge. Shaded areas indicate standard error. Grey outlines around stimuli in the figure, only show edges of stimuli area, rather than the presence of a colored edge. * indicates statistical significance of $p < 0.05$. The dashed line designates that fish were required to demonstrate avoidance of the aposematic stimulus for 7 sessions and therefore could not achieve the learning criteria until the 7th session.

Toxicity and taste: unequal chemical defences in a mimicry ring

Anne E. Winters[1], Nerida G. Wilson[2,3], Cedric P. van den Berg[1], Martin J. How[4], John A. Endler[5], Justin N. Marshall[6], Andrew M. White[7], Mary J. Garson[7] & Karen L. Cheney[1,6]

[1]*School of Biological Sciences, The University of Queensland, Brisbane, QLD 4072 Australia*

[2]*Molecular Systematics Unit, Western Australian Museum, 49 Kew St, Welshpool 6106 WA, Australia*

[3]*School of Biological Sciences, University of Western Australia, Crawley 6009 WA, Australia*

[4]*School of Biological Sciences, University of Bristol, Bristol BS8 1TQ, UK*

[5]*Centre for Integrative Ecology, School of Life and Environmental Science, Deakin University, Victoria, 3217, Australia*

[6]*Queensland Brain Institute, The University of Queensland, Brisbane, QLD 4072, Australia*

[7]*School of Chemistry and Molecular Biosciences, The University of Queensland, Brisbane, QLD 4072, Australia*

Abstract

Mimicry of warning signals is common, and can be mutualistic when mimetic species harbour equal levels of defence (Müllerian), or parasitic when mimics are undefended but still gain protection from their resemblance to the model (Batesian). However, whether chemically defended mimics should be similar in terms of toxicity (i.e. causing damage to the consumer) and/or unpalatability (i.e. distasteful to consumer) is unclear and in many studies remains undifferentiated. In this study, we investigated the evolution of visual signals and chemical defences in a putative mimicry ring of nudibranch molluscs. First, we demonstrated that the appearance of a group of red spotted nudibranchs molluscs was similar from the perspective of potential fish predators using visual modelling and pattern analysis. Second, using phylogenetic reconstruction, we demonstrated that this colour pattern has evolved multiple times in distantly related individuals. Third, we showed that these nudibranchs contained different chemical profiles used for defensive purposes. Finally, we demonstrated that although levels of distastefulness remained relatively constant between species, toxicity levels varied significantly. We highlight the need to disentangle toxicity and taste when considering chemical defences in aposematic and mimetic species, and discuss the implications for aposematic and mimicry signal evolution.

Key words: mimicry rings, chemical defences, aposematism, marine invertebrates, nudibranch

Introduction

Many animals use visual displays to advertise they are chemically or otherwise defended (aposematism) [1]. The efficacy of aposematic signals in deterring predation is thought to be frequency-dependent, as the warning signal must be encountered multiple times for predators to learn and remember the association between the signal and level of unpalatability [2-5]. Müllerian mimics are defended species that have a mutualistic relationship with co-mimics to increase encounters with predators and spread the burden of predator learning [6-8], whereas Batesian mimics are undefended species that parasitize the warning signal of their defended sympatric model [9]. However, mimicry systems are thought to lie on a spectrum of chemical defence strength, with well-protected Müllerian mimics at one end, unprotected Batesian mimics on the other, and a range of intermediate protection in between (quasi-Batesian mimics) [5, 10-14].

When investigating the relative strength of chemical defences for species in proposed mimicry rings, studies tend to consider the unpalatability of species (i.e. distastefulness to consumer) [15-18] and/or toxicity (i.e. harm to consumer) [19-21]. However, the relationship between distastefulness and toxicity in chemically defended prey is rarely investigated and surprisingly, in many studies remains undifferentiated (but see [22]). Indeed, distastefulness and toxicity are often used synonymously in the literature [5, 19, 23], with perhaps the assumption that they are correlated. Prey species that are distasteful but not toxic, or vice versa, may be common [5, 24], and therefore the relationship between distastefulness and toxic defence needs further consideration [25]. Distasteful compounds that are non-toxic could initially deter predators [26], but may eventually be accepted by predators [26, 27]. This could be dependent on predator satiation, how unpleasant the compound is and the abundance of other palatable prey items [28]. Therefore, toxicity could be considered a more

63 effective deterrent than distastefulness. However, distasteful compounds that are moderately
64 toxic may also protect prey populations more effectively than highly toxic compounds [29].
65 To investigate the relationship between distastefulness and toxicity in mimicry
66 systems, we investigated a putative red spot mimicry ring of nudibranch molluscs that co-
67 occur along the east coast of Australia [30, 31]. Many species of nudibranchs display vibrant
68 warning colours to indicate that they contain defensive secondary metabolites that are
69 sequestered, transformed from dietary sources, or synthesized *de novo* [32]. We have
70 previously shown that one member of the putative red spot mimicry group, *Goniobranchus*
71 *splendidus*, contains distasteful compounds to marine organisms and displays conspicuous
72 colours patterns, components of which are learnt readily by reef fish predators [33]. We first
73 examined the similarity of colour patterns in this group to a potential fish predator using
74 spectral reflectance measurements, visual modelling and pattern geometry analysis. Second,
75 we conducted phylogenetic analysis to investigate shared ancestry of species. Third, we
76 identified and quantified defensive metabolites present in each species and examined the
77 strength of chemical defences using anti-feedant and toxicity assays with shrimp.
78
79 **Methods**
80 *Study species*
81 Nudibranch species (n = 24) were collected between 2012 and 2016 by hand from
82 sites in Queensland (QLD) and New South Wales (NSW) (Table S1) either on SCUBA at
83 depths ranging from 5-18m, or from intertidal zones. Based on previous groupings [30], we
84 identified species that exhibited a similar red spotted or red reticulate colour pattern and/or a
85 distinctive yellow/orange mantle border (Figure 1, A-H). Eight species of nudibranch were
86 assigned a prioiri to a red spot mimicry group: *Goniobranchus splendidus* (Angas, 1864) (n =
87 22), *G. tinctorius* (Rüppell & Leuckart, 1830) (n = 4), *G. daphne* (Angas, 1864) (n = 8), *G.*

88 *hunterae* (Rudman, 1983) (n = 1), *Mexichromis mariei* (Crosse, 1872) (n = 4), *Mexichromis*
89 *festiva* (Angas, 1864) (n = 32), *Hypselodoris bennetti* (Angas, 1864) (n = 26), and *Verconia*
90 *haliclona* (Burn, 1957) (n = 1). We assigned a further four species to a partial red spot pattern
91 group: *G. verrieri* (Crosse, 1875) (n = 2), *G. albonares* (n =5), *G. tasmaniensis* (Bergh,
92 1805) (n = 5), and Chromodorididae *thompsoni* (generic placement unassigned, Johnson &
93 Gosliner 2012) (n = 3). These species exhibit part of the red spot mimicry pattern, either with
94 spots or a coloured mantle border missing, or spots of a different colour (Figure 1, I-L).
95 These twelve species co-occur in the study area, and seven of these species are endemic [30].
96 A further 12 species were assigned to a non-mimic group: *Ceratosoma amoenum*
97 (Cheeseman, 1886) (n = 4), *Chromodoris kuiteri* Rudman, 1982 (n = 4), *C. lochi* Rudman,
98 1982 (n = 3), *C. elisabethina* (Bergh, 1877) (n=6), *Doriprismatica atromarginata* (Cuvier,
99 1804) (n = 4), *Goniobranchus decorus* (Pease, 1860) (n = 2), *G. geometricus* (Risbec, 1928)
100 (n = 2), *Hypselodoris jacksoni* Wilson and Willan 2007 (n = 2), *H. obscura* (Stimpson, 1855)
101 (n = 6), *H. tryoni* (Garrett, 1873) (n = 3), *H. whitei* (Adams and Reeve, 1850) (n = 3),
102 *Risbecia godeffroyana* (Bergh, 1877) (n = 2). These species do not appear to closely resemble
103 the red spot mimicry group in terms of colour combinations or pattern (Figure S1).
104 All specimens were placed in buckets with aerated seawater, transported to the
105 laboratory and placed in a petri dish of seawater for processing. The extended crawling length
106 (cm) of each individual was measured, individuals were photographed, the spectral
107 reflectance of each distinct colour pattern element was measured in the water with a
108 spectrophotometer, and a small portion of tissue from the tail was placed in ethanol for
109 phylogenetic analysis. Species identifications were confirmed through expert examination
110 (N.G.W) and genetic sequencing of Cytochrome *c* Oxidase 1 (COI) and 16S rDNA and
111 comparison with sequences deposited on the database GenBank. All nudibranch specimens
112 were then frozen and stored at -20°C until chemical extraction of chemical defences.

113

114 *Phylogenetic relatedness*

115 Representative individuals of newly-collected species selected for the phylogeny were
116 extracted with a DNeasy blood and tissue kit (Qiagen). These were used in PCR reactions to
117 amplify two mitochondrial genes, COI and 16S, using the primers and methods of Wilson,
118 Maschek [34]. Details of all species used in the phylogenetic analysis are available in Table
119 S2. All available COI and 16S data for the Chromodorididae was downloaded from GenBank
120 and added to newly generated data from this study (COI GenBank XXXXX; 16S GenBank
121 XXXXX). Only individuals that were represented by both genes from the same individual
122 were used. This resulted in a data set with 146 species, representing an estimated 40% taxon
123 completeness for the family (www.marinespecies.org). Data were aligned using the MAFFT
124 v7.222 algorithm implemented in Geneious v 9.0.5, trimmed of primer regions, and checked
125 for translation (COI). Data for each gene fragment were analysed separately in a maximum-
126 likelihood (ML) framework for error checking and then concatenated but partitioned,
127 applying the optimal models of evolution simultaneously estimated and selected with the
128 Bayesian Information Criterion in ModelFinder [35] executed in IQ-TREE [36]. To estimate
129 support at each node we used the ultrafast boostrap function, implementing 1000 replicates
130 using a maximum of 1000 iterations and a minimum correlation coefficient of 0.99 as a
131 stopping rule [37]. Outgroups from the putative sister group Actinocyclidae were added, as
132 well as other members of the Doridídae, allowing for outgroup uncertainty recently
133 highlighted [38]. The tree was rooted with *Doris kerguelenensis*. We mapped ancestral traits
134 of red spot mimic colour signals (0, no red spot pattern; 1, partial red spot pattern; 2, full red
135 spot pattern) using stochastic character mapping (SCM) [39] in Mesquite v 3.2 [40]. We
136 selected 'MK1' as the evolutionary model, which assumes an equal probability for a
137 particular character change.

138

139

140 *Spectral reflectance measurements*

141 Spectral reflectance measurements of each nudibranch colour pattern element were
142 obtained by placing individuals in a dish immersed in seawater and measurements were taken
143 with an Ocean Optics USB2000 spectrophotometer (Dunedin, FL, USA) and Ocean Optics
144 OOIBASE32 software. We used a 200 μm bifurcated optic UV/visible fibre held underwater
145 at 45° angle connected to a PX-2 pulse xenon light (Ocean Optics). The percentage of light
146 reflected at each wavelength from 300-700 nm was calibrated using a Spectralon 99% white
147 reflectance standard (LabSphere, NH, USA) placed in the petri dish of seawater with the
148 nudibranch. At least 10 measurements were taken of each colour pattern element and
149 averaged per individual. Spectral reflectance data were not obtained for specimens of
150 *Verconia haliclona* or Chromodorididae *thompsoni* due to equipment failure and therefore
151 these species were not included in the colour pattern analysis.

152

153 *Colour and pattern analysis*

154 We first quantified colour pattern elements from the perspective of a potential
155 trichromatic fish predator, the triggerfish *Rhinecanthus aculeatus* (photoreceptor λ_{max} of 413
156 nm, 480 nm, 528 nm and transmission measurements through cornea, vitreus and lens, all as
157 per [41]). We used this species to model the visual characteristics of nudibranchs as it is an
158 omnivorous fish known to prey on molluscs, found throughout the range of the proposed red
159 spot mimicry group (OZCAM.com.au) and is also representative of a common trichromatic
160 visual system found in many marine fish species [42].

161 Photon capture generated by each given colour pattern element (i) for each
162 photoreceptor q_i was calculated as per equation 1 in [43]. Irradiance measurements, $I(\lambda)$, were

taken at a depth of 5 m (as per [44]). Photon loss by transmittance in function of distance was ignored due to the relative clarity of the water in shallow reefs and the small distance assumed between object and viewer (max 30cm). In order to incorporate colour constancy, cone capture quanta were transformed using the von Kries correction as per equation 2 in [43].

Each colour pattern element was defined as an internal pattern (spots, stripes, reticulate), overall body (background) colour and, if present, a contrasting rim. Colour pattern elements were plotted in a trichromatic visual space (Maxwell's triangle) and we measured hue (the angle of the colour coordinate relative to the achromatic point), chroma (or saturation, defined as its distance from the achromatic point) and luminance (measured used the combined photon capture of the double cone, which process luminance in reef fish [45]) from each colour pattern element. Methods were modified from [46, 47].

For pattern analysis, we used images of nudibranch that were normalized for size by rescaling the images to a standard body area of 5000 pixels. The outline of each animal was then manually traced using a magnetic lasso tool and extracted from the background using Adobe Photoshop CS5. The nudibranch image was then stylized for analysis by placing a transparent layer over the original image and using the pencil tool to define the red spot pattern [48]. This ensured individual colour pattern elements were correctly recognized by the MATLAB code required to run the analysis. Pattern properties of the entire nudibranch pattern were quantified using the adjacency analysis method [48]. Briefly, the method quantifies the distribution of transitions within and between colour pattern elements on an animal. Three relevant statistics [48] were calculated: 1) aspect ratio, 2) colour diversity and 3) pattern complexity. Aspect ratio was calculated by dividing the vertical patch size by the horizontal patch size (patch size was determined by calculating the average number of pixels along a vertical or horizontal transect until a zone transition). Colour diversity described how

188 spatially evenly colours are represented in the pattern. High values indicate that the relative
189 areas of each colour class are more close to being equal; diversity was calculated by the
190 inverse Simpson index which yields the equivalent number of equally common (area) colours.
191 Pattern complexity was calculated as the density of colour transitions; patterns with a greater
192 number of pixels adjacent to a different colour class will have a higher complexity score.
193
194 *Non-metric multidimensional scaling analysis (NMDS)*
195 Species were differentiated in two-dimensional space using 14 characters of colour
196 and pattern analysis by performing a non-metric multidimensional scaling analysis based on a
197 Euclidean distance matrix with the metaMDS function in the vegan package [49] of R v 3.2.2
198 [50]. Characters were overall pattern (plain = 1, reticulate = 2, spotted = 3 or striped = 4);
199 chromatically contrasting rim (absent = 0, present = 1); hue, chroma, luminance of internal
200 pattern, background colour and rim; and our three pattern geometry statistics (aspect ratio,
201 colour diversity, pattern complexity). If there was more than one pattern present on the
202 species, then the dominant pattern was used as defined by 3 authors and is stated in Table S3.
203 If internal patterns or rims were not present on a particular species, then values calculated for
204 background colour were used.
205
206 *Chemical extraction and identification*
207 To investigate the identity and strength of chemical defences for each species, the
208 whole body tissue of specimens were extracted as per [51]. All extracts were dissolved in
209 deuterated chloroform for ^{1}H NMR analysis on a Bruker AV-500 spectrometer at 500 MHz.
210 If necessary for identification of nudibranch metabolites, a small portion of the extract was
211 analyzed using low-resolution electrospray ionisation mass spectrometry (LRESIMS) on a
212 Bruker Esquire HCT mass spectrometer. The ^{1}H NMR and LRESIMS data of crude extracts

213 were compared with the respective literature to identify known compounds. Where necessary,
214 a small portion of the extract was subjected to silica flash chromatography, and the various
215 fractions produced were further separated into individual compounds by normal phase high
216 performance liquid chromatography (NP HPLC), eluting with various ratios of hexanes/ethyl
217 acetate. Dried extracts were placed in solution with dichloromethane (DCM) at the recorded
218 specimen volume to provide a stock solution at the natural concentration (mg/mL) of extract
219 for use in toxicity and palatability assays.
220
221 *Toxicity Assay*
222 In order to measure the relative toxic properties of crude extracts from each species of
223 nudibranch, brine shrimp (*Artemia* sp.) LD_{50} (Lethal dose at 50%) assays were conducted
224 between November 2013 and September 2015 on six of the twelve red spot species for which
225 there was enough biological material (*G. splendidus, G. tinctorius, G. daphne, G.*
226 *tasmaniensis, M. festiva, H. bennetti*). Comparative studies using extracts from marine
227 sponges have demonstrated that brine shrimp can be a good first indicator of bioactivity, and
228 show similar results to assays tested against fish [52, 56]. Assays were carried out as per
229 methods in [51]. Briefly, a stock solution of the crude extract for each species was prepared
230 by adding a volume of DCM equivalent to that of the extracted tissue. One glass microfiber
231 filter paper (Whatman GF/C 47 mm diam.) was placed into individual glass petri dishes (55
232 mm diam.) then 0.005, 0.05, 0.5 mL of stock solution were transferred on to the filter papers
233 with a glass pipette. The solvent was left to evaporate from the filter paper under a Nederman
234 arm for 10 min. Brine shrimp eggs were hatched in artificial seawater (Tropic Marin) and
235 twenty actively swimming instar I nauplii (< 12 h after hatching) were collected with a glass
236 pipette and added to each petri dish with 5 mL filtered sea water. Lids were placed on top of
237 the petri dishes and kept under constant illumination for 24 hours. Surviving nauplii (instar

238 II/III) were then counted; nauplii were considered dead if no movement was detected after
239 several seconds of observation. Natural mortality was controlled for using control treatments
240 in which 0.5 mL of DCM was added to the filter paper. In all cases control deaths occurred,
241 therefore the data was corrected using Abott's formula % deaths = (test – control)/(100 –
242 control) for analysis [53]. We then calculated the LD_{50} of the crude extract for each
243 nudibranch species by interpolating a line or standard curve, chosen based on R^2 values. LD_{50}
244 values were calculated for species with extracts that induced a response to at least 50% of the
245 brine shrimp. LD_{50} values are interpolated x values (mL stock solution), where 1 mL of
246 extract = 1 mL of tissue, and therefore reflect natural volumetric concentrations. Absolute
247 concentrations of compounds tested are shown in Figures S2 and S3.
248
249 *Anti-feedant assay*
250 To assess the relative distastefulness, and thus feeding deterrence of nudibranch
251 extracts, antifeedant assays were performed using the generalist rock-pool prawn (*Palaemon*
252 *serenus*) between November 2013 and September 2015 as per [51, 54, 55]. This species has a
253 clear carapace and digestive tract, which makes it ideal for feeding observations and
254 preliminary studies have shown that compounds distasteful to marine fish *Tetractenos*
255 *hamiltoni* and *Rhinecanthus aculeatus* are also distasteful to rock-pool shrimp [56].
256 Individuals were collected intertidally in SE Queensland on foot using hand nets and housed
257 in aquaria with ample food (Ocean Nutrition, Formula 2) until used in assays. Artificial food
258 pellets were created to approximate the nutritional content of a nudibranch with roughly 90%
259 water, 7% squid + alginate, and 3% sand following the protocol outlined in [51, 57]. Crude
260 extracts were added in several concentrations up to that which they were found occurring
261 naturally for each species by adding the crude stock solution or DCM without extract (control
262 pellets) to a dry mixture (50 mg freeze-dried squid mantle, 30 mg alginic acid, 30 mg purified

sea sand). The DCM of each treatment and control was allowed to evaporate for 30 minutes under a Nederman arm, and then the mixture was reconstituted in distilled water to make a final pellet volume of 0.5 mL. Shrimps were selected randomly and placed individually in small compartments (135mm x 98mm x 90mm) with adequate aeration and water flow. Shrimp were allowed to acclimatize for at least 3 days and fed green fish flakes (Ocean Nutrition, Formula 2) once per day. Shrimp were then starved for 2 days prior to trials. Ten shrimp were randomly selected for each extract-treated and control group. Pellets were offered to shrimp using tweezers and then observed for 60 min. The presence of a red spot in the transparent gastric mill of the shrimp indicated acceptance, and the absence of a spot indicated rejection. Shrimp that rejected a pellet were then offered a control pellet and observed for a further 30 minutes. Shrimp that did not eat control pellets were removed from the analysis. Shrimp were not re-used. The ED_{50} of crude extracts was calculated as above.

To consider whether a correlation existed between distastefulness and toxicity while considering phylogenetic relatedness between species, we used a Generalized Least Squares (GLS) regression model. We first pruned the tree to leave only the six species on which we had conducted assays and then created a chronogram using the chronos function in the ape package v 5.0 [58]. We used the Brownian model [59] as this had the lowest AIC values using corBrownian, in comparison to models run with corGrafen and corMartin. Phylogenetic regression analysis was conducted in R version 3.2.2 [50].

Results

Colour and pattern analysis

Data for colour and pattern parameters are reported in Table S3 and were visualized in ordinal spacing using NMDS. The red spotted species *Goniobranchus splendidus, G. daphne*, *G. hunterae*, *Mexichromis mariei, M. festiva* and *Hypselodoris bennetti* formed a

close cluster of similar colour pattern characteristics (Figure 2) from the perspective of a potential predator. *Goniobranchus tasmaniensis* also clustered closely with this group, even though it does not have a yellow rim and spots are orange to human eyes. *Goniobranchus tinctorius* did not cluster close to the main species, presumably due to the presence of a reticulate pattern rather than well-defined spots. Partial red spotted species that did not cluster with the main group were *G. verrieri* and *G. albonares* but neither of these possessed a spotted pattern. Species that were placed in the non-mimic group were widely distributed in the plot. Therefore, our *a priori* groupings based on human vision appeared to be validated, with the exception of the exclusion of *G. tinctorius* and the inclusion of *G. tasmaniensis,* which may reflect differences between human and triggerfish vision.

Phylogenetic relatedness

The phylogeny generated and stochastic ancestral state reconstruction demonstrates that the red spot group occurs in six parts of the phylogenetic tree (Figure 3) with these included taxa. However, incomplete taxon sampling may affect the reconstruction for some groups, and more conservative estimates might be warranted. However, although the results indicates that shared ancestry may account for similarities in colour pattern for species within the genus *Goniobranchus* and between those in the genus *Mexichromis*, it would not do so between these genera or the other red spot species *Verconia haliclona*, or *Hypselodoris bennetti*. Thus, the red spot pattern has been independently acquired within the family Chromodorididae.

Chemical identification

Nudibranch species from the red spot mimicry group contained different compounds (Table 1). Species from the genus *Goniobranchus* possessed spongian diterpenes, rearranged

diterpenes, and norditerpenes as per [60], and there were significant differences in chemical profiles between species. Species from *Hypselodoris* and *Mexichromis* species possessed furanosesquiterpenes (Table 1), and the extracts of *M. festiva* from Nelson Bay and the Gold Coast possessed the same compounds. Compound names and structures are listed in Table S4.

Toxicity and palatability assays

Red spot species differed both in terms of toxicity and distastefulness (Figure 4). Species with extracts that were toxic to brine shrimp included *G. tasmaniensis*, *H. bennetti*, and *M. festiva* (Figure 4A). A dose response was also observed for the extract of *G. daphne*, but this response did not reach above 50% mortality, and no dose response was observed for *G. tinctorius* or *G. splendidus*. All extracts produced a dose response to the shrimp *Palaemon serenus*, though this response did not reach above 50% for the extract of *M. festiva* (Figure 4B). Importantly, using the phylogenetic generalised least square (GLS) regression model, we did not find an association between toxicity and distastefulness ($t_6 = 0.89$, $p = 0.42$; Figure S3).

Discussion

This study presents quantitative evidence of visual similarities between species in a putative mimicry group using colour and pattern analysis, and demonstrates that shared pattern elements of these co-occurring species are distinct from other, closely related species. Phylogenetic analysis indicates that this red spot pattern evolved at multiple times, suggesting this pattern has resulted from convergent evolution rather than shared ancestry. Members of the mimicry group possess different chemical profiles used for defensive purposes, and these suites of compounds provide unequal levels of defence in terms of a toxic response. However, the level of distastefulness of these compounds appears to be relatively similar to a marine

338 shrimp. These data therefore do not support the assumption that distasteful compounds
339 honestly signal levels of toxicity, at least in this mimicry system, and in many systems,
340 toxicity may not be related to distastefulness [25]. However, cumulative ingestion could be
341 toxic over time and cause incremental damage or illness. This study should encourage
342 researchers to disentangle terms such as toxicity and distastefulness as modes of chemical
343 defences when investigating aposematic and mimicry systems.

344 Many theoretical models of mimicry rings with unequal defences exist [e.g. 13, 56-
345 63]. Weakly defended co-mimics may degrade the warning signal of the model [15, 64]; for
346 instance, in an experiment using birds, an increase in abundance of a moderately defended
347 artificial prey increased per capita predation on both the mimic and the highly defended
348 model prey when population densities were low [15]. However, the relationship between
349 species with comparably weak defences and that of their co-mimics remains unclear. In
350 some studies, unequal defences still appear to be mutualistic [14, 65]. For example, highly
351 defended models coupled with moderately defended mimics can have a decrease in per capita
352 mortality when population densities are high [14].

353 However, the mode of chemical defence is often not defined in such models and
354 unequal defences in mimicry systems are sometimes only discussed in terms of quantity (but
355 see [29]). Prey that store distasteful, but otherwise non-toxic compounds that would not
356 damage or incur costs on the host, may repel predators due to their unpleasant nature.
357 Predators may quickly learn they are not harmed after consuming such prey and may still
358 consume distasteful prey when other food is scarce and predators are hungry [61, 62]. If
359 compounds are equally distasteful, we propose that predators may be unable to discriminate
360 levels of toxicity between species. Therefore, non-toxic species may benefit from resembling
361 their toxic counterparts, but not incur costs involved in harbouring toxins. It is also possible
362 that species may mimic the taste of toxic compounds with those that are non-toxic.

363 Our study species had very different chemical profiles: *Hypselodoris* and
364 *Mexichromis* nudibranchs contained furanosesquiterpenes while *Goniobranchus* nudibranchs
365 and Chromodorididae *thompsoni* contained spongian diterpenes, nor-diterpenes, and
366 rearranged diterpenes, which appeared to be less toxic than furanosesquiterpenes. Although
367 all chemical extracts in this study were distasteful to *Palaemon* shrimp, this effect was weak
368 for the extract of *M. festiva* (Nelson Bay), which did not induce a response to 50% of the
369 shrimp. *M. festiva* extracts were more concentrated, but contained fewer metabolites than that
370 of *H. bennetti*, which showed enhanced activity in both assays. Therefore, toxicity of these
371 extracts is instead likely to be largely influenced by differences in metabolites. did not test for
372 an emetic response, which has been shown before in nudibranch compounds [55]. From our
373 results, it appears that chemical defences, both in terms of palatability and of toxicity, are not
374 equal in this mimicry ring. Ideally, toxicity and unpalatability assays would have been
375 conducted on a potential fish predator of nudibranchs, as the response of different taxa to
376 particular compounds may be variable. However, there are considerable ethical implications
377 of conducting toxicity assays with vertebrates.

378 Our red spot mimetic species clustered together and shared very similar visual
379 characteristics; however, there are some species that shared only some visual similarities and
380 may be considered imperfect mimics. It is predicted that selection on quasi-Batesian mimicry
381 rings should be similar to Batesian systems, with an evolutionary arms race in warning signal
382 design between well-defended and weakly defended species [12, 63]. In this scenario species
383 with greater chemical defences would be selected to differentiate their warning signal from
384 those with weaker defences. However, this hypothesis was not supported in this system,
385 where the colour patterns of the two species with the most potent chemical defences (*G.*
386 *tasmaniensis* and *H. bennetti*) clustered well with other co-mimics. Alternatively, predators
387 may select for imperfect mimicry in complex Müllerian systems when defended and

388 palatable prey types are discriminated based on certain components of the visual signal [64],
389 with relaxed selection on other components of the visual signal that are generalized [65].
390 Indeed, we have recently shown that when learning a red spot / yellow rim colour pattern,
391 triggerfish paid most attention to the yellow border when learning to avoid distasteful food,
392 and disregarded the internal red pattern. We also found that the yellow rim was a more
393 consistent part of the visual signal in populations of *Goniobranchus splendidus*, although
394 there was considerable variation in the red spot component [33] . Highly contrasting body
395 outlines may help nudibranchs to stand out against their background and increase
396 conspicuousness, which is an important characteristic of warning signal designs [5].
397 However, this does not explain the lack of mantle border in five species in this study.
398 We believe that this is the first study of an aposematic mimicry ring to include
399 detailed chemical profiles and to assess both the toxicity and distastefulness of contributing
400 species. We have demonstrated that there may not be a correlation between toxicity and
401 distastefulness, and therefore highlight the importance of testing multiple modes of defence
402 to inform future models of mimicry systems. It is likely that warning signal designs and
403 chemical profiles vary geographically [56]; therefore, the impact of geographical differences
404 in dietary resources and predation pressure on warning signal design, chemical profiles, and
405 anti-predator activity of co-mimics would be an interesting direction for future research.
406
407 **Data accessibility**
408 Data will be made available through Dryad prior to publication.
409
410 **Competing interests**
411 We have no competing interests.
412

Author's contributions

AEW participated in fieldwork, lab-work, data analyses, design of the study, and drafted the manuscript; NGW participated the conception of the study, fieldwork, lab-work, data analyses, and drafting the manuscript. CPvdB participated in data analyses, MJH participated in data analyses and drafting the manuscript, JAE participated in data analyses, NJM advised on data analyses, AMW conducted lab-work and identified metabolites. MJG advised on lab-work, assisted with metabolite identification and participated in drafting the manuscript. KLC conceived of, coordinated, and designed the study, participated in fieldwork, lab-work, data analyses, and drafting the manuscript. All authors provided comments on final version and gave approval for publication.

Acknowledgements

We thank Rachael Templin, Derek Sun, and Will Feeney for help in the field and with spectral reflectance measurements, Holly Urquhart for help with antifeedant assays, and Kara Layton and Diana Prada for assistance with sequencing. This work was supported by The Australian Geographic Society, Experiment.com, The Australia & Pacific Science Foundation (APSF) (to K.L.C, M.J.G. and N.J.M.), UQ Postdoctoral Fellowship (to K.L.C), an Endeavour Postgraduate Award (to A.E.W), the Molecular Systematics Unit at the Western Australian Museum, The University of Queensland, and the Australian Research Council (grants awarded to K.L.C. and N.J.M.).

References

1. Poulton EB. 1890 *The colours of animals: their meaning and use, especially considered in the case of insects*. New York, NY, D. Appleton and Company.
2. Endler JA, Mappes J. 2004 Predator mixes and the conspicuousness of aposematic signals. *Am Nat* **163**(4), 532-547.

439 3. Mappes J, Marples N, Endler JA. 2005 The complex business of survival by
440 aposematism. *Trends Ecol Evol* **20**(11), 598-603.
441 4. Speed MP. 2000 Warning signals, receiver psychology and predator memory. *Anim*
442 *Behav* **60**(3), 269-278.
443 5. Ruxton GD, Sherratt TN, Speed MP. 2004 *Avoiding attack: the evolutionary ecology*
444 *of crypsis, warning signals, and mimicry*. Oxford, UK, Oxford University Press
445 6. Müller F. 1879 Ituna and Thyridia: a remarkable case of mimicry in butterflies. *Trans*
446 *Ent Soc Lond* **1879**, 20-29.
447 7. Stuckert AM, Venegas PJ, Summers K. 2014 Experimental evidence for predator
448 learning and Müllerian mimicry in Peruvian poison frogs (Ranitomeya, Dendrobatidae). *Evol*
449 *Ecol* **28**(3), 413-426.
450 8. Kapan DD. 2001 Three-butterfly system provides a field test of Müllerian mimicry.
451 *Nature* **409**(6818), 338-340.
452 9. Bates HW. 1862 Contributions to an insect fauna of the Amazon Valley. Lepidoptera:
453 Heliconidae. *Trans Linn Soc Lond* **23**(3), 495-566.
454 10. Balogh ACV, Gamberale-Stille G, Leimar O. 2008 Learning and the mimicry
455 spectrum: from quasi-Bates to super-Muller. *Anim Behav* **76**, 1591-1599.
456 (doi:10.1016/j.anbehav.2008.07.017).
457 11. Turner JR. 1987 The evolutionary dynamics of Batesian and Muellerian mimicry:
458 similarities and differences. *Ecol Entomol* **12**(1), 81-95.
459 12. Speed MP. 1993 Muellerian mimicry and the psychology of predation. *Anim Behav*
460 **45**(3), 571-580.
461 13. Rowland HM, Ihalainen E, Lindström L, Mappes J, Speed MP. 2007 Co-mimics have
462 a mutualistic relationship despite unequal defences. *Nature* **448**(7149), 64-67.
463 14. Rowland HM, Mappes J, Ruxton GD, Speed MP. 2010 Mimicry between unequally
464 defended prey can be parasitic: evidence for quasi-Batesian mimicry. *Ecol Lett* **13**(12), 1494-
465 1502.
466 15. Arias M, Mappes J, Thery M, Llaurens V. 2016 Inter-species variation in
467 unpalatability does not explain polymorphism in a mimetic species. *Evol Ecol* **30**(3), 419-
468 433. (doi:10.1007/s10682-015-9815-2).
469 16. Brower LP, Brower JVZ, Collins CT. 1963 Experimental studies of mimicry: Relative
470 palatability and Müllerian mimicry among Neotropical butterflies of the subfamily
471 Heliconiinae. *Zoologica* **48**, 65-84.

17. Bowers MD, Farley S. 1990 The behaviour of grey jays, *Perisoreus canadensis*, towards palatable and unpalatable Lepidoptera. *Anim Behav* **39**(4), 699-705.
18. Sargent TD. 1995 On the relative acceptabilities of local butterflies and moths to local birds. *J Lepid Soc* **49**(2), 148-162.
19. Amézquita A, Ramos O, Gonzalez MC, Rodriguez C, Medina I, Simoes PI, Lima AP. 2017 Conspicuousness, color resemblance, and toxicity in geographically diverging mimicry: The pan-Amazonian frog *Allobates femoralis*. *Evolution* **71**(4), 1039-1050. (doi:10.1111/evo.13170).
20. Darst CR, Cummings ME. 2006 Predator learning favours mimicry of a less-toxic model in poison frogs. *Nature* **440**(7081), 208-211.
21. Darst CR, Cummings ME, Cannatella DC. 2006 A mechanism for diversity in warning signals: Conspicuousness versus toxicity in poison frogs. *Proc Natl Acad Sci U S A* **103**(15), 5852-5857.
22. Marples NM. 1993 Toxicity assays of ladybirds using natural predators. *Chemoecology* **4**(1), 33-38.
23. Alatalo RV, Mappes J. 1996 Tracking the evolution of warning signals. *Nature* **382**(6593), 708.
24. Ruxton GD, Kennedy MW. 2006 Peppers and poisons: the evolutionary ecology of bad taste. *J Anim Ecol* **75**(5), 1224-1226. (doi:10.1111/j.1365-2656.2006.01133.x).
25. Pawlik JR. 2012 Antipredatory defensive roles of natural products from marine invertebrates. In *Handbook of Marine Natural Products* (eds. Fattorusso W., Gerwick W.H., Taglialatela-Scafati O.), pp. 677-710, Springer Netherlands.
26. Glendinning JI. 1994 Is the bitter rejection response always adaptive. *Physiol Behav* **56**(6), 1217-1227. (doi:Doi 10.1016/0031-9384(94)90369-7).
27. Glendinning JI. 2007 How do predators cope with chemically defended foods? *Biol Bull-Us* **213**(3), 252-266.
28. Turner JR, Kearney EP, Exton LS. 1984 Mimicry and the Monte Carlo predator: the palatability spectrum, and the origins of mimicry. *Biol J Linn Soc* **23**(2-3), 247-268.
29. Holen OH. 2013 Disentangling taste and toxicity in aposematic prey. *P Roy Soc B-Biol Sci* **280**(1753).
30. Rudman W. 1991 Purpose in pattern: the evolution of colour in chromodorid nudibranchs. *J Molluscan Stud* **57**(Supplement Part 4), 5-21.

504 31. Rudman WB. 1983 The Chromodorididae (Opisthobranchia, Mollusca) of the Indo-
505 West Pacific - *Chromodoris splendida*, *Chromodoris aspersa* and *Hypselodoris placida*
506 Color Groups. *Zool J Linn Soc* **78**(2), 105-173. (doi: 10.1111/J.1096-3642.1983.Tb00864.X).
507 32. Cimino G, Ghiselin MT. 2009 *Chemical defense and the evolution of opisthobranch*
508 *gastropods*. San Francisco, California, California Academy of Sciences.
509 33. Winters AE, Green NF, WIlson NG, How MJ, Garson MJ, Marshall NJ, Cheney KL.
510 2017 Stabilizing selection on individual pattern elements of aposematic signals. *P Roy Soc B-*
511 *Biol Sci* **284**(1861), 20170926. (doi:10.1098/rspb.2017.0926).
512 34. Wilson NG, Maschek JA, Baker BJ. 2013 A species flock driven by predation?
513 Secondary metabolites support diversification of slugs in Antarctica. *PLoS ONE* **8**(11),
514 e80277. (doi:10.1371/journal.pone.0080277).
515 35. Kalyaanamoorthy S, Minh BQ, Wong TKF, von Haeseler A, Jermiin LS. 2017
516 ModelFinder: fast model selection for accurate phylogenetic estimates. *Nat Methods* **14**(6),
517 587-+.
518 36. Nguyen LT, Schmidt HA, von Haeseler A, Minh BQ. 2015 IQ-TREE: A fast and
519 effective stochastic algorithm for estimating Maximum-Likelihood phylogenies. *Mol Biol*
520 *Evol* **32**(1), 268-274.
521 37. Hoang DT, Chernomor O, von Haeseler A, Minh BQ, Vinh LS. 2018 UFBoot2:
522 Improving the ultrafast bootstrap approximation. *Mol Biol Evol* **35**(2), 518-522.
523 38. Hallas JM, Chichvarkhin A, Gosliner TM. 2017 Aligning evidence: concerns
524 regarding multiple sequence alignments in estimating the phylogeny of the Nudibranchia
525 suborder Doridina. *Roy Soc Open Sci* **4**(10).
526 39. Huelsenbeck JP, Nielsen R, Bollback JP. 2003 Stochastic mapping of morphological
527 characters. *Syst Biol* **52**(2), 131-158. (doi:/10.1080/10635150390192780).
528 40. Maddison WP, Maddison DR. 2017 Mesquite: a modular system for evolutionary
529 analysis. (3.2 ed. http://mesquiteproject.org/.
530 41. Cheney KL, Newport C, McClure EC, Marshall NJ. 2013 Colour vision and response
531 bias in a coral reef fish. *J Exp Biol* **216**(15), 2967-2973.
532 42. Losey G, McFarland W, Loew E, Zamzow J, Nelson P, Marshall N, Montgomery W.
533 2003 Visual biology of Hawaiian coral reef fishes. I. Ocular transmission and visual
534 pigments. *Copeia* **2003**(3), 433-454.
535 43. Vorobyev M, Osorio D. 1998 Receptor noise as a determinant of colour thresholds. *P*
536 *Roy Soc B-Biol Sci* **265**(1394), 351-358.

537 44. Cheney KL, Marshall NJ. 2009 Mimicry in coral reef fish: how accurate is this
538 deception in terms of color and luminance? *Behav Ecol* **20**(3), 459-468.
539 45. Siebeck UE, Wallis GM, Litherland L, Ganeshina O, Vorobyev M. 2014 Spectral and
540 spatial selectivity of luminance vision in reef fish. *Front Neural Circuit* **8**.
541 46. Endler JA. 1990 On the measurement and classification of color in studies of animal
542 color patterns. *Biol J Linn Soc* **41**(4), 315-352.
543 47. Endler JA, Houde AE. 1995 Geographic variation in female preferences for male
544 traits in *Poecilia reticulata*. *Evolution* **49**(3), 456-468.
545 48. Endler JA. 2012 A framework for analysing colour pattern geometry: adjacent
546 colours. *Biol J Linn Soc* **107**(2), 233-253.
547 49. Oksanen J, Blanchet FG, Kindt R, Legendre P, Minchin P, O'Hara R, Simpson G,
548 Solymos P, Stevens M, Wagner H. 2013 Vegan: Community ecology package. R package
549 version 2.0-10.
550 50. Team RC. 2013 R: A language and environment for statistical computing. (Vienna,
551 Austria, R Foundation for Statistical Computing. URL http://www.r-project.org/.
552 51. Cheney KL, White A, Mudianta IW, Winters AE, Quezada M, Capon RJ, Mollo E,
553 Garson MJ. 2016 Choose your weaponry: selective storage of a single toxic compound,
554 latrunculin A, by closely related nudibranch molluscs. *PLoS ONE* **11**(1).
555 52. Thompson JE, Walker RP, Faulkner DJ. 1985 Screening and bioassays for
556 biologically active substances from 40 marine sponge species from San-Diego, California,
557 USA. *Mar Biol* **88**(1), 11-21.
558 53. Abbott WS. 1925 A method of computing the effectiveness of an insecticide. *J Econ*
559 *Entomol* **18**, 265-267.
560 54. Carbone M, Gavagnin M, Haber M, Guo YW, Fontana A, Manzo E, Genta-Jouve G,
561 Tsoukatou M, Rudman WB, Cimino G, et al. 2013 Packaging and delivery of chemical
562 weapons: A defensive Trojan Horse stratagem in Chromodorid nudibranchs. *PLoS ONE* **8**(4),
563 e62075.
564 55. Giordano G, Carbone M, Ciavatta ML, Silvano E, Gavagnin M, Garson MJ, Cheney
565 KL, Mudianta IW, Russo GF, Villani G, et al. 2017 Volatile secondary metabolites as
566 aposematic olfactory signals and defensive weapons in aquatic environments. *Proc Natl Acad*
567 *Sci U S A* **114**(13), 3451-3456.
568 56. Winters AE. 2016 Understanding colour and chemical diversity in nudibranchs
569 [PhD], The University of Queensland.

570 57. Mollo E, Gavagnin M, Carbone M, Castelluccio F, Pozone F, Roussis V, Templado J,
571 Ghiselin MT, Cimino G. 2008 Factors promoting marine invasions: a chemoecological
572 approach. *Proc Natl Acad Sci U S A* **105**(12), 4582-4586.
573 58. Paradis E, Claude J, Strimmer K. 2004 APE: analyses of phylogenetics and evolution
574 in R language. *Bioinformatics* **20**, 289-290.
575 59. Felsenstein J. 1985 Phylogenies and the Comparative Method. *Am Nat* **125**(1), 1-15.
576 60. Keyzers RA, Northcote PT, Davies-Coleman MT. 2006 Spongian diterpenoids from
577 marine sponges. *Nat Prod Rep* **23**(2), 321-334.
578 61. Skelhorn J, Rowe C. 2007 Predators' toxin burdens influence their strategic decisions
579 to eat toxic prey. *Curr Biol* **17**(17), 1479-1483.
580 62. Sherratt TN, Speed MP, Ruxton GD. 2004 Natural selection on unpalatable species
581 imposed by state-dependent foraging behaviour. *J Theor Biol* **228**(2), 217-226.
582 63. Huheey JE. 1988 Mathematical models of mimicry. *Am Nat* **131**, S22-S41.
583 64. Beatty CD, Beirinckx K, Sherratt TN. 2004 The evolution of Müllerian mimicry in
584 multispecies communities. *Nature* **431**(7004), 63-66.
585 65. Chittka L, Osorio D. 2007 Cognitive dimensions of predator responses to imperfect
586 mimicry. *PLoS Biol* **5**, e339.
587
588

589 **Figure Legends**

590 **Figure 1.** Representative photographs of the putative mimicry species investigated in this
591 study. **Top panel:** Full pattern including yellow-orange mantle border, white mantle, and
592 spots. **Bottom panel:** partial pattern missing either spots or border. From upper left:
593 *Goniobranchus splendidus* (A), *Goniobranchus tinctorius* (B), *Goniobranchus daphne* (C),
594 *Goniobranchus hunterae* (D), *Mexichromis mariei* (E), *Mexichromis festiva* (F),
595 *Hypselodoris bennetti* (G), *Verconia haliclona* (H), *Goniobranchus verrieri* (I),
596 *Goniobranchus albonares* (J), *Goniobranchus tasmaniensis* (K), Chromodorididae *thompsoni*
597 (L).
598
599 **Figure 2.** Nudibranch colour patterns differentiated in ordinal space (NMDS) based on 14
600 metrics of the hue, chroma and luminance of colour pattern element and overall nudibranch
601 pattern geometry. The *a priori* predicted red spotted group is shown in red. Partial red
602 spotted pattern species are shown in orange and non-red spot group are shown in black. The
603 red ellipse shows the clustering of many red spotted species.
604
605 **Figure 3.** Maximum-likelihood topology of Chromodorididae taxa. Species that were
606 assigned to a red spotted group are shown in red, the partial red spot group in orange, and
607 those not assigned to the non-red spot group in blue. Bootstrap values are shown for clades
608 with over 70% support. Ancestral state reconstruction of the red colour pattern was
609 performed using ML analysis and marginal probability reconstruction with model Mk1
610 (rate 0.24 Log likelihood, −54.77).
611
612
613 **Figure 4. a*) Toxicity assay:*** LD_{50} values based on mortality of Brine shrimp, *Artemia* sp. ***b)***
614 **Anti-feedant assay**. ED_{50} values based on rejection of pellets by Palaemon shrimp,
615 *Palaemon serenus*. Values are represented as proportion of natural concentration found in the
616 mantle of the nudibranchs. Circles indicate LD_{50} values calculated from the data, nr indicate
617 no response at the highest concentration tested. Absolute concentrations are shown in Figure
618 S2.
619
620
621

Figure 1.

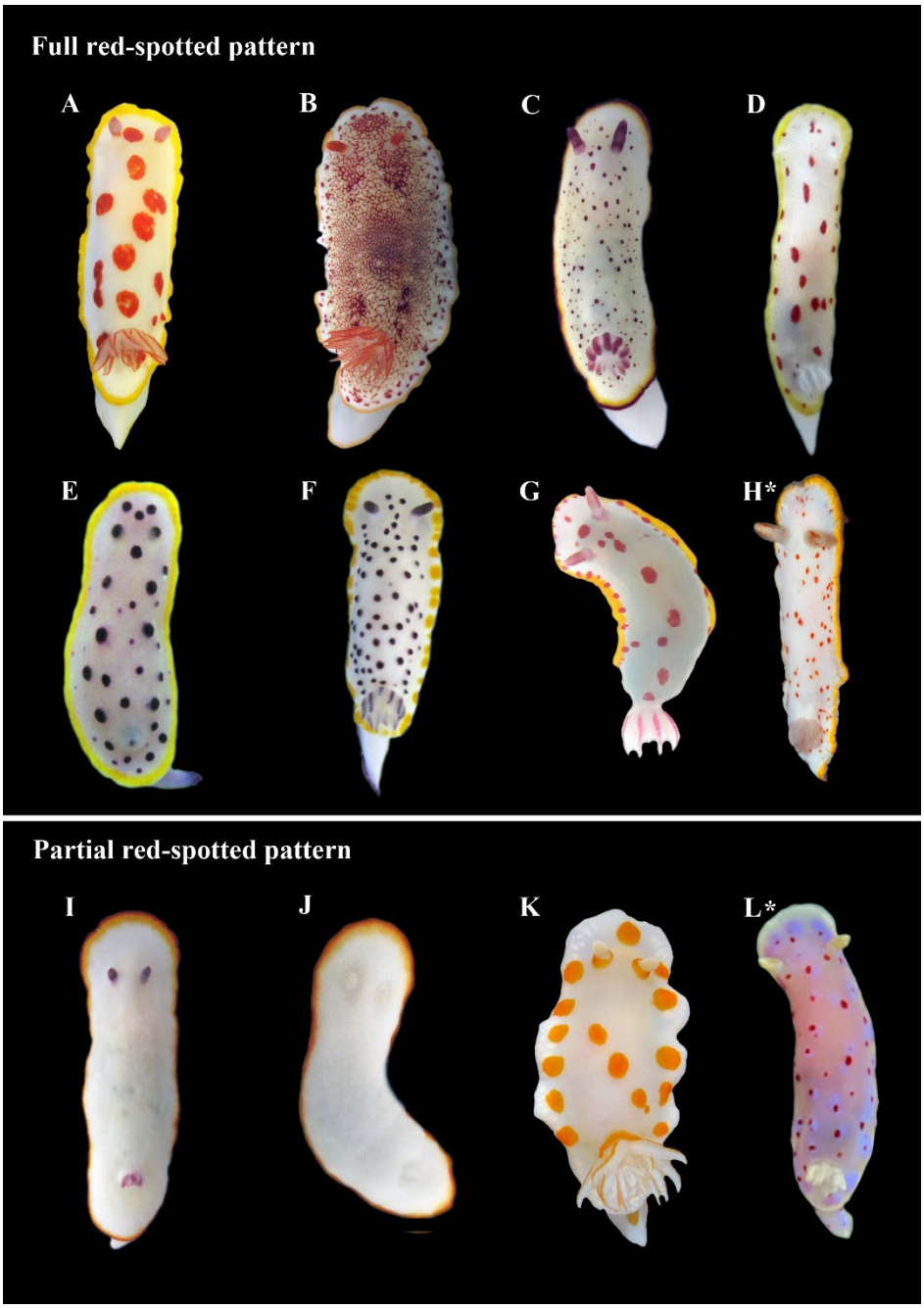
Full red-spotted pattern
A
B
C
D
E
F
G
H*
Partial red-spotted pattern
I
J
K
L*

Figure 2.

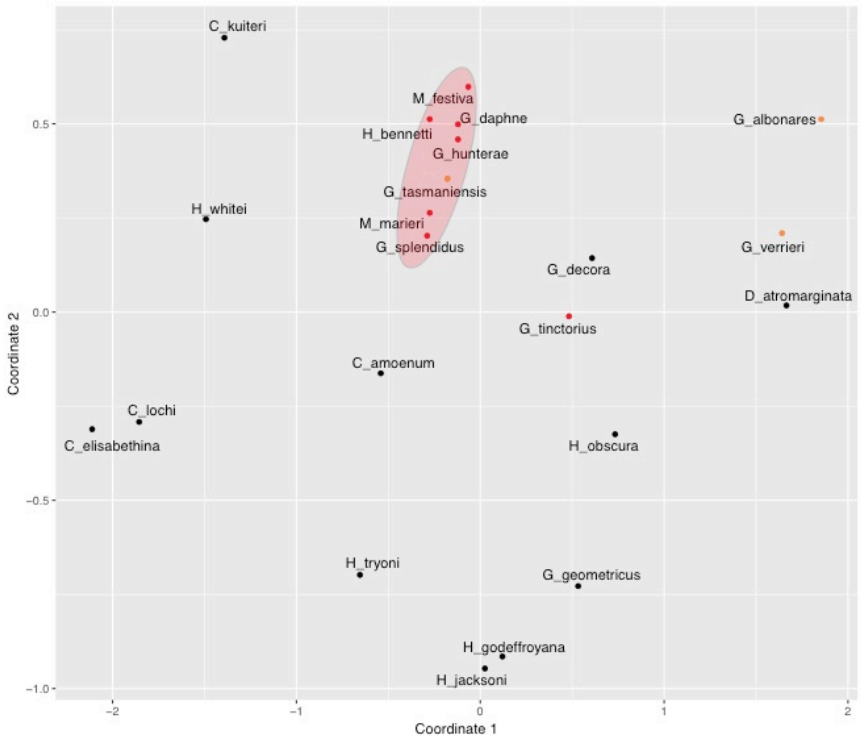
C_kuiteri
M_festiva
G_daphne
H_bennetti
G_hunterae
G_albonares
G_tasmaniensis
H_whitei
M_marieri
G_splendidus
G_verrieri
G_decora
D_atromarginata
G_tinctorius
C_amoenum
C_lochi
C_elisabethina
H_obscura
H_tryoni
G_geometricus
H_godeffroyana
H_jacksoni
Coordinate 2
Coordinate 1
0.5
0.0
−0.5
−1.0
−2
−1
0
1
2

Figure 3.

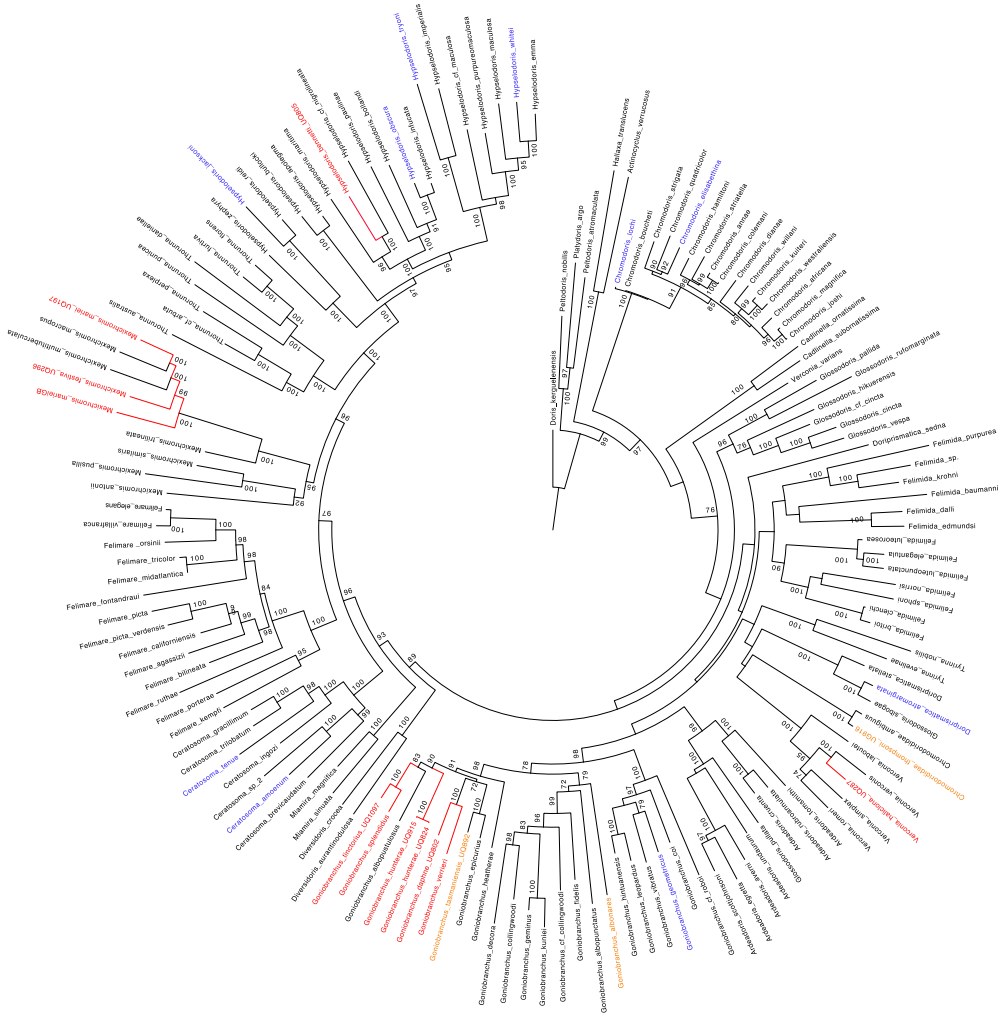
Hypseelodoris_emma
Hypseelodoris_whitei
Hypseelodoris_maculosa
Hypseelodoris_sanctaecrucensis
Hypseelodoris_d_tuvu
Hypselodoris_tryoni
Hypselodoris_rubrolineata
Hypselodoris_d_capricornia
Hypselodoris_bullocki
Hypselodoris_obscura
Hypselodoris_infucata
Hypselodoris_d_ligulifera
Hypselodoris_d_quinnamata
Hypselodoris_Dominica_LQ855
Hypselodoris_nuanua
Hypselodoris_apolegma
Hypselodoris_rubi
Hypselodoris_agassizii
Hypselodoris_royoi
Hypselodoris_aurae
Hypselodoris_picta
Hypselodoris_zephyra
Hypselodoris_bennetti
Thorunna_d_arturi
Thorunna_aurae
Thorunna_papposa
Thorunna_purpurea
Thorunna_royoi
Thorunna_nivea
Thorunna_daneae
Mexichromis_aurantiaca
Mexichromis_multituberculata
Mexichromis_marcgrave
Mexichromis_mariae_U0197
Mexichromis_bertha_U0298
Mexichromis_mariae_U0168
Mexichromis_antonii
Mexichromis_pusilla
Mexichromis_similaris
Mexichromis_villenata
Felimare_edgens
Felimare_villafranca
Felimare_orsinii
Felimare_tricolor
Felimare_midatlantica
Felimare_fontandraui
Felimare_picta
Felimare_picta_verdensis
Felimare_californiensis
Felimare_agassizii
Felimare_bilineata
Felimare_ruthae
Felimare_porterae
Felimare_kempfi
Ceratosoma_gracillimum
Ceratosoma_trilobatum
Ceratosoma_tenue
Ceratosoma_ingozi
Ceratosoma_sp_2
Ceratosoma_amoenum
Ceratosoma_brevicaudatum
Miamira_magnifica
Miamira_sinuata
Diversidoris_aurantiodolorosa
Diversidoris_crocea
Gondobranchus_fontinica_UQ1009
Gondobranchus_splendidus
Gondobranchus_allopolitanus
Gondobranchus_kuniense_LQ915
Gondobranchus_kuniense_LQ903
Gondobranchus_kuniense_LQ902
Gondobranchus_kuniense_LQ901
Gondobranchus_vernieri_LQ900
Gondobranchus_ephoronus
Gondobranchus_hadenense
Gymnodoris_alba
Gymnodoris_striata
Gymnodoris_d_rubra
Gymnodoris_d_colombiensis
Gymnodoris_d_rubropapillata
Gymnodoris_d_rubrocincta
Gymnodoris_d_rubrolineata
Gymnodoris_d_rubrocornuta
Gymnodoris_d_rubrocerata
Gymnodoris_d_rubrofrontalis
Gymnodoris_d_rubrocaudata
Gymnodoris_d_rubrocapensis
Gymnodoris_d_rubrocaerulea
Gymnodoris_d_rubrocandida
Gymnodoris_d_rubrocaledonica
Gymnodoris_d_rubrocinnabarina
Gymnodoris_d_rubrocinnamomea
Gymnodoris_d_rubrocingulata
Gymnodoris_d_rubrocitrina
Gymnodoris_d_rubrocoerulea
Gymnodoris_d_rubrocoralliphila
Gymnodoris_d_rubrocornea
Gymnodoris_d_rubrocruenta
Gymnodoris_d_rubrocyanea
Gymnodoris_d_rubrodiadema
Gymnodoris_d_rubrodigitata
Gymnodoris_d_rubrodorsalis
Gymnodoris_d_rubroelegans
Gymnodoris_d_rubroflammea
Gymnodoris_d_rubrofulgens
Gymnodoris_d_rubrogemmata
Gymnodoris_d_rubrogranulosa
Gymnodoris_d_rubrohamata
Gymnodoris_d_rubrohirsuta
Gymnodoris_d_rubrohispida
Gymnodoris_d_rubrohyalina
Gymnodoris_d_rubroinsignis
Gymnodoris_d_rubrojacksoni
Gymnodoris_d_rubrolaevis
Gymnodoris_d_rubrolamellata
Gymnodoris_d_rubrolanata
Gymnodoris_d_rubrolentiginosa
Gymnodoris_d_rubrolepida
Gymnodoris_d_rubrolineata
Gymnodoris_d_rubrolobata
Gymnodoris_d_rubrolongicirrata
Gymnodoris_d_rubrolucida
Gymnodoris_d_rubrolutea
Gymnodoris_d_rubromaculata
Gymnodoris_d_rubromarginata
Gymnodoris_d_rubromaxima
Gymnodoris_d_rubromedia
Gymnodoris_d_rubromelanocephala
Gymnodoris_d_rubromelanogrammata
Gymnodoris_d_rubromelanopleura
Gymnodoris_d_rubromelanopus
Gymnodoris_d_rubromelanosticta
Gymnodoris_d_rubromicrocerata
Gymnodoris_d_rubromicrotuberculata
Gymnodoris_d_rubromilitaris
Gymnodoris_d_rubromimetica
Gymnodoris_d_rubrominuta
Gymnodoris_d_rubromirabilis
Gymnodoris_d_rubromitis
Gymnodoris_d_rubromollis
Gymnodoris_d_rubromonilifera
Gymnodoris_d_rubromorosa
Gymnodoris_d_rubromucosa
Gymnodoris_d_rubromultifida
Gymnodoris_d_rubromultilineata
Gymnodoris_d_rubromultiramosa
Gymnodoris_d_rubromuricata
Gymnodoris_d_rubromurrayi
Gymnodoris_d_rubromuscosa
Gymnodoris_d_rubromutabilis
Gymnodoris_d_rubromyrmecophila
Gymnodoris_d_rubronebulosa
Gymnodoris_d_rubronigrocincta
Gymnodoris_d_rubronigrocristata
Gymnodoris_d_rubronigrodigitata
Gymnodoris_d_rubronigrolineata
Gymnodoris_d_rubronigrolutea
Gymnodoris_d_rubronigromaculata
Gymnodoris_d_rubronigromarginata
Gymnodoris_d_rubronigromedia
Gymnodoris_d_rubronigrotuberculata
Gymnodoris_d_rubronodosa
Gymnodoris_d_rubronotata
Gymnodoris_d_rubronovaezelandiae
Gymnodoris_d_rubronubila
Gymnodoris_d_rubronucleata
Gymnodoris_d_rubroocellata
Gymnodoris_d_rubroocularis
Gymnodoris_d_rubroornata
Gymnodoris_d_rubropapillata
Gymnodoris_d_rubroparva
Gymnodoris_d_rubropedata
Gymnodoris_d_rubropelagica
Gymnodoris_d_rubropellucida
Gymnodoris_d_rubropenicillata
Gymnodoris_d_rubroperforata
Gymnodoris_d_rubroperlucida
Gymnodoris_d_rubropersonata
Gymnodoris_d_rubropetechialis
Gymnodoris_d_rubrophaeostoma
Gymnodoris_d_rubrophilippinensis
Gymnodoris_d_rubrophoenicea
Gymnodoris_d_rubrophotogenica
Gymnodoris_d_rubropicta
Gymnodoris_d_rubropilosa
Gymnodoris_d_rubropinnata
Gymnodoris_d_rubroplicata
Gymnodoris_d_rubropolycera
Gymnodoris_d_rubropolyphylla
Gymnodoris_d_rubroporosa
Gymnodoris_d_rubroprasina
Gymnodoris_d_rubroprolifera
Gymnodoris_d_rubropsychedelica
Gymnodoris_d_rubropulchra
Gymnodoris_d_rubropulchrocincta
Gymnodoris_d_rubropulchrodigitata
Gymnodoris_d_rubropulchrolineata
Gymnodoris_d_rubropulchrolutea
Gymnodoris_d_rubropulchromaculata
Gymnodoris_d_rubropulchromarginata
Gymnodoris_d_rubropulchromedia
Gymnodoris_d_rubropulchrotuberculata
Gymnodoris_d_rubropunctata
Gymnodoris_d_rubropurpurea
Gymnodoris_d_rubroquadrata
Gymnodoris_d_rubroquinquelineata
Gymnodoris_d_rubroradiata
Gymnodoris_d_rubroramosa
Gymnodoris_d_rubrorectangulata
Gymnodoris_d_rubrorhinophora
Gymnodoris_d_rubrorosea
Gymnodoris_d_rubrorotundata
Gymnodoris_d_rubrorubra
Gymnodoris_d_rubrosanguinea
Gymnodoris_d_rubroscabra
Gymnodoris_d_rubroscripta
Gymnodoris_d_rubrosculptura
Gymnodoris_d_rubrosimplex
Gymnodoris_d_rubrosinuata
Gymnodoris_d_rubrospinosa
Gymnodoris_d_rubrostellata
Gymnodoris_d_rubrostigmatica
Gymnodoris_d_rubrostriata
Gymnodoris_d_rubrosubmarginata
Gymnodoris_d_rubrosubmedia
Gymnodoris_d_rubrosubtuberculata
Gymnodoris_d_rubrotaeniata
Gymnodoris_d_rubrotentaculata
Gymnodoris_d_rubrotessellata
Gymnodoris_d_rubrotricolor
Gymnodoris_d_rubrotuberculata
Gymnodoris_d_rubroundulata
Gymnodoris_d_rubrovariegata
Gymnodoris_d_rubrovenosa
Gymnodoris_d_rubroverrucosa
Gymnodoris_d_rubrovesiculata
Gymnodoris_d_rubrovirgata
Gymnodoris_d_rubrovirgulata
Gymnodoris_d_rubrovirgultifera
Gymnodoris_d_rubrovirgultifera
Gymnodoris_d_rubrovirgultifera

Figure 4.

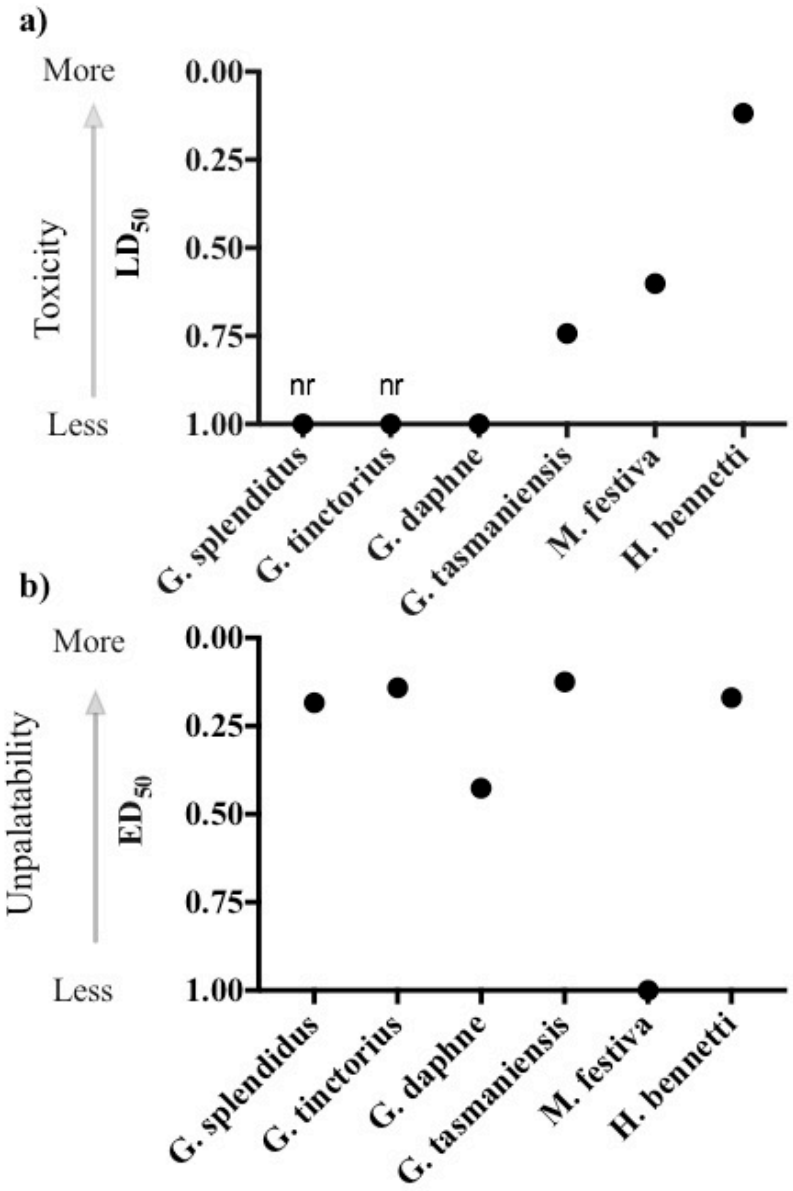
a)
More
Toxicity
Less
LD50
0.00
0.25
0.50
0.75
1.00
nr
nr
G. splendidus
G. tinctorius
G. daphne
G. tasmaniensis
M. festiva
H. bennetti
b)
More
Unpalatability
Less
ED50
0.00
0.25
0.50
0.75
1.00
G. splendidus
G. tinctorius
G. daphne
G. tasmaniensis
M. festiva
H. bennetti

Table 1.

	Species	Type	Crude mg/ml
Red-spot mimicry species	*Goniobranchus splendidus*	A, B, C, D	32.4
	Goniobranchus tinctorius	A, B	19.9
	Goniobranchus daphne	B, C	12.3
	Goniobranchus hunterae	B	35.0
	Mexichromis mariei	E	15.3
	Mexichromis festiva	E	17.8 (gcbs) 29.2 (nbps)
	Hypselodoris bennetti	E	15.2
	Veronica haliclona	NA	NA
Partial red-spot species	*Goniobranchus verrieri*	B, C	19.3
	Goniobranchus albonares	NA	NA
	Goniobranchus tasmaniensis	A, B	37.6
	Chromodorididae *thompsoni*	B	19.1

Appendix E - Animal Ethics Approval Form

THE UNIVERSITY OF QUEENSLAND
AUSTRALIA

Office of Research Ethics
Director
Nicole Shively

Animal Ethics Approval Certificate

20-Sep-2017

Please check all details below and inform the Animal Ethics Unit within 10 working days if anything is incorrect.

Activity Details

Chief Investigator:	Dr Karen Cheney, Biological Sciences
Title:	How do fish perceive and learn colour patterns in the marine environment?
AEC Approval Number:	SBS/077/17
Previous AEC Number:	SBS/111/14/ARC
Approval Duration:	28-Jun-2017 to 28-Jun-2020
Funding Body:	ARC
Group:	Native and exotic wildlife and marine animals
Other Staff/Students:	Justin Marshall, Erin Watson, Laurie Mitchell, Fabio Cortesi, Cedric van den Berg, Naomi Green
Location(s):	St Lucia Bldg 8 - Goddard Moreton Bay Research Centre

Summary

Subspecies	Strain	Class	Gender	Source	Approved	Remaining
Fish	Rhinecanthus sp. (Balistidae)	Adults	Unknown		350	350
Fish	Damsel (Pomacentridae)	Adults	Unknown		300	300
Fish	Tetractenos sp. (Tetradontidae)	Adults	Unknown		200	200

Permits

Provisos

Collection within the Moreton Bay area is not permitted under this protocol until permits have been received and provided to the AEU.

Approval Details

Description	Amount	Balance
Fish (Damsel (Pomacentridae), Unknown, Adults,)		
28 Jun 2017 Initial approval	300	300
Fish (Rhinecanthus sp. (Balistidae), Unknown, Adults,)		
28 Jun 2017 Initial approval	350	350
Fish (Tetractenos sp. (Tetradontidae), Unknown, Adults,)		
28 Jun 2017 Initial approval	200	200

Animal Ethics Unit
Office of Research Ethics
The University of Queensland

Cumbrae-Stewart Building
Research Road
St Lucia Qld 4072 Australia

+61 7 336 52925 (Enquiries)
+61 7 334 68710 (Enquiries)
+61 7 336 52713 (Coordinator)

animal.ethics@research.uq.edu.au
uq.edu.au/research

Please note the animal numbers supplied on this certificate are the total allocated for the approval duration

Please use this Approval Number:

1. When ordering animals from Animal Breeding Houses
2. For labelling of all animal cages or holding areas. In addition please include on the label, Chief Investigator's name and contact phone number.
3. When you need to communicate with this office about the project.

It is a condition of this approval that all project animal details be made available to Animal House OIC.
(UAEC Ruling 14/12/2001)

The Chief Investigator takes responsibility for ensuring all legislative, regulatory and compliance objectives are satisfied for this project.

This certificate supercedes all preceeding certificates for this project (i.e. those certificates dated before 20-Sep-2017)

Literature Cited

Adelson, E. H. (1993). Perceptual organization and the judgment of brightness. *Science*, *262*(5142), 2042. doi:10.1126/science.8266102

Adelson, E. H. (2000). Lightness perception and lightness illusions. *The New Cognitive Neurosciences*, *3*, 339–351. doi:10.1068/p230869

Alatalo, R. V., & Mappes, J. (1996). Tracking the evolution of warning signals. *Nature*, *382*(6593), 708–710. doi:10.1038/382708a0

Allen, W. L., & Higham, J. P. (2013). Analyzing visual signals as visual scenes. *American Journal of Primatology*, *75*(7), 664–682. doi:10.1002/ajp.22129

Allen, W. L., Moreno, N., Gamble, T., & Chiari, Y. (2019). Ecological, behavioral, and phylogenetic influences on the evolution of dorsal color pattern in geckos. *Evolution*, 1–15. doi:10.1111/evo.13915

Amey, A., Worthington Wilmer, J., Blomberg, S., & Couper, P. (2018). Range extension and genetic structure of the narrowly-restricted slider skink, Lerista rochfordensis Amey and Couper, 2009 (Reptilia: Scincidae). *Memoirs of the Queensland Museum - Nature*, *61*(1), 29–41. doi:10.17082/j.2204-1478.61.2018.2017-09

Anderson, B. L. (2011). Visual perception of materials and surfaces. *Current Biology*, *21*(24), R978–R983. doi:10.1016/j.cub.2011.11.022

Arenas, L. M., Troscianko, J., & Stevens, M. (2014). Color contrast and stability as key elements for effective warning signals. *Frontiers in Ecology and Evolution*, *2*(June), 1–12. doi:10.3389/fevo.2014.00025

Aronsson, M., & Gamberale-Stille, G. (2013). Evidence of signaling benefits to contrasting internal color boundaries in warning coloration. *Behavioral Ecology*, *24*(2), 349–354. doi:10.1093/beheco/ars170

Arrese, C. A., Hart, N. S., Thomas, N., Beazley, L. D., & Shand, J. (2002). Trichromacy in Australian marsupials. *Current Biology*, *12*(02), 657–660.

Aurorès-Weber, A., de Brito Sanchez, M. G., Giurfa, M., & Dyer, A. G. (2010). Aversive reinforcement improves visual discrimination learning in free-flying honeybees. *PLoS ONE*, *5*(10). doi:10.1371/journal.pone.0015370

Backhaus, W. (1991). Color opponent coding in the visual system of the honeybee. *Vision Research*, *31*(7–8), 1381–1397. doi:10.1016/0042-6989(91)90059-E

Baden, T., & Osorio, D. (2019). The retinal basis of vertebrate color vision. *Annual Review of Vision Science*, *5*(1), 1–24. doi:10.1146/annurev-vision-091718-014926

Bandaranayake, W. M. (2006). The nature and role of pigments of marine invertebrates. *Natural Product Reports*, *23*(2), 223–255. doi:10.1039/b307612c

Barnett, J. B., & Cuthill, I. C. (2015). Distance-dependent defensive coloration. *Current Biology*, *24*(24), R1157–R1158. doi:10.1016/j.cub.2014.11.015

Barnett, J. B., Scott-samuel, N. E., Cuthill, I. C., & Barnett, J. B. (2016). Aposematism : balancing salience and camouflage. doi:10.1098/rsbl.2016.0335

Barth, J. (1964). Intracellular recordings from photoreceptor neurons in the eyes of a nudibranch mollusc (Hermissenda crassicornis). *Comparative Biochemistry and Physiology*, *11*, 311–315.

Baylor, D. A., Hodgkin, A. L., & Lamb, T. D. (1974). The electrical response of turtle cones to flashes and steps of light. *The Journal of Physiology*, *242*(3), 685–727. doi:10.1113/jphysiol.1974.sp010731

Behrens, D. W., Petrinos, C., & Schrurs, C. (2005). *Nudibranch Behaviour*. Jacksonville, Fla: New World Publications.

Benjamini, Y., & Hochberg, Y. (1995). Controlling the false discovery rate: a practical and powerful approach to multiple testing. *Journal of the Royal Statistical Society: Series B (Methodological)*, *57*(1), 289–300. doi:10.1111/j.2517-6161.1995.tb02031.x

Bex, P. J., & Makous, W. (2002). Spatial frequency, phase, and the contrast of natural images. *Journal of the Optical Society of America A*, *19*(6), 1096. doi:10.1364/JOSAA.19.001096

Bland, j. M., & Altman, D. G. (1995). Multiple significance tests: the Bonferroni method. *BMJ*, *310*(6973), 170. doi:10.1136/bmj.310.6973.170

Boos, D. D. (2003). Introduction to the bootstrap world. *Statistical Science*, *18*(2), 168–174. doi:10.1214/ss/1063994971

Bouchet, P., Rocroi, J.-P., Hausdorf, B., Kaim, A., Kano, Y., Nützel, A., … Strong, E. E. (2017). Revised classification, nomenclator and typification of gastropod and monoplacophoran families. *Malacologia*, *61*(1–2), 1–526. doi:10.4002/040.061.0201

Bowen, R. W., Pokorny, J., & Smith, V. C. (1989). Sawtooth contrast sensitivity: decrements have the edge. *Vision Research*, *29*(11), IN1-1509. doi:https://doi.org/10.1016/0042-6989(89)90134-X

Bowmaker, J. K., Heath, L. A., Wilkie, S. E., & Hunt, D. M. (1997). Visual pigments and oil droplets from six classes of photoreceptor in the retinas of birds. *Vision Research*, *37*(16), 2183–2194. doi:10.1016/S0042-6989(97)00026-6

Bradburry, J. W., & Vehrencamp, S. L. (2011). *Principles of animal communication* (Second Edi). Sunderland, Massachusetts: Sinauer Associates.

Bradley, a, & Ohzawa, I. (1986). A comparison of contrast detection and discrimination. *Vision Research*, *26*(6), 991–997. doi:10.1016/0042-6989(86)90155-0

Breitman, M. F., Morando, M., & Avila, L. J. (2013). Past and present taxonomy of the Liolaemus lineomaculatus section (Liolaemidae): Is the morphological arrangement hypothesis valid? *Zoological Journal of the Linnean Society*, *168*(3), 612–668. doi:10.1111/zoj.12037

Briolat, E. S., Zagrobelny, M., Olsen, C. E., Blount, J. D., & Stevens, M. (2018). Sex differences but no evidence of quantitative honesty in the warning signals of six-spot burnet moths (Zygaena filipendulae L.). *Evolution*. doi:10.1111/evo.13505

Briscoe, A. D., & Chittka, L. (2001). The evolution of color vision in insects. *Annual Review of Entomology*, *46*, 471–510. doi:10.1146/annurev.ento.46.1.471

Brooks, J. L. (2014). Traditional and new principles of perceptual grouping. *Oxford Handbook of Perceptual Organization*, 1–31. doi:10.1093/oxfordhb/9780199686858.013.060

Brooks, S. P., & Gelman, A. (1998). General methods for monitoring convergence of iterative simulations)? *Journal of Computational and Graphical Statistics*, *7*(4), 434–455. doi:10.1080/10618600.1998.10474787

Bruce, V., Green, P. R., Georgeson, M. A., & Dynan, L. (2010). *Visual perception: physiology, psychology, & ecology* (Fourth edi). Hove, England ; New York, New York: Psychology Press.

Buades, A., Coll, B., & Morel, J.-M. J.-M. (2005). A non-local algorithm for image denoising. *Computer Vision and Pattern Recognition, 2005. CVPR 2005. IEEE Computer Society Conference On*, *2*(0), 60–65 vol. 2. doi:10.1109/CVPR.2005.38

Carbone, M., Gavagnin, M., Haber, M., Guo, Y.-W., Fontana, A., Manzo, E., … Mollo, E. (2013). Packaging and delivery of chemical weapons: a defensive trojan horse stratagem in chromodorid nudibranchs. *PloS One*, *8*(4), e62075. doi:10.1371/journal.pone.0062075

Caro, T., Merilaita, S., & Stevens, M. (2008). The colours of animals. from Wallace to the present day. I. cryptic colouration. In C. H. Smith & G. Beccaloni (Eds.), *Natural Selection and Beyond: The Intellectual Legacy of Alfred Russel Wallace* (pp. 125–143). Oxford, UK: Oxford University Press.

Caro, T., Sherratt, T. N., & Stevens, M. (2016). The ecology of multiple colour defences. *Evolutionary Ecology*, *30*(5), 797–809. doi:10.1007/s10682-016-9854-3

Caves, E. M., Frank, T. M., & Johnsen, S. (2016). Spectral sensitivity, spatial resolution, and temporal resolution and their implications for conspecific signalling in cleaner shrimp. *Journal of Experimental Biology*, *219*(4), 597–608. doi:10.1242/jeb.122275

Caves, E. M., Green, P. A., Zipple, M. N., Peters, S., Johnsen, S., & Nowicki, S. (2018). Categorical perception of colour signals in a songbird. *Nature*, *560*(7718), 365–367. doi:10.1038/s41586-018-0377-7

Caves, E. M., & Johnsen, S. (2017). AcuityView: An R package for portraying the effects of visual acuity on scenes observed by an animal. *Journal of Engineering and Applied Sciences*, *12*(10), 3218–3221. doi:10.1111/ijlh.12426

Champ, C. M., Vorobyev, M., & Marshall, N. J. (2016). Colour thresholds in a coral reef fish. *Royal Society Open Science*, *3*(9), 160399. doi:10.1098/rsos.160399

Champ, C. M., Wallis, G., Vorobyev, M., Siebeck, U., & Marshall, N. J. (2014). Visual acuity in a species of coral reef fish: Rhinecanthus aculeatus. *Brain, Behavior and*

Evolution, *83*, 31–42. doi:10.1159/000356977

Chan, I. Z. W., Chang, J. J. M., Huang, D., & Todd, P. A. (2019). Colour pattern measurements successfully differentiate two cryptic Onchidiidae Rafinesque, 1815 species. *Marine Biodiversity*, 1–8. doi:10.1007/s12526-019-00940-4

Chang, Y.-W., Chen, T.-C., Willan, R. C., Mok, H.-K., & Yu, M.-H. (2013). Diel variation affects estimates of biodiversity and abundance of nudibranch (Gastropoda) faunas. *The Nautilus*, *127*(1), 19–28.

Chen, I. P., Stuart-Fox, D., Hugall, A. F., & Symonds, M. R. E. (2012). Sexual selection and the evolution of complex color patterns in dragon lizards. *Evolution*, *66*(11), 3605–3614. doi:10.1111/j.1558-5646.2012.01698.x

Cheney, K. L., Cortesi, F., How, M. J., Wilson, N. G., Blomberg, S. P., Winters, A. E., … Marshall, N. J. (2014). Conspicuous visual signals do not coevolve with increased body size in marine sea slugs. *Journal of Evolutionary Biology*, *27*(4), 676–87. doi:10.1111/jeb.12348

Cheney, K. L., Green, N. F., Vibert, A. P., Vorobyev, M., Marshall, N. J., Osorio, D., & Endler, J. A. (2019). An Ishihara-style test of animal colour vision. *The Journal of Experimental Biology*, *222*(Pt 1), jeb189787. doi:10.1242/jeb.189787

Cheney, K. L., Newport, C., McClure, E. C., & Marshall, N. J. (2013). Colour vision and response bias in a coral reef fish. *The Journal of Experimental Biology*, *216*(Pt 15), 2967–73. doi:10.1242/jeb.087932

Cheney, K. L., White, A., Mudianta, I. W., Winters, A. E., Quezada, M., Capon, R. J., … Garson, M. J. (2016). Choose your weaponry: Selective storage of a single toxic compound, latrunculin a, by closely related nudibranch molluscs. *PLoS ONE*, *11*(1), 1–16. doi:10.1371/journal.pone.0145134

Chiao, C. C., Chubb, C., & Hanlon, R. T. (2007). Interactive effects of size, contrast, intensity and configuration of background objects in evoking disruptive camouflage in cuttlefish. *Vision Research*, *47*, 2223–2235. doi:10.1016/j.visres.2007.05.001

Chirimuuta, M. (2016). Why the ‘stimulus-error’ did not go away. *Studies in History and Philosophy of Science Part A*, *56*, 33–42. doi:10.1016/j.shpsa.2015.10.007

Chittka, L., & Osorio, D. (2007). Cognitive dimensions of predator responses to imperfect mimicry? *PLoS Biology*, *5*(12), 2754–2758. doi:10.1371/journal.pbio.0050339

Clark, R. C., Santer, R. D., & Brebner, J. S. (2017). A generalized equation for the calculation of receptor noise limited colour distances in n-chromatic visual systems. *Royal Society Open Science*, *4*(9), 170712. doi:10.1098/rsos.170712

Clery, S., Bloj, M., Harris, J. M., Ephane Clery, S., Bloj, M., & Harris, J. M. (2013). Interactions between luminance and color signals: effects on shape. *Journal of Vision*, *13*(5), 16. doi:10.1167/13.5.16

Colman, A. M. (2008). *A Dictionary of Psychology*. Oxford University Press. doi:10.1093/acref/9780199534067.001.0001

Cook, S. E., & Roper, T. J. (1989). Responses of chicks to brightly coloured insect prey. *Behaviour*, *110*(1), 276–293. doi:10.1163/156853989X00510

Corney, D., & Lotto, R. B. (2007). What are lightness illusions and why do we see them? *PLoS Computational Biology*, *3*(9), 1790–1800. doi:10.1371/journal.pcbi.0030180

Cornsweet, T. N., & Pinsker, H. M. (1965). Luminance discrimination of brief flashes under various conditions of adaptation. *The Journal of Physiology*, *176*(2), 294–310. doi:10.1113/jphysiol.1965.sp007551

Cortesi, F., & Cheney, K. L. (2010). Conspicuousness is correlated with toxicity in marine opisthobranchs. *Journal of Evolutionary Biology*, *23*(7), 1509–18. doi:10.1111/j.1420-9101.2010.02018.x

Cott, H. B. (1940). *Adaptive Coloration in Animals*. doi:10.1038/146144a0

Craik, K. J. (1938). The effect of adaptation on differential brightness discrimination. *The Journal of Physiology*, *92*(4), 406–21. Retrieved from http://www.jstor.org/stable/10.2307/82255

Cronin, T. W., & Bok, M. J. (2016). Photoreception and vision in the ultraviolet. *The Journal of Experimental Biology*, *219*(18), 2790–2801. doi:10.1242/jeb.128769

Cronin, T. W., Johnsen, S., Marshall, N. J., & Warrant, E. (2014). *Visual Ecology*. *Journal of Chemical Information and Modeling* (Vol. 53). Princeton, N.J: Princeton

University Press. doi:10.1017/CBO9781107415324.004

Cuthill, I. C. (2019). Camouflage. *Journal of Zoology*, jzo.12682. doi:10.1111/jzo.12682

Cuthill, I. C., Allen, W. L., Arbuckle, K., Caspers, B., Chaplin, G., Hauber, M. E., … Caro, T. (2017). The biology of color. *Science*, *357*(6350), 1–7. doi:10.1126/science.aan0221

Cuthill, I. C., Matchette, S. R., & Scott-Samuel, N. E. (2019). Camouflage in a dynamic world. *Current Opinion in Behavioral Sciences*, *30*, 109–115. doi:10.1016/j.cobeha.2019.07.007

Cuthill, I. C., & Székely, A. (2009). Coincident disruptive coloration. *Philosophical Transactions of the Royal Society of London. Series B, Biological Sciences*, *364*(November 2008), 489–496. doi:10.1098/rstb.2008.0266

da Silva Souza, G., Gomes, B. D., & Silveira, L. C. L. (2011). Comparative neurophysiology of spatial luminance contrast sensitivity. *Psychology & Neuroscience*, *4*(1), 29–48. doi:10.3922/j.psns.2011.1.005

Dalton, B. E., de Busserolles, F., Marshall, N. J., & Carleton, K. L. (2017). Retinal specialization through spatially varying cell densities and opsin coexpression in cichlid fish. *The Journal of Experimental Biology*, *220*(2), 266–277. doi:10.1242/jeb.149211

Daly, I. M., How, M. J., Partridge, J. C., & Roberts, N. W. (2018). Complex gaze stabilization in mantis shrimp. *Proceedings of the Royal Society B*, *285*(1878), 20180594. doi:10.1098/rspb.2018.0594

Dalziell, A. H., & Welbergen, J. A. (2016). Mimicry for all modalities. *Ecology Letters*, *19*(6), 609–619. doi:10.1111/ele.12602

Darst, C. R., Cummings, M. E., & Cannatella, D. C. (2006). A mechanism for diversity in warning signals: conspicuousness versus toxicity in poison frogs. *Proceedings of the National Academy of Sciences of the United States of America*, *103*(Track II), 5852–5857. doi:10.1073/pnas.0600625103

Dawkins, M. S. (1993). Are there general principles of signal design? *Philosophical Transactions of the Royal Society of London. Series B, Biological Sciences*, *340*(1292), 251–255. doi:10.1098/rstb.1993.0065

Day, W. H. E., & Edelsbrunner, H. (1984). Efficient algorithms for agglomerative hierarchical clustering methods. *Journal of Classification*, *1*(1), 7–24. doi:10.1007/BF01890115

Dimitrova, M., & Merilaita, S. (2010). Prey concealment: Visual background complexity and prey contrast distribution. *Behavioral Ecology*, *21*(1), 176–181. doi:10.1093/beheco/arp174

Domingos, P., & Pazzani, M. (1997). On the optimality of the simple Bayesian classifier under zero-one loss. *Machine Learning*, *29*, 103–130.

Douglas, R. H., & Partridge, J. C. (1997). On the visual pigments deep-sea fish. *Journal of Fish Biology*, *50*(1), 68–85. doi:10.1006/jfbi.1996.0277

Dugas, M. B., Halbrook, S. R., Killius, A. M., del Sol, J. F., & Richards-Zawacki, C. L. (2015). Colour and escape behaviour in polymorphic populations of an aposematic poison frog. *Ethology*, n/a-n/a. doi:10.1111/eth.12396

Dzhafarov, E. N., & Colonius, H. (1999). Fechnerian metrics in unidimensional and multidimensional stimulus spaces. *Psychonomic Bulletin & Review*, *6*(2), 239–68. doi:10.3758/BF03212329

Eagleman, D. M., Jacobson, J. E., & Sejnowski, T. J. (2004). Perceived luminance depends on temporal context. *Nature*, *428*(6985), 854–856. doi:10.1038/nature02467

Eakin, R. M., Westfall, J. a, & Dennis, M. J. (1967). Fine structure of the eye of a nudibranch mollusc, Hermissenda crassicornis. *Journal of Cell Science*, *2*, 349–358.

Edmunds, M. (1987). Color in opisthobranchs. *American Malacological Bulletin*, *5*(January), 185–196.

Edmunds, M. (1991). Does warning coloration occur in nudibranchs. *Malacologia*, *32*, 241–255.

Einhäuser, W., & König, P. (2003). Does luminance-contrast contribute to a saliency map for overt visual attention? *European Journal of Neuroscience*, *17*(5), 1089–1097. doi:10.1046/j.1460-9568.2003.02508.x

Elder, J. H., & Sachs, A. J. (2004). Psychophysical receptive fields of edge detection

mechanisms. *Vision Research*, *44*(8), 795–813. doi:10.1016/j.visres.2003.11.021

Elder, J. H., & Velisavljević, L. (2009). Cue dynamics underlying rapid detection of animals in natural scenes. *Journal of Vision*, *9*(7), 7. doi:10.1167/9.8.787

Emran, F., Rihel, J., Adolph, A. R., Wong, K. Y., Kraves, S., & Dowling, J. E. (2007). OFF ganglion cells cannot drive the optokinetic reflex in zebrafish. *Proceedings of the National Academy of Sciences*, *104*(48), 19126 LP – 19131. doi:10.1073/pnas.0709337104

Endler, J. A. (1978). A predator's view of animal color patterns. *Evolutionary Biology*, *11*(5), 320–364.

Endler, J. A. (1984). Progressive background in moths, and a quantitative measure of crypsis. *Biological Journal of the Linnean Society*, *22*(3), 187–231. doi:10.1111/j.1095-8312.1984.tb01677.x

Endler, J. A. (1987). Predation, light intensity and courtship behaviour in Poecilia reticulata (Pisces: Poeciliidae). *Animal Behaviour*, *35*(5), 1376–1385. doi:10.1016/S0003-3472(87)80010-6

Endler, J. A. (1990). On the measurement and classification of colour in studies of animal colour patterns. *Biological Journal of the Linnean Society*, *41*(4), 315–352. doi:10.1111/j.1095-8312.1990.tb00839.x

Endler, J. A. (1991). Variation in the appearance of guppy color patterns to guppies and their predators under different visual conditions. *Vision Research*, *31*(3), 587–608. doi:10.1016/0042-6989(91)90109-I

Endler, J. A. (1993). The color of light in forests and its implications. *Ecological Monographs*, *63*(1), 1–27. Retrieved from http://www.jstor.org/stable/2937121

Endler, J. A. (2012). A framework for analysing colour pattern geometry: Adjacent colours. *Biological Journal of the Linnean Society*, *107*(2), 233–253. doi:10.1111/j.1095-8312.2012.01937.x

Endler, J. A., Cole, G. L., & Kranz, A. M. (2018). Boundary strength analysis: Combining colour pattern geometry and coloured patch visual properties for use in predicting behaviour and fitness. *Methods in Ecology and Evolution*, *9*(12), 2334–2348. doi:10.1111/2041-210X.13073

Endler, J. A., & Greenwood, J. J. D. (2006). Frequency-dependent predation, crypsis and aposematic coloration [and discussion]. *Philosophical Transactions of the Royal Society B: Biological Sciences*, *319*(1196), 505–523. doi:10.1098/rstb.1988.0062

Endler, J. A., & Houde, A. E. (1995). Geographic variation in female preferences for male traits in Poecilia reticulata. *Evolution*, *49*(3), 456. doi:10.2307/2410270

Endler, J. A., & Mappes, J. (2017). The current and future state of animal coloration research. *Philosophical Transactions of the Royal Society B: Biological Sciences*, *372*(1724), 20160352. doi:10.1098/rstb.2016.0352

Endler, J. A., & Mielke, P. W. (2005). Comparing entire colour patterns as birds see them. *Biological Journal of the Linnean Society*, *86*(4), 405–431. doi:10.1111/j.1095-8312.2005.00540.x

Enright, J. T. (1977). Diurnal vertical migration: Adaptive significance and timing. Part 1. Selective advantage: A metabolic model. *Limnology and Oceanography*, *22*(5), 856–872. doi:10.4319/lo.1977.22.5.0856

Escobar-Camacho, D., Marshall, N. J., & Carleton, K. L. (2017). Behavioral color vision in a cichlid fish: Metriaclima benetos. *The Journal of Experimental Biology*, *220*(16), 2887–2899. doi:10.1242/jeb.160473

Escobar-Camacho, D., Taylor, M. A., Cheney, K. L., Green, N. F., Marshall, N. J., & Carleton, K. L. (2019). Color discrimination thresholds in a cichlid fish: Metriaclima benetos . *The Journal of Experimental Biology*, *222*(17), jeb201160. doi:10.1242/jeb.201160

Eskew, R. T. (2009). Higher order color mechanisms: A critical review. *Vision Research*, *49*(22), 2686–2704. doi:10.1016/j.visres.2009.07.005

Faulkner, D., & Ghiselin, M. (1983). Chemical defense and evolutionary ecology of dorid nudibranchs and some other opisthobranch gastropods . *Marine Ecology Progress Series*, *13*, 295–301. doi:10.3354/meps013295

Fennell, J. G., Talas, L., Baddeley, R. J., Cuthill, I. C., & Scott-Samuel, N. E. (2019). Optimizing colour for camouflage and visibility using deep learning: The effects of the environment and the observer's visual system. *Journal of the Royal Society Interface*, *16*(154). doi:10.1098/rsif.2019.0183

Field, D. J. (1987). Relations between the statistics of natural images and the response properties of cortical cells. *Journal of the Optical Society of America. A, Optics and Image Science*, *4*(12), 2379–94. doi:10.1364/JOSAA.4.002379

Fleishman, L. J. (1986). Motion detection in the presence and absence of background motion in an Anolis lizard. *Journal of Comparative Physiology A*, *159*(5), 711–720. doi:10.1007/BF00612043

Fleishman, L. J., Perez, C. W., Yeo, A. I., Cummings, K. J., Dick, S., & Almonte, E. (2016). Perceptual distance between colored stimuli in the lizard Anolis sagrei: comparing visual system models to empirical results. *Behavioral Ecology and Sociobiology*, *70*(4), 541–555. doi:10.1007/s00265-016-2072-8

Forsman, A., & Herreträm, J. (2004). Asymmetry in size, shape, and color impairs the protective value of conspicuous color patterns. *Behavioral Ecology*, *15*(1), 141–147. doi:10.1093/beheco/arg092

Foster, J. J., Temple, S. E., How, M. J., Daly, I. M., Sharkey, C. R., Wilby, D., & Roberts, N. W. (2017). Polarization vision: Overcoming challenges of working with a property of light we barely see. *The Science of Nature*, *105*(27). doi:10.1101/207217

Friedman, J. H. (1989). Regularized discriminant analysis. *Journal of the American Statistical Association*, *84*(405), 165–175. doi:10.1080/01621459.1989.10478752

Furchner, C. S., Thomas, J. P., & Campbell, F. W. (1977). Detection and discrimination of simple and complex patterns at low spatial frequencies. *Vision Research*, *17*(7), 827–836.

Galván, I., Vargas-Mena, J. C., & Rodríguez-Herrera, B. (2020). Tent-roosting may have driven the evolution of yellow skin coloration in Stenodermatinae bats. *Journal of Zoological Systematics and Evolutionary Research*, *58*(1), 519–527. doi:10.1111/jzs.12329

Garcia, J. E., Dyer, A. G., Greentree, A. D., Spring, G., & Wilksch, P. a. (2013). Linearisation of RGB camera responses for quantitative image analysis of visible and UV photography: A comparison of two techniques. *PLoS ONE*, *8*(11). doi:10.1371/journal.pone.0079534

Garcia, J. E., Shrestha, M., & Dyer, A. G. (2018). Flower signal variability overwhelms

receptor-noise and requires plastic color learning. *Behavioral Ecology*, *In press*, Accepted Sept 3 2018. doi:10.1093/beheco/ary127

Garcia, J. E., Spaethe, J., & Dyer, A. G. (2017). The path to colour discrimination is S-shaped: behaviour determines the interpretation of colour models. *Journal of Comparative Physiology A: Neuroethology, Sensory, Neural, and Behavioral Physiology*, *203*(12), 983–997. doi:10.1007/s00359-017-1208-2

Gaskett, A. C., & Herberstein, M. E. (2010). Colour mimicry and sexual deception by Tongue orchids (Cryptostylis). *Naturwissenschaften*, *97*(1), 97–102. doi:10.1007/s00114-009-0611-0

Gawryszewski, F. M. (2018). Color vision models: Some simulations, a general n -dimensional model, and the colourvision R package. *Ecology and Evolution*, *8*(16), 8159–8170. doi:10.1002/ece3.4288

Gegenfurtner, K. R., & Kiper, D. C. (1992). Contrast detection in luminance and chromatic noise. *J Opt. Soc. Am. A.*, *9*(11), 1880–1888. doi:10.1364/JOSAA.9.001880

Geisbauer, G., Griebel, U., Schmid, A., & Timney, B. (2004). Brightness discrimination and neutral point testing in the horse. *Canadian Journal of Zoology*, *82*(4), 660–670. doi:10.1139/z04-026

Gelman, A., & Rubin, D. B. (1992). Inference from iterative simulation using multiple sequences. *Statistical Science*, *7*(4), 457–472. doi:10.1214/ss/1177011136

Gescheider, G. A. (1997). *Psychophysics : the fundamentals* (3rd ed.). Mahwah, N.J.: L. Erlbaum Associates.

Gilchrist, A. L. (2008). Perceptual organization in lightness. In *Oxford Handbook of Perceptual Organisation* (pp. 1–25). Retrieved from http://medcontent.metapress.com/index/A65RM03P4874243N.pdf

Gilchrist, A. L. (2014). Response to Maniatis critique of anchoring theory. *Vision Research*, *102*, 93–96. doi:10.1016/j.visres.2014.07.006

Gilchrist, A. L., Kossyfidis, C., Agostini, T., Li, X., Bonato, F., Cataliotti, J., … Economou, E. (1999). An anchoring theory of lightness perception. *Psychological Review*, *106*(4), 795–834. doi:10.1037/0033-295X.106.4.795

Gilchrist, A. L., & Radonjić, A. (2009). Anchoring of lightness values by relative luminance and relative area. *Journal of Vision*, *9*(2009), 13.1–10. doi:10.1167/9.9.13

Giurfa, M., Vorobyev, M., Brandt, R., Posner, B., & Menzel, R. (1997). Discrimination of coloured stimuli by honeybees: Alternative use of achromatic and chromatic signals. *Journal of Comparative Physiology - A Sensory, Neural, and Behavioral Physiology*, *180*(3), 235–243. doi:10.1007/s003590050044

Godfrey, D., Lythgoe, J. N., & Rumball, D. a. (1987). Zebra stripes and tiger stripes: the spatial frequency distribution of the pattern compared to that of the background is significant in display and crypsis. *Biological Journal of the Linnean Society*, *32*(4), 427–433. doi:10.1111/j.1095-8312.1987.tb00442.x

Goldsmith, T. H., & Butler, B. K. (2003). The roles of receptor noise and cone oil droplets in the photopic spectral sensitivity of the budgerigar, Melopsittacus undulatus. *Journal of Comparative Physiology A*, *189*(2), 135–142. doi:10.1007/s00359-002-0385-8

Gordon, I. E. (2004). *Theories of visual perception* (3rd ed.). East Sussex: Psychology Press.

Grafen. (1989). The Phylogenetic Regression. *Philosophical Transactions of the Royal Soociety of London, Series B*, *326*(1233), 119–157. doi:10.1098/rstb.1989.0106

Grande, C., Templado, J., Cervera, J. L., & Zardoya, R. (2004). Phylogenetic relationships among Opisthobranchia (Mollusca: Gastropoda) based on mitochondrial cox 1, trnV, and rrnL genes. *Molecular Phylogenetics and Evolution*, *33*, 378–388. doi:10.1016/j.ympev.2004.06.008

Gray, S. M., & McKinnon, J. S. (2007). Linking color polymorphism maintenance and speciation. *Trends in Ecology & Evolution*, *22*(2), 71–9. doi:10.1016/j.tree.2006.10.005

Green, N. F., Urquhart, H. H., Van Den Berg, C. P., Marshall, N. J., & Cheney, K. L. (2018). Pattern edges improve predator learning of aposematic signals. *Behavioral Ecology*, *29*(July), 1–6. doi:10.1093/beheco/ary089

Greig, D. M., Porteous, B. T., Seheult, A. H., & Seheultt, A. H. (1989). Exact maximum a posteriori estimation for binary images. *Source Journal of the Royal Statistical*

Society. Series B (Methodological) Journal of the Royal Statistical Society. Series B J. R. Statist. Soc. B, *51*(2), 271–279. doi:10.2307/2345609

Griebel, U., & Schmid, A. (1997). Brightness discrimination ability in the West Indian manatee (Trichechus manatus). *The Journal of Experimental Biology*, *200*(Pt 11), 1587–92. Retrieved from http://www.ncbi.nlm.nih.gov/pubmed/9202447

Griffiths, T. L., Chater, N., Kemp, C., Perfors, A., & Tenenbaum, J. B. (2010). Probabilistic models of cognition: exploring representations and inductive biases. *Trends in Cognitive Sciences*, *14*(8), 357–364. doi:10.1016/j.tics.2010.05.004

Guilford, T., & Dawkins, M. S. (1993). Receiver psychology and the design of animal signals. *Trends in Neurosciences*, *16*(August 1990), 430–436. doi:10.1016/S0003-3472(05)80600-1

Haber, M., Cerfeda, S., Carbone, M., Calado, G., Gaspar, H., Neves, R., … Mollo, E. (2010). Coloration and defense in the nudibranch gastropod Hypselodoris fontandraui. *Biological Bulletin*, *218*(April), 181–188. doi:218/2/181 [pii]

Hadfield, J. D. (2010). MCMCglmm: MCMC Methods for Multi-Response GLMMs in R. *Journal of Statistical Software*, *33*(2), 1–22. doi:10.1002/ana.22635

Hanlon, R. T., Naud, M.-J., Forsythe, J. W., Hall, K., Watson, A. C., & McKechnie, J. (2007). Adaptable night camouflage by cuttlefish. *American Naturalist*, *169*(4), 543–551. doi:10.1086/512106

Hanson, H. M. (1959). Effects of discrimination training on stimulus generalization. *Journal of Experimental Psychology*, *58*(5), 321–334. doi:10.1037/h0042606

Hart, N. S. (2001a). The visual ecology of avian photoreceptors. *Progress in Retinal and Eye Research*, *20*(5), 675–703.

Hart, N. S. (2001b). Variations in cone photoreceptor abundance and the visual ecology of birds. *Journal of Comparative Physiology - A Sensory, Neural, and Behavioral Physiology*, *187*(9), 685–697. doi:10.1007/s00359-001-0240-3

Hartigan, J. A., & Wong, M. A. (1979). Algorithm AS 136: A K-means clustering algorithm. *Journal of the Royal Statistical Society. Series C (Applied Statistics)*, *28*(1), 100–108. Retrieved from https://www.jstor.org/stable/2346830

Hausdorf, B., & Bouchet, P. (2005). *Working classification of the Gastropoda.*

Pulmonata. Classification and nomenclator of gastropod families. Malacologia (Vol. 47).

Hebets, E. A., & Papaj, D. R. (2005). Complex signal function: Developing a framework of testable hypotheses. *Behavioral Ecology and Sociobiology*, *57*(3), 197–214. doi:10.1007/s00265-004-0865-7

Heinemann, E. G., & Chase, S. (1995). A quantitative model for simultaneous brightness induction. *Vision Research*, *35*(14), 2007–2020. doi:10.1016/0042-6989(94)00281-P

Hempel de Ibarra, N., Giurfa, M., & Vorobyev, M. (2001). Detection of coloured patterns by honeybees through chromatic and achromatic cues. *Journal of Comparative Physiology A: Sensory, Neural, and Behavioral Physiology*, *187*(3), 215–224. doi:10.1007/s003590100192

Henze, M. J., Lind, O., Mappes, J., Rojas, B., & Kelber, A. (2018). An aposematic colour-polymorphic moth seen through the eyes of conspecifics and predators - sensitivity and colour discrimination in a tiger moth. *Functional Ecology*, *32*(7), 0–3. doi:10.1111/1365-2435.13100

Henze, M. J., & Oakley, T. H. (2015). The dynamic evolutionary history of pancrustacean eyes and opsins. *Integrative and Comparative Biology*, *55*(5), 830–842. doi:10.1093/icb/icv100

Hering, E. (1861). *Beiträge zur Physiologie: Hft. Zur Lehre vom Ortsinne der Netzhaut. 1861*. W. Engelmann. Retrieved from https://books.google.com.au/books?id=-VtVAAAAMAAJ

Hochberg, J. E., & Beck, J. (1954). Apparent spatial arrangement and perceived brightness. *Journal of Experimental Psychology*, *47*(4), 263–266. doi:10.1037/h0056283

Hollander, M., & Wolfe, D. A. (1973). *Nonparametric Statistical Methods*. New York: John wiley & Sons Ltd.

Honma, A., Mappes, J., & Valkonen, J. K. (2015). Warning coloration can be disruptive: Aposematic marginal wing patterning in the wood tiger moth. *Ecology and Evolution*, *5*(21), 4863–4874. doi:10.1002/ece3.1736

Howard, S. R., Avarguès-Weber, A., Garcia, J. E., Greentree, A. D., & Dyer, A. G. (2019). Surpassing the subitizing threshold: appetitive–aversive conditioning improves discrimination of numerosities in honeybees. *The Journal of Experimental Biology*, *222*(19), jeb205658. doi:10.1242/jeb.205658

Hughes, A. E. (2018). Dissociation between perception and smooth pursuit eye movements in speed judgments of moving Gabor targets. *Journal of Vision*, *18*(4), 4. doi:10.1167/18.4.4

Hughes, A. E., Troscianko, J., & Stevens, M. (2014). Motion dazzle and the effects of target patterning on capture success. *BMC Evolutionary Biology*, *14*(1), 1–10. doi:10.1186/s12862-014-0201-4

Isaac, L. A., & Gregory, P. T. (2013). Can snakes hide in plain view? Chromatic and achromatic crypsis of two colour forms of the Western Terrestrial Garter Snake (Thamnophis elegans). *Biological Journal of the Linnean Society*, *108*(4), 756–772. doi:10.1111/bij.12020

Itti, L., Koch, C., & Niebur, E. (1998). A model of saliency-based visual attention for rapid scene analysis. *IEEE Transactions on Pattern Analysis and Machine Intelligence*, *20*(11), 1254–1259. doi:10.1109/34.730558

Jacobs, G. H. (2009). Evolution of colour vision in mammals. *Philosophical Transactions of the Royal Society B: Biological Sciences*, *364*(1531), 2957–2967. doi:10.1098/rstb.2009.0039

Jameson, D., & Hurvich, L. M. (1955). Some quantitative aspects of an opponent-colors theory I. Chromatic responses and spectral saturation. *Journal of the Optical Society of America*, *45*(7), 546. doi:10.1364/josa.45.000546

Jerlov, N. G. (1976). *Marine Optics*. (Elsevier, Ed.). Amsterdam.

Johnsen, S. (2005). The red and the black: Bioluminescence and the color of animals in the deep sea. *Integrative and Comparative Biology*, *45*(2), 234–246. doi:10.1093/icb/45.2.234

Johnsen, S., & Mobley, C. (2012). *The Optics of Life: A Biologist's Guide to Light in Nature. American Journal of Physics* (Vol. 80). Woodstock, Oxfordshire: Princeton University Press. doi:10.1119/1.4739054

Johnson, R. F., & Gosliner, T. M. (2012). Traditional taxonomic groupings mask evolutionary history: A molecular phylogeny and new classification of the chromodorid nudibranchs. *PLoS ONE*, *7*(4), 29–31. doi:10.1371/journal.pone.0033479

Jörges, B., Slupinski, L., & López-Moliner, J. (2018). The use of visual cues in gravity judgements on parabolic motion. *Vision Research*, *149*(March), 47–58. doi:10.1101/301077

Kachinsky, E. S., Smith, V. C., & Pokorny, J. (2003). Discrimination and identification of luminance contrast stimuli. *Journal of Vision*, *3*(10), 599–609. doi:10:1167/3.10.2

Kamilar, J. M. (2009). Interspecific variation in primate countershading: Effects of activity pattern, body mass, and phylogeny. *International Journal of Primatology*, *30*(6), 877–891. doi:10.1007/s10764-009-9359-9

Kang, C., Stevens, M., Moon, J. Y., Lee, S. I., & Jablonski, P. G. (2015). Camouflage through behavior in moths: The role of background matching and disruptive coloration. *Behavioral Ecology*, *26*(1), 45–54. doi:10.1093/beheco/aru150

Katoh, K., & Standley, D. M. (2013). MAFFT multiple sequence alignment software version 7: Improvements in performance and usability. *Molecular Biology and Evolution*, *30*(4), 772–780. doi:10.1093/molbev/mst010

Kearse, M., Moir, R., Wilson, A., Stones-Havas, S., Cheung, M., Sturrock, S., … Drummond, A. (2012). Geneious Basic: An integrated and extendable desktop software platform for the organization and analysis of sequence data. *Bioinformatics*, *28*(12), 1647–1649. doi:10.1093/bioinformatics/bts199

Kelber, A. (2019). Bird colour vision – from cones to perception. *Current Opinion in Behavioral Sciences*, *30*, 34–40. doi:10.1016/j.cobeha.2019.05.003

Kelber, A., Balkenius, A., & Warrant, E. J. (2002). Scotopic colour vision in nocturnal hawkmoths. *Nature*, *419*(6910), 922–925. doi:10.1038/nature01065

Kelber, A., Vorobyev, M., & Osorio, D. (2003). Animal colour vision--behavioural tests and physiological concepts. *Biological Reviews of the Cambridge Philosophical Society*, *78*, 81–118. doi:10.1017/S1464793102005985

Kelley, L. A., & Kelley, J. L. (2014). Animal visual illusion and confusion: The importance of a perceptual perspective. *Behavioral Ecology*, *25*(3), 450–463. doi:10.1093/beheco/art118

Kemp, D. J., Herberstein, M. E., Fleishman, L. J., Endler, J. A., Bennett, A. T. D., Dyer, A. G., … Whiting, M. J. (2015). An integrative framework for the appraisal of coloration in nature. *The American Naturalist*, *185*(6), 705–724. doi:10.1086/681021

Kingdom, F. A. A. (2011). Lightness, brightness and transparency: A quarter century of new ideas, captivating demonstrations and unrelenting controversy. *Vision Research*, *51*(7), 652–673. doi:10.1016/j.visres.2010.09.012

Koleček, J., Šulc, M., Piálková, R., Troscianko, J., Požgayová, M., Honza, M., & Procházka, P. (2019). Rufous Common Cuckoo chicks are not always female. *Journal of Ornithology*, *160*(1), 155–163. doi:10.1007/s10336-018-1591-7

Kurki, I., Peromaa, T., Hyvärinen, A., & Saarinen, J. (2009). Visual features underlying perceived brightness as revealed by classification images. *PLOS ONE*, *4*(10), e7432.

Laming, D. (1988). Precis of sensory analysis. *Behavioral and Brain Sciences*, (11), 275–339.

Laming, D., & Laming, J. (1992). F. Hegelmaier: On memory for the length of a line. *Psychological Research*, *54*(4), 233–239. doi:10.1007/BF01358261

Land, E. H. (1986). Recent advances in retinex theory. *Vision Research*, *26*(1), 7–21. doi:10.1016/0042-6989(86)90067-2

Land, M. F. (1999). Motion and vision: Why animals move their eyes. *Journal of Comparative Physiology - A Sensory, Neural, and Behavioral Physiology*, *185*(4), 341–352. doi:10.1007/s003590050393

Land, M. F., & Nilsson, D.-E. (2012). *Animal eyes* (2nd ed..). Oxford ; New York: Oxford University Press.

Larkin, M. F., Smith, S. D. A., Willan, R. C., & Davis, T. R. (2017). Diel and seasonal variation in heterobranch sea slug assemblages within an embayment in temperate eastern Australia. *Marine Biodiversity*, 1–10. doi:10.1007/s12526-017-

0700-9

Layton, K. K. S., Gosliner, T. M., & Wilson, N. G. (2018). Flexible colour patterns obscure identification and mimicry in Indo-Pacific Chromodoris nudibranchs (Gastropoda: Chromodorididae). *Molecular Phylogenetics and Evolution*, *124*(February), 27–36. doi:10.1016/j.ympev.2018.02.008

Ligon, R. A., Diaz, C. D., Morano, J. L., Troscianko, J., Stevens, M., Moskeland, A., … Scholes, E. (2018). Evolution of correlated complexity in the radically different courtship signals of birds-of-paradise. *PLOS*, 351437. doi:10.1371/2006962

Linares, D., & Lopez-Moliner, J. (2015). quickpsy: An R package to fit psychometric functions for multiple groups, (1), 1–11.

Lind, O. (2016). Colour vision and background adaptation in a passerine bird, the zebra finch (Taeniopygia guttata). *Royal Society Open Science*, *3*(9), 160383. doi:10.1098/rsos.160383

Lind, O., Karlsson, S., & Kelber, A. (2013). Brightness discrimination in budgerigars (Melopsittacus undulatus). *PLoS ONE*, *8*(1), 8–10. doi:10.1371/journal.pone.0054650

Lind, O., Sunesson, T., Mitkus, M., & Kelber, A. (2012). Luminance-dependence of spatial vision in budgerigars (Melopsittacus undulatus) and Bourke's parrots (Neopsephotus bourkii). *Journal of Comparative Physiology A: Neuroethology, Sensory, Neural, and Behavioral Physiology*, *198*(1), 69–77. doi:10.1007/s00359-011-0689-7

Lindstedt, C., Lindström, L., & Mappes, J. (2009). Thermoregulation constrains effective warning signal expression. *Evolution*, *63*(2), 469–478. doi:10.1111/j.1558-5646.2008.00561.x

Livingstone, M., & Hubel, D. (1988). Segregation of form, color, movement, and depth: Anatomy, physiology, and perception. *Science*. doi:10.1126/science.3283936

Loew, E. R. (1995). Determinants of visual pigment spectral location and photoreceptor cell spectral sensitivity. *Neurobiology and Clinical Aspects of the Outer Retina*, 57–77. doi:10.1007/978-94-011-0533-0_3

Long, C., & Sweet, J. (2006). Hyperspectral imaging of cuttlefish camouflage indicates

good color match in the eyes of fish predators. *South East Asia Research*, *14*(3), 445–469. doi:10.1073/pnas.

Losey, G. S., McFarland, W. N., Loew, E. R., Zamzow, J. P., Nelson, P. a., & Marshall, N. J. (2003). Visual biology of Hawaiian coral reef fishes. I. Ocular transmission and visual pigments. *Copeia*, *2003*(3), 433–454. doi:10.1643/01-053

Lotto, R. B., Clarke, R., Corney, D., & Purves, D. (2011). Seeing in colour. *Optics and Laser Technology*, *43*(2), 261–269. doi:10.1016/j.optlastec.2010.02.006

Lotto, R. B., & Purves, D. (2000). An empirical explanation of color contrast. *Proceedings of the National Academy of Sciences of the United States of America*, *97*(23), 12834–9. doi:10.1073/pnas.210369597

Lowe, D. G. (1999). Object recognition from local scale-invariant features. In *Proceedings of the Seventh IEEE International Conference on Computer Vision* (pp. 1150–1157 vol.2). IEEE. doi:10.1109/ICCV.1999.790410

Lu, Z.-L., & Sperling, G. (2012). Black-white asymmetry in visual perception. *Journal of Vision*, *12*(10), 8–8. doi:10.1167/12.10.8

Lythgoe, J. N. (1979). *The ecology of vision*. Oxford University Press.

Maan, M. E., & Cummings, M. E. (2012). Poison Frog colors are honest signals of toxicity, particularly for bird predators. *The American Naturalist*, *179*(1), E1–E14. doi:10.1086/663197

Macuda, T., & Timney, B. (1999). Luminance and chromatic discrimination in the horse (Equus caballus). *Behavioural Processes*, *44*(3), 301–307. doi:10.1016/S0376-6357(98)00039-4

Maia, R., Eliason, C. M., Bitton, P. P., Doucet, S. M., & Shawkey, M. D. (2013). pavo: An R package for the analysis, visualization and organization of spectral data. *Methods in Ecology and Evolution*, *4*(10), 906–913. doi:10.1111/2041-210X.12069

Maia, R., Gruson, H., Endler, J. A., & White, T. E. (2019). pavo 2: New tools for the spectral and spatial analysis of colour in r. *Methods in Ecology and Evolution*, (September), 0–2. doi:10.1111/2041-210X.13174

Maia, R., & White, T. E. (2018). Comparing colors using visual models. *Behavioral*

Ecology, *29*(3), 649–659. doi:10.1093/beheco/ary017

Maître, H. (2017). *From Photon to Pixel*. *From Photon to Pixel*. Hoboken, NJ, USA: John Wiley & Sons, Inc. doi:10.1002/9781119402442

Majerus, M. E. N. (2009). Industrial melanism in the peppered moth, Biston betularia: An excellent teaching example of darwinian evolution in action. *Evolution: Education and Outreach*, *2*(1), 63–74. doi:10.1007/s12052-008-0107-y

Mallet, J., & Joron, M. (1999). Evolution of diversity in warning color and mimicry: polymorphisms, shifting balance, and speciation. *Annual Review of Ecology and Systematics*, *30*(30), 201–233. doi:0066-4162/99/1120-0201$08.00

Mangiafico, S. S. (2016). Summary and analysis of extension program evaluation in R. Retrieved from rcompanion.org/documents/RHandbookProgramEvaluation.pdf

Maniatis, L. M. (2014). A theory divided: Current representations of the anchoring theory of lightness contradict the original's core claims. *Vision Research*, *102*, 89–92. doi:10.1016/j.visres.2014.04.010

Marr, D. (2010). *Vision: A Computational Investigation into the Human Representation and Processing of Visual Information*. The MIT Press. doi:10.7551/mitpress/9780262514620.001.0001

Marr, D., & Hildreth, E. (1980). Theory of edge detection. *Proceedings of the Royal Society of London B: Biological Sciences*, *207*(1167), 187–217. doi:10.1098/rspb.1980.0020

Marshall, K. L. A., Philpot, K. E., & Stevens, M. (2016). Microhabitat choice in island lizards enhances camouflage against avian predators. *Scientific Reports*, *6*(January), 19815. doi:10.1038/srep19815

Marshall, N. J. (2000). Communication and camouflage with the same 'bright' colours in reef fishes. *Philosophical Transactions of the Royal Society of London. Series B, Biological Sciences*, *355*(1401), 1243–1248. doi:10.1098/rstb.2000.0676

Marshall, N. J., Cortesi, F., de Busserolles, F., Siebeck, U. E., & Cheney, K. L. (2018). Colours and colour vision in reef fishes: Past, present and future research directions. *Journal of Fish Biology*, jfb.13849. doi:10.1111/jfb.13849

Marshall, N. J., Jennings, K., McFarland, W. N., Loew, E. R., & Losey, G. S. (2003).

Visual biology of Hawaiian coral reef fishes. III. Environmental light and an integrated approach to the ecology of reef fish vision. *Copeia*, *2003*(3), 467–480. doi:10.1643/01-056

Marshall, N. J., & Johnsen, S. (2017). Fluorescence as a means of colour signal enhancement. *Philosophical Transactions of the Royal Society B: Biological Sciences*, *372*(1724), 20160335. doi:10.1098/rstb.2016.0335

Marshall, N. J., Land, M. F., King, C. A., & Cronin, T. W. (1991). The compound eyes of mantis shrimps (Crustacea, Hoplocarida, Stomatopoda). II. Colour pigments in the eyes of stomatopod crustaceans: polychromatic vision by serial and lateral filtering. *Philosophical Transactions of the Royal Society of London. Series B: Biological Sciences*, *334*(1269), 57–84. doi:10.1098/rstb.1991.0097

Marshall, N. J., Vorobyev, M., & Siebeck, U. (2006). What does a reef fish see when it sees a reef fish? Eating Nemo. In F. Laddich, S. Collin, P. Moller, & B. Kapoor (Eds.), *Communication in Fishes* (pp. 393–422). Plymouth, UK: Science Publishers Inc.

Martin Schaefer, H., Schaefer, V., Vorobyev, M., Schaefer, H. M., Schaefer, V., & Vorobyev, M. (2007). Are fruit colors adapted to consumer vision and birds equally efficient in detecting colorful signals? *American Naturalist*, *169*(1), S159–S169. doi:10.1086/510097

Matchette, S. R., Cuthill, I. C., & Scott-Samuel, N. E. (2019). Dappled light disrupts prey detection by masking movement. *Animal Behaviour*, *155*, 89–95. doi:10.1016/j.anbehav.2019.07.006

MathWorks. (2000). Matlab. Natick, MA.

McGarigal, K., & Marks, B. J. (1994). BJ Marks. 1995. FRAGSTATS: spatial pattern analysis program for quantifying landscape structure. *USDA Forest Service General Technical Report PNW*, *97331*(503).

Merilaita, S., Lyytinen, A., & Mappes, J. (2001). Selection for cryptic coloration in a visually heterogeneous habitat. *Proceedings. Biological Sciences / The Royal Society*, *268*(1479), 1925–1929. doi:10.1098/rspb.2001.1747

Merilaita, S., Scott-Samuel, N. E., & Cuthill, I. C. (2017). How camouflage works. *Philosophical Transactions of the Royal Society B: Biological Sciences*,

372(1724). doi:10.1098/rstb.2016.0341

Michalis, C., Scott-samuel, N. E., Gibson, D. P., Cuthill, I. C., & Michalis, C. (2017). Optimal background matching camouflage.

Miquilini, L., Walker, N. A., Odigie, E. A., Guimarães, D. L., Salomão, R. C., Lacerda, E. M. C. B., … Souza, G. S. (2017). Influence of spatial and chromatic noise on luminance discrimination. *Scientific Reports*, *7*(1), 1–11. doi:10.1038/s41598-017-16817-0

Mochida, K., Zhang, W.-Y., & Toda, M. (2015). The function of body coloration of the hai coral snake Sinomicrurus japonicus boettgeri. *Zoological Studies*, *54*(1), 33. doi:10.1186/s40555-015-0110-2

Monnier, P., & Shevell, S. K. (2003). Large shifts in color appearance from patterned chromatic backgrounds. *Nature Neuroscience*, *6*(8), 801–802. doi:10.1038/nn1099

Moulden, B., Kingdom, F., & Gatley, L. F. (1990). The standard deviation of luminance as a metric for contrast in random-dot images. *Perception*, *19*(1), 79–101. doi:10.1068/p190079

Mullen, K. T., & Kulikowski, J. J. (1990). Wavelength discrimination at detection threshold K. *Journal of the Optical Society of America*, *7*(4). doi:10.1080/15320383.2018.1423023

Murali, G. (2018). Now you see me, now you don't: dynamic flash coloration as an antipredator strategy in motion. *Animal Behaviour*, *142*, 207–220. doi:10.1016/j.anbehav.2018.06.017

Neumeyer, C., Wietsma, J. J., & Spekreijse, H. (1991). Separate processing of 'color' and 'brightness' in goldfish. *Vision Research*, *31*(3), 537–549. doi:10.1016/0042-6989(91)90104-D

Newport, C., Green, N. F., McClure, E. C., Osorio, D., Vorobyev, M., Marshall, N. J., & Cheney, K. L. (2017). Fish use colour to learn compound visual signals. *Animal Behaviour*, *125*, 93–100. doi:10.1016/j.anbehav.2017.01.003

Ng, L., Garcia, J. E., & Dyer, A. G. (2018). Why colour is complex: Evidence that bees perceive neither brightness nor green contrast in colour signal processing.

FACETS, *3*(1), 800–817. doi:10.1139/facets-2017-0116

Nguyen-Tri, D., & Faubert, J. (2003). The fluttering-heart illusion: A new hypothesis. *Perception*, *32*(5), 627–634. doi:10.1068/p3228

Nilsson, D., Warrant, E., & Johnsen, S. (2014). Computational visual ecology in the pelagic realm. *Philosophical Transactions of the Royal Society of London. Series B, Biological Sciences*, *369*(1636), 20130038. doi:10.1098/rstb.2013.0038

Nimbs, M. J., & Smith, S. D. A. (2017). An illustrated inventory of the sea slugs of new south wa les, Australia (ga stropoda: Heterobranchia). *Proceedings of the Royal Society of Victoria*, *128*, 44–113. doi:10.1071/RS16011

Nityananda, V., Tarawneh, G., Henriksen, S., Umeton, D., Simmons, A., & Read, J. C. A. (2018). A novel form of stereo vision in the Praying Mantis. *Current Biology*, *28*(4), 588-593.e4. doi:10.1016/j.cub.2018.01.012

Nock, R., & Nielsen, F. (2004). Statistical region merging. *IEEE Transactions on Pattern Analysis and Machine Intelligence*, *26*(11), 1452–1458. doi:10.1109/TPAMI.2004.110

Norwich, K. H. (1987). On the theory of Weber fractions. *Perception & Psychophysics*, *42*(3), 286–298. doi:10.3758/BF03203081

Okuda, R. K., & Scheuer, P. J. (1985). Latrunculin-A, ichthyotoxic constituent of the nudibranch Chromodoris elisabethina. *Experientia*, *41*(10), 1355–1356. doi:10.1007/BF01952094

Olsson, P., Lind, O., & Kelber, A. (2015). Bird colour vision: behavioural thresholds reveal receptor noise. *Journal of Experimental Biology*, *218*(2), 184–193. doi:10.1242/jeb.111187

Olsson, P., Lind, O., & Kelber, A. (2018). Chromatic and achromatic vision: parameter choice and limitations for reliable model predictions. *Behavioral Ecology*, *29*(2), 273–282. doi:10.1093/beheco/arx133

Ortea, J., Valdes, A., & Espinosa, J. (1994). North Atlantic nudibranchs of the Chromodoris clenchi colour group (Opisthobranchia: Chromodorididae). Journal of Molluscan Studies 60(3):237.248. [Chromodoris binza, Chromodoris britoi, Chromodoris clenchi, Chromodoris neona, Glossodoris clenchi, Glossod, 237–

248.

Osborne, J., Osborne, J. W., Costello, A. B., & Kellow, J. T. (2011). Best practices in exploratory factor analysis. *Best Practices in Quantitative Methods*, 86–99. doi:10.4135/9781412995627.d8

Osorio, D. (1996). Symmetry detection by categorization of spatial phase, a Model. *Proceedings of the Royal Society B: Biological Sciences*, *263*(1366), 105–110. doi:10.1098/rspb.1996.0017

Osorio, D., & Anderson, J. (2007). Measuring skin colour and spectral reflectance using a digital camera. *Http://Www.Chrometrics.Com/*. Retrieved from http://www.chrometrics.com/

Osorio, D., Jones, C. D., & Vorobyev, M. (1999). Accurate memory for colour but not pattern contrast in chicks. *Current Biology*, *9*, 199–202. doi:10.1016/S0960-9822(99)80089-X

Osorio, D., Mikló, A., & Gonda, Z. (1999). Visual ecology and perception of coloration patterns by domestic chicks. *Evolutionary Ecology*, *13*(7–8), 673–689. doi:10.1023/A:1011059715610

Osorio, D., Smith, A. C., Vorobyev, M., & Buchanan-Smith, H. M. (2004). Detection of fruit and the selection of primate visual pigments for color vision. *The American Naturalist*, *164*(6), 696–708. doi:10.1086/425332

Osorio, D., & Vorobyev, M. (2005). Photoreceptor spectral sensitivities in terrestrial animals: Adaptations for luminance and colour Vision. *The Royal Society*, *272*(1574), 1745–1752.

Osorio, D., & Vorobyev, M. (2008). A review of the evolution of animal colour vision and visual communication signals. *Vision Research*, *48*, 2042–2051. doi:10.1016/j.visres.2008.06.018

Paradis, E., & Schliep, K. (2019). ape 5.0: an environment for modern phylogenetics and evolutionary analyses in R. *Bioinformatics*, *35*(3), 526–528. doi:10.1093/bioinformatics/bty633

Párraga, C. A., Troscianko, T., & Tolhurst, D. J. (2002). Spatiochromatic properties of natural images and human vision. *Current Biology : CB*, *12*(6), 483–487.

doi:10.1016/s0960-9822(02)00718-2

Pearson, P. M., & Kingdom, F. A. A. (2002). Texture-orientation mechanisms pool colour and luminance contrast. *Vision Research*, *42*(12), 1547–1558. doi:10.1016/S0042-6989(02)00067-6

Pelli, D. G., & Bex, P. J. (2013). Measuring contrast sensitivity. *Vision Research*, *90*, 10–14. doi:10.1016/j.visres.2013.04.015

Pignatelli, V., Champ, C., Marshall, N. J., & Vorobyev, M. (2010). Double cones are used for colour discrimination in the reef fish, Rhinecanthus aculeatus. *Biology Letters*, *6*(4), 537–539. doi:10.1098/rsbl.2009.1010\

Poulson, T. L., & White, W. B. (1969). The cave environment. *Science*, *165*(3897), 971–981.

Poulton, E. B. (1890). *The Colours of Animals*. Kegan Paul, Trench & Trubner.

Pretterer, G., Bubna-Littitz, H., Windischbauer, G., Gabler, C., & Griebel, U. (2004). Brightness discrimination in the dog. *Journal of Vision*, *4*(3), 10. doi:10.1167/4.3.10

Price, T. D. (2017). Sensory drive, color, and color vision. *The American Naturalist*, *190*(2), 157–170. doi:10.1086/692535

Price, T. D., Stoddard, M. C., Shevell, S. K., & Bloch, N. I. (2019). Understanding how neural responses contribute to the diversity of avian colour vision. *Animal Behaviour*, 1–9. doi:10.1016/j.anbehav.2019.05.009

Prudic, K. L., Skemp, A. K., & Papaj, D. R. (2007). Aposematic coloration, luminance contrast, and the benefits of conspicuousness. *Behavioral Ecology*, *18*(October), 41–46. doi:10.1093/beheco/arl046

Pugh, E. N., & Lamb, T. D. (2000). Chapter 5 Phototransduction in vertebrate rods and cones: Molecular mechanisms of amplification, recovery and light adaptation. In D. G. Stavenga, W. J. DeGrip, & E. N. Pugh (Eds.), *Molecular Mechanisms in Visual Transduction* (Vol. 3, pp. 183–255). North-Holland. doi:https://doi.org/10.1016/S1383-8121(00)80008-1

Purchon, R. D. (1977). *The Biology of the Mollusca*. Exeter: Pergamon Press Ltd.

Purves, D., Lotto, R. B., & Nundy, S. (2002). Why we see what we do. Retrieved from http://discovery.ucl.ac.uk/29109/

Purves, D., Lotto, R. B., Williams, S. M., Nundy, S., & Yang, Z. (2001). Why we see things the way we do: evidence for a wholly empirical strategy of vision. *Philosophical Transactions of the Royal Society of London. Series B, Biological Sciences*, *356*(1407), 285–97. doi:10.1098/rstb.2000.0772

R Core Team. (2015). R: A language and environment for statistical computing. Vienna, Austria: R Foundation for Statistical Computing. Retrieved from http://www.r-project.org/

Rajabizadeh, M., Adriaens, D., Kaboli, M., Sarafraz, J., & Ahmadi, M. (2015). Dorsal colour pattern variation in Eurasian mountain vipers (genus Montivipera): A trade-off between thermoregulation and crypsis. *Zoologischer Anzeiger*, *257*, 1–9. doi:10.1016/j.jcz.2015.03.006

Ramírez-Delgado, V. H., & Cueva del Castillo, R. (2020). Background matching, disruptive coloration, and differential use of microhabitats in two neotropical grasshoppers with sexual dichromatism. *Ecology and Evolution*, (December 2019), ece3.5995. doi:10.1002/ece3.5995

Ramos, J. A., & Peters, R. A. (2017). Motion-based signaling in sympatric species of Australian agamid lizards. *Journal of Comparative Physiology A: Neuroethology, Sensory, Neural, and Behavioral Physiology*, *203*(8), 661–671. doi:10.1007/s00359-017-1185-5

Randall, J. E., Allen, G. R., & Steene, R. C. (1997). *Fishes of the Great Barrier Reef and Coral Sea*. Crawford House Press.

Renoult, J. P., Kelber, A., & Schaefer, H. M. (2017). Colour spaces in ecology and evolutionary biology. *Biological Reviews*, *92*(1), 292–315. doi:10.1111/brv.12230

Renoult, J. P., & Mendelson, T. C. (2019). Processing bias: Extending sensory drive to include efficacy and efficiency in information processing. *Proceedings of the Royal Society B: Biological Sciences*, *286*(1900). doi:10.1098/rspb.2019.0165

Revell, L. J. (2009). Size-correction and principal components for interspecific comparative studies. *Evolution*, *63*(12), 3258–3268. doi:10.1111/j.1558-5646.2009.00804.x

Revell, L. J. (2012). phytools: An R package for phylogenetic comparative biology (and other things). *Methods in Ecology and Evolution*, *3*(2), 217–223. doi:10.1111/j.2041-210X.2011.00169.x

Riesenhuber, M., & Serre, T. (2004). Realistic modeling of simple and complex cell tuning in the HMAX model, and implications for invariant object recognition in cortex. *AI Memo*, (July). Retrieved from http://www.stormingmedia.us/29/2969/A296954.pdf

Rocha, F. A. F., Saito, C. A., Silveira, L. C. L., De Souza, J. M., & Ventura, D. F. (2008). Twelve chromatically opponent ganglion cell types in turtle retina. *Visual Neuroscience*, *25*(3), 307–315. doi:10.1017/S0952523808080516

Rodriguez-Morales, D., Rico-Gray, V., Garcia-Franco, J., Ajuria-Ibarra, H., Hernandez-Salazar, L. T., Robledo-Ospina, L. E., & Rao, D. (2018). Context-dependent crypsis : a prey ' s perspective of a color polymorphic predator. *The Science of Nature*, (351). doi:https://doi.org/10.1007/s00114-018-1562-0

Rojas, B., Devillechabrolle, J., & Endler, J. A. (2014). Paradox lost: Variable colour-pattern geometry is associated with differences in movement in aposematic frogs. *Biology Letters*, *10*(6), 20140193. doi:10.1098/rsbl.2014.0193

Rojas, B., & Endler, J. A. (2013). Sexual dimorphism and intra-populational colour pattern variation in the aposematic frog Dendrobates tinctorius. *Evolutionary Ecology*, *27*(4), 739–753. doi:10.1007/s10682-013-9640-4

Roper, T., & Wistow, R. (1986). Aposematic colouration and avoidance learning in chicks. *The Quarterly Journal of Experimental Psychology*, *38B*(March 2015), 37–41. doi:10.1080/14640748608402225

Rosenholtz, R., Li, Y., Jin, Z., & Mansfield, J. (2010). Feature congestion: A measure of visual clutter. *Journal of Vision*, *6*(6), 827–827. doi:10.1167/6.6.827

Rowe, C. (1999). Receiver psychology and the evolution of multicomponent signals. *Animal Behaviour*, *58*(5), 921–931. doi:10.1006/anbe.1999.1242

Rowe, C. (2013). Receiver psychology: A receiver's perspective. *Animal Behaviour*, *85*(3), 517–523. doi:10.1016/j.anbehav.2013.01.004

Rowe, C., & Guilford, T. (1999). The evolution of multimodal warning displays.

Evolutionary Ecology, 655–672. Retrieved from http://link.springer.com/article/10.1023/A:1011021630244

Rudman, W. B. (1986). The Chrornodoridídae (Opisthobranchia : Mollusca). *Zoological Journal of the Linnean Society*, *86*(1986), 101–184.

Rudman, W. B. (1991). Purpose in pattern - the evolution of color in chromodorid Nudibranchs. *Journal of Molluskan Studies*, *57*(1991), 5–21.

Rudman, W. B., & Bergquist, P. R. (2007). A review of feeding specificity in the sponge-feeding Chromodoridídae (Nudibranchia: Mollusca). *Molluscan Research*.

Russell, B. J., & Dierssen, H. M. (2015). Use of hyperspectral imagery to assess cryptic color matching in Sargassum associated crabs. *PLoS ONE*, *10*(9), 4–11. doi:10.1371/journal.pone.0136260

Ruxton, G. D., Allen, W. L., Sherratt, T. N., & Speed, M. P. (2018). *Avoiding Attack*. New York: Oxford University Press.

Sagi, D., & Julesz, B. (1984). Detection versus discrimination of visual orientation. *Perception*, *14*(5), 619–628. doi:10.1068/p130619

Sankeralli, M. J., Mullen, K. T., & Hine, T. J. (2002). Ratio model serves suprathreshold color-luminance discrimination. *Journal of the Optical Society of America A-Optics Image Science and Vision*, *19*(3), 425–435. doi:Doi 10.1364/Josaa.19.000425

Schiller, P. H., Sandell, J. H., & Maunsell, J. H. R. (1986). Functions of the On and Off channels of the visual system. *Nature*, *322*(6082), 824–825. doi:10.1038/322824a0

Scholtyssek, C., & Dehnhardt, G. (2013). Brightness discrimination in the South African fur seal (Arctocephalus pusillus). *Vision Research*, *84*, 26–32. doi:10.1016/j.visres.2013.03.003

Scholtyssek, C., Kelber, A., & Dehnhardt, G. (2008). Brightness discrimination in the harbor seal (Phoca vitulina). *Vision Research*, *48*(1), 96–103. doi:10.1016/j.visres.2007.10.012

Serre, T. (2014). Hierarchical models of the visual system. In *Encyclopedia of Computational Neuroscience* (Vol. 6, pp. 1–12). New York, NY: Springer New York. doi:10.1007/978-1-4614-7320-6_345-1

Servedio, M. R. (2000). The effects of predator learning, forgetting, and recognition errors on the evolution of warning coloration. *Evolution; International Journal of Organic Evolution*, *54*(3), 751–763. doi:10.1111/j.0014-3820.2000.tb00077.x

Shapiro, A. G., & Todorovic, D. (2017). *The Oxford Compendium of Visual Illusions*. (A. G. Shapiro & D. Todorovic, Eds.) (Vol. 1). Oxford University Press. doi:10.1093/acprof:oso/9780199794607.001.0001

Shapley, R., & Hawken, M. J. (2011). Color in the Cortex: single- and double-opponent cells. *Vision Research*, *51*(7), 701–717. doi:10.1016/j.visres.2011.02.012

Shepard, T. G., Swanson, E. A., McCarthy, C. L., & Eskew, R. T. (2016). A model of selective masking in chromatic detection. *Journal of Vision*, *16*(9), 3. doi:10.1167/16.9.3

Shevell, S. K. (2003). *The Science of Colour*. Elsevier.

Shevell, S. K., & Kingdom, F. A. A. (2008). Color in complex scenes. *Annual Review of Psychology*, *59*(1), 143–166. doi:10.1146/annurev.psych.59.103006.093619

Sibeaux, A., Cole, G. L., & Endler, J. A. (2019a). Success of the receptor noise model in predicting colour discrimination in guppies depends upon the colours tested. *Vision Research*, *159*(December 2018), 86–95. doi:10.1016/j.visres.2019.04.002

Sibeaux, A., Cole, G. L., & Endler, J. A. (2019b). The relative importance of local and global visual contrast in mate choice. *Animal Behaviour*, *154*, 143–159. doi:10.1016/j.anbehav.2019.06.020

Sibeaux, A., Keser, M. L., Cole, G. L., Kranz, A. M., & Endler, J. A. (2019). How viewing objects with the dorsal or ventral retina affects colour-related behaviour in guppies (Poecilia reticulata). *Vision Research*, *158*(February), 78–89. doi:10.1016/j.visres.2019.02.007

Siddiqi, A., Cronin, T. W., Loew, E. R., Vorobyev, M., & Summers, K. (2004). Interspecific and intraspecific views of color signals in the strawberry poison frog Dendrobates pumilio. *The Journal of Experimental Biology*, *207*(Pt 14), 2471–85. doi:10.1242/jeb.01047

Siebeck, U. E., Wallis, G. M., Litherland, L., Ganeshina, O., & Vorobyev, M. (2014). Spectral and spatial selectivity of luminance vision in reef fish. *Frontiers in Neural*

Circuits, *8*(September), 118. doi:10.3389/fncir.2014.00118

Simmons, D. R., & Kingdom, F. A. A. (2002). Interactions between chromatic- and luminance-contrast-sensitive stereopsis mechanisms. *Vision Research*, *42*(12), 1535–1545. doi:10.1016/S0042-6989(02)00080-9

Simpson, E. E., Marshall, N. J., & Cheney, K. L. (2016). Coral reef fish perceive lightness illusions. *Scientific Reports*, *6*(October), 35335. doi:10.1038/srep35335

Skorupski, P., & Chittka, L. (2011). Is colour cognitive? *Optics and Laser Technology*, *43*(2), 251–260. doi:10.1016/j.optlastec.2008.12.015

Smith, S. D. A. (2005). Rapid assessment of invertebrate biodiversity on rocky shores: Where there's a whelk there's a way. *Biodiversity and Conservation*, *14*(14), 3565–3576. doi:10.1007/s10531-004-0828-3

Smith, V. C., Pokorny, J., & Sun, H. (2000). Chromatic contrast discrimination : Data and prediction for stimuli cone excitation. *Color Reseach and Application*, *25*(2).

Smithers, S. P., Roberts, N. W., & How, M. J. (2019). Parallel processing of polarization and intensity information in fiddler crab vision. *Science Advances*, *5*(8), eaax3572. doi:10.1126/sciadv.aax3572

Solomon, J. A. (2009). The history of dipper functions. *Attention, Perception & Psychophysics*, *71*(3), 435–443. doi:10.3758/APP.71.3.435

Speed, M. P., & Ruxton, G. D. (2005). Aposematism: what should our starting point be? *Proceedings. Biological Sciences / The Royal Society*, *272*(September 2004), 431–438. doi:10.1098/rspb.2004.2968

Spinner, M., Kovalev, A., Gorb, S. N., & Westhoff, G. (2013). Snake velvet black: hierarchical micro- and nanostructure enhances dark colouration in Bitis rhinoceros. *Scientific Reports*, *3*, 1846. doi:10.1038/srep01846

Spottiswoode, C. N., & Stevens, M. (2010). Visual modeling shows that avian host parents use multiple visual cues in rejecting parasitic eggs. *Proceedings of the National Academy of Sciences of the United States of America*, *107*(19), 8672–8676. doi:10.1073/pnas.0910486107

Stevens, M. (2015). Anti-predator coloration and behaviour : a longstanding topic with many outstanding questions. *Current Zoology*, *61*(4), 702–707.

doi:10.1093/czoolo/61.4.702

Stevens, M. (2016). *Cheats and Deceits* (1st ed.). Oxford, UK: Oxford University Press.

Stevens, M., Broderick, A. C., Godley, B. J., Lown, A. E., Troscianko, J., Weber, N., … Weber, S. B. (2015). Phenotype – environment matching in sand fleas, 10–13.

Stevens, M., & Cuthill, I. C. (2006). Disruptive coloration, crypsis and edge detection in early visual processing. *Proceedings. Biological Sciences / The Royal Society*, *273*(May), 2141–2147. doi:10.1098/rspb.2006.3556

Stevens, M., Lown, A. E., & Wood, L. E. (2014). Camouflage and individual variation in shore crabs (Carcinus maenas) from different habitats. *PLoS ONE*, *9*(12), 1–31. doi:10.1371/journal.pone.0115586

Stevens, M., & Merilaita, S. (2011). *Animal Camouflage*. Cambridge: Cambridge University Press.

Stevens, M., Parraga, C. A., Cuthill, I. C., Partridge, J. C., & Troscianko, T. S. (2007). Using digital photography to study animal coloration. *Biological Journal of the Linnean Society*, *90*, 211–237.

Stevens, M., & Ruxton, G. D. (2012). Linking the evolution and form of warning coloration in nature. *Proceedings of the Royal Society B*, *279*(November 2011), 417–426. doi:10.1098/rspb.2011.1932

Stich, H.-B., & Lampert, W. (1981). Predator evasion as an explanation of diurnal vertical migration by zooplankton. *Nature*, *293*(5831), 396–398. doi:10.1038/293396a0

Stoddard, M. C., Kilner, R. M., & Town, C. (2014). Pattern recognition algorithm reveals how birds evolve individual egg pattern signatures. *Nature Communications*, *5*(May), 1–10. doi:10.1038/ncomms5117

Stoddard, M. C., & Osorio, D. (2019). Animal Coloration Patterns: Linking Spatial Vision to Quantitative Analysis. *The American Naturalist*, *193*(2), 000–000. doi:10.1086/701300

Stoddard, M. C., & Prum, R. O. (2008). Evolution of avian plumage color in a tetrahedral color space: A phylogenetic analysis of New World Buntings. *The American Naturalist*, *171*(6), 755–776. doi:10.1086/587526

Stoddard, M. C., & Stevens, M. (2010). Pattern mimicry of host eggs by the common cuckoo, as seen through a bird's eye. *Proceedings. Biological Sciences / The Royal Society*, *277*(January), 1387–1393. doi:10.1098/rspb.2009.2018

Strannegård, C., Xu, W., Engsner, N., Endler, J. A., & Marshall, J. (2020). Combining evolution and learning in computational ecosystems. *Journal of Artificial General Intelligence*, *11*(1), 1–37. doi:10.2478/jagi-2020-0001

Straube, S., & Fahle, M. (2011). Visual detection and identification are not the same: Evidence from psychophysics and fMRI. *Brain and Cognition*, *75*(1), 29–38. doi:10.1016/j.bandc.2010.10.004

Summers, K., & Clough, M. E. (2001). The evolution of coloration and toxicity in the poison frog family (Dendrobatidae). *Proceedings of the National Academy of Sciences of the United States of America*, *98*(11), 6227–6232. doi:10.1073/pnas.101134898

Switkes, E., Mayer, M. J., & Sloan, J. A. (1978). Spatial frequency analysis of the visual environment: Anisotropy and the carpentered environment hypothesis. *Vision Research*, *18*(10), 1393–1399. doi:10.1016/0042-6989(78)90232-8

Syrkin, G., & Gur, M. (1997). Colour and luminance interact to improve pattern recognition. *Perception*, *26*(2), 127–140. doi:10.1068/p260127

Tabata, M., & Alkon, D. L. (1982). Positive synaptic feedback in visual system of nudibranch mollusk Hermissenda crassicornis. *Journal of Neurophysiology*, *48*(1), 174–191.

Talas, L., Fennell, J. G., Kjernsmo, K., Cuthill, I. C., Scott-Samuel, N. E., & Baddeley, R. J. (2020). CamoGAN: Evolving optimum camouflage with Generative Adversarial Networks. *Methods in Ecology and Evolution*, *11*(2), 240–247. doi:10.1111/2041-210X.13334

Tartarotti, B., & Sommaruga, R. (2006). Seasonal and ontogenetic changes of mycosporine-like amino acids in planktonic organisms from an alpine lake. *Limnology and Oceanography*, *51*(3), 1530–1541. doi:10.4319/lo.2006.51.3.1530

Taylor, C. H., Gilbert, F., & Reader, T. (2013). Distance transform: A tool for the study of animal colour patterns. *Methods in Ecology and Evolution*, *4*(8), 771–781. doi:10.1111/2041-210X.12063

Thayer, G. H. (1909). *Concealing-Colouration in the Animal Kingdom: An Exposition of the Laws of Disguise through Color and Pattern: Being a summary of Abbott H. Thayer's Discoveries*. New York: Macmillan.

Thoen, H. H., How, M. J., Chiou, T.-H., & Marshall, N. J. (2014). A Different form of color vision in Mantis Shrimp. *Science*, *343*(January), 411–413. doi:10.1126/science.1245824

Treisman, M. (1964). Noise and Weber's law: The discrimination of brightness and other dimensions. *Psychological Review*, *71*(4), 314–330. doi:10.1037/h0042445

Trifinopoulos, J., Nguyen, L. T., von Haeseler, A., & Minh, B. Q. (2016). W-IQ-TREE: a fast online phylogenetic tool for maximum likelihood analysis. *Nucleic Acids Research*, *44*(W1), W232–W235. doi:10.1093/nar/gkw256

Troscianko, J., Skelhorn, J., & Stevens, M. (2017). Quantifying camouflage: how to predict detectability from appearance. *BMC Evolutionary Biology*, *17*(1), 7. doi:10.1186/s12862-016-0854-2

Troscianko, J., & Stevens, M. (2015). Image calibration and analysis toolbox - a free software suite for objectively measuring reflectance, colour and pattern. *Methods in Ecology and Evolution*, *6*(11), 1320–1331. doi:10.1111/2041-210X.12439

Troscianko, J., Wilson-Aggarwal, J., Spottiswoode, C. N., & Stevens, M. (2016). Nest covering in plovers: How modifying the visual environment influences egg camouflage. *Ecology and Evolution*, *6*(20), 7536–7545. doi:10.1002/ece3.2494

Troscianko, J., Wilson-Aggarwal, J., Stevens, M., & Spottiswoode, C. N. (2016). Camouflage predicts survival in ground-nesting birds. *Scientific Reports*, *6*, 19966. doi:10.1038/srep19966

Tullberg, B. S., Merilaita, S., & Wiklund, C. (2005). Aposematism and crypsis combined as a result of distance dependence: functional versatility of the colour pattern in the swallowtail butterfly larva. *Proceedings. Biological Sciences / The Royal Society*, *272*(1570), 1315–1321. doi:10.1098/rspb.2005.3079

Tullrot, A. (2013). The evolution of unpalatability and warning coloration in soft-bodied marine invertebrates. *Evolution*, *48*(3), 925–928.

Tullrot, A., & Sundberg, P. (1991). The conspicuous nudibranch Polycera

quadrilineata: aposematic coloration and individual selection. *Animal Behaviour*, (41), 175–176.

Umeton, D., Tarawneh, G., Fezza, E., Read, J. C., & Rowe, C. (2019). Pattern and speed interact to hide moving prey. *Current Biology*, 1–5. doi:10.1016/j.cub.2019.07.072

v. Campenhausen, M., Kirschfeld, K., Campenhausen, M. V., & Kirschfeld, K. (1998). Spectral sensitivity of the accessory optic system of the pigeon. *Journal of Comparative Physiology - A Sensory, Neural, and Behavioral Physiology*, *183*(1), 1–6. doi:10.1007/s003590050229

Valdés, Á. (2002). A phylogenetic analysis and systematic revision of the cryptobranch dorids (Mollusca, Nudibranchia, Anthobranchia). *Zoological Journal of the Linnean Society*, *136*(4), 535–636. doi:10.1046/j.1096-3642.2002.00039.x

Van Belleghem, S. M., Papa, R., Ortiz-Zuazaga, H., Hendrickx, F., Jiggins, C. D., Mcmillan, W. O., & Counterman, B. A. (2018). Patternize : An R package for quantifying color pattern variation. *Methods in Ecology and Evolution*, *9*(2), 390–398. doi:10.1111/2041-210X.12853

van den Berg, C. P., Troscianko, J., Endler, J. A., Marshall, N. J. J., Cheney, K. L., Berg, C. P., … Cheney, K. L. (2020). Quantitative Colour Pattern Analysis (QCPA): A comprehensive framework for the analysis of colour patterns in nature. *Methods in Ecology and Evolution*, *11*(2), 316–332. doi:10.1111/2041-210X.13328

Vasas, V., Brebner, J. S. J. S., & Chittka, L. (2018). Color discrimination is not just limited by photoreceptor noise: a comment on Olsson et al. *Behavioral Ecology*, *29*(2), 285–28. doi:10.1093/beheco/arx157

Veale, R., Hafed, Z. M., & Yoshida, M. (2017). How is visual salience computed in the brain ? Insights from behaviour , neurobiology and modelling. *Philosophical Transactions of the Royal Society B*, *372*, 20160113. doi:10.1098/rstb.2016.0113

Veilleux, C. C., & Cummings, M. E. (2012). Nocturnal light environments and species ecology: implications for nocturnal color vision in forests. *Journal of Experimental Biology*, *215*(23), 4085–4096. doi:10.1242/jeb.071415

Vereecken, N. J. (2008). Pollinator-mediated selection, reproductive isolation and floral evolution in Ophrys orchids. *Proc. Neth. Entomol. Soc. Meet.*, *19*(January 2008),

9–22.

Vingrys, A. J., & Mahon, L. E. (1998). Color and luminance detection and discrimination asymmetries and interactions. *Vision Research*, *38*(8), 1085–1095. doi:10.1016/S0042-6989(97)00250-2

Vorobyev, M., Brandt, R., Peitsch, D., Laughlin, S. B., & Menzel, R. (2001). Colour thresholds and receptor noise: Behaviour and physiology compared. *Vision Research*, *41*, 639–653. doi:10.1016/S0042-6989(00)00288-1

Vorobyev, M., & Osorio, D. (1998). Receptor noise as a determinant of colour thresholds. *Proceedings of the Royal Society B: Biological Sciences*, *265*(1394), 351–358. doi:10.1098/rspb.1998.0302

Voss, K. J., & Zhang, H. (2006). Bidirectional reflectance of dry and submerged Labsphere Spectralon plaque. *Applied Optics*, *45*(30), 7924–7. doi:10.1364/AO.45.007924

Wägele, H., & Klussmann-Kolb, A. (2005). Opisthobranchia (Mollusca, Gastropoda) - More than just slimy slugs. Shell reduction and its implications on defence and foraging. *Frontiers in Zoology*, *2*, 1–18. doi:10.1186/1742-9994-2-3

Wägele, H., & Willan, R. (2000). Phylogeny of the Nudibranchia. *Zoological Journal of the Linnean …*, 83–181. doi:10.1006/zjls

Wagemans, J., Elder, J. H., Kubovy, M., Palmer, S. E., Peterson, M. A., Singh, M., & von der Heydt, R. (2012). A century of Gestalt psychology in visual perception: I. Perceptual grouping and figure–ground organization. *Psychological Bulletin*, *138*(6), 1172–1217. doi:10.1037/a0029333

Wallach, H. (1948). Brightness constancy and the nature of achromatic colors. *Journal of Experimental Psychology*, *38*(3), 310–324. doi:10.1037/h0053804

Warrant, E. J. (1999). Seeing better at night: Life style, eye design and the optimum strategy of spatial and temporal summation. *Vision Research*, *39*(9), 1611–1630. doi:10.1016/S0042-6989(98)00262-4

Warrant, E. J. (2007). Visual ecology: Hiding in the dark. *Current Biology*, *17*(6), R209–R211. doi:10.1016/j.cub.2007.01.043

Warrant, E. J. (2017). The remarkable visual capacities of nocturnal insects: Vision at

the limits with small eyes and tiny brains. *Philosophical Transactions of the Royal Society B: Biological Sciences*, *372*(1717). doi:10.1098/rstb.2016.0063

Warrant, E. J. (2019). Animal signals: Dirty dancing in the dark? *Current Biology*, *29*(17), R834–R836. doi:10.1016/j.cub.2019.07.046

Webber, E. S., Chambers, N. E., Kostek, J. A., Mankin, D. E., & Cromwell, H. C. (2015). Relative reward effects on operant behavior: Incentive contrast, induction and variety effects. *Behavioural Processes*, *116*(4), 87–99. doi:10.1016/j.beproc.2015.05.003

White, T. E., Dalrymple, R. L., Noble, D. W. A., O'Hanlon, J. C., Zurek, D. B., & Umbers, K. D. L. (2015). Reproducible research in the study of biological coloration. *Animal Behaviour*, *106*, 51–57. doi:10.1016/j.anbehav.2015.05.007

White, T. E., Rojas, B., Mappes, J., Rautiala, P., Kemp, D. J., & White, T. E. (2017). Colour and luminance contrasts predict the human detection of natural stimuli in complex visual environments. *Biology Letters*, *13*, 20170375. Retrieved from http://dx.doi.org/10.1098/rsbl.2017.0375

Whittle, P. (1986). Increments and decrements: Luminance discrimination. *Vision Research*, *26*(10), 1677–1691. doi:10.1016/0042-6989(86)90055-6

Whittle, P. (1992). Brightness, discriminability and the 'Crispening Effect'. *Vision Research*, *32*(8), 1493–1507. doi:10.1016/0042-6989(92)90205-W

Wickham, J. D., Riitters, K. H., O'Neill, R. V., Jones, K. B., & Wade, T. G. (1996). Landscape 'contagion' in raster and vector environments. *International Journal of Geographical Information Systems*, *10*(7), 891–899. doi:10.1080/02693799608902115

Wiebe, P. H., Copley, N. J., & Boyd, S. H. (1992). Coarse-scale horizontal patchiness and vertical migration of zooplankton in Gulf Stream warm-core ring 82-H. *Deep Sea Research Part A. Oceanographic Research Papers*, *39*, 247–278. doi:10.1016/S0198-0149(11)80015-4

Wiener, M. (1957). Animal eyes. *American Orthoptic Journal*, *7*(1), 137–142. doi:10.1080/0065955X.1957.11981216

Willis, A., & Anderson, S. J. (2002). Colour and luminance interactions in the visual

perception of motion. *Royal Society*, *269*(1495), 1011–1016. Retrieved from http://www.jstor.org/stable/3068182

Wilson, N. G., & Lee, M. S. Y. (2005). Molecular phylogeny of Chromodoris (Mollusca, Nudibranchia) and the identification of a planar spawning clade. *Molecular Phylogenetics and Evolution*, *36*(3), 722–727. doi:10.1016/j.ympev.2005.04.003

Winters, A. E., Green, N. F., Wilson, N. G., How, M. J., Garson, M. J., Marshall, N. J., & Cheney, K. L. (2017). Stabilizing selection on individual pattern elements of aposematic signals. *Proceedings of the Royal Society B*, *284*(1861).

Winters, A. E., Wilson, N. G., van den Berg, C. P., How, M. J., Endler, J. A., Marshall, N. J., … Cheney, K. L. (2018). Toxicity and taste: Unequal chemical defences in a mimicry ring. *Proceedings of the Royal Society B: Biological Sciences*, *285*(1880), 20180457. doi:10.1098/rspb.2018.0457

Wu, S., Chang, C. M., Mai, G. S., Rubenstein, D. R., Yang, C. M., Huang, Y. T., … Shen, S. F. (2019). Artificial intelligence reveals environmental constraints on colour diversity in insects. *Nature Communications*, *10*(1), 1–9. doi:10.1038/s41467-019-12500-2

Wyszecki, G., & Stiles, W. (2000). *Color Science: Concepts and Methods, Quantitative Data and Formulae* (second edt). Wiley.

Xiao, F., & Cuthill, I. C. (2016). Background complexity and the detectability of camouflaged targets by birds and humans. *Proceedings of the Royal Society B: Biological Sciences*, *283*(1838), 20161527. doi:10.1098/rspb.2016.1527

Yokoyama, S., & Yokoyama, R. (1996). Adaptive evolution of photoreceptors and visual pigments in vertebrates. *Annual Review of Ecology and Systematics*, *27*, 543–567. doi:10.1146/annurev.ecolsys.27.1.543

Yssaad-Fesselier, R., & Knoblauch, K. (2006). Modeling psychometric functions in R. *Behavior Research Methods*, *38*(1), 28–41. doi:10.3758/BF03192747

Zylinski, S., How, M. J., Osorio, D., Hanlon, R. T., & Marshall, N. J. (2011). To be seen or to hide: Visual characteristics of body patterns for camouflage and communication in the Australian Giant Cuttlefish Sepia apama. *The American Naturalist*, *177*(5), 681–690. doi:10.1086/659626